Isolation and characterization of xanthine oxidase inhibitor(s) from endophytic fungi

A

thesis submitted

in the partial fulfilment of the requirements for the award of degree of

DOCTOR OF PHILOSOPHY

IN

BIOTECHNOLOGY

Submitted By

NEHA KAPOOR

(Reg. No. 901000008)

Under the supervision of

Dr. SANJAI SAXENA

Professor

Department of Biotechnology

Thapar University, Patiala, 147004, Punjab

January 2017

CERTIFICATE

Certified that the thesis entitled "Isolation and characterization of xanthine oxidase inhibitor(s) from endophytic fungi" submitted by Ms. Neha Kapoor, Reg. no. 901000008 in the partial fulfilment of the requirements for the award of the degree of Doctor of Philosophy in the Department of Biotechnology, Thapar University, Patiala, Punjab is a record of candidate's own independent and original research work carried out by himself under my supervision and guidance. The material embodied in this thesis has not been submitted in part or full to any other University or institute for the award of any degree.

27/1/2017

Dr. Sanjai Saxena

Supervisor

Department of Biotechnology

Thapar University, Patiala, Punjab

CANDIDATE'S DECLARATION

I, hereby declare that the work presented in the thesis entitled "Isolation and characterization of xanthine oxidase inhibitor(s) from endophytic fungi" in the partial fulfilment of the requirements for the award of the degree of Doctor of Philosophy at Department of Biotechnology, Thapar University, Patiala is an authentic record of my own work during the period from January 2011 to December 2016, under the supervision of Prof. Sanjai Saxena, Professor, Department of Biotechnology, Thapar University. This report has not been submitted for the award of any degree or certificate in this or any other university.

Place: Patiala, Punjab

Date: January 30, 2017

Neha Kapoor

(Reg no. 901000008)

ACKNOWLEDGMENT

I feel this thesis became a reality with the kind help and support of many individuals and I would like to extend my sincere thanks to all of them.

Foremost, I would like to express deep sense of gratitude to my supervisor, **Prof. Sanjai Saxena**, Dr., Department of Biotechnology (DBT), Thapar University, Patiala, Punjab for his direction, support and inspiration throughout this work. I sincerely thank him for providing me endless learning opportunities during my tenure who continue moulding me to work to my extremities. I owe heartfelt thanks to my mentor for the tremendous efforts and every possible help to finish this thesis. His constructive and valuable suggestions have always worked for me in professional as well as personal life. I truly thank him for being a Man Of Solutions (MOS) for my every problem.

My sincere gratitude to visionary director of TU, **Prof. Dr. Prakash Gopalan**, for providing necessary infrastructure and excellent research environment.

I am highly thankful to **Prof. Dinesh Goyal**, Head, DBT, **Dr. Siddarth Sharma**, Assistant professor and **Dr. Manoj Baranwal**, Assistant Professor, DBT, Thapar University, Patiala for their valuable suggestions and constant encouragement. I am highly obliged to them for their kind support in carrying out present research work.

I am grateful to **Mr. Avtar Singh**, **Mr. Maneesh Kumar**, **Mr. Anoop Patyal,** Technical officer, SAIF, Panjab University, Chandigarh for their kind cooperation in NMR and ESI-MS analysis. I am also thankful to **Mr. Mukesh Kumar,** SAI Lab, Thapar University, Patiala and **Ms. Maneesha,** Ph.D scholar, School of Chemistry and Biochemistry, Thapar University for their kind help in NMR and FTIR analysis.

I am thankful to **Department of Biotechnology**, Ministry of Science and Technology, Government of India, New Delhi and **Council of Scientific & Industrial Research** (CSIR), New Delhi for providing me financial help under the sponsored project BT/PR/10083/NDB/52/95/2007; 38(1308)/11/EMR-II. I also appreciate the financial help received from **Thapar University,** Patiala in lieu of Teaching Assistantship.

I owe my heartfelt thanks to **Dr. Satyendra K. Pandey,** Assistant Professor, School of Chemistry and Biochemistry, Thapar University for his kind guidance, constructive suggestions and cooperation in compound purification and structure elucidation. A special thanks to **Mr. Ram Naval**, **Mr. Surinder Pal** and other lab staff members of DBT, TU without whom's help many experiments would not be have been possible.

I am especially indebted to my seniors **Mr. Birinderjit singh**, **Dr. Vineet Meshram** and **Dr. Mahiti Gupta** and for their constant love, cooperation and help. I extend my heartfelt thanks to all of them

from inspiring discussion sessions to cherishable moments. My special thanks to **Mr. Vagish Dwibedi**, Ph. D scholar for all the kind support, co-operation and for providing nice atmosphere in the lab.

I would also like to acknowledge love, care and cooperation of my friends Dr. Sumit Jaiswal, Anugya Shrivastava, Noorpreet Dhanjal, Himadri, Palak, Jayishnu, Rahil and Devendera Sillu. I thank all of them for all fun filled and wonderful memories.

I sincerely thank Amma and Baba (**Dr. Devendra Kumar Saxena** and **Smt. Savita Saxena**) and **Mrs. Merry Saxena** for their parental love, care and affection. I am genuinely appreciative of countless efforts of Baba for being very co-operative and patient while checking my thesis. I am thankful to sweet Mehak for all the wonderful memories. I always felt like home while spending time with them.

I would like to thank **Mr. Virender Gambhir and Mrs. Pushpa Gambhir** for their constant love, care and encouragement without which this thesis would not have been possible.

A special vote of thanks to **Dr. Lokesh Gambhir**, Assistant Professor, SGRRITS, Dehradun for continual support, encouragement and for always being by my side during my rough times. I highly appreciate his unlimited encouragement, compassion, patience when the times got rough. Thanks for being a compassionate and trustworthy individual.

Above all, my sincere and heartfelt thanks to my loving parents, **Mr. Ashok Kumar and Mrs. Meenu Kapoor** for immense love, care, encouragement and motivation to complete my work. You are the guiding light of my life that had always provided me strength, peace, enthusiasm and courage to keep pushing. I owe my earnest thanks to my brothers, **Mr. Kunal Kapoor**, **Mr. Karan Kapoor** and bhabhi, **Mrs. Pooja Kapoor** for their endless love, care, patience, and encouragement. Love to my two cutie pies, **Ananya** and **Hardik**.

Thanks to almighty for bestowing wisdom, peace, strength and good health in this endeavour.

Date: Jan 30, 2016

Place: Patiala **Neha Kapoor**

Dedicated

to

My Family

Publications

1. Kapoor N and Saxena S (2016): Xanthine oxidase inhibitory and antioxidant potential of Indian *Muscodor* species. 3Biotech. 6:248. ISSN 2190-5738. (IF-0.992)
2. Kapoor and Saxena S (2014): Potential xanthine oxidase inhibitory activity of endophytic *Lasiodiplodia psuedotheobromae*. Applied Biochemistry and Biotechnology. 173(6):1360-74. ISSN: 0273-2289. (IF-1.606)
3. Saxena S, Meshram V and Kapoor N (2015): *Muscodor tigerii* sp. nov.-Volatile antibiotic producing endophytic fungus from North-eastern Himalayas. Annals of Microbiology. 65:47–57. ISSN 1590-4261. (IF- 1.232)
4. Saxena S, Meshram V and Kapoor N (2014): *Muscodor darjeelingensis*, a new endophytic fungus of *Cinnamomum camphora* collected from Northeastern Himalayas. Sydowia. 66(1):2014-0055. ISSN 0082-0598. (IF-1.02)

Other Publications

1. Meshram V, Kapoor N and Saxena S (2016): Endophytic *Fusarium* isolates from *Aegle marmelos* in Western Ghats of India and their fibrinolytic ability. Sydowia. 68 (30): 113-119. ISSN 0082-0598. (IF-1.02)
2. Meshram V, Saxena S, Paul K, Gupta M and Kapoor N (2016): Production, Purification and Characterisation of a Potential Fibrinolytic Protease from Endophytic *Xylaria curta* by Solid Substrate Fermentation. Applied Biochemistry and Biotechnology. zOI 10.1007/s12010-016-2298-y. ISSN: 0273-2289. (IF-1.606)
3. Meshram V, Saxena S and Kapoor N (2014): *Muscodor strobelii*, a new endophytic species from South India. Mycotaxon. 128:93-104. ISSN 0093-4666. (IF: 0.705).
4. Meshram V, Kapoor N and Saxena S (2013): *Muscodor kashayum* sp. nov. – a new volatile antimicrobial producing endophytic fungus. Mycology: an international journal of fungal biology. 4(4): 196-204.

5. Meshram V, Saxena S and Kapoor N (2012)*: In vitro a*nti-staphylococcal potential of endophytic fungi from *Aegle marmelos.* Journal of Pure and Applied Microbiology. 6(4):1859-1868. (IF: 0.073).

Submitted Manuscripts

1. **Kapoor N** and Saxena S (2016): Speciation of *Muscodor* based on ITS phylogeny and secondary structure prediction. Annals of Microbiology (Revision Submitted).
2. **Kapoor N** and Saxena S (2017): Xanthine oxidase inhibitory potential of fungal endophytes isolated from Indian Medicinal Plants. 3Biotech (Submitted).
3. Meshram V, **Kapoor N,** Chopra G and Saxena S (2016): *Muscodor camphora:* a new endophytic fungus from *Cinnamomum camphora.* Symbiosis. Submitted.
4. Meshram V, **Kapoor N,** Shrivastava A, Dwibedi V and Saxena S (2016): Endophytic Quamblaria cyanescens: a new bioresource for resveratrol production. Journal of Industrial Microbiology. Submitted.

Conference Proceedings

<u>Poster Presentations</u>

1. **Kapoor N** and Saxena S (2015): Xanthine oxidase inhibitory and cytotoxic potential of Lasiodiplodia species, an endophytic fungus in *Aegle marmelos* at 41st Annual meeting of MSI and National symposium on "Mycological research-Emerging trends, applications and prospects" held at Punjabi University, Patiala.
2. **Kapoor N**, Meshram V and Saxena S (2015): Antimicrobial and mycofumigation potential of endophytic Muscodor species from Western Ghats of India. at DAE-BRNS Life science symposium on "Advances in Microbiology of Food, Agriculture, Health and Environment held at BARC, Mumbai.

3. **Kapoor N** and Saxena S (2014): Endophytic fungi: A Novel source of Gout Therapeutics at 4th Biennial International Conference on "New Developments in Drug Discovery from Natural Products and Traditional Medicines" held at NIPER, Mohali.
4. **Kapoor N** and Saxena S (2014): Phylogenetic Character Mapping of Indian Muscodor species at International symposium on "Role of fungi and microbes in the 21st century- A Global scenario" held at Kolkata, West Bengal.
5. **Kapoor N** and Saxena S (2013): Gout Therapeutics from Endophytic fungi: New Source for old disease at 39th Annual MSI and conference on "Current prospectives of fungi in health care and environment (KAAVASTHA)" at Bangalore university, Bangalore.
6. **Kapoor N** and Saxena S (2012): Bio-prospecting endophytic fungi as the potential source of Xanthine oxidase inhibitors at 3rd Biennial International Conference on "New Developments in Drug Discovery from Natural Products and Traditional Medicines" held at NIPER, Mohali.
7. Meshram V, Saxena S and **Kapoor N** (2012): Antibacterial effect of VOCs produced by Indian Muscodor isolates. National conference on "Mycodiversity with its sustainable exploration and biotechnological application" and 38th annual meeting of Mycological Society of India at Sant Gadke Baba University, Amravati, Maharashtra
8. Saxena S, Meshram V and **Kapoor N** (2015) Mycofumigation potential of novel Indian Muscodor isolates. DAE-BRNS life science symposium (LSS-2015): Advances in microbiology of food, agriculture, health and environment. Bhabha Atomic research centre, Mumbai, Maharashtra
9. Saxena S, Meshram V and **Kapoor N** (2013) Endophytic fungi: A treasure trove of bioactive compounds. XIth International Fungal Biology Conference. Karlsruhe Institute of Technology. Karlsruhe, Germany.

AWARDS

1. Best Poster Award (2014) at 4th Biennial International conference on new developments in drug discovery from natural products and traditional medicines. National institute of pharmaceutical education and research (NIPER), Mohali, Punjab.

WORKSHOPS/ TRAININGS

1. Kapoor N (2010): National conference on “Emerging trends in Biopharmaceuticals relevance to human health & 4th Annual convention of Association of biotechnology and pharamacy” held at Thapar University, Patiala.
2. Kapoor N (2013): National seminar on “Innovation and Entrepreneurship” held at Thapar University, Patiala.
3. Kapoor N (2013): National Workshop on “Natural vinegar and naturally carbonated beverage production” at Science and Technology Entrepreneur’s Park, Thapar University, Patiala
4. Kapoor N (2013): Workshop on “Intellectual Property rights”. Science and Technology Entrepreneur’s Park, Thapar University, Patiala

Table of Contents

List of Tables

List of figures

List of symbols

S. no	Symbol	
1.	%	percentage
2.	′	minute
3.	≥	equals to or greater than
4.	°	degree
5.	°C	degree celsius
6.	µg	microgram
7.	µl	microliter
8.	µm	micrometer
9.	cm	centimeter
10.	g	gram
11.	h	hour
12.	kDa	kilo Dalton
13.	K_m	Michaelis constant
14.	l	litre
15.	M	molar
16.	mA	milliampere
17.	mg	milligram
18.	min	minute
19.	ml	milliliter
20.	mm	millimeter
21.	mM	millimolar
22.	mPa	megapascel
23.	nm	nanometer
24.	psi	pounds per square inch
25.	rpm	revolutions per minute
26.	s	second
27.	U	unit (activity)
28.	mU	milliunit
29.	v	volume
30.	v/v	volume by volume
31.	V_{max}	maximum reaction velocity
32.	w/v	weight by volume
33.	µg /ml	microgram per milligram
34.	mg/dl	Milligram per decilitre
35.	µM	micromolar
36.	U/ml	units per milliliter
37.	ng/µl	nanograms per microliter
38.	bp	base pair
39.	α	alpha
40.	β	beta
41.	γ	gamma
42.	±	plus minus
43.	MJ/Kg	millijoule per kiligram
44.	~	approximately
45.	mm^2	millimeter square
46.	mAU	milli Absorbance Unit
47.	$	dollar

List of abbreviations

S. no	Abbreviations	Full form
1.	ADP	Adenosine diphosphate
2.	ADSL	Adenylosuccinte lyase
3.	ADSS	Adenylosuccinate sythase
4.	Ag^{+}	Silver ion
5.	agalA	α-galactosidase A
6.	AHS	Allopurinol hypersensitivity syndrome
7.	AICAR	Aminoimidazole-4-carboxamide ribonucleotide
8.	AICAR Tfase	5-aminoimidazole-4-carboxamide ribonucleotide formyltransferase
9.	AIR	Aminoimidazole ribonucleotide
10.	AIRS	Phosphoribosylaminoimidazole synthetase
11.	AMP	Adenosine monophosphate
12.	AMPS	Adenylosuccinate
13.	ANOVA	Analysis of variance
14.	APRT	Adenine phosphoribosyl transferase
15.	AR	Analytical reagent
16.	Asp	Asparagine
17.	ATP	Adenosine triphosphate
18.	BLAST	Basic local alignment search tool
19.	BRT	Billiranga swami temple
20.	Ca^{2+}	Calcium
21.	CAD	coronary artery diseases
22.	CAIRS	Phosphoribosyl aminoimidazole carboxylase
23.	CDA	Czapek dox agar
24.	CDB	Czapek dox Broth
25.	CF-LCMS	Centrifugal force liquid chromatography mass spectrometry
26.	CH_3	Methyl
27.	CH_3OH	Methanol
28.	$CHCl_2$	Dichloromethane
29.	CHF	Chronic heart failure
30.	CKD	Chronic kidney disease
31.	CMA	Corn meal agar
32.	CVDs	Cardiovascular disorders
33.	Cys	Cystine
34.	DDW	Double distilled water
35.	DNA	Deoxyribonucleic acid
36.	dNTP	Deoxy nucleotide triphosphate
37.	DPX	Distrene plasticiser xylene
38.	DRESS	Drug rash with eosinophilia and systematic symptoms
39.	EHT	Extra high tension
40.	eNO	Endothelial nitric oxide
41.	ESI	Electron spray ionization
42.	ESI-MS	Electrospray ionisation -mass spectrometry

43.	FAICAR	N-formylaminoimidazole-4-carboxyamide ribonucleotide
44.	FDA	Food and Drug administration
45.	$FeSO_4$	Ferrous sulphate
46.	FGAM	N-formylglycinamide ribonucleotide
47.	FGAMS	Phosphoribosylformylglycinamide synthase
48.	FGAR	N-formylglycinamide ribonucleotide
49.	FIA	Flow injection analysis
50.	FTIR	Fourier transform infrared spectroscopy
51.	GAR	Phosphoribosyl glycinamide
52.	GARfase	Phosphoribosylglycinamide formyltransferase
53.	GARS	Phosphoribosyl glycinamide synthetase
54.	GC	Gas chromatography
55.	GERD	Gastroesophage reflux disease
56.	Gln	Glutamine
57.	Glu	Glucose
58.	Gly	Glycine
59.	GMP	Guanosine monophosphate
60.	GMPS	GMP synthase
61.	GTP	Guanosine triphosphate
62.	GTR	General time reversible
63.	H_2O_2	Hydrogen peroxide
64.	H_2SO_4	Sulphuric acid
65.	HCl	Hydrochloric acid
66.	HCO^{3-}	Bicarbonate ion
67.	HF	Heart failure
68.	HGPRT	Hypoxanthine guanine phosphoribosyl transferase
69.	His	Histidine
70.	HLA-B	Human leukocyte antigen type B
71.	HMG-CoA	3-hydroxy-3-methyl-glutaryl-CoA reductase
72.	HOMA-IR	Homeostasis model assessment of insulin resistance
73.	HPLC	High pressure liquid chromatography
74.	HPRT	Hypoxanthine guanine phosphoribosyl transferase
75.	HSCCC	High speed counter current chromatography
76.	IC_{50}	Inhibitory concentration 50
77.	IMP	Inosine monophosphate
78.	IMPCH	IMP cyclohydrolase
79.	IMPDH	IMP dehydrogenase
80.	ITS	Internal transcribed spacer
81.	Kb	Kilobase pair
82.	KH_2PO_4	Potassium dihydrogen phospahte
83.	K_i	Inhibition constant
84.	K_m	Michaelis-menten constant
85.	LC	Liquid chromatography
86.	m/z	Mass to charge ratio
87.	MCL	Maximum composite likelihood

88.	MEA	Malt extract agar
89.	MEB	Malt extract broth
90.	MEGA	Molecular evolutionary genetics analysis
91.	MFE	Minimum free energy
92.	$MgCl_2$	Magnesium chloride
93.	$MgSO_4$	Magnesium sulphate
94.	MHz	Mega hertz
95.	MLST	Multi locus sequence typing
96.	$MnSO_4$	Magnese sulphate
97.	MPE	Maculopapular eruptions
98.	MS	Mass spectroscopy
99.	NaClO	Sodium hypochlorite
100.	NAD	Nicotinamide dinucleotide
101.	NADH	Nicotinamide dinucleotide (reduced)
102.	NADPH	Nicotinamide dinucleotide phospahte
103.	NAFLD	Non-alcoholic fatty acid liver disease
104.	NBT	Nitroblue tetrazolium
105.	NCBI	National centre for biotechnology Information
106.	NMR	Nuclear magnetic resonance
107.	NO	Nitric oxide
108.	NP-SIXO	Non purine selective inhibitor of xanthine oxidase
109.	NRPS	non-ribosomal peptide synthetase
110.	NSAID	Non steroidal anti-inflammatory drugs
111.	O_2	oxygen
112.	$\cdot O^{2-}$	Superoxide anion
113.	·OH	Hydroxyl radical
114.	OD	Optical Density
115.	PAICS	Phosphoribosyl aminoimidazole succinocarboxamide synthetase
116.	PCR	Polymerase chain reaction
117.	PDA	Potato dextrose Agar
118.	PDB	Potato dextrose Broth
119.	PEG	Polyethylene glycol
120.	PEP	Phosphoenol pyruvate
121.	pH	Pouvoir hydrogen or Power of Hydrogen
122.	Phy	Phenylalanine
123.	PK	Pyruvate kinase
124.	PKS	Polyketide synthase
125.	PNJ	Profile neighbour joining
126.	PNP	Purine nucleoside phosphorylase
127.	PPAT	PRPP amidotransferase
128.	PPi	Pyrophosphatase
129.	PRA	5-Phosphoribosylamine
130.	PRPP	Phosphoribosyl pyrophosphate
131.	QSAR	Quantitative structure activity relationship
132.	R5P	Ribose-5-phospahte

133.	RB	Richard's broth
134.	RBOH	Respiratory burst oxidative homolog
135.	rDNA	Ribosomal DNA
136.	R_f	Retention factor
137.	RNA	Ribonucleic acid
138.	RNase	Ribonuclease
139.	ROS	Reactive oxygen species
140.	rpm	Revolutions per minute
141.	RyR	Ryanodine receptor
142.	SAICAR	N-Succinocarboxyamide-5-aminoimidazole ribonucleotide
143.	SAM	S-adenosyl methionine
144.	SCAR	severe cutaneous adverse reactions
145.	SD	Standard deviation
146.	SDW	Sterile distilled water
147.	SEM	Scanning electron microscopy
148.	SJS	Stevens – Johnson syndrome
149.	SmF	Submerged fermentation
150.	SNA	Synthetischer nahourstoffarmer agar
151.	SR	Sarcoplasmic reticulum
152.	SRL	Sisco research laboratories
153.	SSF	Solid state fermentation
154.	sUA	Serum uric acid
155.	SURI	selective uric acid re-absorption Inhibitor
156.	T2DM	Type 2 diabetes mellitus
157.	TAE	Tris acetate EDTA
158.	TCA	Trichloro acetic acid
159.	THF	Tetrahydrofolate
160.	TLC	Thin layer chromatography
161.	TOF MS	Time of flight mass spectrometry
162.	Tris	Tris(hydroxymethyl)aminomethane
163.	TSB	Tryptone soya broth
164.	UF-UPLC-MS	Ultrafiltration ultra-performance liquid chromatography mass spectrometry
165.	ULT	Urate lowering therapy
166.	URAT 1	Urate re absorption transporter 1
167.	US	United states
168.	USA	United states of America
169.	USFDA	United States Food and Drug Administrations
170.	UV	Ultraviolet
171.	V_{max}	Maximum velocity
172.	VOCs	Volatile organic compounds
173.	WA	Water agar
174.	WHO	World Health Organization
175.	XMP	Xanthosine monophosphate
176.	XO	Xanthine oxidase

177.	XOI	Xanthine oxidase inhibitor
178.	YEPB	Yeast extract peptone dextrose broth
179.	$ZnSO_4$	Zinc sulphate

Executive Summary

The present study was oriented towards the exploration of xanthine oxidase inhibitory potential of fungal endophytes isolated from Indian medicinal plants inhabiting biodiversity hotspots of India. Of 181 endophytic isolates, culture filtrates of 38 isolates were found to exhibit XO inhibitory activity over xanthine-NBT agar plate preliminary assay. Both the quantitative assays indicated ten fungal isolates to be potent producers of xanthine oxidase inhibitory entities. The crude chloroform residue of endophytic fungal isolate, #1 CCSTITD was found to be non-purine in nature and exhibited maximum XO inhibitory activity with IC_{50} of 0.54 µg/ml which was better than positive control Allopurinol (IC_{50}- 0.93 µg/ml). The potential endophytic fungus was identified using morphological and molecular tools as novel Muscodor species named as *Muscodor darjeelingensis*. Further, the crude chloroform residue of *M. darjeelingensis* was fractionated into 18 major fractions using TLC and column chromatography.

The fraction 9 was found to exhibit mixed type XO inhibitory potential with K_i value of 17.54 µM which was quite close to the febuxostat (K_i- 14.5 µM). The fraction 9 was pale yellow in color, light sensitive, slightly polar having a melting point >200 ˚C. H^1-NMR and C^{13}-NMR spectra of bioactive fraction 9 suggested it to be a long chain unsaturated, hydroxylated terpenoid. Further, IR spectra confirmed the presence of carboxyl group. Mass spectra of bioactive fraction showed parent ion peak at *m/z* 569 and molecular ion peak at *m/z* 553. The NMR, IR and ESI-MS spectral data of bioactive fraction 9 was found to be identical to that of dihydroxy-carotenoid Lutein. Hence, the bioactive fraction was proposed to be Lutein. This is the first report of a plant carotenoid being produced by an endophytic fungus which is also a potent XO inhibitor. The present study establishes that endophytic fungi are prolific sources of novel non-purine selective inhibitors of xanthine oxidase (NP-SIXO's). The isolation of Lutein, as XO inhibitor from endophytic fungi further warrants its further evaluation by *in silico* docking studies and optimizing using QSAR (Quantitative Structure Activity Relationship) for its development into a pharmacophore in management of long term hyperuricemia and oxidative stress related diseases since lutein is already being used as a nutraceuticals.

Chapter 1

Introduction

1.0 Background

Purines (adenine and guanine) are a series of heterocyclic compounds which are diversely substituted in the nature, abundantly found in the mammalian cells. Functionally, purines are responsible for biosynthesis of nucleic acids i.e. DNA and RNA apart from playing a crucial role in the intracellular signaling and cellular energy in the form of Adenosine Triphosphate (ATP) and Guanosine Triphosphate (GTP). The purines are also incorporated in the formation of complex molecules such as NADH and Coenzyme A (Pedley and Benkovic, 2016). The purine metabolism is tightly regulated and can be divided into three pathways. The first pathway is the biosynthetic pathway or the *de novo* pathway which begins with Phosphoribosyl pyrophosphate (PRPP) and leads to the formation of Inosine monophosphate (IMP), a precursor of AMP (adenosine monophosphate) and GMP (Guanosine monophosphate). The second pathway is also known as catabolic pathway wherein AMP, GMP and IMP are converted into Uric acid (7,9-dihydro-1H-purine-2,6,8(3H)-trione), a poorly soluble compound and tends to crystallize once the serum uric acid (sUA) level rises over a concentration of 6.5-7 mg/dl. The third pathway is the salvage pathway wherein IMP, GMP and AMP are synthesized from the purine bases i.e. Hypoxanthine, Guanine and Adenine respectively (Van der Berghe et al., 2006). Thus, it can be easily realized that any disturbance in these metabolic pathways will lead to clinical consequence (Fig. 1.1).

Hyperuricemia is a biochemical abnormality which occurs when the sUA level is higher than 7 mg/dl (Shi et al., 2003). Exogenous pool of purine as well as endogenous purine catabolism primarily contributes to the sUA level. Hyperuricemia generally results due to overproduction of uric acid or under excretion of uric acid by the kidneys. However, the latter case is predominantly responsible for the occurrence of hyperuricemia (Liote, 2003).

Hyperuricemia has already been established to be a pre-disposing factor for gout (Billet et al., 2014). However, recently after understanding the pathophysiology of uric acid accumulation, hyperuricemia has also been incriminated in diseases such as hypertension, type 2 diabetes, metabolic syndrome, renal and cardiovascular diseases (Gliozzi et al., 2016). Uric acid accumulation

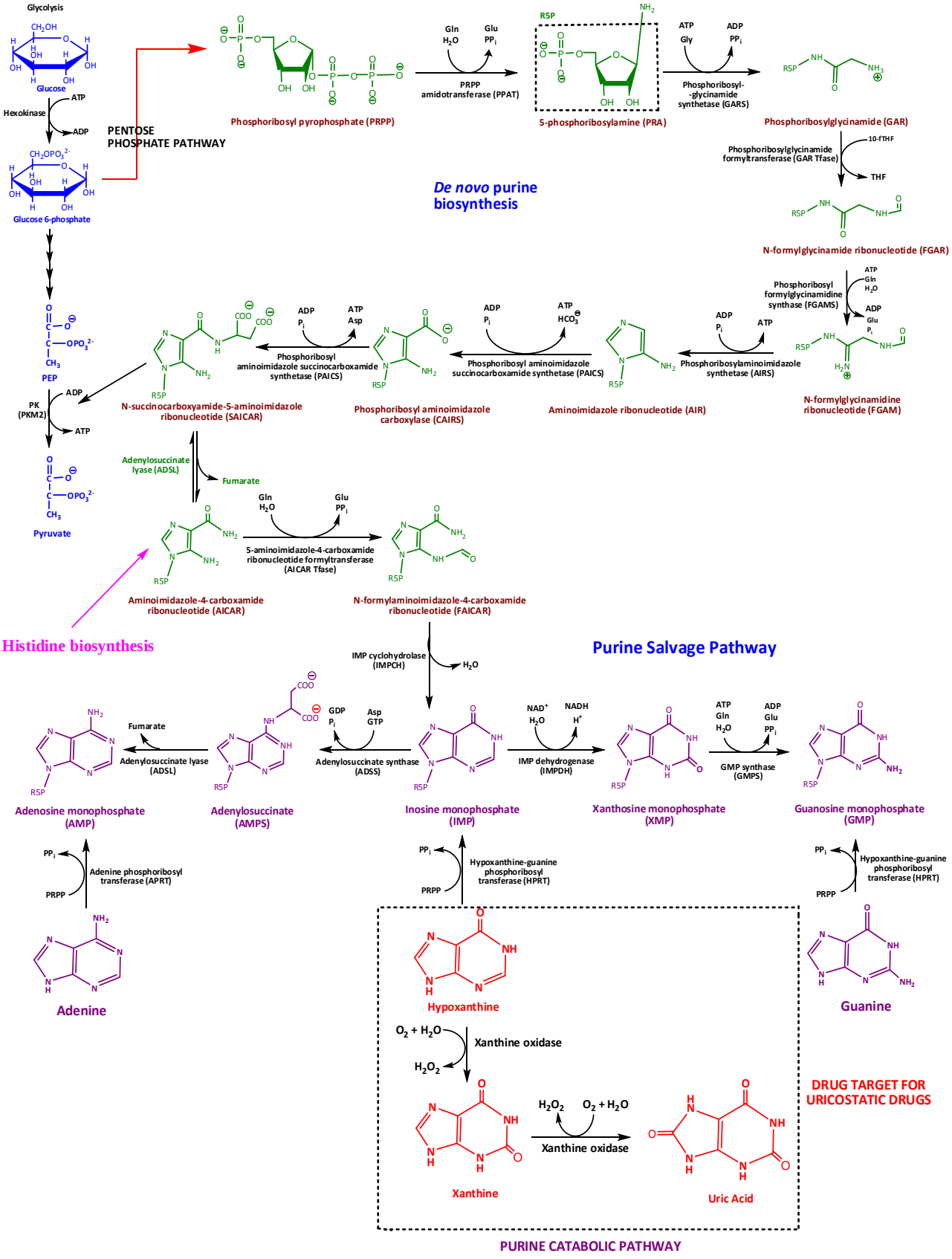

Fig 1.1 Purine metabolic pathways and their cross link with other metabolic pathways.
(PK- Pyruvate kinase, Gln- Glutamine, Glu- Glucose, PP_i- pyrophosphate, THF- tetrahydrofolate, 10-fTHF- 10-formyltetrahydrofolate, Asp- Asparagine, H_2O_2- hydrogen peroxide)

beyond physiological limits, i.e. hyperuricemia is responsible for fat storage in adipose tissue as well as in liver (Lanaspa et al., 2012a; 2012b). One of the earliest associations of hyperuricemia is with hypertension (Cannon et al., 1966). There is ample literature which provides epidemiological evidence that hyperuricemia is present in type 2 diabetes as well as predicts the development of insulin resistance and type 2 diabetes (Johnson et al., 2013b). It has been observed that the patients with established coronary heart disease have increased concentration of plasma uric acid as compared to those who are healthy. Further, it has been reported that the increased plasma uric acid is associated with increased risk of incident coronary heart disease (Wheeler et al., 2005). It has also been hypothesized that uric acid overproduction/accumulation can trigger oxidative stress and the enzyme xanthine oxidoreductase (XO), which is responsible for urate formation and plays a critical role in this context (Agarwal et al., 2011; Puddu et al., 2012).

First line treatment of chronic hyperuricemia (long term therapy) is based on lowering the sUA into normal physiological range and this is referred as urate lowering therapy (ULT). Long term management of hyperuricemia generally targets the key enzymes which are responsible for metabolism and excretion of sUA i.e. XO and Uric Acid Transporter 1 (URAT1) respectively. There are two main classes of drugs used for ULT- Uricostatics and Uricosurics. Uricostatic drugs inhibit the enzyme XO which plays a key role in the production of uric acid from purines while the uricosurics increases the urinary excretion of uric acid by blocking the renal tubular re-absorption of uric acid (Suresh and Das, 2012). The United States Food and Drug Administration (USFDA) approved uricostatic drugs are Allopurinol and Febuxostat. The first uricosuric developed was Probenecid, however it was withdrawn in USA due to its side effects. Uricosurics which are generally used outside USA comprise of Sulfinpyrazone, Probenecid and Benzbromarone.

USFDA has recently approved Lesinurad as a selective uric acid re-absorption Inhibitor (SURI) (Fleischmann et al., 2014). Allopurinol (analog of hypoxanthine) has been the cornerstone of urate lowering therapy for over five decades. It gets converted into oxypurinol which competitively binds XO, thereby, inhibiting the production of uric acid. Allopurinol also has direct scavenging effect on

free radicals. However, prolonged use of allopurinol in some individuals results in Allopurinol Hypersensitivity Syndrome (AHS), currently known as Drug Rash with Eosinophilia and Systematic Symptoms (DRESS) which at times can be fatal with a mortality rate of ~20% (Yaylaci et al., 2012). Allopurinol also has dose related and idiosyncratic side effects in patients with renal impairment.

Febuxostat was approved by USFDA in 2009 as a non-purine selective inhibitor of XO (NP-SIXO) which undergoes hepatic metabolism. Febuxostat has a better efficacy and low dose regimen as compared to allopurinol, being a selective inhibitor of XO. It is also less toxic as compared to allopurinol and is used on patients with mild to moderate renal impairment since the drug is metabolized in liver. However, the commonly reported adverse reactions of the drug are abnormality in liver function, diarrhea, headache, nausea and rash (Gliozzi et al., 2016).

Despite febuxostat and allopurinol being commonly recommended for gout therapy, clinical studies have shown that the effective reduction of sUA to < 6 mg/dl in case of allopurinol is in the range of 20-40 % while for febuxostat is 45-67 % thus indicating the need of additional therapies or new drugs in long term management of hyperuricemia and gout. This has led to a renaissance in the area of pharma gout research. As per GlobalData, the acute gout market size is going to increase to US$ 337 million by 2018 and the chronic gout market comprising of prophylactic anti-inflammatory therapies and urate lowering therapy is going to reach over US$ 1.9 billion (GlobalData, 2016).

XO has been recognized as a key enzyme responsible for uric acid production, apart from its role in inducing oxidative stress in mammalian system. During the production of uric acid, the XO has been found to produce reactive oxygen species (ROS). ROS have been found to play an important role in cell signaling and likely act as key players in many diseases and homeostasis. ROS generated by XO oxidize the cellular proteins and membranes resulting in myocardial cellular injury (Thompson-Gorman and Zweier, 1990). XO has been found to be expressed by failing heart where it uncouples the cardiac energy consumption from cardiac contraction in setting up chronic heart failure (Sesh et al., 2015; Raghuvanshi et al., 2007; Pandey et al., 2000). Hyperuricemia appears to be surrogate biomarker for high levels of damaging oxidative stress associated with increased XO activity. Hence,

XO inhibition using uricostatic drugs represents a therapeutic approach which will have dual benefit, reduction in circulating uric acid as well as reducing vascular oxidative stress. Therefore, XO inhibitors (XOI's) also appear to be an emerging class of drugs for heart failure apart from their potential use in hyperuricemia management (Kittleson and Hare, 2005; Higgins et al., 2011).

1.1 Bio-prospecting for new Xanthine oxidase inhibitors (XOI's)

The currently used uricostatic drugs, allopurinol and febuxostat are predominantly synthetic compounds. Allopurinol is an analog of hypoxanthine which inhibits XO, while febuxostat is a 2-aryl thiazole based (non-purine) compound which has been chemically synthesized and tested for use as a potent XOI by Tejin Pharmaceuticals, Japan. Nature has been a brilliant chemist providing a variety of chemical templates which have been exploited by the medicinal chemists and pharmacologists in developing potent drugs for treatment of various diseases.

The folklore medicine began with the discovery of medicinal properties of plants and their extracts where further isolation of bioactive moieties and their evaluation formed the basis of modern medicine. Isolation of morphine from *Papaver somniferum* in 1806 marked the beginning of early chemotherapeutics in modern medicine. Modern pharmacology is highly dependent on plant based drugs. Natural compounds resourced from plants could be directly used as drugs, precursors for semi-synthetic drugs or as templates for the design of novel synthetic agents. Thus, natural product research is an integral part of pharmaceutical drug discovery programs.

Seed extracts of *Cassia fistula*, *Swietenia mahagoni* and *Erythrina indica* exhibited potential inhibition of XO (Jothy et al., 2011; Sahgal et al., 2009; Sowndhararajan et al., 2012). A vast literature abounds wherein different plant extracts have exhibited *in vitro* XO inhibition (Umamaheswari et al., 2007; Hudaib et al., 2011). Several phytochemicals such as Liquiritigenin, Isoliquiritigenin (Kong et al., 2000b), cinnamaldehyde (Wang et al., 2008) and hesperidin (Liu et al., 2016) have been found to be potent xanthine oxidase inhibitors. One compound which has been approved as an uricostatic drug by USFDA in 2009 is Colchicine, isolated from the plant *Colchicum autumnale.* Traditionally, this plant has been used to treat rheumatic conditions especially gout. Colchicine is currently

recommended for acute gout flares and prophylaxis for gout flares (Zhang and Zhang, 2016). However, the major issues with plant extracts is their standardization and for phytochemicals is their bulk requirement which cannot be resourced from plants since they are generally present in low concentration and would lead to massive annihilation of the flora and biodiversity.

Microorganisms have been long recognized by the pharmaceutical industry as a prolific source of structurally diverse secondary metabolites which have propelled the discovery of numerous antibiotics beginning with the discovery of the miracle drug Penicillin (Demain, 2009). Apart from antibiotics, microbial natural products have also been exploited in the development of immunosuppressive, hypocholesterolemic, anti-parasitic, anti-cancer and anti-diabetic drugs (Demain, 1999; Berdy, 2005; Demain and Sanchez, 2009). 5-formyluracil from *Streptomyces sp.* and *Bacillus cereus* (Umezawa et al., 1972; Sunahara et al., 1977), Akalone and Hydroxyakalone isolated from marine bacterium, *Agrobacterium auranticum* N-81106 were reported to be potent XO inhibitors (Izumida et al., 1995; 1997).

1.2 Fungi as a source of XOI's

Fungi have been intensively explored for bioactive secondary metabolites for pharmaceutical drug discovery ever since the discovery of penicillin. Novel therapeutic moieties which have been discovered from fungi and subsequently deployed in pharmaceutical industry as antibacterial agents like Cephalosporins, immunosuppressive agents such as cyclosporine and cholesterol lowering agents such as Mevastatin and Lovastatin. Various wild and edible mushrooms are reported to be producers of XO inhibitors. Methanolic and aqueous extracts of *Pleurotus citrinopileatus* (Alam et al., 2011a), *Pleurotus salmoneostramineus* (Alam et al., 2011b), *Pleurotus cornucopiae* (Alam et al., 2011c), *Pleurotus nebrodensis* (Alam et al., 2011d) and *Lentinus edodes* (Yoon et al., 2011a) are found to possess remarkable XOI potential.

Approximately 20 % of fungi are obligate symbionts in lichens which have been overlooked by mycologists as well as industrial microbiologists despite the fact that lichen and lichen products have been used in traditional medicines since centuries and still hold considerable interest in

alternative treatments in various parts of the world (Crittenden and Porter, 1991; Boustie and Grube, 2005). Various species of lichens have been bio-prospected in search of novel xanthine oxidase inhibitors. Thallus extract of foliose lichen *Bulbothrix setschwanensis* was found to exhibit profound xanthine oxidase inhibitory activity (Behera and Makhija, 2002). *Graphina pyrrhocheiloides* thallus extract exhibited 41 % inhibition in XO activity (Behera et al., 2004).

1.3 Fungal endophytes: A promising resource of XOI

Fungi ubiquitously exist within the plants i.e. internally without any apparent signs of their existence and are known as endophytes (Schulz and Boyle, 2006). In contrast to their pathogenic fungal counterparts, the endophytic fungi exist in a mutualistic association with their host plants, and in few cases, enhance the ability of plants to tolerate abiotic and biotic stresses (Rodriguez et al., 2009; White and Torres, 2010; White and Bacon, 2012). Discovery of *Taxomyces andreanae*, a taxol producing endophytic fungus from *Taxus brevifolia* (Stierle et al., 1993) embarked research on fungal endophytes as producers of phytochemicals similar to their host plants (Strobel et al., 2004).

It has been amply demonstrated that the endophytic fungi possess the capacity to biosynthesize the host metabolites like Podophyllotoxin, Camptothecin and Huperzine, therefore, they promise to be an alternative source of secondary metabolites known from plants (Aly et al., 2010; Kaul et al., 2012; Aly et al., 2013; Nisa et al., 2015; Venugopalan and Srivastava, 2015). However, endophytic fungi have also been reported to be lucrative sources of novel organic compounds possessing anti-cancer, anti-microbial, neuroprotective and anti-oxidant properties since last two decades and many compounds have entered into clinical studies (Gunatilaka, 2006; Suryanarayanan et al., 2009; Baker and Satish, 2012; Newman and Cragg, 2015; Muller et al., 2016).

Plants in tropical rainforests are exposed to different biotic as well abiotic stresses and therefore endophytes existing within them are metabolically active in biosynthesizing myriad chemical structures which could possess novel bioactivities. Enzymes have been recognized as potential drug targets for the treatment of several diseases and therefore molecules which inhibit their activity could be effectively used as drugs. Several enzyme inhibitors have been reported to be

produced by endophytic fungi. Khafrefungin which inhibits phosphoceramide synthase has been exploited for treatment of drug resistant infections caused by *Candida albicans* since this molecule does not interfere with human sphingolipid metabolism (Mandala et al., 1997). Cytonic acids A and B isolated from endophytic fungus *Cytonaema* sp. are found to inhibit human cytomegalovirus protease (Guo et al., 2000). More recently, a cholinesterase inhibitor has been isolated from endophytic *Alternaria alternata* (Bhagat et al., 2016). Leptin inhibitors have also been isolated from endophytic fungi for their possible use as anti-obesity agents (Chandra Mouli et al., 2016). Nectriacids B and C have been isolated from endophytic *Nectria* sp. of Mangrove plant *Sonneratia ovate* and are found to inhibit α-glucosidase activity for possible use as an anti-diabetic agent (Cui et al., 2016).

However, exploration of XO inhibitors from endophytic fungi is limited. Predominantly, the XO inhibitory activities of endophytic fungi have been correlated with their anti-oxidant activity. Fusaruside is an XO inhibitory cerebroside which has been isolated from *Fusarium* sp. IFB-121, an endophytic fungus in *Quercus Variabilis* (Shu et al., 2004). Similarly, Endophytic *Chaetomium* sp. obtained from aerial tissues of *Nerium oleander* L (Apocyanaceae) produced phenolic compounds exhibiting XO inhibition (Huang et al., 2007a). Rubrofusarin B and Auraseprone A obtained from the culture of *Aspergillus niger* IFR-E003, an endophytic fungus harboring in the well growing leaves of *Cynodon dactylon* showed XO inhibitory activity (Song et al., 2004). Lumichrome, a compound isolated from the ethyl acetate extract of liquid culture of endophyte *Myrothecium roridum* IFB-E012 in *Artemisia annua* exhibited cytotoxicity against the human tumor cell line nasopharyngeal epidermoid KB and inhibition activity against XO (Shen et al., 2009). An endophytic fungal strain, *Alternaria brassicicola* (ML-P08), was isolated from the fresh leaves of *Malus halliana* has been found to produce two compounds named Alternariol and Alternariol monomethyl ether showing strong XO inhibitory activity (Gu et al., 2009).

Thus, in the present work we have systematically screened endophytic fungi from the biodiversity hotspots of India for their potential to inhibit XO with a future implication of their

clinical evaluation in management of hyperuricemia as well as for prevention against chronic heart failure by reducing the oxidative stress which are two major health hazards worldwide, especially in India.

Chapter 2

Present Approach

Chapter 2

Plant microbiome comprises of microbial communities which can be classified as pathogens, epiphytes, saprophytes and endophytes. Endophytic fungi are phylogenetically diverse and large group of fungi which colonize internally without exhibiting any obvious signatures of their existence (Bacon and White, 2000; Strobel and Daisy, 2003). Endophytes differ from mycorrhizal fungi by the fact that they reside entirely within the plant tissues (Stone et al., 2004). It has been reported that all terrestrial plants are colonized with endophytic fungi (Arnold and Lutzoni, 2007). Endophytic fungi trace back their association with plants for over 400 million years (Krings et al., 2007) and have been studied in plants existing in various geographical and climatic zones (Sun and Guo, 2012).

Plant-fungus interaction is mediated by a variety of chemical/biochemical molecules which mediate the interactions to establish an association. This is referred to as “balanced antagonism”, a hypothesis which proposes how endophytic fungi avoids activating the host defense responses, ensures self-resistance prior to getting incapacitated by the toxic metabolites of the host thereby manages to grow within host without causing the visible manifestation of infection or disease (Arnold, 2005; 2007; 2008; Schulz and Boyle, 2006).

Fungal endophytes have been effectively used for improving growth, health and adaptation of plants to stress conditions and therefore hold promise for agriculture and horticulture (Singh et al., 2011; Iqbal et al., 2013; Card et al., 2015; Wani et al., 2015; Rai and Agarkar, 2014). There are several reviews which highlight the potential to overcome biotic and abiotic stresses by fungal endophytes (Rodriguez et al., 2008; Aly et al., 2011; Porras-Afarno and Bayman, 2011; Friensen, 2013; Johnson et al., 2013a). Exploring biosynthetic capabilities of fungal endophytes has gained impetus owing to ever increasing discovery of fungal endophytes synthesizing plant compounds such as Paclitaxel, Camptothecin, Podophyllotoxin and Hypericin (Stierle et al., 1993; Puri et al., 2006; Kusari et al., 2009b; Shweta et al., 2010). Apart from their biosynthetic potential to synthesize putative phytochemicals,

endophytes are a lucrative source of bioactive secondary metabolites which have agrochemical as well as pharmaceutical applications (Chen et al., 2016; Strobel, 2015).

Biosynthesis of these novel chemistries by endophytic fungi is a result of their cross-talk with the host defense and other biotic/abiotic stresses as propounded in the balanced antagonism hypothesis. The endophyte derived compounds belong to diverse chemical classes such as terpenoids, steroids, xanthones, chinones, phenols, isocoumarins, benzopyrans, cytochalasins etc. It has been estimated that more than 51 % of the bioactive compounds isolated from endophytes are novel structures or chemical templates (Firakova et al., 2007).

As it has been proved that endophytic fungi are fountainheads of novel bioactive compounds possessing anti-microbial, anti-cancer, anti-oxidant, anti-parasitic, anti-viral, insecticidal and immunomodulatory activities for possible use in pharmaceutical and agrochemical industries (Aly et al., 2010; Kaul et al., 2012; Elsebai et al., 2014), the present work was therefore oriented towards exploring fungal endophytes for bioactive compounds which could inhibit the enzyme Xanthine Oxidase (XO), a key molecule in uric acid formation apart from being a key player in inducing cellular oxidative stress.

2.1 Hypothesis

Aerobic metabolism results in the production of reactive oxygen species (ROS) which comprises of superoxide anion ($\cdot O_2^-$), hydroxyl radical ($\cdot OH$) as well as non-radical molecules like Hydrogen peroxide (H_2O_2), singlet oxygen (O_2) etc. ROS have been found to be associated with most processes in plant development and acclimatization. They are usually generated in various sub-cellular components such as chloroplasts, mitochondria and peroxisomes as well as in the cellular environment. ROS play a dual role- beneficial as well as harmful which depends upon their concentration inside the plants. More recently, ROS have been implicated in generation of systematic whole plant signals in response to biotic and abiotic stresses.

Generation and quenching of ROS is strictly balanced to avoid the oxidative stress in all living systems. However, when the level of ROS exceeds the defense mechanism, the cell is said to be in a state of "Oxidative Stress". ROS scavenging is perturbed under a number of stressful conditions such as salinity, drought, metal toxicity and pathogens etc. ROS generating enzymes such as Respiratory Burst Oxidative Homolog (RBOH) of NADPH oxidase has demonstrated that plant cells like mammalian cells can initiate and amplify ROS production for signaling. RBOH has been recognized as central hub of cellular ROS signaling network (Sierla et al., 2016; Gilroy et al., 2016). More recently, Xanthine dehydrogenase has also been implicated in this systematic response (Ma et al., 2016).

In fungal system, xanthine oxidase has been found to be localized in the cytoplasmic membrane in close association with cell membrane lipids and inward cell wall protruding lipids. It has been well documented that the hydrophobic nature of XO drives its association over membrane or fat globule (Bruder et al., 1982; Cheng et al., 1988). The ROS produced by membrane bound XO was found to exhibit key role in sclerotial differentiation and phytopathogenic potential (Papapostolou and Georgiou, 2010). It has also been implicated that asymptomatic fungi can produce anti-oxidants in response to both biotic/abiotic stresses when grown in culture as well as *in planta.* There are a variety of anti-oxidants originating from fungal endophyte mediated host metabolism (Hamilton et al., 2012).

Hence, it is hypothesized that during plant-endophytic fungal interaction, endophytic fungi secrete certain molecules that neutralize the oxidative attack of plant XO which may be helpful in developing a symbiotic association. Thus, these inhibitors of plant oxidases could also be used as inhibitors of oxidases of mammalian origin. Based on the above premise, the present work is oriented on screening endophytic fungi for XO inhibitors with the following objectives:

I. Isolation and characterization of Xanthine oxidase inhibitor(s) producing endophytic fungi
II. Characterization of xanthine oxidase inhibitors from potential endophytic fungi
III. To study the Inhibition kinetics of selected XOI

Chapter 3

Review of Literature

3.1 Background

Purines are the ubiquitous component of life, performing many important functions at the cellular level. They are considered to be major energy carriers and precursors for the synthesis of nucleic acids (DNA and RNA). Despite being structural components of nucleotide cofactors such as Nicotinamide adenine dinucleotide (NAD) and S-Adenosyl methionine (SAM), purines are reported to perform vital role in the physiology of muscles, thrombocytes and synaptic transmission (Maiuolo et al., 2016). Under physiological environment, the enzymes involved in the purine metabolism maintain equilibrium between synthesis and degradation of purines. However, nucleic acid turnover (synthesis and degradation) is an ongoing metabolic process which liberates free purines in the form of adenine, guanine and hypoxanthine. These free purine counterparts are considered to be metabolic investment of the cells for development, proliferation and survival. In humans, uric acid is the final end product of purine catabolism and is primarily produced by oxidative degradation of hypoxanthine to xanthine and xanthine to uric acid which is catalyzed by the enzyme XO (Fig 3.1). All other mammals possess the uricases enzyme involved in conversion of uric acid to allantoin that is eliminated through urinary excretion (Sundy and Hershfield, 2007).

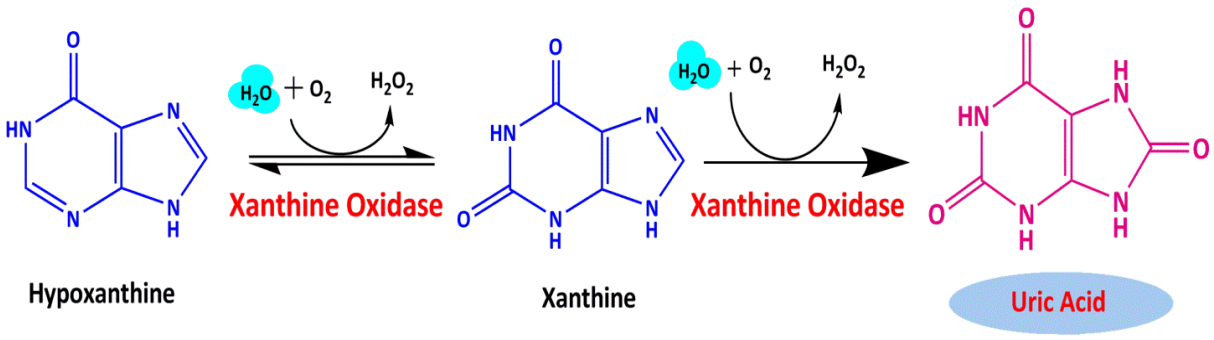

Fig 3.1: Reaction catalyzed by Xanthine oxidase in purine catabolic pathway

The major disorders of purine degradation are either due to block or increased degradation of purines. In the former i.e. during the block in purine degradation, syndromes like immune deficiency, myopathy or renal calculi may occur while enhanced purine degradation leads to syndromes like hyperuricemia and gout, renal calculi, anemia and hypoxia apart from oxidative stress (Lomax et al., 1975). The block in the purine catabolism is generally attributed to deficiency or

malfunction of some important enzymes such as 5'-nucelotidase, adenosine deaminase, purine nucleotide phosphorylase (PNP), myoadenylate deaminase, XO deficiency and guanine deaminase deficiency. While increased purine nucleotide degradation may occur via different pathways which may alter the regulated pathway. Hence, if the purine catabolism pathway is not blocked, it shall lead to enhanced uric acid biosynthesis which will clinically result in hyperuricemia, hyperuricosuria and gout (Fox, 1981; Nyhan, 2005; Jiao et al., 2006).

3.2 Hyperuricemia: the underlying cause of Gout

Hyperuricemia is a biochemical abnormality characterized by elevated sUA level exceeding above the normal threshold limit of 6.8-7.0 mg/dL. Epidemiological association between hyperuricemia and gout has been established over 150 years ago (Garrod, 1848; Campion et al., 1987). Recent studies have indicated an increasing prevalence of gout in the age group of 30-50 years (Kuo et al., 2015). Though main focus of global surveys has been gout, but the incidence of hyperuricemia has also increased accordingly as sustained hyperuricemia is a physiological pre-requisite for gout. There are four phases of gout- asymptomatic hyperuricemia, acute gouty arthritis, intercritical gout and chronic tophaceous gout (So and Thorens, 2010).

Diseases which are responsible for over production of urate include myeloproliferative disorders, lymphomas, exfoliative psoriasis and genetic diseases such as deficiency of Hypoxanthine guanine phosphoribosyl transferase (HGPRT) and in tumor lysis syndrome (Luk and Simkin, 2005). Dietary factors which contribute to hyperuricemia includes high alcohol intake which results in increased purine production and decreases urate excretion, consumption of purine rich foods such as red meat or sea food (Choi et al., 2004a; 2004b). Apart from being a physiological pre-requisite for gout, today hyperuricemia is responsible for a variety of metabolic and oxidative stress related diseases.

3.3 Hyperuricemia and other diseases

Numerous experimental as well as clinical studies provide sufficient evidence that hyperuricemia may play a role in development and pathogenesis of a number of metabolic, hemodynamic and

systemic pathological diseases comprising of metabolic syndrome, hypertension, stroke and atherosclerosis. It also plays a role in renal and endothelial dysfunction (Rahman et al., 2012).

Hyperuricemia has been identified as an early marker for hypertensive diseases (Ward, 1998) i.e. it predicts the development of hypertension and is associated with coronary artery disease (Tuttle et al., 2001) and cardiovascular mortality (Fang et al., 2000). Yet, another important pathogenic mechanism by which high concentrations of uric acid raised the blood pressure is by activation of NADPH oxidases in the cytoplasm as well as in mitochondrion. Thus blocking the oxidative stress could lower hypertension in hyperuricemic rat models (Yu et al., 2010; Lanaspa et al., 2012b). Initially, it was proposed that the high concentration of uric acid in the blood suppresses the insulin secretion and possibly exerts cytotoxic effect on the β- cells in pancreas (Scott et al., 1981). Today, there are numerous epidemiological evidences, which confirm the role of hyperuricemia in insulin resistance and type 2 diabetes (Mundhe and Mhasde, 2016; Shah et al., 2016). More recently, hyperuricemia has been found to be an independent predictor of coronary artery diseases (CAD) among Asian Indian subjects having type 2 diabetes (Jayashankar et al., 2016). It has also been reported that the hyperuricemia is associated with increased prevalence, incidence as well as disease severity of Non-alcoholic fatty acid liver disease (NAFLD) (Lonardo et al., 2002; Li et al., 2009). sUA has been used as a predictive biomarker to predict NAFLD (Ryu et al., 2011).

Recently, hyperuricemia has also been associated with the development of chronic kidney disease (CKD) by inducing renal inflammation, endothelial dysfunction and activation of the renin-angiotensin system (Mallat et al., 2016). High plasma uric acid has also been found to be associated with stroke risk factors in women (Jimenez et al., 2016). High levels of uric acid has also been identified as a marker for mortality and morbidity in Fabry's disease (an X-linked lysosomal storage disorder due to decrease or absence of α-galactosidase A (agalA) enzymatic activity, as a result of gene mutations), apart from adverse cardiac outcomes such as progression of left ventricular hypertrophy and progression of renal dysfunction (Rob et al., 2016). Thus, hyperuricemia or high uric

acid concentration is being implicated as the master conductor of the worldwide symphony of diabetes, obesity and cardio-renal diseases apart from gout (Kanbay et al., 2016).

3.3.1 Role of high XO activity

High concentrations of circulating XO have also been reported in patients suffering with hyperuricemia which is released by the damaged cells due to elevated level of uric acid in plasma. XO is a source of ROS and generates superoxide anion radicals. An elevated level of circulating XO is an important marker of hepatic as well as interstitial damage and is responsible for remote organ injury in several patho-physiological conditions such as hepatic ischemia and reperfusion, hemorrhagic attack and sickle cell disease (Houston et al., 1999; Aslan et al., 2001). It also plays a key role in vascular injuries, acute arthritis, chronic heart failure (CHF) and type 2 diabetes (T2DM) (Desco et al., 2002; Berry and Hare, 2004).

S-nitrosylation is a ubiquitous post-translational modification which is involved in the regulation of diverse biological processes. Ryanodine receptor (RyR) is an intracellular calcium channel present in excitable animal tissues such as the muscle and neurons. All the three isoforms of this receptor get S-nitrosylated and play a critical role in signaling responsible for metabolic events. It has been reported that hypernitrosylation of RyR1 leads to sarcoplasmic reticulum (SR) calcium leakage accompanied by skeletal muscle dysfunction. On the other hand, hyponitrosylation resulted in RyR2 leakage and decreased contractile reserve in the cardiomyocytes. Global S- nitrosylation was found to be decreasing in the failing hearts compared to non-failing. XO inhibition has been found to reverse or restore the global as well as RyR2 nitrosylation thereby reverting the SR Ca^{2+} leak and improving the calcium handling and contractility. Thus, nitroso- redox balance plays a critical role is heart failure (HF) by causing RyR2 oxidation, hyponitrosylation, and SR Ca^{2+} leakage. However, it has been experimentally demonstrated that the inhibition of XO is helpful in the reversal of this patho-physiological condition thereby reducing the oxidative stress on heart (Gonzalez et al., 2010).

It has been reported that oxidative stress i.e. the imbalance between the free radical levels and the anti-oxidant capacity plays a significant role in the cardiovascular disease and diabetes (Furukawa et al., 2004; Palmieri et al., 2006). ROS have also been implicated in the endothelial dysfunction in experimental atherosclerosis and also in patients with CAD. This basically occurs via the inactivation of endothelial NO (nitric oxide) by the superoxide radicals (White et al., 1996; Cai and Harrison, 2000; Heitzer et al., 2001; Spiekermann et al., 2003). It has also been demonstrated that the endothelial XO activity and protein levels are substantially increased in patients suffering from CAD or carotid stenosis (Berry and Hare, 2004; Guzik et al., 2006). More recently, the relationship between hyperuricemia and NAFLD has been attributed to XO which may be possibly used as a novel therapeutic target linking the two diseases possibly mediated via inflammasomes which are expressed due to hyperuricemia as a result of higher XO activity (Xu et al., 2015; Sun et al., 2016).

As XO plays a critical role in hyperuricemia as well as in host of oxidative stress related diseases, it can be a potent therapeutic target not only for the long term management of hyperuricemia but also for reducing the oxidative stress which is a hallmark of variety of metabolic/ oxidative stress related diseases including HF.

3.4 Therapeutic options for treatment of hyperuricemia

The main stay in successful long term management of hyperuricemia and gout is urate lowering therapy (ULT). The ULT is an effective anti-hyperuricemic alternative targeting uric acid excretion, production and degradation by utilizing uricosurics, xanthine oxidase inhibitors (XOI's) and uricases respectively (Fig 3.2).

3.4.1 Uricosurics

Uricosurics enhance the renal uric acid excretion by inhibiting the urate re-absorption by renal anion transporters in the proximal tubule. Probenecid was first FDA approved (1951) uricosuric drug for gout treatment followed by Sulfinpyrazone in 1959 (Gutman and Yu, 1951; Gutman, 1966). However, both probenecid and sulfinpyrazone caused nephrotoxicity among patients suffering with chronic

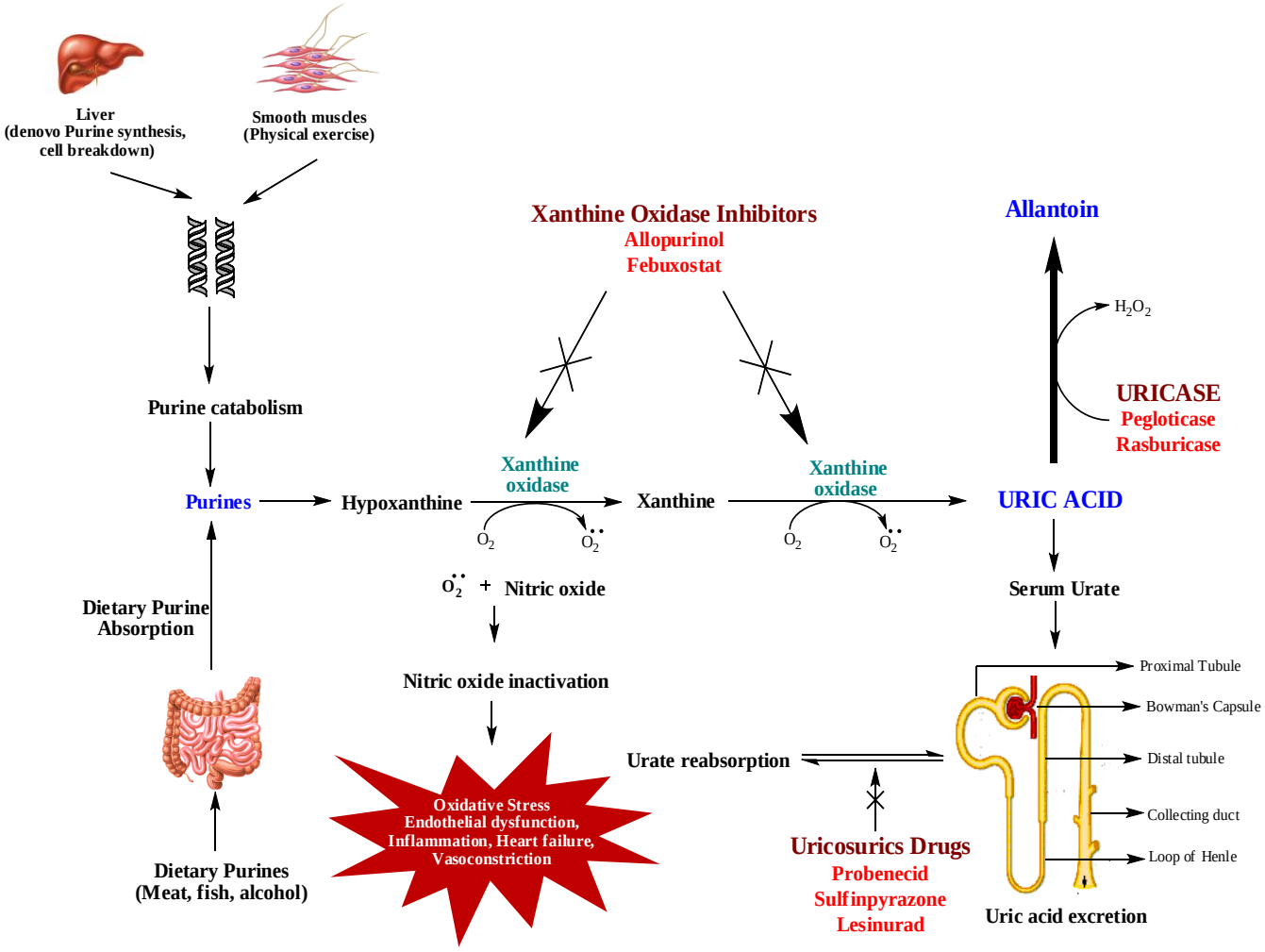

Fig 3.2: Sites of action of urate lowering drugs (ULT)- uricosurics, uricostatics and uricases.

renal insufficiency disorder. Moreover, probenecid was reported to alter the human metabolism by increasing the potency of other drugs such as penicillin, non-steroidal inflammatory drugs (NSAIDs), methotrexate by reducing the renal clearance efficacy (Burns and Wortmann, 2012). Benzbromarone, another uricosuric agent, never got approval from USFDA despite being far potent and well tolerated as compared to probenecid and sulfinpyrazone in patients with moderate renal insufficiency (Perez-Ruiz et al., 2000). However in France, benzbromarone was withdrawn in 2003 due to reports of fulminant hepatotoxicity among the population (Chaibriant, 2003).

Lesinurad is the newest molecule which has been approved by USFDA in 2015 for ULT in combination with an XOI for long term management of chronic hyperuricemia and gout (Fig 3.3). This molecule acts as an inhibitor of urate transporter URAT1 which is responsible for the renal re-

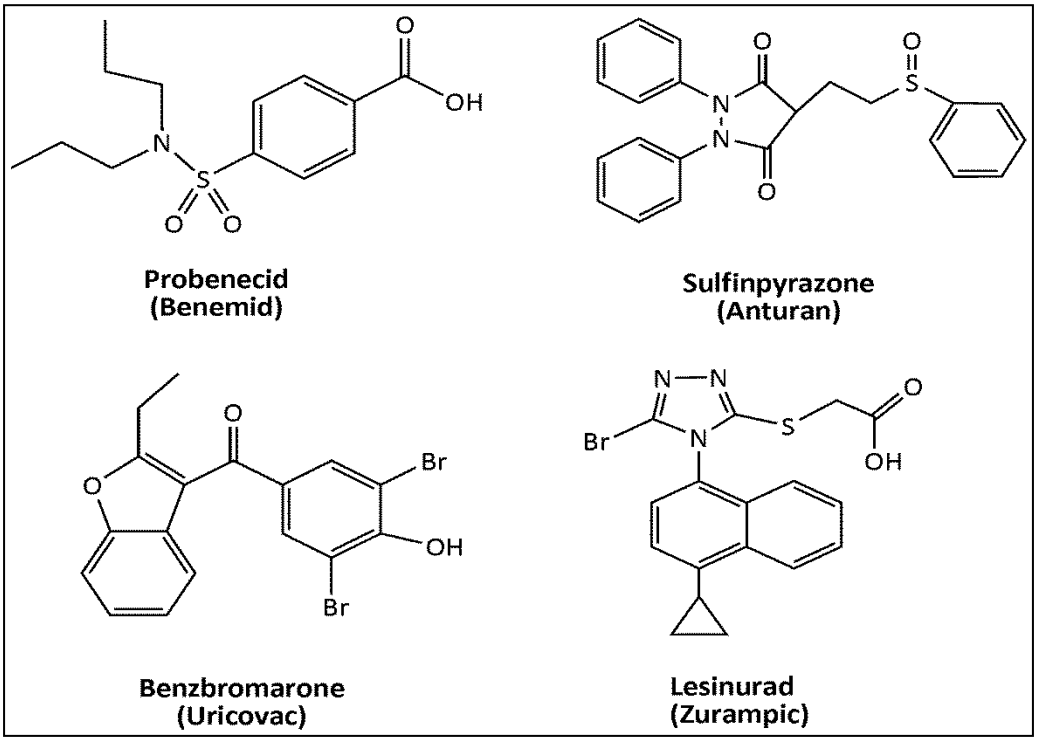

Fig 3.3: Various uricosuric agents used in ULT.

absorption of uric acid (So and Thorens, 2010; Bardin et al., 2016; Saag et al., 2016). The common side effects of Lesinurad (Zurampic®, AstraZeneca) includes headache, influenza, increases blood creatinine and gastroesophage reflux disease (GERD). However, if used without XOI it can result in acute kidney failure among patients (Hoy, 2016).

3.4.2 Uricostatics

XOI's block the xanthine oxidase catalyzed oxidation of hypoxanthine and xanthine to uric acid of purine metabolic pathway. The first XOI, allopurinol or 1,5-dihydro-4H-pyrazolo[3,4-d]pyrimidin-4-one), is a purine analogue which was approved by FDA in 1966 (Fig 3.4). Allopurinol was initially discovered in the drug discovery program of Burroughs Wellcome by Gertrude B. Elion and George H. Hitchings in 1963 (Elion, 1988; 1993). It rapidly gets oxidized to oxypurinol which acts as a suicide inhibitor of XO by altering the hydroxyl ligand of the molybdenum at the active site of the enzyme. Allopurinol is metabolized in the liver and has plasma half-life of 1-3 h, while oxypurinol is excreted in the urine and has 12–17 h half-life. Allopurinol has remained as the cornerstone of hyperuricemia management and gout therapy for over 40 years. However, continued use of allopurinol results in

acute problems like fever and rash to the gradually developing leukocytosis, eosinophilia, vasculitis, aseptic meningitis, nephritis, renal and hepatic dysfunction (Hande et al., 1984; Greenberg et al., 2001).

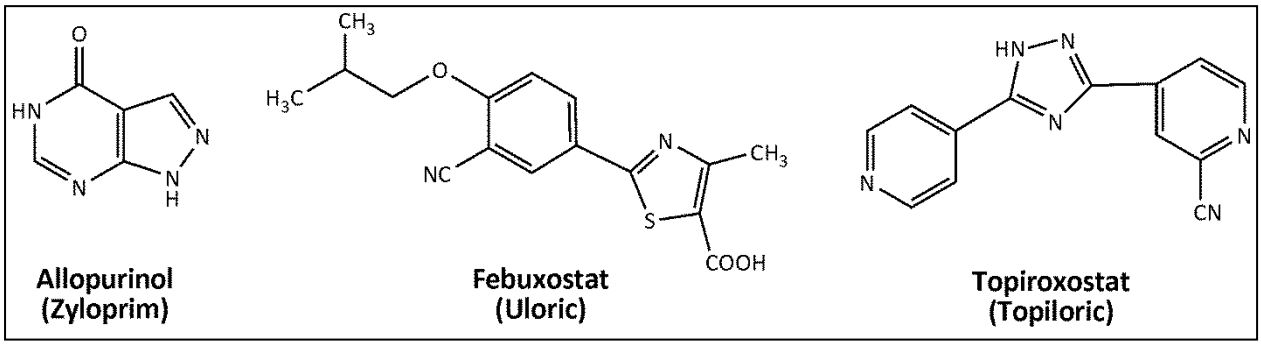

Fig 3.4: Currently used XO inhibitors

Allopurinol is an efficient drug; however, it is a weak inhibitor of XO in the *in vitro* assays with IC_{50} value ranging between 0.2 to 50 µM. Hence, research was fuelled to explore synthetic purine and pyrimidine compounds which exhibited better XO inhibition. The early research influenced by the success of allopurinol was focused on synthetic purines and pyrimidine derivatives. However, these did not meet the clinical structure since the purine and pyrimidine motifs induced a similar side effect as allopurinol. The synthetic purines and pyrimidine derivative so developed can possibly undergo conversion into corresponding nucleotides *in vivo* and may interfere with other pathways of purine metabolism thereby inducing severe adverse effects (Pacher et al., 2006)

Today, allopurinol should be tested prior to being recommended for therapeutic use as it may result in adverse reaction which can be fatal. This is attributed to presence of the HLA-B*58:01 allele and other factors that influence drug concentration. The adverse reactions of Allopurinol sensitivity may include maculopapular eruptions (MPE), severe cutaneous adverse reactions (SCAR), Stevens - Johnson syndrome (SJS), drug reactions with eosinophilia and systemic symptoms (DRESS) and the rare, but life-threatening, systemic manifestation, allopurinol hypersensitivity syndrome (AHS)(Stamp et al., 2016).

Hence, the focus of research shifted on development of non-purine based XO inhibitors for their possible role in long term hyperuricemia management as well as combating gout. Structure

elucidation of the XO led to rational drug discovery and many potent XOI belonging to steroids, imidazoles and triazoles derivatives, flavonoids and many other classes have been either synthesized or screened from natural product libraries (Borges et al., 2002). Two synthetic compounds viz. [2-[3-cyano-4-(2-methylpropoxy)phenyl)-4-methylthiazole-5-carboxylic acid], abbreviated as TMX-67, TEI-6720 and Y-700 [1-(-3-cyano-4-neopentyloxyphenyl)-pyrazole-4-carboxylic acid] were found to exhibit a more potent, selective XO inhibition, long lasting hyperuricemic control as compared to allopurinol with a favorable toxicological profile and high bioavailability (Becker et al., 2004).

TMX-67, TEI-6720 (Teijen Pharmaceuticals, Japan) successfully cleared the clinical trial and eventually was approved by USFDA in 2009 for treatment of chronic hyperuricemia and gout (Schumacher et al., 2009). Commercially this is known as Febuxostat with trade names Adenuric (Europe and New Zealand), Uloric (USA), Goturic (Latin America) and Feburic (Japan). With the development and deployment of Febuxostat, the first non-purine selective inhibitor of XO (NP-SIXO), it was clearly established that xanthine or purine like structural framework is not a pre-requisite for the development of potent XOI inhibitors.

CONFIRMS trial on over 2000 human subjects proved the superiority of Febuxostat (80 mg/day) over Allopurinol (300-800 mg/day) in long term ULT (Becker et al., 2010). Febuxostat is an excellent alternative for allopurinol sensitive patients suffering hyperuricemia with mild renal insufficiency (Faruque et al., 2013; Weng et al., 2016). Febuxostat has been reported to effectively control sUA and increase insulin sensitivity by reducing the HOMA-IR (Homeostasis Model Assessment of Insulin Resistance) index (Meng et al., 2016). It is implicated to reduce the renal oxidative stress and inhibition of profibrotic signaling (Tsuda et al., 2012; Komers et al., 2016). However, febuxostat has adverse effects also. The common adverse effects associated with febuxostat include diarrhea, dizziness, headache, liver abnormalities and altered thyroid function tests. A new XO inhibitor, Topiroxostat was approved and developed in Japan for treatment of hyperuricemia in 2013 (Matsumoto et al., 2011; Hosoya et al., 2014; Diaz-Torne et al., 2015).

Yet, another strategy to treat gout is enzymatic. It involves the use of uricases, a class of enzyme which converts uric acid into allantoin. As humans lack this pathway due to missense mutation in the uricase encoding gene (Wu et al., 1989), exogenous uricases have been developed as a therapeutic intervention to dissolve uric acid deposits. Rasburicase is a recombinant uricases cloned from *Aspergillus flavus*, approved for hyperuricemia due to tumor lysis syndrome in cancer patients (Kennedy and Ajiboye, 2010). However, the major drawback is the immunogenicity of the exogenous protein for which it has to be PEGylated. Pegloticase is a PEGylated mammalian (porcine-like) recombinant uricases approved by USFDA in 2010 for the treatment of chronic tophaceous gout (Baraf et al., 2008a; 2008b). However, despite specific prophylaxis, gout flares, infusion reactions and serious adverse effects were significantly more frequent in patients over pegloticase therapy. The ideal candidate for pegloticase therapy includes patients with tophaceous and persistent gout flares or arthropathic disorders who are intolerant to conventional ULT (Hamburger et al., 2010). Further, uricases do not demonstrate long term efficacy and sustainable tolerability in hyperuricemic patients (Richette et al., 2007). It also does not ameliorate oxidative stress conditions like XO inhibitors. Hence, XO inhibitors serve as key molecule of hyperuricemia management as well as oxidative stress related diseases.

3.5 Exploration of new XO inhibitors for ULT and related diseases

Today, XO is identified as a key molecule of purine catabolism and is constitutively being expressed in liver, kidney, epithelial lining of heart and brain. Being a hepatic enzyme, XO is also responsible for production of uric acid, nitric oxide and reactive oxygen species which potentially degrade DNA, RNA, protein, inhibit enzymatic systems and cause lipid per-oxidation (Freeman and Crapo, 1982; Meerson et al., 1982; Halliwell and Gutteridge, 1982). Further, ROS has been implicated in the endothelial dysfunction also. With excessive production of ROS due to over expression of XO, the activity of eNO (endothelial nitric oxide) is reduced which affects the production of NO (Higashi et al., 2009; Yang et al., 2009; Tousoulis et al., 2012; Higashi et al., 2014). Inhibiting XO is also a part of ULT for long term hyperuricemia management apart from its presumptive role in cardiovascular and

metabolic syndrome. As xanthine oxidase inhibition plays a plausible role in management of hyperuricemia and oxidative stress diseases like cardiovascular diseases, metabolic syndrome, so newer classes XO inhibitors are being explored to be used for management of oxidative stress related diseases as well as hyperuricemia.

Much emphasis is being laid on non-purine based selective inhibitors (NP-SIXO) as they do not lead to allele based hypersensitivity and adverse reactions as encountered in case of allopurinol which restricts its further use in long term hyperuricemia management. NP-SIXO's can be broadly classified as synthetic and natural product based. Presently approved NP-SIXO is Febuxostat 92-(3-cyano-4-[2-methylpropoxyl] phenyl-4-methylthiazole-5-carboxylic acid) which was approved by USFDA as a second line treatment when allopurinol failed to manage hyperuricemia or the patients exhibit Allopurinol hypersensitivity syndrome.

3.6 Bio-prospecting Xanthine oxidase inhibitors (XOI's)

Nature is an excellent chemist and produces scaffolds which are beyond the imagination of synthetic organic chemists. Thus it become pertinent to explore plants and microbes for the presence of bioactive compounds which could selectively inhibit XO for developing novel drugs to combat oxidative stress related disorders and chronic hyperuricemia.

3.6.1 XO inhibitors from plants

The dependence of humans on plants and plant extracts to combat diseases began with the settlement of humans and taking up agrarian practices. According to World Health Organization (WHO), approximately 80 % of the world's population relies mainly on conventional medication for their primary health care and about 50 % of the drugs introduced to the market during the last 20 years are derived directly or indirectly from small biogenic molecules (Luo et al., 2014, Harvey et al., 2015; Amirkia and Heinrich, 2016). A comprehensive study of US Food and Drug Administration (FDA) approved drugs between 1981 and 2010 (Newman and Cragg, 2012; 2016; Cragg and Newman, 2013) revealed that 34 % of medicines that were based on small molecules were traced to or were inspired by natural products including the statins, tubulin-binding anticancer drugs and immunosuppressant's.

Table 3.1: Xanthine oxidase inhibitors from plants

Name of Compound/Drug	**Host Plant**	**Class of compound**	**Reference**
Valoneic acid dilactone	*Lagerstroemia speciosa*	Lactone	Unno et al., 2004
Ellagic acid	*Lagerstroemia speciosa*	Lactone	Unno et al., 2004
Carallidin	*Carallia brachiata*	Proanthocyanidin	Phuwapraisirisan et al., 2006
Anacardic acid	*Anacardium occidentale L*	Phenolic lipid	Kubo et al., 2006
Apigenin-4'-O-(2"-O-p-coumaroyl)-β-D-glycopyranoside	*Pallhinhaea cernua*	Glycoside	Jiao et al., 2006
2-metylester-1-h-pyrrole-4-carboxylic acid	*Salacca edulis*	Pyrrole	Priyanto and Sukandar, 2007
Geraniin	*Phyllanthus urinaria*	tannin	Lin et al., 2008
Cinnamaldehyde	*C. osmophloeum*	Flavanoid	Wang et al., 2008b
Loniceraflavone	*Lonicera hypoglauca*	Flavanoid	Chien et al., 2009
Okanin	*Acacia confusa*	chalconoid	Tung and Chang, 2010
Mucusamide, Mucusoside	*Ficus mucuso*	sphingolipids	Gojayev et al., 2011
28-O-β-D-glucopyranosyl ester of platanic acid	*Tetracera scandens*	nor-lupane triterpene	Nguyen and Nguyen, 2013
Epihyprhombin B	*Hyptis rhomboides*	Neolignan	Tsai and Lee, 2014
Hyprhombin C	*Hyptis rhomboides*	Neolignan	Tsai and Lee, 2014
Riparsaponin	*Homonoia riparia*	Saponin	Xu et al., 2014
Heraclinin	*Tamus communis*	Furanocoumarins	Zerargui et al., 2015
Nudibaccatumin A and B	*Piper nudibaccattumin*	hydroxychavicol	Liu et al., 2015
Hesperetin	*Citrus auranticum*	Flavanone	Liu et al., 2016

Plants have been extensively explored for bioactive compounds which could be developed as potent and efficient XO inhibitors. Different phytochemicals from plants have been evaluated for the possible anti-oxidant as well as XO inhibitory activity (Table 3.1). These predominantly belong to phenolics and flavonoids (Lespade and Bercion, 2010). It has been reported that among flavonoids,flavones exhibited a higher XO inhibition as compared to flavonols. Luteolin exhibited the least IC_{50} as XOI amongst a battery of plant flavonoids tested using allopurinol as standard. Flavonoid

derivatives are exhibiting a higher IC_{50} when compared to flavonoids. These have been classified into six groups based on their XO and superoxide scavenging potential (Cos et al., 1998). Some other flavonoids such as Chrysin, Kaempferol, myricetin and isorhamnetin have been found to exhibit mixed type XO inhibition (Nagao et al., 1999). Isoliquirigenin and Liquiritigenin have been identified as the main compounds present in the methanolic extract of *Sinofranchetia chinensis* stem and exhibiting XO inhibition with IC_{50} of 55.8 µM and 49.3 µM respectively (Kong et al., 2000b).

Biota orientalis is a chinese medicinal plant which has been used for gout, rheumatism, diarrhea and chronic tracheitis. Quercetin and rutin were identified as flavonoid constituents and exhibited hyperuricemic effects comparable to allopurinol (Zhu et al., 2004). Two iridoids namely specioside and 6-feruloylcatpol purified from the acetonic stem bark extract of traditional Indian medicinal plant *Stereopermum personatum* significantly inhibited XO with IC_{50} of 79.88 µM and 150.44 µM respectively (Kumar et al., 2005). Geraniin, a tannin purified from 70 % water-acetonic extract of *Phyllanthus winaria* showed a dose dependent XO inhibition with IC_{50} of 30.49 µM (Lin et al., 2008). Lithospermic acid isolated from *Salvia mitiorrhiza* has been found to competitively inhibit XO with an IC_{50} of 5.2 µg/ml (Liu et al., 2008). Hydroxychavicol, a phenolic compound from *Piper* plants displayed potent inhibitory activity against XO (Murata et al., 2009).

Extracts prepared from different parts of medicinal plants are the primary target of researchers for exploration of novel industrially important pharmaceuticals. Numerous studies on *in vitro* XO inhibition by plant extracts have been attempted to identify key molecules which could be used as XO inhibitors in future (Table 3.2)

Of the 288 extracts from 96 medicinal plants of Vietnamese traditional medicine, 188 have exhibited XO inhibitory activity at a concentration of 100 µg/ml. The methanol extracts of *Artemisia vulgaris*, *Caeselpinia sappan, Blumea balsamiflora* and *Chrysanthemum sinense* exhibited a strong XO inhibition with IC_{50} less than 20 µg/ml (Nguyen et al., 2004). Among Indian plant extracts screened for XO inhibitory activity, methanolic extracts of *Coccinia grandis, Datura metel, Strychnosnux vomica* and *Vitex negundo* exhibited more than 50 % inhibition (Umamaheswari et al.,

2007). Among Czech medicinal plants which are traditionally used for gout, arthritis and rheumatism, the highest XO inhibitory activity was exhibited by *Populus nigra* and *Betula pendula* methylene chloride-methanol extract which exhibited an IC_{50} of 8.3 and 25.9 µg/ml respectively (Havlik et al., 2010). Moderate XO inhibition was exhibited by the methanol extracts of *Chrysanthemum coronarum, Achillea biebersteinii, Rosmarinus officinalis* and *Ginkgo biloba* with IC_{50} of 199.5 µg/ml, 360 µg/ml, 650 µg/ml and 595.8 µg/ml respectively (Hudaib et al., 2011).

Table 3.2: Xanthine oxidase inhibitors from different plants extracts

Name of extract	**Host Plant**	**Class of compound**	**IC_{50} (µg/ml)**	**Reference**
Methanol	*Cinnamomum cassia*	Complex	18.0	Kong et al., 2000a
Methanol	*Chrysanthemum indicum*	Complex	22.0	Kong et al., 2000a
Methanol	*Rhus coriaria*	Complex	172.5	Candan, 2003
Chloroform	*Coccinia grandis*	Complex	17.8	Umamaheswari and Chatterjee, 2008
Chloroform	*Erythrina stricta*	Complex	21.2	Umamaheswari et al., 2009
Ethyl acetate	*Tinospora cordifolia*	Complex	21.2	Raju et al., 2011
Methanol	*Erythrina indica*	Phenolics	52.7	Sowndhararajan et al., 2012
Aqueous	*Carica papaya*	Complex	4.3	Azmi et al., 2012
Methanol	*Flacoutia sepiaria*	Complex	8.3	Sreejith et al., 2013
Methanol	*Memecylon talbotianum*	Complex	1265	Bharathi et al., 2014
Hexane	*Pandiaka angustifolia*	Complex	-	Thiombiano et al., 2014
Ethyl acetate	*Lycium arabicum*	phenolics	17.0	Trabsa et al., 2015
Ethanol	*Prunus salicina*	Polyphenols	179	Li et al., 2016
Aqueous	*Plectranthus scutellariodes*	Complex	6.0	Levita et al., 2016
Ethyl acetate	*Psidium guajava*	Polyphenols	38.2	Irondi et al., 2016

Root extract of *Tephrosia pupurea,* an Indian folk medicinal plant displayed a concentration dependent, non competitive XO inhibition (Nile and Khobragade, 2011). N-butanol leaf extract of *Ruellia tuberosa Linn* (Ahmad et al., 2012), *Sida rhombifolia* and *Sonchus arvensis* (Hendriani et al., 2016) exhibited potent XO inhibitory activity with IC_{50} of 0.15 µg/ml, 21.43 µg/ml and 23.64 µg/ml

respectively. Further, six Indian medicinal plants viz. *Asparagus racemosus, W. somnifera, V. negundo, Plumbago zeylanica, Butea monosperma* and *T. purpurea* were evaluated for their antioxidant and XO inhibitory potency. All methanolic fractions were found to exhibit moderate XO inhibition with IC_{50} ranging from 3-6 µg/ml (Nile and Park, 2014). However, the major issue with plant extracts is the requirement of a standard raw material as well as bulk plant material for continuous drug supply. This threatens the plant diversity and thus demands development of methods to produce these plant chemical scaffolds in other organisms or through chemical route in case the synthesis is not cumbersome.

3.6.2 Bacteria

There are few reports of XO inhibitors from bacterial sources since 1970s. First report was from *Streptomyces sp* producing 5-formyluracil as potent XO inhibitor (Umezawa et al., 1972). Further, various bacterial isolates from soil were screened for xanthine oxidase inhibitory activity, out of which *Bacillus cereus* A-73 produced 5-formyluracil and *Alcaligenes aquamarinus* produced a purine based XO inhibitor namely 2,8-dihydoxyadenine showing competitive mode of inhibition with IC_{50} and K_i value of 2.0 µM and 0.7 µM respectively (Sunahara et al., 1976). Akalone and Hydroxyakalone isolated from marine bacterium, *Agrobacterium auranticum* N-81106 were reported to be potent XO inhibitors (Izumida et al., 1995; 1997).

3.6.3 Algae

Over the years, algae have emerged as a novel source of putative compounds with hyper diverse biological and structural variability (Borowitzka, 2011; Michalak and Chojnacka, 2015). A sesquiterpenoid named caulerperyne, purified from marine alga *Caulerpa prolifera* was reported to non-competitively inhibiting XO with IC_{50} of 26.92 µM (Cengiz et al., 2012).

3.6.4 Fungi as a source of XOI's

Fungi have been known to produce important inhibitors like statins which have been clinically used for the treatment of hypercholesterolemia. Majority of literature wherein XO inhibition was reported from fungi belongs to basidiomycetes or the mushrooms i.e. macrofungi. Aqueous extract

of *Fistulina hepatica* (beefsteak fungus) was found to possess a concentration dependent XO inhibitory activity with IC_{50} of 1444 µg/ml (Ribeiro et al., 2007).

Table 3.3: Xanthine oxidase inhibitors from microbial sources

Name of Organism	Source	Name of Compound/extract	Reference
Bacteria			
Bacillus cereus	Soil	5-formyluracil	Sunahara et al., 1977
Alcaligenes aquamarines	Soil	2,8-dihydoxyadenine	Sunahara et al., 1977
Agrobacterium auranticum	Marine source	Akalone	Izumida et al., 1995
Agrobacterium auranticum	Marine source	Hydroxyakalone	Izumida et al., 1997
Fungi			
Aspergillus sp. F184	Soil	Terric acid	Hyoung et al., 2000
Phellinus linteus	local farm, Chowon Sangwhang Microbios, Chuncheon, Korea	Ethanolic extract	Song et al., 2003
Fistulina hepatica	Chest nut orchard in Braganca region, Portugal	Aqueous extract	Ribeiro et al., 2007
Agaricus brazillensis	Korea	Water extract	Zanabaatar et al., 2010
Pleurotus cornucopiae	Mushroom Research Institute of Gyeonggi Province, Korea	Acetonic extract	Alam et al., 2011c
Lentinus lepideus	Mushroom Research Institute of Gyeonggi Province, Korea	Acetonic and Methaolic extract	Yoon et al., 2011b
Lichen			
Bulbothrix setschwanensis	Various parts of India	Acetonic extract	Behera and Makhija, 2002
Graphidaceae family	Various parts of India	Methanolic extract	Behera et al., 2003; 2004
Algae			
Caulerpa prolifera	Marine	caulerperyne	Cengiz et al., 2012
Marine Sources			
Halicdona sp.	Marine sponge	Renierol	Wang et al., 2008a

In a study from Korea, aqueous extract of *Agaricus brazillensis* was found to exhibit maximum XOI activity of 72.9 % followed by *P. salmoneostramineus*, *Phellinus baumii*, *A. bisporus* and *Hericium erinaceum* with 60.1 %, 57.7 %, 56.7 % and 52.4 % XO inhibitory activity respectively (Zanabaatar et

al., 2010). Acetone, methanol and aqueous extracts of *Pleurotus cornucopiae*, *P. citrinopileatus*, *P. salmoneostramineus, P. nebrodensis* and *Lentinus lepideus* were found to exhibit dose dependent XO inhibitory activity. However, acetone extract was found to exhibit best XO inhibition when compared to other extracts from the above mushroom species (Alam et al., 2011a; 2011b; 2011c; 2011d; Yoon et al., 2011b). A tripeptide with sequence Phy-Cys-His purified from aqueous fruiting body extract of *Pleurotus ostreatus* exhibited a dose dependent XO inhibitory activity (IC_{50} – 0.9 µM) on potassium oxanate treated rats (Jang et al., 2014). Potent XO inhibition was exhibited by *Hypholoma fasciculare*, *Suillus grevillei*, *Tricholoma populinum* with IC_{50} values of 67.76 ± 11.05 µg/ml, 13.28 ± 1.58 µg/ml and 85.08 ± 15.02 µg/ml respectively (Vanyolos et al., 2014). Terric acid from *Aspergillus sp*. F184 isolated from soil sample of Korea has also exhibited XO inhibition non-competitively (Hyoung et al., 2000).

3.7 Endophytic fungi as a novel source of XOI

Endophytic fungi are heterogeneous group of micro-organisms colonizing the living interstitial tissues of plant cells without any apparent signature of their existence (Schulz et al., 2002). Endophytes presumably exist in a symbiotic association with the host plant by secreting novel bioactive metabolites to strengthen the host plant defense mechanism (Aly et al., 2011; Rosa et al., 2011; Kaul et al 2012; Alvin et al., 2014; Elsebai et al., 2014; Tiwari, 2015; Deshmukh et al., 2015; Aharwal et al., 2016; Gouda et al., 2016). The era of endophytic research was revolutionized with the discovery of million dollar anticancer drug paclitaxel produing endophytic fungus *Taxomyces andreanae* that had been originally isolated from yew tree *Taxomyces breviofolia* (Stierle et al., 1993; 1995). The fascinating discovery of paclitaxel from endophytic fungi evoked the interest of researchers towards endophytes as potential novel source of therapeutic agents. Camptothecin originally isolated from *Camptotheca accuminata*, is a potent anti-neoplastic agent and was also isolated from endophytic *Entrophospora infrequens* inhabiting *Nothapodytes foetida* (Puri et al., 2005). Endophytic *Fusarium solani* isolated from *Camptotheca accuminata* has also been reported to produce camptothecin (Kusari et al., 2009b). On the same lines Podophyllotoxin, a well known anti-

cancer drug is also reported from the endophytic fungus *Phialocephala fortinii* inhabiting its host plant *Podophyllum peltatum* (Eyberger et al., 2006). Podophyllotoxin have also been reported to be produced by another novel endophytic fungus, *Trametes hirsute* (Puri et al., 2006), *Aspergillus fumigatus* isolated from *Juniperus communis* (Kusari et al., 2009a) and *Fusarium oxysporum* inhabiting *Juniperus recurva* (Kour et al., 2008). Apart from production of putative phytochemicals, endophytic fungi also produce a plethora of bioactive secondary metabolites which possess anti-parasitic, neuroprotective, antioxidant, immunosuppressant, anticoagulants and anticancer activities (Mitchell et al., 2008; Guo et al., 2008; Verma et al., 2009; Kusari et al., 2014).

The chemical diversity produced by endophytes is remarkable and it includes polyketides, shikimate derivative, terpenes, steroids, flavanoids, alkaloids, enzymes and peptides. These bioactive metabolites offer an enormous potential for the finding of novel agrochemicals and drugs of natural origin thereby being an alternative source of bioactive metabolites of pharamaceutical importance (Tan and Zou, 2001; Priti et al., 2009; Chandra et al., 2012; Kusari et al., 2012; Nisa et al., 2015).

Endophytic fungi are reported to be prolific source of various enzyme inhibitors for regulation of enzymatic activity. The catalytic activity of enzymes is considered to be vital for the normal metabolism and dysregulation of any of the enzyme can result in fatal disorders. Various classes of compounds viz. polyphenol, terpenes, peptides, alkaloid produced by endophytic fungi with potent inhibitory action against lipases, aldose reductase, HMG-CoA reductase and α-glucosidase are reported (Table 3.3).

Bio-prospecting endophytic fungi in search of novel and effective XO inhibitor is a nascent area with much skewed preliminary data. Endophytic *Fusarium sp*. IFB-121 isolated from *Quercus variabilis* produced a cerebroside named Fusaruside exhibiting potent mixed type XO inhibition with IC_{50} of 43.8 ± 3.6 μM (Shu et al., 2004). Rubrofusarin B and Auraseprone A obtained from the *Aspergillus niger* IFB-E003, an endophytic fungus residing in healthy leaves of *Cynodon dactylon*

Table 3.4: Enzyme inhibitors reported from different endophytic fungi

Name of Compound	Name of endophytic fungus	Host Plant	Target enzyme	Clinical application	Reference
Khafrefungin	*Mycelia sterilia*	Costa Rican plant	Inositol phosphoceramide synthase	Fungal infections	Mandala et al., 1997
Altenusin	*Alternaria sp.*	*Trixis vauthieri*	Trypanotthione reductase	Trypanosomiasis and leishmaniasis	Cota et al., 2008
Koninginins	*Trichoderma koningii*	*Strychnos cogens*	Phospholipase A_2	anti-inflammatory agent, neural disorders	Souza et al., 2008
Corynesidone A	*Corynespora cassiicola*	*Lindenbergia philippensis*	Aromatase	Breast cancer	Chomcheon et al., 2009
Unsaturated fatty acids	*Colletotrichum sp.*	*Taxus sumatrana*	α-glucosidase	Diabetes mellitus	Artanti et al., 2012
Thielavins	*Chaetomium sp*	*Hintonia latiflora*	α-glucosidase	Diabetes mellitus	Rivera-Chavez et al., 2013
Tetrapeptide	*Fusarium incarnatum*	*Aegle marmelos*	Pancreatic lipase	Obesity	Gupta et al., 2015
Bipolarisenol	*Bipolaris sorokiniana*	*Rhazya stricta*	Urease and Acetyl cholinesterase	Alzheimer's disease	Khan et al., 2015
Lovastatin	*Phomopsis vexans*	*Solanum xanthocarpum*	HMG-CoA reductase	Hypercholesterolemia	Parthasarathy and Sathiyabama, 2015
Sorokiniol	*Bipolaris sorokiniana*	*Rhazya stricta*	Acetyl cholinesterase	Alzheimer's disease	Ali et al., 2016
Altenuene	*Alternaria alternata*	*Catharanthus roseus*	Acetyl cholinesterase	Alzheimer's disease	Bhagat et al., 2016
benzyl benzoate	*Emericiella quadrilineata*	*Pteris pellucida*	tyrosinase	Anti- melanogenesis and anti-browning	Goutam et al., 2016

showed potent xanthine oxidase inhibition activity with IC_{50} value of 16.8 µM and 10.9 µM respectively (Song et al., 2004). Further, extract of *Cladosporium herbarum*, an endophytic fungal counterpart of *Cynodon dactylon* yielded aspernigrin A, 7-hydroxy-4-methoxy5-methylcoumarin, orlandin, 3β,5α,6β trihydroxyergosta-7,22-diene, kotanin and two previously reported xanthine oxidase inhibitors rubrofusarin B and fonsecinone A (Ye et al., 2005). Endophytic fungal strain *Chaetomium* sp. obtained from aerial tissues of *Nerium oleander* produced polyphenols exhibiting XO inhibitory activity (Huang et al., 2007a). Lumichrome, a compound isolated from ethyl acetate extract of liquid culture of endophyte

Myrothecium roridum IFB-E012 in *Artemisia annua* exhibited cytotoxicity against the human tumor cell line nasopharyngeal epidermoid KB and inhibition activity against xanthine oxidase (Shen et al., 2009). An endophytic fungal strain, *Alternaria brassicicola* (ML-P08) isolated from leaves of *Malus halliana* has been found to produce two compounds named Alternariol and Alternariol monomethyl ether showing strong xanthine oxidase inhibitory activity (Gu et al., 2009). Recently, chloroform extract of *Lasiodiplodia pseudotheobromae* species isolated from *Aegle marmelos* has been found to inhibit XO with an IC_{50} of 0.61 µg/ml, which was better than positive control, i.e. Allopurinol exhibiting IC_{50} value of 0.937 µg/ml (Kapoor and Saxena, 2014). Thus, endophytic fungi offers immense opportunities in exploration of NP-SIXO's which could be developed into novel therapeutic moieties for combating oxidative stress related diseases and long term hyperuricemia management.

Chapter 4

Materials & Methods

4.0 Materials and Methods

4.1 Plant sample collection

Asymptomatic samples of leaves, twigs and bark of *Aegle marmelos* (Rutaceae family); *Cinnamomum camphora*, *Cinnamomum malabaricum*, *Cinnamomum zeylanicum* (Lauraceae family); *Catharanthus roseus, Rauvolfia serpentina*, *Nerium oleander, Tabernaemontana divaricata* (Apocynaceae); *Tinospora cordifolia* (Menispermaceae family); *Camellia sinensis* (Theaceae); *Piper nigrum* (Piperaceae Family) were collected from the biodiversity hotspots of India including conserved tropical rainforest region of Western Ghats and North-eastern Himalayan region (Table 4.1). The collected plant samples were stored at 4 °C in sterile zip pouches till further use.

Table 4.1: Sampling sites for collection of plant samples

S.No	Biodiversity Hot spot	Sampling site	State	Geographical coordinates
1.	Western Ghats	BRT wildlife Sanctuary	Karnataka	11°59'38"N, 77°8'26"E
2.		Yelandur wildlife Sanctuary	Karnataka	12.07°N, 77.03°E
3.		Wayanad wildlife Sanctuary	Kerala	11°38'46"N 76°21'50"E
4.		Neyyar wildlife Sanctuary	Kerala	8°24'N 77°10'E
5.	North–eastern	Darjeeling	West Bengal	27°3'N 88°16'E
6.		Palampur	Himachal Pradesh	32.11° N, 76.53° E

*BRT: Biligiriranganatha Swamy Temple Wildlife Sanctuary

4.2 Isolation of endophytic fungi

Endophytic fungi were isolated from fresh disease free plant samples (leaves, bark and stems) by following the method of Mitchell et al. (2008). Plant samples were thoroughly washed under running tap water and air dried. Subsequently, the samples were surface sterilised by soaking them in 1 % sodium hypochlorite (NaClO) solution for 5 min followed by 70 % ethanol for 2 min and 30 % ethanol for 45 sec to suppress/remove the epiphytic microflora. These were then finally rinsed with sterile distilled water (SDW) and were allowed to surface dry over sterile blotting sheets aseptically. Subsequently,

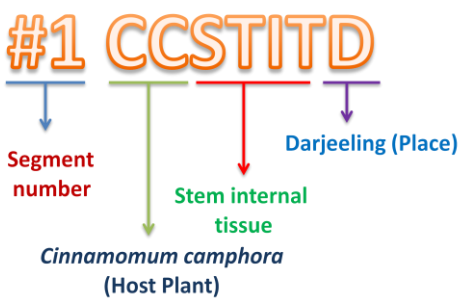

Fig 4.1: Coding outline of pure isolates of endophytic fungi

the sterilized samples were chopped into 2–3 mm pieces with the help of sharp sterile blade and were inoculated onto Potato dextrose agar (PDA, HiMedia, India) plates with ventral side facing towards the medium. The PDA plates were supplemented with 100 µl of streptomycin (100 mg/l, HiMedia, India) to check the bacterial growth. The inoculated PDA plates were then incubated at 26 ± 2 °C for 15 days with 12 h light and dark period. The imprints of disinfected plant samples were also taken on to PDA plates to check the efficiency of sterilization and to ensure that the subsequent fungal growth is of endophytic species. The plates were frequently monitored for any fungal growth and hyphae emerging out from inoculated samples were picked from the edge with sterile fine needle and transferred onto fresh PDA plate. These cultures were considered as pure isolates (Schulz et al., 1993; Zhang et al., 2010). Further, each isolate was encoded based on the host plant, its part and the place from where it was collected (Fig 4.1).

4.3 Maintenance and long-term preservation of endophytic fungal isolates

The fungal isolates so obtained were cultured on to glycerol–PDA slants which were prepared by dissolving 39 g of PDA (HiMedia, India) in one litre of lukewarm double distilled water (DDW) supplemented with 10 % glycerol. This was followed by autoclaving at 121 °C for 15 min at 15 psi. Actively growing fungal mass was then transferred into the slants of glycerol-PDA aseptically and incubated at 26 ± 2 °C till the proper growth was observed. For each isolate, three slants were prepared which were further stored at 4 °C till further use (Ezra et al., 2004).

4.4 Production of culture filtrate for assaying XO inhibition

Culture filtrate production is a pre-requisite for assessing the extracellular XO inhibition potential of endophytic fungi. The culture filtrate production was carried out in a semi-synthetic medium by following the procedure of Raviraja et al. (2006). Briefly the method comprised of aseptically inoculating 25 ml of pre–sterilized Potato Dextrose broth (PDB, HiMedia, India) with a 5 mm mycelial plug prepared aseptically from 7-day old culture of the endophytic fungus followed by incubation at 26 ± 2 °C, 120 rpm (revolutions per minutes) for 10 days. After the culmination of incubation period, the mycelial mass was separated using Whatmann filter paper No. 4 (GE Healthcare Life Sciences,

USA) followed by centrifugation (Hitachi RX II series, Japan) at 8000 g for 10 min at room temperature. The supernatant so obtained was passed through 0.2 µm nitrocellulose membrane (GE Healthcare Life Sciences, USA) to make it cell free and stored at -20 ˚C.

4.5 Preliminary screening for XO inhibition by culture filtrates of endophytic fungi

To assess the xanthine oxidase inhibitory potential of the culture filtrates of endophytic fungi qualitatively, a Xanthine – Nitroblue Tetrazolium (NBT) agar plate assay was designed for preliminary screening. The method was based upon reduction in the diameter of blue/purple colored halo formed by formazan due to presence of ROS produced by xanthine oxidase during conversion of xanthine into uric acid (Kapoor and Saxena, 2014)

Briefly, Xanthine-NBT agar plates were prepared by pouring 23 ml of pre-sterilized molten agar (0.8 %) comprising of 1.5 mg/ml xanthine and 0.11 mg/ml NBT in 90 mm sterile petri plates (Tarsons, India). After solidification, 5 mm wells were scooped out by using sterile cork borer. Subsequently, 40 µl of master-mix containing pre-incubated 15 µl of xanthine oxidase (110 mU; Source: Bovine milk, Sigma- Aldrich) with 25 µl of culture filtrate were dispensed in each well. The control well comprised of 15 µl of xanthine oxidase and 25 µl of sterile un-inoculated PDB. Allopurinol and Febuxostat were used as the positive control and the plates were incubated at 37 °C for 24 h. A reduction or absence of blue colored zone formation was noted to ascertain the XO inhibitory activity of the culture filtrate of the endophytic fungi. The relative inhibition was determined by measuring the zone diameter of the control and the test wells. All the tests were performed in replicates and data was represented as mean ± standard deviation (SD) values.

4.6 Optimization of assay conditions for maximum XO activity

As a pre-requisite for quantitative assay of XO inhibition, optimization of XO activity was carried out to determine its K_m and V_{max}. The various parameters used for XO activity optimization comprised of substrate concentration, enzyme concentration, incubation time and pH.

4.6.1 Effect of substrate concentration

Different concentrations of the xanthine (SRL, India) ranging from 0.5 mM to 5 mM were prepared

from a stock solution of 5 mM xanthine. Subsequently, 135 µl of each concentration was dispensed in separate wells in a 96 well microtiter plate followed by addition of 15 µl of xanthine oxidase (110 mU/ml) and 15 µl of 50 mM Tris-HCl buffer (pH 7.4). The plate was incubated at 37 ˚C for 30 min. Subsequently, 35 µl of 2 mM NBT was added to make the final volume of 200 µl and re-incubated at 37 °C for a minimum of 6 hours. After the incubation is over, the amount of formazan produced was measured at 575 nm using BIOTEK® Powerwave 340 microplate reader. Each substrate concentration was tested in triplicates and data was represented as mean ± SD (Egwim et al., 2005).

4.6.2 Effect of enzyme concentration

To establish optimal enzyme concentration, different concentrations of XO ranging between 100 - 400 mU were prepared from a stock solution of 500 mU. The assay format was same as used for the optimization of substrate concentration as described in section 4.6.1. The formazan formed was quantified at 575 nm using BIOTEK® Powerwave 340 microplate reader. Each test was performed in triplicate and data was represented as mean ± SD.

4.6.3 Effect of incubation time

After the optimization of substrate and enzyme concentration, the incubation time was optimized to assess the optimal incubation time for XO to exhibit maximum activity. The assay format was same as described in previous sections however, optimized concentration of substrate and enzyme were used in the assay. The incubation time was varied from 0 h to 24 h. The absorbance of reaction mixture was recorded at different time intervals using Kinetic and incubation temperature (37 ˚C) mode of BIOTEK® Powerwave 340 microplate reader at 575 nm. A curve was plotted between absorbance and time to ascertain the optimum incubation time. The time interval after which there was no significant increase in XO activity was considered as optimum incubation time. The experiment was conducted in triplicates and data was represented as mean ± SD.

4.6.4 Effect of pH

The effect of pH on the optimal activity of XO with optimized substrate and enzyme concentration was assessed by varying the pH of Tris-HCl buffer used in the reaction mixture. The pH range tested

was between 6.8 to 9.0 (6.8, 7.0, 7.4, 7.8, 8.0, 8.5 and 9.0). A curve was plotted between absorbance and pH of buffer to determine optimum pH value. Each test was performed in triplicates and data was expressed as mean ± SD (Egwim et al., 2005).

4.7 Determination of kinetic constants of xanthine oxidase

The initial reaction mixture comprised of fixed concentration of XO (200 mU/ml) and varying concentration of substrate i.e. xanthine ranging between 0.5 mM to 5 mM. 50 mM Tris-HCl buffer (pH 7.8) was further added to the reaction mixture, incubated for 2h at 37 °C and the kinetic read was recorded at intervals of 10 min using BIOTEK® Powerwave 340 microplate reader at 575 nm. The K_m and V_{max} of XO was determined by non–linear regression fit in GraphPad Prism 5.0 (Hanaee et al., 2004; Lin et al., 2014).

4.8 Quantitative assays for screening XO inhibitors from endophytic fungi

The cell free culture filtrate of endophytic fungi exhibiting potential XO inhibition in the qualitative xanthine-NBT assay were further screened for their inhibitory potential quantitatively by using two spectrophotometric assays viz. NBT microtiter plate assay and the Uric acid estimation assay.

4.8.1 Nitroblue tetrazolium (NBT) reduction microtiter plate assay

The cell free filtrates of selected endophytic isolates exhibiting potential XO inhibition in the preliminary assay were subjected to *in vitro* NBT assay as described by Agarwal and Banerjee (2009) with minor modifications (Fig 4.2). The NBT is reduced to blue colored formazan produced due to interaction with superoxide radicals generated during the oxidation of xanthine to uric acid with XO. The reduction in the intensity of blue colored product indicated the XO inhibition. Briefly, 25 µl of culture filtrate was incubated with 15 µl of XO (200 mU/ml) for 30 min at 37 °C and the reaction was initiated by adding 135 µl of 2 mM xanthine followed by addition of 25 µl of 2mM NBT. The microtiter plate was incubated at 37 °C for 2 h. After the completion of incubation, the amount of formazan produced in the reaction was estimated by measuring the absorbance at 575 nm using Biotek throughput reader, Powerwave 340. The negative control well comprised all reagents except

culture filtrate. Allopurinol and Febuxostat of concentration 1 mM were used as positive controls. Each test was carried out in triplicate and the data was represented as mean ± SD values.

	1	2	3	4	5	6	7	8	9	10	11	12
A	C1	S1	S3	S6	S9	S10	S13	S15	S18	B	B	B
B	C1	S1	S4	S6	S9	S10	S13	S16	S18	B	B	B
C	C1	S1	S4	S7	S9	S11	S13	S16	C3	B	B	B
D	C2	S2	S4	S7	S10	S11	S14	S16	C3	B	B	B
E	C2	S2	S5	S7	B	S11	S14	S17	C3	B	B	B
F	C2	S2	S5	S8	B	S12	S14	S17	C3	B	B	B
G	B	S3	S5	S8	B	S12	S15	S17	B	B	B	B
H	B	S3	S6	S8	B	S12	S15	S18	B	B	B	B

← Fig 4.2: Template for *in vitro* XO inhibitory activity. C1 refers to the negative control i.e. Xanthine + Xanthine oxidase; C2 and C3 refers to positive controls i.e. xanthine + xanthine oxidase+ Allopurinol and xanthine + xanthine oxidase+ Febuxostat respectively; S1 to S18 refers to culture filtrates of different endophytic fungi; B refers to Blank well.

4.8.2 *In vitro* uric acid estimation Assay

This assay was carried out as per the method of Chang et al. (1993) to establish the production of uric acid from xanthine which is dependent on the XO activity. Briefly, 200 µM of xanthine buffer solution was prepared by dissolving xanthine (3.0 mg) in the 100 ml of 100 mM phosphate buffer (pH 7.8) solution by mild heating. The initial assay mixture was prepared by adding 10 µl of culture filtrate to 990 µl of xanthine buffer solution. The reaction was initiated by adding 15 µl of xanthine oxidase (200 mU/ml) followed by incubation at 37 ˚C for 15 min. Further, the reaction was stopped by adding 1 N HCl solution. The concentration of uric acid produced was measured by taking absorbance value at 290 nm. Allopurinol and Febuxostat served as positive control. The inhibitory percentage of xanthine oxidase was calculated by:

$$\% \text{ Inhibition} = [(A-B) - (C-D)] / (A-B) \times 100\ \%$$

Where A is the OD at 290 nm with enzyme but without sample, B is the OD at 290 nm without sample and enzyme, C is the OD at 290 nm with sample and enzyme, D is the OD at 290 nm with sample but without enzyme.

4.9 Isolation of the bioactive moiety using liquid-liquid extraction

The culture filtrates of endophytic isolates exhibiting XO inhibitory activity of 70 % and above were subjected to liquid-liquid extraction (Choudhary et al., 2004). The culture filtrate of each selected

culture was extracted with a series of solvents with increasing polarity viz. hexane, diethylether, dichloromethane, ethyl acetate and chloroform (Fig 4.3). Briefly, 150 ml of culture filtrate was mixed with the equal volume of hexane and shaken vigorously for 15 min a 500 ml separating funnel (Borosil, India) and allowed to settle down to have separate aqueous and hexane layer. The hexane layer was withdrawn from the separating funnel and this step was further repeated twice. All the organic layers of hexane were pooled followed by dehydration by using anhydrous sodium sulphate. Subsequently, the obtained aqueous layer was further extracted with diethylether, dichloromethane, ethyl acetate and chloroform following the above scheme (Figure 4.2). The organic phase of each solvent was evaporated to dryness by Rotatory Evaporator (IKA RV10, Germany) at 25 ˚C. The crude fractions so obtained were weighed and reconstituted in methanol. The fractions were stored at 4˚C till further use.

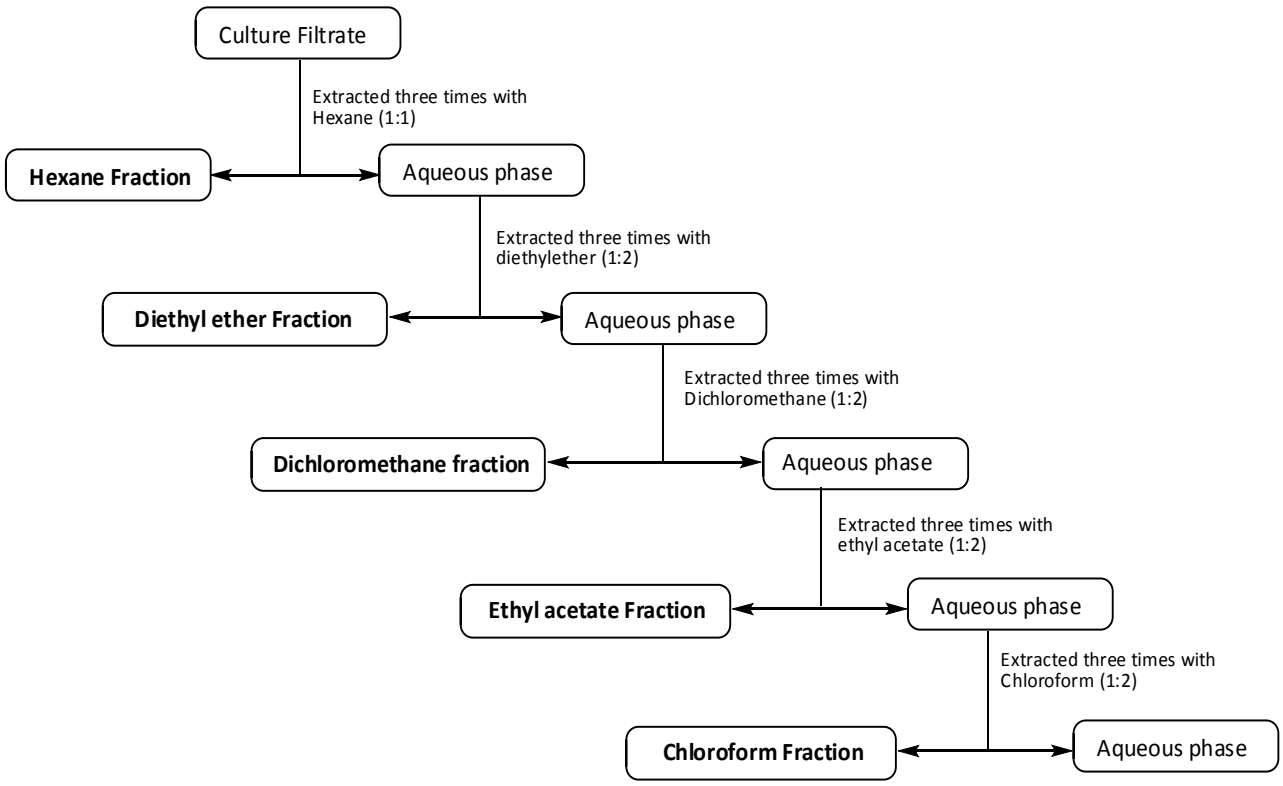

Fig 4.3: Solvent extraction scheme of culture filtrates of selected endophytic fungi

4.10 Quantitative screening of crude fractions for XO inhibitory activity

The crude fractions of hexane, diethylether, dichloromethane, ethyl acetate, chloroform and aqueous residue (spent broth) of selected cultures were further subjected to quantitative NBT-XO

inhibitory assay as described in section 4.8.1. Methanol was used as a negative control. Allopurinol and Febuxostat served as positive controls. The relative decline in the absorbance of crude fractions in comparison to negative control was indicative of XO inhibitory activity. The relative percentage XO inhibitory activity was determined by taking ratio of % age XO inhibition in presence and absence of crude fractions.

4.11 Test for purine detection

The solvent fractions exhibiting *in vitro* XO inhibition was further subjected to purine detection test based on precipitation of Ag^+ ions with purine (Salkowski, 1897). Briefly, 1 ml of solvent fraction (stock- 1 mg/ml) was mixed with excess of ammonium hydroxide followed by addition of few drops of 0.1 M silver nitrate solution. Formation of white precipitate, which is a purine complex with Ag^+ ions, confirms the presence of purine**.** Allopurinol (purine analogue) and xanthine was used as positive control and Febuxostat being non-purine in nature was used as negative control**.**

4.12 Identification of potential endophytic fungi

The crude fraction of endophytic fungal isolate exhibiting maximum XO inhibitory activity was identified by macro and microscopic characteristics along with molecular taxonomic tools.

4.12.1 Morphotaxonomy

The potential endophytic fungus was grown over six different media namely Potato Dextrose Agar (PDA), Malt Extract Agar (MEA), Corn Meal Agar (CMA), Czapek Dox Agar (CDA), Synthetischer Nahrstoffarmer agar (SNA) and Water Agar (WA) to assess its sporulation potential under different stress conditions. The plates were incubated at 26 ± 2˚C for 2-3 weeks under 12 h light/dark period cycles. The morphological properties such as growth rate, colony color, colony diameter, texture, pigmentation and presence of any odor was observed to identify the fungus (Guo et al., 1998; Mitchell et al., 2008; Kudalkar et al., 2012; Saxena et al., 2014).

4.12.2 Microscopic identification

For microscopic characteristics examination, mycelial mass was picked up with a fine tip needle and placed over a clean glass slide containing a drop of water. The mycelial mass was teased properly

with the help of sharp needle followed by addition of a drop of Lactophenol Cotton Blue (Himedia, India) over it and was slightly teased again. A clean cover slip was placed over it carefully to avoid formation of any air bubbles. The cover slip was pressed gently to remove excess stain and air followed by mounting with DPX (HiMedia, India). The prepared slide was then observed under different magnification (10X-1000X) lenses of Nikon Eclipse Compound microscope (E100). Further, the microscopic characteristics were critically studied under Nikon Stereo zoom microscope (Nikon SMZ 745T, Japan) coupled with NIS element D 3.2 software. Microscopic measurements were made using Image J software with at least 30 observations per structure. Colony texture, color, growth rate, pigment and VOCs production along with microscopic structures like hyphal characteristics and presence of other cellular bodies were critically observed and recorded (Zhang et al., 2010; Suwannarach et al., 2010; 2013).

4.12.3 Scanning Electron Microscopy

Scanning electron microscopy of selected endophytic fungus was carried out according to the method described by Ezra et al. (2004). Mycelial blocks of seven days old fungus were immersed in 2.5 % glutaraldehyde solution prepared in 0.1 M phosphate buffer (pH 7.2) for overnight at 4 °C. Next day, the mycelia blocks were washed twice with the same buffer for 10 min each. Further, fungal mycelia were slowly dehydrated by sequential washing with different gradients of acetone (30–100 %) and critical-point dried with hexamethyldisilazane (Sigma Aldrich, USA). The dehydrated fungal sample was coated with gold palladium using putter coater and the images were recorded in high vacuum mode using Zeiss Evo40 scanning electron microscope between 307 X – 2.02 KX magnification at 15 kV EHT (Kudalkar et al., 2012).

4.12.4 Molecular Taxonomy

For accurate and precise speciation of potential endophytic fungus, the culture was subjected to DNA isolation followed by amplification of internal transcribed spacer (ITS) region and further construction of phylogenetic tree to ensure its accurate taxonomic placement.

4.12.4.1 Genomic DNA isolation

Fungal genomic DNA extraction was carried out by using the Wizard® Genomic DNA purification kit (Promega, Madison, USA) as per the manufacturer's instructions. For the isolation of genomic DNA, about 0.2-0.3 g of cultured mycelia was scrapped off from 3-4 day old culture plate with sterile inoculation loop. The mycelial mass was then crushed to very fine powder in pestle mortar using liquid nitrogen. Subsequently, 600 µl of nuclei lysis buffer was added and was gently crushed again. The contents were then transferred into 2 ml sterile micro-centrifuge tube (Tarsons, India), vortexed followed by incubation at 65 °C for 15 min in water bath (Stuart Water Bath SBS40) with intermittent mixing after every 5 min. After 15 min, micro-centrifuge tubes were allowed to cool down at room temperature for 2 min and 5 µl of RNase (10 mg/ml) was added to each micro-centrifuge tube followed by incubation at 37 °C for 15 min. After the incubation is over, the micro-centrifuge tubes were centrifuged at 10,000 × g for 5 min to remove cell debris. Further, the supernatant was transferred to fresh micro-centrifuge tube, to which 200 µl of protein precipitating solution was added, vortexed for 20 s and subsequently centrifuged at 12000 × g for 3 min to precipitate and remove interfering protein particles. Further, the supernatant free from protein impurities was transferred to fresh micro-centrifuge tubes containing 600 µl of chilled isopropanol and inverted gently to ensure proper mixing for precipitation of DNA. Initially, the white shining threads of DNA were seen in the tubes which were then centrifuged at 12000 × g for 3 min to precipitate DNA. The obtained DNA pellet was given a quick wash with 70 % ethanol (AR grade, Merck, US) followed by centrifugation at 12000 × g for 1 min. The pellet was air dried, dissolved in 50 µl of DNA rehydration buffer and was stored at 4 °C till further use.

4.12.4.2 Qualitative and quantitative estimation of Genomic DNA

The extracted gemonic DNA was further visualized on 0.8 % agarose gel (HiMedia, India) prepared in 1 X Tris acetate EDTA (TAE) containing 0.5 µg /ml of ethidium bromide (HiMedia, India). The gel was casted in a mini gel electrophoresis unit (BioRad, India) and allowed to solidify. After solidification, the comb was carefully removed and running buffer (1 X TAE) was poured into the electrophoretic

tank so that the gel remains fully immersed in the buffer. The DNA samples mixed with 5X loading buffer were loaded into the respective wells. The molecular weight marker of 1 Kb (Step up, Genei, Bangalore) was loaded along with samples. A constant voltage of 60 volts was maintained till the tracking dye reached three fourth of the gel during the electrophoretic separation. The gel was then observed under UV transilluminator to confirm the presence of DNA. Further, the gel imaging was performed under UV light in Bio–Rad Gel documentation System using Quantity–1–D analysis software. Quantitative estimation of the genomic DNA was done by spectrophotometric analysis of the sample. The absorbance of the sample was taken at 260 nm, to determine the concentration of the sample. 1 OD is equivalent to 50 µg/ml DNA sample. The concentration of the DNA was calculated by using formula:

$$\text{DNA Concentration (µg/ml)} = OD_{260nm} \times 50 \text{ µg/ml} \times \text{Dilution factor}$$

The purity and quantity of DNA was checked using NanoDrop 2000 (Thermo Scientific™) at 260 nm and 280 nm

4.12.4.3 ITS gene amplification

The conserved internal transcribed spacer region (ITS1-5.8S-ITS2) was amplified using the *Muscodor* specific primer pair *M. albus* F (5'-GGGAGGCTACCCTATAGGGGATAC-3') and *M. albus* R (5'-CAGGGGCCGGAACCACTACAGAGG-3') as described by Ezra et al. (2010). The master mix contained 50 ng of extracted genomic DNA, 2.5 mM dNTP, 10 pmol/µl of each primer, 1.5 U of Taq DNA polymerase, 1.5 mM $MgCl_2$ (Bangalore Genei) in 10X Taq buffer making the reaction volume to 25 µl. The thermal cycling parameters for ITS region amplification was as follows: initial denaturation at 96 °C for 5 min followed by 35 cycles of 95 °C for 45 s, annealing at 60 °C for 45 s, extension at 72 °C for 45 s followed by final extension at 72 °C for 5 min (Saxena et al., 2014). The PCR products were visualized in 1.5 % agarose gel and gel imaging was carried out in BioRad gel documentation system. The amplicon of approximately 450-500 bp was purified by Wizard® SV Gel and PCR clean up system kit Promega, USA). The purified amplicon was sequenced by Xcleris Genomics Pvt. Ltd, Ahmadabad, Gujarat, India.

4.12.4.4 Sequence assembly and phylogenetic tree construction

The chromatograms obtained after sequencing was checked for their purity (≥ 95%) and assembled using Sequencher ver 5.0 (Gene Codes, Ann, Arbor, MI). The final consensus sequence was then submitted to GenBank and sequence similarity search was performed using BLAST against the database maintained by NCBI to establish the homology with closely related organisms. Sequences showing highest sequence similarity with the respective sequence under study were aligned using Clustal W in MEGA 5.2 (Tamura et al., 2011). Distance based analysis of the ITS region alignment was done by Neighbor-joining method (Saitou and Nei, 1987) using the Tamura-Nei model (Tamura and Nei, 1993) of nucleotide substitution and the rate variation among sites was modeled with a gamma distribution (shape parameter = 5). Gaps were coded as missing characters. 1000 bootstrap replicates were taken into account to infer the consensus tree for the representation of evolutionary relationship (Saxena et al., 2014).

4.13 Secondary structure prediction

Secondary structures of ITS1, 5.8S and ITS2 marker region of selected endophytic isolate was generated using LocaRNA-P simultaneous RNA alignment and folding option of the Freiburg RNA Tools web server (http://rna.informatik.uni-freiburg.de:8080/LocARNA/Input.jsp) (Smith et al., 2010; Will et al., 2012) and RNAfold web server (rna@tbi.univie.ac.at) hosted by Institute of Theoretical Chemistry, University of Vienna (Hofacker, 2004). The three conserved motifs M1, M2 and M3 among eukaryotes were also predicted.

4.14 Sequence-structure assembly, alignment and phylogenetic tree construction

The sequence and structure data of endophytic isolate under study and the respective species of same genus were synchronously aligned using ClustalW (Larkin et al., 2007) to generate a multiple sequence-structure alignment in 4SALE v 1.7 (Seibel et al., 2006). Further, Phylogenetic relationship among all the species was inferred by Profile Neighbor Joining as implemented in ProfDistS 0.9.9 (Wolf et al., 2008; Friedrich et al., 2005) by employing the use of sequence structure specific General

Time Reversible (GTR) model of substitution and 1000 bootstrap replicates. The visualization of phylogenetic tree was carried out in FigTree v1.4.2 (Rambaut, 2007).

4.15 Optimization of suitable culture conditions

Culture conditions of the selected endophytic isolate exhibiting maximum extracellular *in vitro* XO inhibitory activity during preliminary screening were further evaluated for optimal production on solid substrate fermentation and submerged fermentation methods. Further, a correlation of XO inhibitory activity with fungal biomass production was also studied

4.15.1 SSF for *in vitro* XO inhibition

Different solid substrates such as rice chaff, wheat bran, egg shell and banana peel were collected from the local market, dried for several days and grounded into a fine powder. 10 g powder of each of the substrate was moistened with 50 % of salt solution (KH_2PO_4: 0.5 g, $MgSO_4$: 0.5 g, $MnSO_4$: 0.001 g, $ZnSO_4$: 0.002 g, $FeSO_4$: 0.0005 g, double distilled water: 10 ml) in 250 ml Erlenmeyer flask followed by autoclaving at 121 °C for 15 min and then cooled at room temperature and inoculated with 2 ml (0.91 % physiological saline) of the finely ground mycelium of #1 CCSTITD aseptically. Further, the flasks were incubated at 26 ± 2 °C for 15 days. After incubation, each flask was soaked with 50 ml of chloroform and incubated in orbital shaker at 120 rpm for 2 h at 28 °C. Further, the crude chloroform extract was obtained by filtration through Whatmann filter paper. The crude extract obtained from each substrate was checked for its *in vitro* XO inhibitory activity as described previously in section 4.8.1. The data was analysed using one way ANOVA followed by Tukey's post hoc analysis (GraphPad Prism 5.0) to determine significant difference between the mean values.

4.15.2 Selection of suitable medium for production of XOI

To ascertain the optimal medium for maximum *in vitro* XO inhibitory activity, six different medium viz. CDB (HiMedia, India), malt extract broth (MEB, HiMedia, India), potato dextrose broth (PDB, HiMedia, India), Richard's broth (HiMedia, India), Tryptone soya broth (TSB, HiMedia, India) and yeast extract peptone dextrose broth (YEPB, HiMedia, India) were inoculated with the 5 mm mycelial plug of 7-day old culture of selected endophytic isolate and XO inhibitory activity was determined

using quantitative *in vitro* NBT assay. Briefly, 50 ml of each pre–sterilized broth was inoculated with 5 mm mycelial plug of selected 7-day old culture followed by incubation at 26 ± 2 °C, 120 rpm for 15 days. After the termination of incubation period, the spent broths were separated from the fungal biomass by filtration to obtain the culture filtrates. Subsequently, the culture filtrates were extracted with various solvents as described in section 4.9 and the crude extracts so obtained were tested for its *in vitro* XO inhibitory activity using quantitative NBT assay as described previously in section 4.8.1.

4.15.3 Correlation between fungal biomass and XOI activity

To evaluate the correlation between the growth of the potential endophytic fungus and XO inhibitory activity, 50 ml of pre-sterilized potato dextrose broth (PDB) in 250 ml of Erlenmeyer flask was inoculated with 5 mm mycelial plug of active culture. Subsequently, all the 30 flasks were incubated at 26 ± 1°C at 120 rpm. After each day, two flasks were removed from the shaking and supernatant was separated by filtration through Whatmann filter paper no. 4. The collected filtrate was subjected to XO inhibition assay using quantitative plate assay. However, the mycelium collected on Whatmann filter paper no. 4 was kept in oven at 80˚C to get the dry weight of the biomass. Correlation was established between the % XO inhibition, Dry weight of biomass and incubation days.

4.16 Phytochemical testing of crude bioactive residue

Phytochemical analysis involves the assessment for the presence of broad chemical classes of compounds like saponins, glycosides, flavonoids, alkaloids and tannins in the crude solvent residues. Different phytochemical tests were performed to establish the qualitative chemical profile of the crude bioactive residue.

4.16.1 Test for alkaloids

The method used to confirm the presence of alkaloids involves the addition of few drops of Dragendorff's reagent (Bismuth sub-nitrate-1.7 g, glacial acetic acid-20 ml, water-80 ml and 50% solution of Potassium iodide in water-100 ml) to the 100 µl of crude residue. The appearance of turbidity or red precipitation indicated the presence of alkaloids (Oloyede et al., 2005).

4.16.2 Test for anthraquinones

For the detection of anthraquinones, 100 µl of each test sample was mixed with 500 µl of benzene. Subsequently, 300 µl of 10 % ammonia solution was added followed by vigorous shaking. The formation of violet color in the ammonical (lower) phase indicated the presence of free hydroxyl anthraquinones (Bandoni et al., 1976; Govindappa et al., 2013).

4.16.3 Test for tannins

Briefly, few drops of ferric chloride reagent were added to 100 µl of crude residue. Appearance of a blue–black precipitate, which disappears on addition of H_2SO_4 and further results in formation of yellow brown precipitate, indicates the presence of tannin in the sample (Senthilmurugan et al., 2013).

4.16.4 Test for saponins

The presence of saponins in the test sample was detected by frothing test. Briefly, 100 µl of crude residue was mixed with 400 µl of distilled water followed by vigorous vortexing. The appearance of stable froth formation upon slight warming of the vortexed mixture indicated the presence of saponins (Desire et al., 2012).

4.16.5 Test for flavonoids

The presence of flavonoids was tested by mixing 100 µl of crude residue with 500 µl of water and ethanol mixture (1:1) and centrifuged. The solution was further mixed with 500 µl of concentrated hydrochloric acid (HCl) and 100 mg of zinc turnings. The presence of flavonoids was indicated by the appearance of pink/ magenta color within two minutes which could be extracted with butanol (Aynehchi et al., 1981).

4.16.6 Test for glycosides and glycolipids

To test the presence of glycosides and glycolipids, diphenylamine reagent was used. Diphenylamine reagent was prepared by adding 10 ml of 10 % diphenylamine in ethanol, 100 ml HCl and 80 ml glacial acetic acid. This reagent was added to 100 µl of crude residue followed by heating for 30-40

min at 110 °C. Appearance of blue coloration indicates the presence of glycosides/ glycolipids (Narasimhan et al., 1982).

4.16.7 Test for carbohydrates

To test the presence of carbohydrates, 100 µl of the crude residue were mixed with few drops of Molisch reagent (α-napthol in ethanol). After mixing, few drops of concentrated sulfuric acid were slowly added along the walls, without mixing, to form a layer. Appearance of a purple ring at the interface between the acid and test layers indicates presence of carbohydrates (Sawhney et al., 2011).

4.16.8 Test for amino acids

To confirm the presence of amino acids, 200 µl of ninhydrin solution was added to 100 µl of crude residue and in micro–centrifuge and then kept in boiling water bath for 5 min. Appearance of blue purple coloration confirms the presence of amino acids (Sawhney et al., 2011).

4.16.9 Test for fats

Briefly, 100 µl of crude residue was mixed with 200 µl of sudan dye IV. Formation of red coloration confirms the presence of fats (Zhu et al., 2015).

4.16.10 Test for terpenoids and steroids

1 mg of crude compound was suspended in 1 ml of chloroform in micro-centrifuge tube, placed in an ice bath for 10 minutes. Subsequently, 1ml of acetic acid was added followed by a few drops of concentrated sulphuric acid (H_2SO_4) along the walls. Appearance of pink or pinkish-brown ring/ colour indicates the presence of terpenoids and the appearance of bluish-green or a rapid change from pink to blue color indicates the presence of steroids (Kantamreddi et al., 2010; Chandrappa et al., 2013).

4.17 Purification and characterization of bioactive residue

For purification of xanthine oxidase inhibitor, the potential isolate was grown on PDB to obtain 15 l of culture filtrate which was then subjected to liquid-liquid extraction to obtain crude bioactive residue. The selected bioactive crude fraction of potential endophytic fungus was further subjected

to purification by thin layer chromatography (TLC) and column chromatography. Further, the purified fraction was characterized by employing various analytical techniques viz. HPLC, MS, FTIR and NMR.

4.17.1 Thin layer chromatography (TLC) of bioactive residue

Firstly, the bioactive crude fraction was subjected to preparative thin layer chromatography (TLC) on pre-coated silica gel alumina plates (GF_{254}, 20 cm x 20 cm, Merck Millipore). In order to achieve good separation on TLC plate, different mobile phase (Binary and tertiary) comprising of solvents of different polarities mixed in different ratios was used. The mobile phase in which the fraction was resolved into maximum number of bands were considered as optimum mobile system. In brief, the bioactive fraction was spotted on to pre activated TLC plate just 1 cm above the edge of the plate with the help of capillary tube. The spotted TLC plate was then allowed to develop in TLC chamber pre saturated with optimum mobile system. The TLC plate was dipped in the solvent system in such a way that spotted sample is above the solvent front. The TLC plates were allowed to develop till the solvent front reaches at a distance of 16 cm through capillary action. Further, the TLC plate was taken out from developing chamber and solvent was allowed to evaporate. After that, the developed TLC plate was visualized under short and long wave UV light followed by development in iodine chamber to accurately check the location of all separated bands. The distance travelled by each band was marked and noted to calculate the Retention factor (R_f) value by using following formula

$$\text{Retention Factor } (R_f) = \frac{\text{Distance travelled by solute}}{\text{Distance travelled by solvent}}$$

4.17.2 Purification of bioactive residue by column chromatography

The optimum mobile phase for the separation of bioactive fraction formed the basis to decide the mobile system for silica based column chromatography. Briefly, prior to packing the silica column, the silica gel (60-120 mesh, Merck Millipore) was dried in an oven for one hour at 100 °C. Approximately, 50 g of dried silica was suspended in dichloromethane and packed in a glass column

(50 x 5 cm, Borosil, India) fitted with a G_0 filter. The packed column was allowed to be equilibrated with dichloromethane for 1h. Around 2 g of the bioactive residue (Bed height- 2.5 cm). absorbed on dried silica was loaded on to the pre-packed column (Length- 45 cm) The gradient elution was carried out using a gradient of $CHCl_2$- CH_30H (100:0 → 0:100). The fractions so obtained were analyzed by TLC using optimized solvent system and R_f value was determined. Further, all the fractions were subjected to quantitative XOI assay as described in section 4.8.1 and 4.8.2 respectively. The fraction with positive XOI activity was further subjected to structure elucidation studies.

4.18 Structure elucidation of bioactive fraction

4.18.1 Liquid chromatography mass spectrometry (LC–MS)

The bioactive fraction (Stock- 1 mg/ml) in chloroform-d (Merck) was analyzed in LC–MS system (Waters, Micromass Q–TOF micro using Waters Alliance 2795 separation module). Briefly, 20 µl of purified compound was injected into LC-MS system using a Waters Symmetry–C_{18} Unisol chromatographic column (4.6 mm x 250 mm, 5 µm). Initially, the column was equilibrated with methanol to ensure clear base line. The mobile phase comprised of a mixture of methanol (phase A): water (phase B) in the ratio 9:1.

The peaks so obtained were analyzed using Time of Flight–Mass spectrometry (TOF MS) (Waters 2795, Micromass Q–TOF micro) with electro spray ionization in positive mode (ES^+). The ion optics used was capillary with voltage of 3000 V and cone voltage of 30 V. The flow of desolvation and cone gas was adjusted to 750 L/h and 30 L/h. The source block temperature was 110 °C and desolvation temperature was 300 °C. The electron spray probe flow was adjusted to 400 µl/min and continuous mass spectra was recorded over a range *m/z* 0 to 1000 with scan time of 1 sec and inter scan delay 0.1 s.

4.18.2 Fourier Transform Infrared Spectroscopy (FTIR)

IR spectrum was obtained on Agilent Resolutions Pro using 600 FT-IR spectrometer fitted with a beam condensing ATR accessory. The peaks were reported within the range of 7500-500 cm^{-1} using

rapid scans of 65 spectra/s at 16 cm^{-1}. 100 µl of bioactive fraction (1 mg/ml) dissolved in chloroform was loaded onto the cell. The spectral resolution was 0.2 cm^{-1} containing temperature control stage. For each spectrum, 32 scans were used (Jiao et al., 2006).

4.18.3 Nuclear magnetic resonance spectroscopy (NMR)

Approximately, 5 mg of the bioactive fraction dissolved in 0.5 ml of deuterated-chloroform (Sigma Aldrich) was used for recording the NMR spectra. NMR spectra were recorded at 400 MHz on a Bruker Avance II-400 NMR spectrometer (400.131 MHz proton and 100.525 MHz carbon frequencies) at 18 °C. Proton and carbon 90 ° pulse widths were 10.9 sec and 8.37 sec µs respectively (Liu et al., 2016).

4.18.4 Melting point

1 mg of the bioactive fraction was packed in a capillary tube sealed at one end. The capillary was placed over oil bath heater with a thermometer. The temperature was read manually till the compound starts melting. The temperature at which compound was melted was recorded as Melting point of the compound.

4.19 Kinetic studies on inhibition of bovine xanthine oxidase by bioactive fraction

To study the K_m, V_{max}, K_i (inhibition constant) and mode of inhibition, Lineweaver-Burke plot was prepared. Different concentrations of the isolated XO inhibitor (100, 200, 400, 700 µg/ml) were incubated with 15 mU of XO for 30 min at 37 °C. The reaction was then started by adding different concentrations of xanthine (0.5-3 mM). The microtiter plate was incubated at 37 °C for 30 min followed by addition of 30 µl of NBT. The plate was further incubated at 37 ˚C for 4 h. The amount of formazan released was recorded at 575 nm by BIOTEK® Powerwave 340 microplate reader. All the tests were performed in triplicates each having a substrate control. The values of K_m, V_{max} and K_i were calculated using Non linear regression fit in Graph pad prism 5. Lineweaver-Burk plot was used to verify the type of inhibition (Lin et al., 2014).

Chapter 5

Results

5.1 Isolation of endophytic fungi from plant samples

A total of 181 endophytic fungal isolates belonging to 25 taxa were isolated from different parts of the host plants collected during the forays. Each of the endophytic isolate was assigned a unique code on the basis of name of the host plant, plant part and place of collection (Table 5.1, Appendix A). These endophytic isolates were tentatively identified on the basis of morphological and microscopic characteristics (Barnett and Hunter, 1998) (Figure 5.1, 5.2).

Fig 5.1: Endophytic fungal isolates from various medicinal plants used in the study. (a,h) *Fusarium solani* (b) *Fusarium incarnatum* (c) *Muscodor tigerii* (d) *Lasiodiplodia pseudotheobromae*, (e) *Hypoxylon sp.* (f,l) Unidentified (g) *Muscodor strobelii* (i) *Fusarium oxysporum* (j) *Xylaria* sp (k) *Muscodor kashayum* (Bar: 10 mm)

Maximum endophytic fungal isolates were recovered from *Cinnamomum zeylanicum* (27 %) followed by *Aegle marmelos* (23 %) and *Cinnamomum malabaricum* (20 %). The host tissue of each plant sample exhibited a variation in colonization of the endophytic mycoflora (Table 5.2; Fig 5.3a). The maximum colonization of fungal endophytes was observed in internal tissue/vascular tissue in the stem (30 %) followed by leaf (27 %), stem (25 %) and bark (18 %) (Table 5.2; Fig 5.3b). Further,

the total endophytic fungi isolated were grouped in different classes viz. hyphomycetes, coelomycetes, ascomycetes, basidiomycetes and some could not be identified being non sporulating in nature. The maximum number of endophytic isolates belonged to hyphomycetes (45.8 %) followed by ascomycetes (22 %), coelomycetes (9.9 %), unidentified (20.4 %) and basidiomycetes (1.65 %). No member of zygomycetes was reported during the study (Fig 5.4).

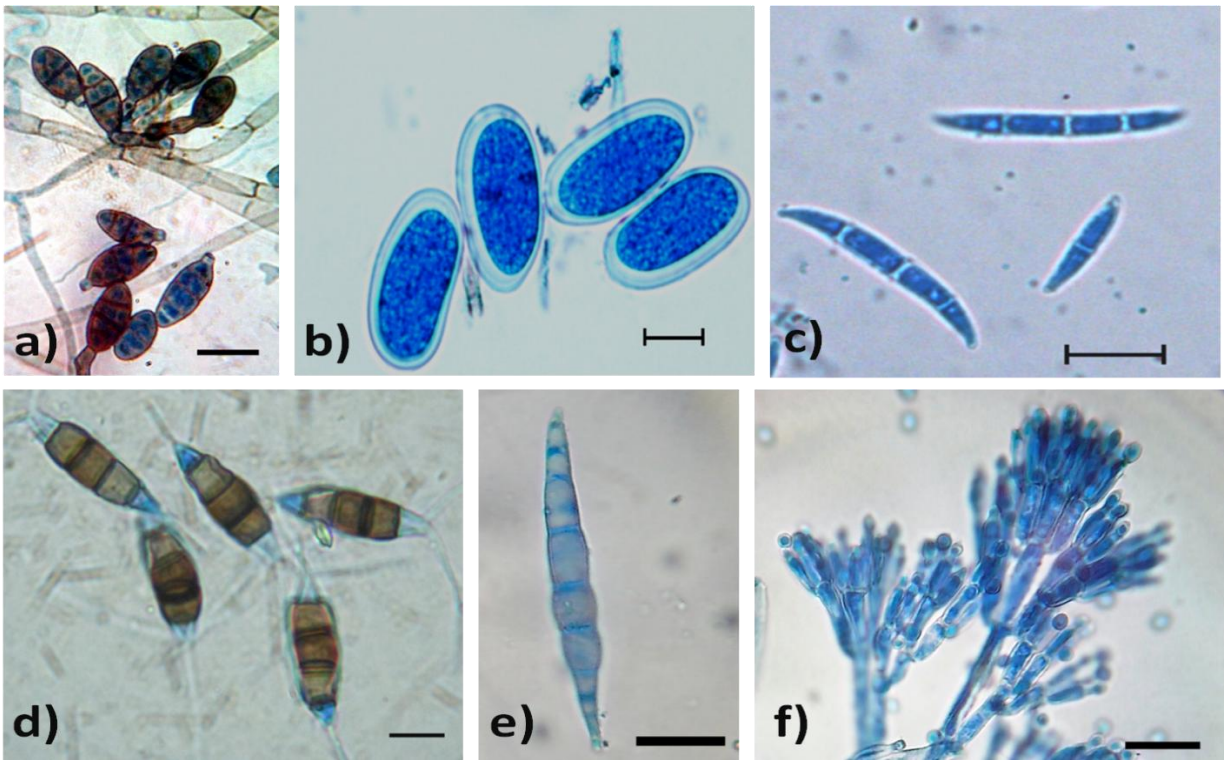

Fig 5.2: Microscopic features of endophytic fungi isolated during the study. (a) Conidia of *Alternaria* sp. (b) immature conidia of *Lasiodiplodia psuedotheobromae*, (c) macroconidia of *Fusarium oxysporum,* (d) Conidia of *Pestalotiopsis* sp. (e) macroconidia of *Fusarium equiseti,* (f) Stipe, metulae and phialides of *Penicillium* sp. (Bar: 10 µm)

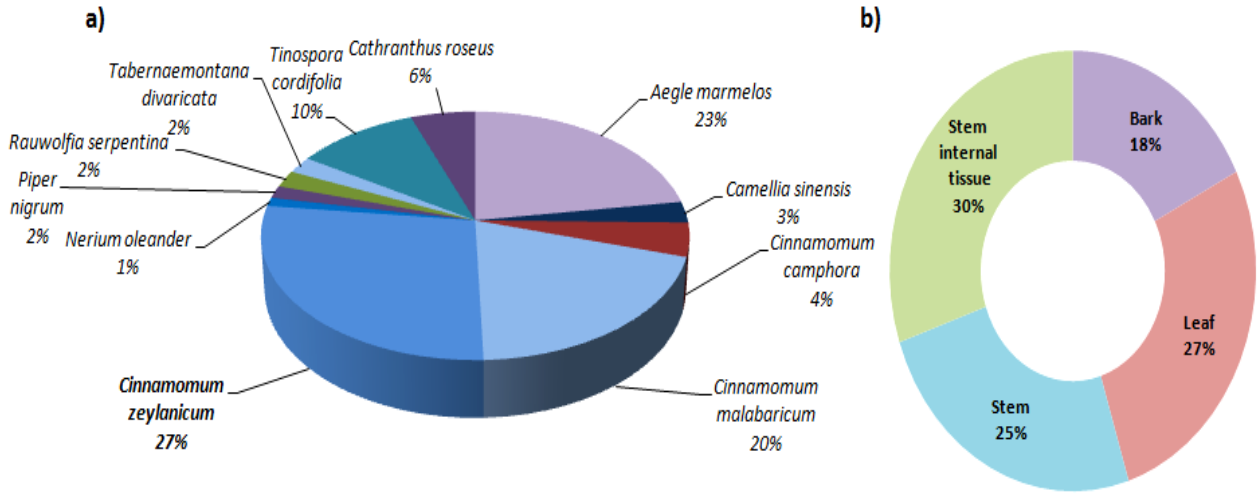

Fig 5.3: Distribution of endophytic fungi (%) among (a) host plants (b) different plant tissues

Table 5.2: Summary of endophytic fungi isolated from different tissues of host plant

S. no	Host plant	Endophytic fungi				Total
		Leaf	Bark	Stem	Stem internal tissue	
1.	*Aegle marmelos*	7	1	16	17	41
2.	*Camellia sinensis*	0	0	5	0	5
3.	*Cinnamomum camphora*	0	2	0	6	8
4.	*Cinnamomum malabaricum*	13	7	10	6	35
5.	*Cinnamomum zeylanicum*	24	19	0	7	50
6.	*Nerium oleander*	0	2	0	0	2
7.	*Piper nigrum*	3	0	0	0	3
8.	*Rauvolfia serpentina*	2	1	1	0	4
9.	*Tabernaemontana divaricata*	0	0	4	0	4
10.	*Tinospora cordifolia*	0	0	0	19	19
11.	*Cathranthus roseus*	1	0	9	0	10
	Total	**50**	**32**	**45**	**55**	**181**

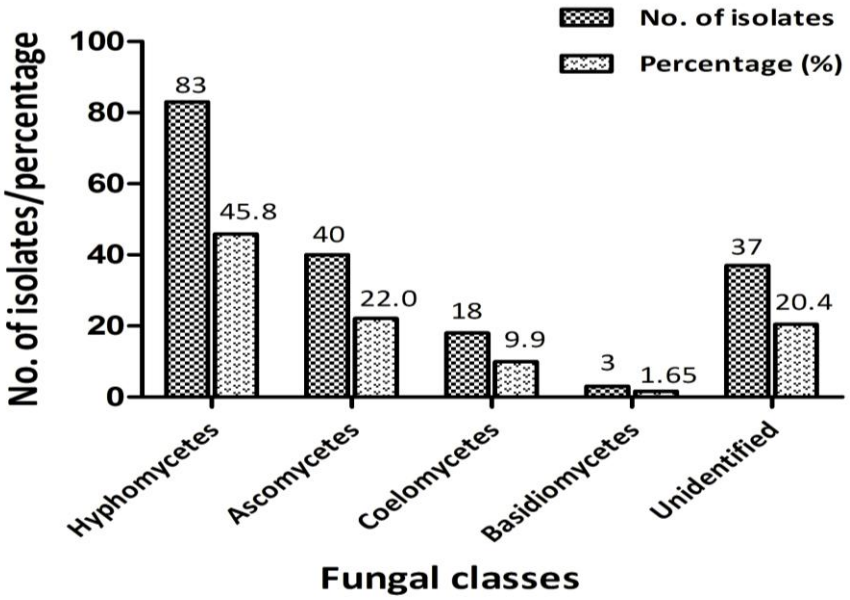

Fig 5.4: Distribution of endophytic fungal isolates in different classes of fungi

Among the taxa identified, frequency of occurrence of *Fusarium, Alternaria, Pestalotiopsis* and *Botryosphaeria* species was much higher when compared to the *Acremonium*, *Arthrinium, Phomopsis* and *Chaetomium* sp. (Table 5.3). *Fusarium* species was dominant endophytic colonizer among *Aegle marmelos*, *Cinnamomum malabaricum* and *Tinospora cordifolia.* Further, volatile organic compound (VOC) producing *Muscodor* species have also been isolated from *A. marmelos* and *C. camphora* for the first time in India (Meshram et al., 2013; Saxena et al., 2014; Saxena et al., 2015).

Table 5.3: Summary of endophytic fungal isolates obtained during the study from different medicinal plants

S. no	Endophytic fungi	*Rutaceae*	*Lauraceae*			*Apocynaceae*				*Piperaceae*	*Menispermaceae*	*Theaceae*	Total
		AM	CM	CZ	CC	CR	TMD	RS	NO	PN	TC	CS	
1.	*Acremonium* sp.	–	1	–	–	–	–	–	–	–	–	–	**1**
2.	*Alternaria* sp.	2	3	6	1	1	–	–	–	3	2	–	**18**
3.	*Arthrinium* sp.	–	–	1	–	–	–	–	–	–	–	–	**1**
4.	*Aspergillus* sp.	–	2	1	–	–	–	–	–	–	–	–	**3**
5.	*Barriopsis* sp.	2	–	–	–	–	–	–	–	–	–	–	**2**
6.	*Bionectria* sp	–	3	–	–	–	–	–	–	–	–	–	**3**
7.	*Botryosphaeria* sp.	6	–	3	–	–	–	–	–	–	–	–	**8**
8.	*Chaetomium* sp.	–	–	1	–	–	–	–	–	–	–	–	**1**
9.	*Cladosporium* sp.	–	–	1	–	1	–	–	–	–	–	–	**2**
10.	*Colletotrichum* sp.	–	–	2	–	–	–	–	–	–	1	–	**3**
11.	*Curvularia* sp	–	1	–	–	–	–	–	–	–	1	–	**2**
12.	*Fusarium* sp.	15	2	13	1	3	3	3	–	–	8	–	**48**
13.	*Glomerella* sp.	–	–	2	–	–	–	–	–	–	–	–	**2**
14.	*Gibberella sp*	–	–	–	–	–	–	1	1	–	–	–	**2**
15.	*Hypoxylon* sp.	–	–	1	–	1	–	–	–	–	2	–	**4**
16.	*Lasiodiplodia* sp.	4	1	3	–	–	–	–	–	–	–	–	**8**
17.	*Muscodor* sp.	1	–	1	5	–	–	–	–	–	–	–	**7**
18.	Mycelia sterilia	–	1	1	–	–	–	–	–	–	–	–	**2**
19.	*Neofussicoccum* sp.	2	–	–	–	–	–	–	–	–	–	1	**3**
20.	*Nigrospora* sp.	–	1	1	–	–	–	–	–	–	–	–	**2**
21.	*Penicillium* sp.	–	–	1	1	–	–	–	–	–	–	–	2
22.	*Pestalotiopsis* sp.	–	4	3	–	2	–	–	–	–	–	–	**9**
23.	*Pheoacremonium* sp.	1	1	–	–	–	–	–	–	–	–	–	**2**
24.	*Phomopsis* sp.	–	–	1	–	–	–	–	–	–	–	–	1
25.	*Schizophyllum* sp.	–	–	–	–	–	–	–	–	–	–	3	**3**
26.	*Xylaria* sp.	–	1	3	–	–	–	–	–	–	–	–	**4**
27.	Unidentified	8	14	5	–	2	1	–	1	–	5	1	**37**
	Total	**41**	**35**	**50**	**8**	**10**	**4**	**4**	**2**	**3**	**19**	**5**	**181**
	Grand Total												

AM: *A. marmelos*, CM: *C. malabaricum,* CZ*: C. zeylanicum,* CC*: C. Camphora,* CR*: C. roseus,* TMD: *T. divaricata,* RS: *R. serpentina, NO:N. oleander, PN: P. nigrum, TC: T. cordifolia, CS: C. Sinensis*

5.2 Preliminary screening of endophytic fungal isolates for XO inhibition

5.2.1 *In vitro* xanthine-NBT plate assay

Of the 181 endophytic isolates screened, culture broth of only 20.9 % endophytic fungi i.e. 38 isolates exhibited XO inhibition ≥ 40 % in the *in vitro* xanthine-NBT agar plate assay (Table 5.4). The reduction in blue zone/halo diameter ranged between 5.0-7.6 mm as compared to 12.6 mm of negative control i.e. without any inhibitor (Figure 5.5). An inverse relation was observed between the diameter of blue zone and XO inhibition.

Table 5.4: *in vitro* xanthine-NBT agar plate assay of culture broth of different endophytic fungi

S. No	Culture Code	XO Inhibition (%)	S. No	Culture Code	XO Inhibition (%)
1.	Febuxostat	$60.31^{a} \pm 0.54$	21.	#2 CSSTOT	$44.97^{defghi} \pm 0.85$
2.	Allopurinol	$55.81^{ab} \pm 1.32$	22.	#1 TCSTITPLM	$44.97^{defghi} \pm 0.85$
3.	#1 CCSTITD	$60.31^{a} \pm 0.54$	23.	##11 AMSTITYEL	$44.96^{defghi} \pm 1.66$
4.	#1048 AMSTITYEL	$59.51^{a} \pm 1.72$	24.	#1079 AMSTITYEL	$44.44^{defghi} \pm 0.75$
5.	#2 CCSTITD	$57.93^{a} \pm 0.98$	25.	#2 CCBD	$44.17^{efghi} \pm 1.06$
6.	#16 AMLWLS	$55.81^{ab} \pm 1.32$	26.	#1058 AMSTITYEL	$44.17^{efghi} \pm 1.06$
7.	#1 CSSTOT	$51.04^{bc} \pm 2.69$	27.	#7 CSSTOT	$43.64^{fghi} \pm 1.88$
8.	#3 CZLPLM	$50.01^{cd} \pm 1.05$	28.	#23 JTLSVNP	$43.64^{fghi} \pm 1.88$
9.	#6610 CZSTITBRT	$49.74^{cde} \pm 2.05$	29.	#9(b) AMSTYEL	$43.14^{ghi} \pm 1.49$
10.	#24 CZLPLM	$49.71^{cde} \pm 2.95$	30.	#53 TCSTITPLM	$43.14^{ghi} \pm 1.49$
11.	#6 AMLWLS	$49.21^{cdef} \pm 1.20$	31.	#20 CMBANEY	$43.10^{ghi} \pm 2.76$
12.	#33 CZSTITBRT	$49.19^{cdef} \pm 2.05$	32.	#23(a) RSSTNEY	$42.34^{ghi} \pm 1.44$
13.	#1639 CCSTITD	$47.89^{cdefg} \pm 0.96$	33.	#55 CMSTNEY	$42.30^{ghi} \pm 2.72$
14.	#18 CMBANEY	$47.10^{cdefgh} \pm 1.55$	34.	#105 TCSTITPLM	$41.80^{hi} \pm 2.02$
15.	#38 CZLPLM	$47.07^{cdefgh} \pm 2.73$	35.	#22 AMSTYEL	$41.77^{hi} \pm 3.06$
16.	#96 CMSTITNEY	$47.07^{cdefgh} \pm 2.73$	36.	#2123 CZSTITG	$40.74^{i} \pm 0.70$
17.	#9 AMLBRT	$44.97^{defghi} \pm 0.85$	37.	#2 PNLNEY	$40.74^{i} \pm 0.70$
18.	#2013AMBARS	$44.97^{defghi} \pm 0.85$	38.	#1104 AMSTITYEL	$40.72^{i} \pm 1.98$
19.	#12CMBANEY	$44.97^{defghi} \pm 0.85$	39.	#15 RSLBRT	$40.47^{i} \pm 0.81$
20.	#19NOBASVNP	$44.97^{defghi} \pm 0.85$	40.	#7 AMSTYEL	$40.20^{i} \pm 1.11$

*Data presented are mean ± standard deviation of three replications. Means with different superscript letters are different by Tukey's post-hoc test ($p<0.05$)

The positive control febuxostat and culture filtrate of #1 CCSTITD exhibited 60 % relative inhibition of XO in the qualitative xanthine-NBT assay suggesting it to be lead extract for further isolation of NP-SIXO. Further, culture filtrate of #1048 AMSTITYEL and #2 CCSTITD also exhibited a similar relative XO inhibition in the xanthine-NBT plate assay based on Tukey's post-hoc analysis.

Thus, these endophytic isolates could be probable source of new NP-SIXO's while #16 AMLWLS and allopurinol gave a similar relative XO inhibitory activity. Further, 37.5 % fungal isolates of *C. camphora* and 14.6 % isolates of *Aegle marmelos* were found to be potent producers of XO inhibitory moieties.

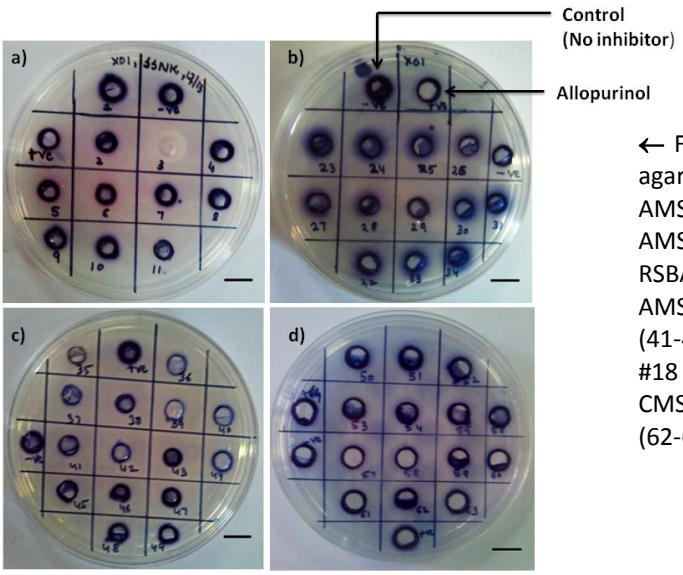

← Fig 5.5: *in vitro* XO inhibitory activity on xanthine-NBT agar plate {Well id a: (1-4): #7 AMSTYEL, (5-7): 9b AMSTYEL, (8-10): #1011 AMSTITYEL, (11): #37(b) AMSTWLS}, {b: (23-25): #1016 AMLBRT, (26-28): #16 RSBANEY, (29-31): #1006 AMLBRT, (32-34): #1069 AMSTITYEL}, {c: (35-37): #1 CSSTOT, (38-40): #1 CCSTITD, (41-43): #1048 AMSTITYEL, (44-46): #6 AMLWLS, (47-49): #18 CMBANEY}, {d: (50-52): #9 AMLBRT, (53-55): #96 CMSTITNEY, (56-58): #2 CCSTITD, (59-61): #16 AMLWLS, (62-64): #6610CZSTITBRT} {-ve: Control, +ve: Allopurinol}

5.3 Optimization of assay conditions for maximum XO activity

To develop quantitative in vitro XO inhibition assay, optimal conditions for maximum XO activity need to be determined. Hence, effect of substrate concentration, enzyme concentration, incubation time and pH were optimized by one factor at a time method.

5.3.1 Effect of substrate concentration

A significant difference in the *in vitro* enzyme activity at different xanthine concentrations was observed by one way ANOVA analysis ($F(6,12) = 75.24$, $p<0.0001$). As evident from Fig 5.6, a linear relationship was observed between substrate concentration and XO activity till 2 mM concentration. Further, Tukey's post-hoc comparisons indicated that the mean *in vitro* xanthine oxidase activity was maximum at the

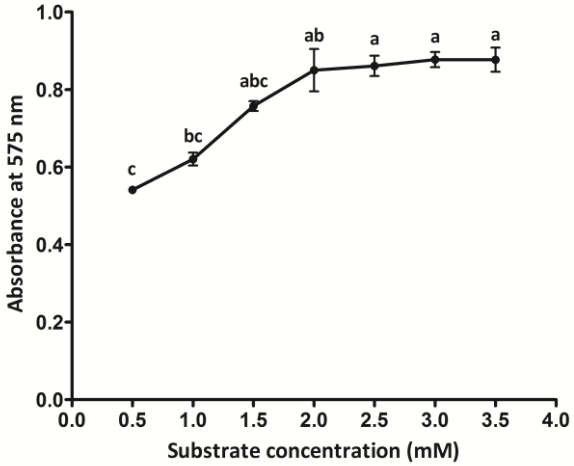

Fig 5.6: Effect of substrate concentration over *in vitro* XO activity. Data are represented Mean ± SD of three replicates. Means with different letters are significantly different by Tukey's Post-hoc test at $p<0.05$

substrate concentration of ≥ 2.5 mM. Hence, optimum substrate concentration of 2.5 mM was further taken up to achieve optimal *in vitro* XO activity.

5.3.2 Effect of enzyme concentration

Varying concentrations of enzyme exhibited a significant difference in the *in vitro* XO activity as observed by one way ANOVA analysis ($F(5,12) = 188.5$, $p<0.0001$) (Fig 5.7). Linearity between enzyme concentration and XO activity was observed till 15 mU/200 µl enzyme concentration. Further, Tukey's post-hoc analysis suggested that the mean *in vitro* XO activity was significantly different and maximum at 15 mU/ 200 µl. Hence, 15 mU of xanthine oxidase was considered to be optimum enzyme concentration to further optimize pH and Incubation time.

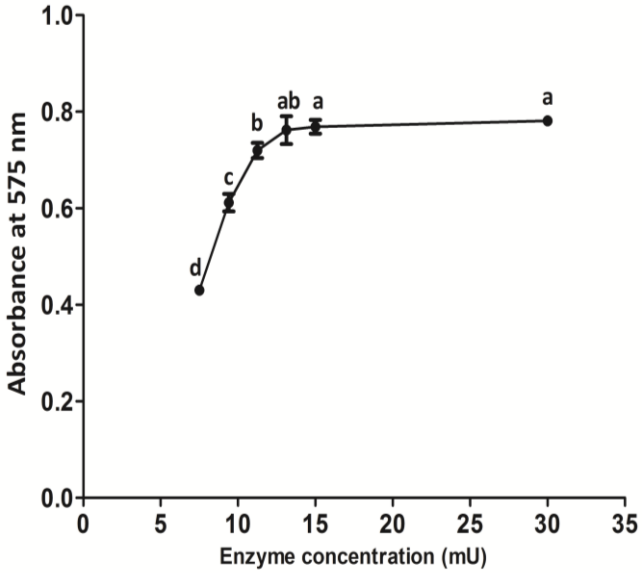

Fig 5.7: Effect of enzyme concentration over *in vitro* XO activity. Data are represented Mean ± SD of three replicates. Means with different letters are significantly different by Tukey's post-hoc test at $p<0.05$.

5.3.3 Optimization of incubation time

Incubation time had a significant effect on the *in vitro* XO activity as evident by One way ANOVA analysis ($F(12, 26) = 796.9$, $p<0.0001$). There was a linear increase in the XO activity till 2 h. However, maximal XO activity was observed at 4 h. which was further confirmed by Tukey's post-hoc analysis (Fig 5.8). Hence, 4 h incubation was selected as optimal time

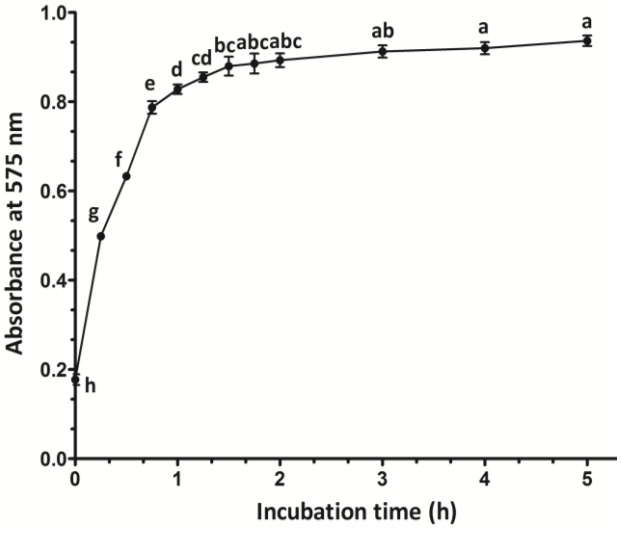

Fig 5.8: Optimization of incubation time for *in vitro* XO activity. Data are represented as Mean ± SD of three replicates. Means with different letters are significantly different by Tukey's post-hoc test at $p<0.05$.

.

5.3.4 Effect of pH

As evident from Fig 5.9, significant difference in the *in vitro* XO activity was observed at different pH levels in the range of 6.8-9.0 by one way ANOVA analysis ($F(6,14) = 453.8$, $p<00001$). There was a linear increase in the *in vitro* XO activity between pH 6.8-8.0 which was evident by Tukey's post-hoc analysis. Further, the activity remained stable between pH 7.8-8.0 and declined beyond pH 8. Hence, the optimum pH for maximum *in vitro* XO activity was found to be 7.8.

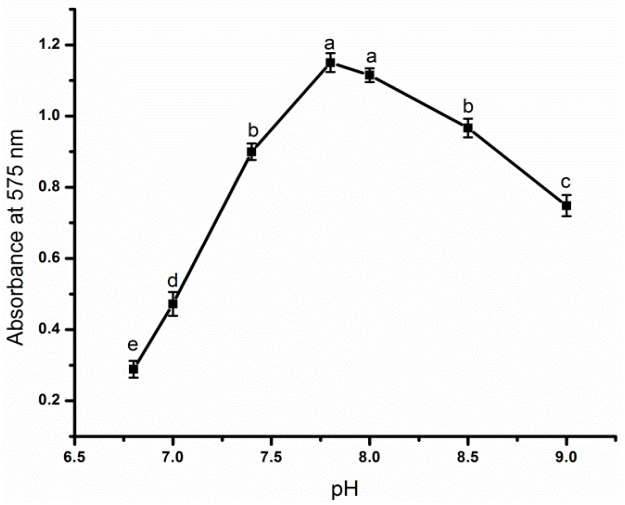

Fig 5.9: Effect of buffer pH over *in vitro* XO activity. Data are represented as Mean ± SD of three replicates. Means with different letters are significantly different by Tukey's post-hoc test at $p<0.05$.

5.4 Determination of the kinetic constants of bovine milk xanthine oxidase

The K_m and V_{max} values of xanthine oxidase (Bovine milk, Sigma Aldrich) was established to later analyze the effect of inhibitor on enzyme activity and further in determination of K_i of the inhibitor. The K_m and V_{max} was found to be 2545 µM and 0.02650 µM/min respectively as deduced from Lineweaver-Burk plot (Fig 5.10).

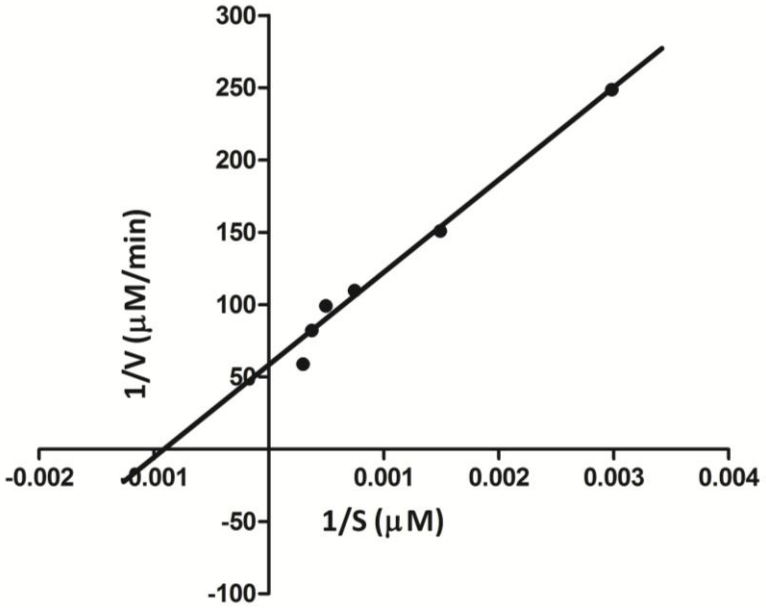

Fig 5.10: Lineweaver-Burk plot representing K_m and V_{max} (reciprocal of substrate at X-axis and reciprocal of velocity at Y-axis).

5.5 Quantitative screening of XOI producing endophytes

5.5.1 NBT microtiter plate assay

Out of the selected 38 endophytic isolates, only 14 isolates were found to exhibit promising XO inhibitory (≥ 70 %) activity (Table 5.5). In NBT microtiter plate assay, the culture filtrate of #1 CCSTITD was found to exhibit maximum XOI activity followed by #1048 AMSTITYEL, #33 CZSTITBRT and #9 AMLBRT. However, the mean *in vitro* XO inhibitory activity of febuxostat was highest and significantly different from #1 CCSTITD as per one way ANOVA analysis ($F(17, 34)= 103.0$, $p<0.0001$) followed by Tukey's post-hoc analysis. Culture filtrate of #1 CCSTITD exhibited highest relative XO inhibition which was significantly different from other endophytic fungi by Tukey's post-hoc analysis. Further, allopurinol and culture filtrate of #1048 AMSTITYEL did not exhibit any significant variation in terms of XO inhibition followed by #33 CZSTITBRT and #9 AMLBRT. The XO inhibitory potential of #2 CCSTITD, #12 CMBANEY and ##11 AMSTITYEL were not significantly different from each other but was significantly lower than #1 CCSTITD. Further, an insignificant difference in the XO inhibitory activity was observed in case of #7 CSSTOT and #1058 AMSTITYEL.

Table 5.5 *in vitro* XO inhibitory activity of fungal endophytes using NBT microtiter and Uric acid estimation assay

S.NO	Culture code	XO inhibition (%)	
		NBT Microtiter assay	Uric acid estimation assay
1.	Febuxostat	$99.24^{a} \pm 0.06$	$99.55^{a} \pm 0.78$
2.	Allopurinol	$88.13^{bc} \pm 0.18$	$86.76^{bc} \pm 0.81$
3.	#1 CCSTITD	$91.25^{b} \pm 0.83$	$88.13^{b} \pm 0.66$
4.	#1048 AMSTITYEL	$84.74^{cd} \pm 0.41$	$83.10^{cd} \pm 1.00$
5.	#33 CZSTITBRT	$82.79^{d} \pm 2.55$	$79.44^{de} \pm 1.51$
6.	#9 AMLBRT	$82.08^{d} \pm 0.57$	$77.16^{ef} \pm 1.51$
7.	#2 CCSTITD	$77.40^{e} \pm 0.77$	$73.97^{fg} \pm 0.35$
8.	# 12 CMBANEY	$77.30^{e} \pm 0.67$	$73.98^{fg} \pm 1.23$
9.	##11 AMSTITYEL	$77.40^{e} \pm 1.55$	$79.00^{e} \pm 0.55$
10.	#16 AMLWLS	$76.15^{ef} \pm 1.05$	$70.33^{ghi} \pm 1.23$
11.	#2 PNLNEY	$75.76^{ef} \pm 0.79$	$73.52^{fgh} \pm 0.50$
12.	#7 CSSTOT	$73.99^{efg} \pm 2.33$	$71.24^{ghi} \pm 1.21$
13.	#1058 AMSTITYEL	$73.98^{efg} \pm 1.88$	$69.85^{hi} \pm 1.78$
14.	#20 CMBANEY	$72.62^{fg} \pm 2.82$	$68.51^{ij} \pm 1.99$
15.	#6 AMLWLS	$71.83^{fg} \pm 1.40$	$69.41^{ij} \pm 0.47$
16.	#18 CMBANEY	$70.46^{gh} \pm 0.42$	$65.74^{j} \pm 1.83$

*Data presented are mean ± standard deviation of three replicates. Means with different superscript letters are different by Tukey's post-hoc test ($p<0.05$)

5.5.2 Uric acid estimation assay

Effective XO inhibition can also be assessed in terms of reduction in uric acid production and therefore uric acid estimation was further carried out. Of the 14 endophytic isolates shortlisted from previous NBT microtiter plate assay, culture filtrates of only 10 endophytic isolates were found to exhibit XO inhibition ≥ 70 % (Table 5.5). Febuxostat exhibited maximum XO inhibition of 99.5 % in terms of uric acid production which was closely followed by culture filtrate of #1 CCSTITD. However, there was a significant difference in the mean *in vitro* XO inhibitory activity between febuxostat and #1 CCSTITD as observed by one way ANOVA ($F(16,32)= 171.9$, $p<0.0001$) and Tukey's post-hoc analysis. An insignificant difference in the mean XOI activity of #2 CCSTITD and #12 CMBANEY was observed. However, four endophytic isolates viz. #1058 AMSTITYEL, #20 CMBANEY, #6 AMLWLS and #18 CMBANEY exhibiting >70% XO inhibition in NBT microtiter plate assay were found to exhibit XOI activity in the range of 65-70 % in uric acid estimation assay.

Hence, #1 CCSTITD was found to exhibit maximum mean XO inhibitory activity in NBT microtiter plate assay as well as in uric acid estimation assay followed by #1048 AMSTITYEL. Thus, both of these isolates were further selected for isolation and evaluation of XO inhibitors.

It was also observed that the selected isolates exhibited significantly higher mean *in vitro* XO inhibitory activity in NBT microtiter plate assay as compared to uric acid determination assay. Hence, NBT microtiter plate assay was considered to be better method for determination of XO inhibitory activity. Further, Bland-Altman analysis of NBT microtiter plate assay and uric acid estimation assay for determining *in vitro* XO inhibitory activity exhibited a significant bias of 1.03 with SD of 0.026 with 95 % limits of agreement ranging between 0.98 to 1.09 which further indicated that NBT microtiter plate assay is a better option for XO inhibition studies.

5.6 Partial purification of bioactive residue of selected endophytes by liquid-liquid extraction

The culture broth of the selected endophytic isolates i.e. #1 CCSTITD and #1048 AMSTITYEL were partially purified by using a series of solvents of different polarity. The maximum yield of crude residue was resided in the aqueous fraction left after extraction of the spent broth in both #1

CCSTITD and #1048 AMSTITYEL (Table 5.6). The organic and aqueous residues of both potential isolates were further screened for *in vitro* XO inhibitory activity using NBT microtiter plate assay for further purification of bioactive residue.

Table 5.6: Weight of residue left after solvent extraction of selected endophytic fungi

Culture Code	**Weight of the extracted residue (mg) in different solvents**					
	HEX*	DEE*	DCM*	EA*	CHL*	Aqueous
#1 CCSTITD	1.12 ± 0.0	2.27 ± 0.00	4.31 ± 0.00	2.43 ± 0.00	5.98 ± 0.00	10.12 ± 0.00
#1048 AMSTITYEL	1.96 ± 0.00	3.03 ± 0.01	2.19 ± 0.00	3.39 ± 0.00	4.46 ± 0.00	7.19 ± 0.00

* HEX- Hexane; DEE- Diethylether; DCM- Dichloromethane; CHL- Chloroform; EA- Ethyl Acetate

5.7 *in vitro* XOI screening of partially purified residues by NBT microtiter plate assay

Out of all the solvent fractions of #1 CCSTITD and #1048 AMSTITYEL tested, chloroform residue of #1 CCSTITD and #1048 AMSTITYEL exhibited maximum XO inhibition in the NBT microtiter plate assay (Fig 5.11, Table 5.7). Rest of the crude residues did not exhibit significant XO inhibition. As per One way ANOVA ($F(6,10)=4451$; $p<0.0001$) and Tukey's post-hoc analysis, maximum XO inhibition of 91.8 % was achieved by crude chloroform residue of #1 CCSTITD followed by 88.1 % XO inhibition by #1048 AMSTITYEL.

Table 5.7: *in vitro* XO inhibitory activity of crude fractions of #1048 AMSTITYEL and #1 CCSTITD

Culture Code	**XO inhibitory activity (%)**					
	HEX*	DEE*	DCM*	EA*	CHL*	Aqueous
#1 CCSTITD	$22.5^{d} \pm 1.28$	$31.0^{b} \pm 1.00$	$33.2^{b} \pm 0.24$	$27.0^{c} \pm 0.33$	$91.8^{a} \pm 0.67$	$6.1^{e} \pm 0.20$
#1048 AMSTITYEL	$15.4^{e} \pm 0.27$	$24.5^{c} \pm 0.60$	$22.0^{d} \pm 0.81$	$33.2^{b} \pm 0.67$	$88.3^{a} \pm 0.39$	$9.2^{f} \pm 0.19$

**Data represented are mean ± standard deviation of three replicates. Means with different superscript letters are different by Tukey's post-hoc test ($p<0.05$)

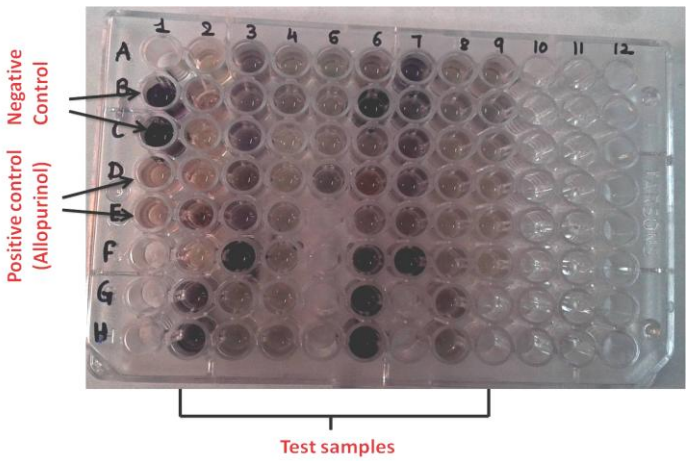

← Fig 5.11: NBT microtiter plate assay for *in vitro* XO inhibitory activity of crude fractions of #1 CCSTITD and #1048 AMSTITYEL. Well B1-C1: Negative control (no inhibitor); D1-E1: positive control (Allopurinol); fractions of #1 CCSTITD: A2-C2: CHL fraction, D2-F2: EA fraction, G2-H2: DCM fraction, A3-C3: DEE fraction, D3-F3: HEX fraction, G3-H3, A4: Aqueous fraction; Crude fractions of #1048 AMSTITYEL: B4-D4: CHL, E4-G4: EA, H4-B5: DCM, C5-D5,A6: DEE, B6-E6: HEX, F6-H6: Aqueous. A7-F7 and A8-F8: control of CHL, EA, DCM and DEE, HEX and Aqueous fraction of #1 CCSTITD respectively. G8-F9: control of all fractions of #1048 AMSTITYEL.

5.8 Purine detection test

Allopurinol and the substrate, xanthine, both formed a white precipitate on addition of silver nitrate thereby confirming them to be purine moieties. However, no white precipitate formation was observed in the chloroform residues of #1 CCSTITD and #1048 AMSTITYEL similar to that of febuxostat, thereby, confirming their non-purine nature (Fig 5.12).

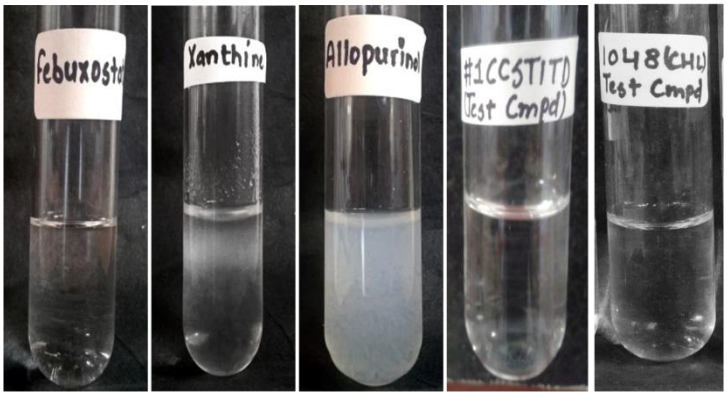

← Fig 5.12: Purine detection test of crude chloroform fraction of #1 CCSTITD and #1048 AMSTITYEL. Allopurinol and Xanthine served as positive control while febuxostat was chosen as negative control.

5.9 Determination of IC_{50} value of potential endophytic isolates

Half maximal inhibitory concentration (IC_{50}) values of crude chloroform residue of #1 CCSTITD and #1048 AMSTITYEL along with Febuxostat and allopurinol were deduced from dose response curve (Fig 5.13). The crude chloroform residue of #1 CCSTITD and #1048 AMSTITYEL exhibited IC_{50} values of 0.54 µg/ml and 0.61 µg/ml respectively. However, IC_{50} value of standard XOI, allopurinol and Febuxostat were found to be 0.93 µg/ml and 0.076 µg/ml respectively.

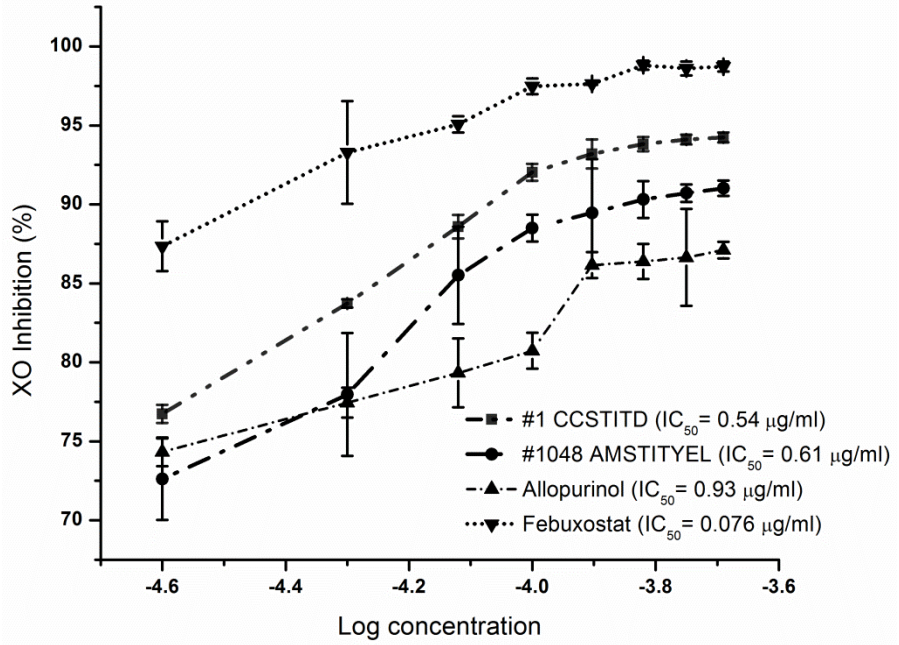

Fig 5.13: Dose response curve of chloroform residue of #1 CCSTITD and #1048 AMSTITYEL for inhibition of xanthine oxidase. Allopurinol and Febuxostat were taken as positive control

It was quite evident that the crude chloroform residue of #1 CCSTITD exhibited better dose response in comparison to allopurinol and #1048 AMSTITYEL for XO inhibition and can be further taken up for the purification of bioactive molecule.

5.10 Identification of potential endophytic fungus

The selected XO inhibitor producing endophytic fungus, #1 CCSTITD, was identified using morphotaxonomic and molecular taxonomic methods.

5.10.1 Morphotaxonomy

The endophytic fungus, #1 CCSTITD produced white, fast growing floccose to downy colonies over different culture media viz. PDA, CMA, CDA, SNA, WA and MEA (Fig 5.14). No reproductive structures like stromata, conidia, conidiogenus cells or ascospores were developed in the fungus even after incubation for over 9 weeks. The fungus did not sporulate despite being subjected to stress conditions like incubation in complete darkness or UV radiation. The macroscopic and morphological features have been summarized in Table 5.8.

Table 5.8: Morphological and microscopic features of #1 CCSTITD produced on different medium after 2 weeks

Medium	Colony colour		Colony diameter (mm)*	Appearance	Elevation	Hyphae/ coiling structures (µm)	Margin	VOC/pigment production
	Front	Back						
PDA	White	Cream	90.0 ± 0.0	Floccose	Flat	6.3 ± 1.7, 37.30	Smooth	VOCs, brown pigment
CMA	Hyaline	Hyaline	32.0 ± 2.0	Downy	Flat	3.5 ± 1.2, 71.3	Smooth	VOCs, no pigment
CDA	White	Off-white	46.6 ± 2.5	Floccose	Flat	6.5 ± 0.9, 149.6	At center	VOCs, no pigment
SNA	White	Hyaline	67.0 ± 2.6	Floccose	Flat	6.6 ± 1.4, 93.8	Smooth	No VOCs, no pigment
WA	White	Hyaline	23.0 ± 3.0	Downy	Flat	6.2 ± 1.3	Smooth	No VOCs, no pigment
MEA	White	Cream	90.0 ± 0.0	Floccose	Flat	7.4 ± 1.7, 134	Smooth	VOCs, no pigment

* Data presented are mean ± standard deviation of thirty readings

The fungus formed hyphal coils which characteristically appeared over all the medium. However, over MEA, the fungus produced a thick mycelium which formed a fishing net like structure. The fungus emanated a strong fruity odour specifically over PDA, MEA and CDA which is due to the presence of volatile organic compounds (VOCs).

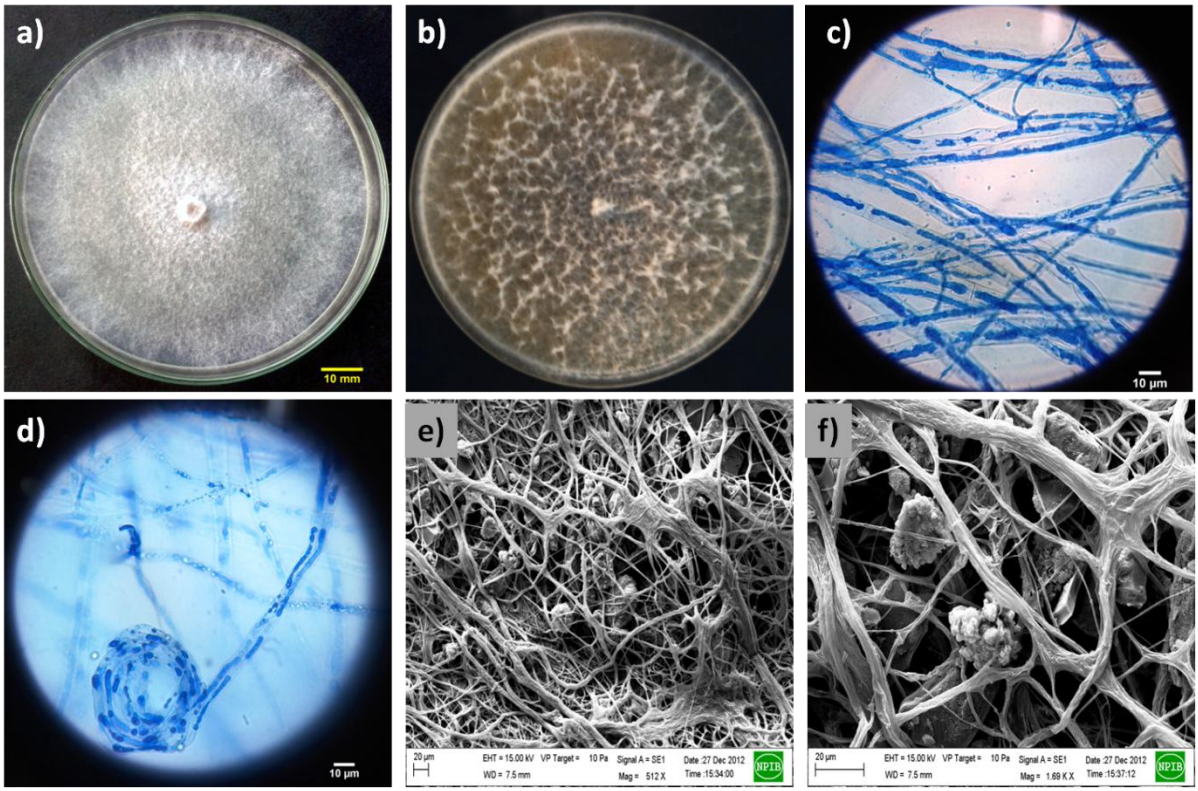

Fig 5.14: Morphological features of #1 CCSTITD after seven days of growth (a-b): Culture characteristics on PDA, (c): Hyphae stained with lactophenol cotton blue on CDA, (d): Hyphae forming coils on SNA, (e-f): SEM of the mycelial arrangement and of cauliflower-like structures.

5.10.2 Scanning electron Microscopy

The scanning electron micrographs of #1 CCSTITD exhibited the characteristic features of *Muscodor* species i.e. long, sterile and right-angled ropy hyphae that terminate into coils. The hyphae further fused to form a ropy mycelium. The isolate also produced cauliflower-like structure but did not produce any sporulating structures (Fig 5.14 e-f). #1 CCSTITD differs in morphology from the other type strains of *Muscodor. Muscodor crispans* and *M. sutura* form a similar cauliflower-like structure but they differ in mycelial arrangement, with *M. crispans* forming a wavy hyphal mass and *M. sutura* showing a 'knitting pattern' mycelium. *Muscodor roseus, M. cinnamomi, M. musae, M. oryzae* and *M. suthepensis* have ropy mycelia with coils but lack cauliflower-like structures. *Muscodor yucatanensis* and *M. equiseti* have ropy mycelia with swollen hyphae. *Muscodor albus* and *M. vitigenus* have straight hyphae without any coils or cauliflower-like structures. Hence, on the basis of morphology, colony characteristics and volatile organic odour, it was tentatively identified as *Muscodor* sp (Table 5.9).

5.10.3 Molecular taxonomy

The endophytic fungus was exhibiting characteristic features of *Muscodor* species morphologically as well as by scanning electron microscopy. Hence, for further speciation the ITS-rDNA was amplified from the purified fungal genomic DNA (concentration 85 ng/µl). The purity of the DNA (A_{260}/ A_{280}) exhibited a ratio of 1.78. The amplicon of ITS1-5.8S-ITS2 region of rDNA was found to be pure (Fig 5.15a) and the size was found to be ranging between 450-550 bp (Fig 5.15b). The sequence data was submitted in GenBank under accession number JQ409997. BLAST analysis of the ITS sequence exhibited close homology with *Muscodor* species with 97 % sequence identity confirming that the fungus belongs to *Muscodor* genus (Table 5.8).

Table 5.10. BLAST search summary of homology analysis of ITS1–5.8S–ITS2 sequence of #1 CCSTITD

GenBank Accession No.	Organism	Query Coverage (%)	Sequence Similarity (%)	e-value
JQ409997	#1 CCSTITD	Present study		
KU659026	*Muscodor sp.* E6011C	98	97	0.00
KU659025	*Muscodor sp.* E3816A	98	97	0.00
KU659024	*Muscodor sp.* E3801A	98	97	0.00
KU204610	*Muscodor albus* INBio:613C	98	97	0.00
LC132715	*Muscodor oryza**e*** JCM 18231	98	97	0.00
KU683934	*Xylariaceae sp.* ARIZ FL1963	98	97	0.00
KF229754	*Muscodor sp.* VC-01	98	97	0.00
JX298899	*Xylariaceae sp*. M26 XS-2012	98	97	0.00
JX089323	*Muscodor musae* CMU-MU3	98	97	0.00
JX089321	*Muscodor oryzae* CMU-WR2	98	97	0.00
JQ760598	*Xylariaceae sp* FL0969	98	97	0.00
JQ760221	*Xylariaceae sp* FL0502	98	97	0.00
JN426991	*Muscodor sp.* AB-2011	98	97	0.00
HM034857	*Muscodor albus* isolate 9-6	98	97	0.00
HM473081	*Muscodor albus* CMU44	98	97	0.00

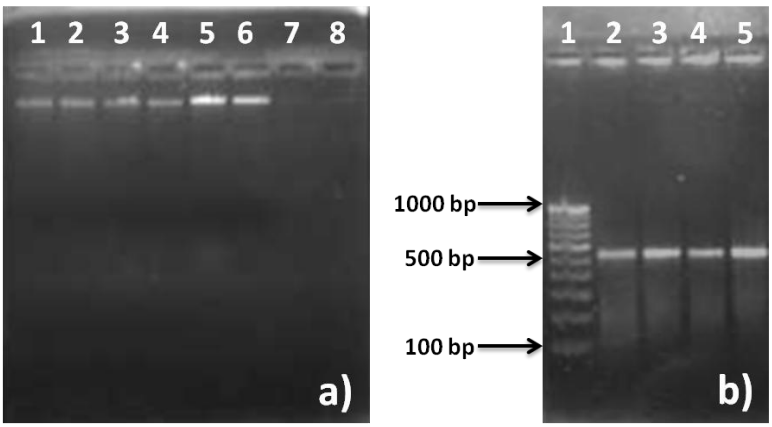

← Fig 5.15: (a) Genomic DNA of #1 CCSTITD (b) ITS rDNA amplification of #1 CCSTITD; Lane 1: 100 bp ladder, Lane 2-5: ITS1–5.8S–ITS2 (~500 bp) amplicon.

For accurate speciation, the phylogenetic tree was constructed based on ITS1-5.8S-ITS2 region which was resolved into two clades- Clade I with *M. albus, M. cinnamomi*, *M. crispans*, *M. musae, M. oryzae* and *M. roseus*. #1 CCSTITD and *M. suthepensis* were appearing as a basal sister to the rest of clade I with 99 % bootstrap support. *Muscodor equiseti, M. fengyangensis, M. sutura, M. vitigenus* and *M. yucatanensis* grouped in Clade II. *Xylaria arbuscula* and *Peziza badia* were taken as outgroup (Saxena et al., 2014) (Fig 5.16).

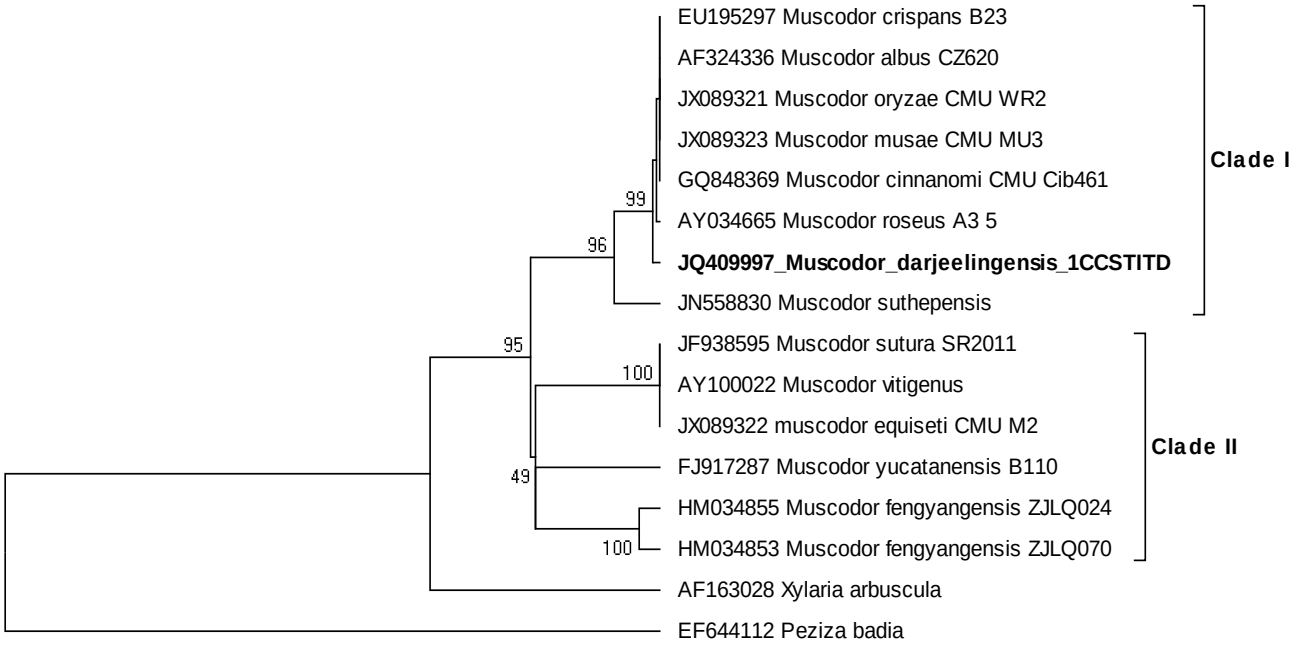

Fig 5.16: The Neighbor-joining tree based on ITS1-5.8S-ITS2 region. The optimal tree with the sum of branch length = 0.68548993 is shown. The percentage of replicate trees in which the associated taxa clustered together in the bootstrap test (1000 replicates)

Thus, the potential endophytic isolate on the basis of molecular and morphological taxonomy was identified as a novel species of *Muscodor,* named as *Muscodor darjeelingensis* sp. nov. (Saxena et al., 2014). Since then many novel species have been added to this genus. Till date, 19 species have been added to this genus from all over the world. ITS rDNA region sequence analysis is most commonly used method for the identification of novel *Muscodor* species. In the present era, Multi-locus sequence based taxonomy (MLST) is commonly adopted for precise speciation of various fungi (Donnell et al., 2012; Marques et al., 2013). However, the strategy is limited by the lack of sequence information from different nuclear regions of *Muscodor* species (Yuan et al., 2011).

Table 5.9: Comparison of morphological and microscopic characteristics of *Muscodor* type species isolated from different geographical regions

***Muscodor* species**	**Host Plant**	**Location**	**Mycelial growth**	**Major VOCs**	**Hyphal growth (at colony front)**	**Pigment production**
M. albus (2001)	*C. zeylanicum*	Honduras, South America	Rope Like	1,2,3,4	Straight	None
M. vitigenus (2002)	*P. paullinioides*	Peruvian, Amazon	Rope Like	3	Straight	None
M. roseus (2002)	*G. pteridifolia*	Northern-Australia	Rope-like, erumpent pie-shaped sectors	5,6,7	Intertwining, rope-like, (coiled)	Red (in light)
M. crispans (2008)	*A. ananassoides*	Bolivian Amazon basin	Rope-like with cauliflower-like bodies	1,2	Heavily wavy new growth	Raddish (in light)
*M .yucatanensis (*2009)	*B. simaruba*	Yucatan peninsula, Mexico	Rope-like with coiled hyphae	8	Multiple rope-like strands interwine to form coils	None
M. fengyangensis (2010)	*A. chinesis*	Fengyangshan Nature reserve, China	Rope-like with coiled hyphae	3,4	Straight	Yellow
M. cinnamomi (2010)	*C. bejolghota*	Doi suthep-pui, National Park, Thailand	Rope-like with coiled hyphae	1,2, 9	Straight	Pale Orange (in light)
M. sutura (2012)	*P. trifidi*	Columbian tropical Pacific rainforest	Rope-like bands extra-cellular bodies	1,2,10	Suture-like pattern on PDA	Reddish (in Dark)
M. musae (2013)	*M. acuminata*	Doi suthep-pui, Thailand	Rope-like with coils structure	11	Straight hairy mycelium	None
M. oryzae (2013)	*O. rufipogon*	Chiang Mai, Thailand	Rope-like with coils structure	12	Straight	Orange
M. suthepensis (2013)	*C. bejolghota*	Doi-Suthep Pui, Thailand	Rope-like with coils structure	11	Straight	Pale pink in light
M. equiseti (2013)	*E. debile*	Chiang Mai, Thailand	Rope-like coils and swollen cell	11	Cottony-like pattern	None
M. kashayum (2013)	*A. marmelos*	Wayanad wild life sanctuary, Kerala, India	Rope like	13,14, 15,16, 17	Straight	none
***M. darjeelingensis* (2014)**	***C. camphora***	**Darjeeling, West Bengal, India**	**Rope like with cauliflower like structures**	**14,15, 17**	**Straight**	**Brown**
M. strobelii (2014)	*C. zeylanicum*	BRT wildlife sanctuary, Karnataka, India	Rope-like, slimy; Zinnia-bud-like bodies	17,18, 19	Straight	Pale Yellow (in light)
M. tigerii (2015)	*C. camphora*	Darjeeling, West Bengal, India	Rope like with swollen hyphae and coils	17,20	Straight	Brown

(1): Propanoic acid; (2): 2-methyl, 2-nonanone; (3): Naphthalene; (4): Azulene derivatives; (5): 2-butenoic acid, Ethyl ester (6): 1,2,4-tri-methyl-benzene; (7): 2-nonadiene; (8): 1R,4S,7S,11R-2,2,4,8-Tetramethyl-tricyclo[5.3.1.0(4,11)]undec-8-ene, Caryophyl-lene, Aroma-dendrene; (9): Methyl ester, b-humulene; (10): Thujopsene; (11): 2-methylpropanoic acid; (12): 3-Methylbutan-1-ol; (13): 3-cyclohexen-1-ol,1-(1,5-dimethyl-4-hexenyl)-4-methyl; (14): 1,6-dioxacyclododecane-7,12-dione; (15): 2, 6-Bis (1, 1-dimethylethyl)-4-(1-oxopropyl) phenol; (16): 2,4-di-tert-butylthiophenol; (17): 4-octadecylmorpholine; (18): Tetraoxa-propellan; (19): Aspido-fractinine-3-methanol; (20): 1 - Te t r a d e c a n a m i n e ,N, N - d i m e t h y l a n d 1 , 2 - Benzenedicarboxylic acid, mono(2-ethylhexyl) ester

5.10.4 Secondary structure Prediction

Secondary structure prediction of ITS rDNA region appears to be a prominent method of delineating species identification and enhancing phylogenetic resolution (Schulz and Wolf, 2009). The sequence length of each marker region ranges from 158-250 nucleotides for ITS1, 157 nucleotides for 5.8S and 125-216 nucleotides for ITS2 region for all *Muscodor* species. The ΔG required for the formation of secondary structure of different *Muscodor* species ranges from -44.80 to -101.20 kcal/mol and -38.50 to -67.10 kcal/mol for ITS1 and ITS2 regions respectively (Table 5.11, Appendix A). The sequence length of ITS1, 5.8S and ITS2 region of *Muscodor darjeelingensis* was found to be 171, 157 and 134 nucleotides respectively.

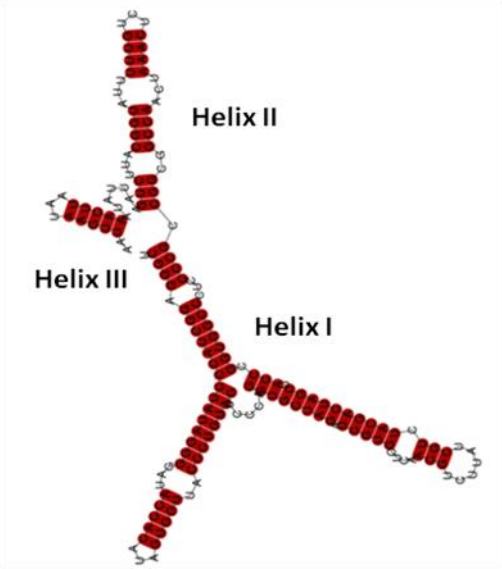

Fig 5.17: The predicted minimum free energy (MFE) secondary structures of ITS1 region of *M. darjeelingensis.*

The ΔG required for the formation of secondary structure of ITS1 region of *M. darjeelingensis* was -60.70 kcal/mol. The ITS1 region of *M. darjeelingensis* produced X-shaped, three-helix core structure (Fig 5.17) differing from other reported type species of *Muscodor* genus due to number of helices, varying nucleotide length of helices as well as the presence and absence of additional bulges and internal loops (Fig 5.18, 5.19, 5.20, Appendix A).

The 5.8S region of all *Muscodor* species spanning 157 nucleotides was highly conserved. The ΔG required for the formation of secondary structure was -44.20 kcal/mol and GC content was estimated to be 43.94 %. The predicted secondary structure comprised of a central internal loop from which four helices emerged (Fig 5.21). All the three motifs viz. M1, M3 and M2 reported in case of angiosperms were identified in the 5.8S region of all *Muscodor* species as (base substitutions are highlighted in bold) M3: (5'-UUUGAACGCA-3'), M1 (5'-CGAUGAAGAACG**C**AGC-3') and M2 (5'-GAAUUGCAGAAU**U**C-3'). There was a single base substitution in motif M1 (C>U) and M2 (U>C).

The ΔG required for the formation of secondary structure of ITS2 region of *M. darjeelingensis* was -46.40 kcal/mol. *M. darjeelingensis* produced a long double helix comprising U-U, A-C mismatch bulges (Fig 5.21) similar to that of *M. kashayum* and *M. tigerii*. However, these species differed from each other due to variation in nucleotide sequence in the small out bulges of unpaired nucleotides. Rest of the members of *Muscodor* genus formed distinct secondary structures differing from each other in terms of number and shape of helices, mismatched and unpaired nucleotides (Fig 5.22, 5.23, 5.24, Appendix A).

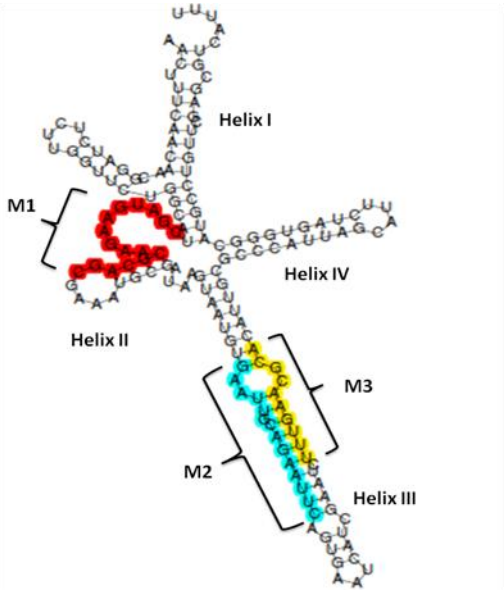

Fig 5.21: The predicted consensus secondary structure of conserved 5.8S region of *Muscodor* species. The three conserved motifs (M1, M2 and M3) were detected and highlighted in yellow color for M3, red for M1 and blue for M2.

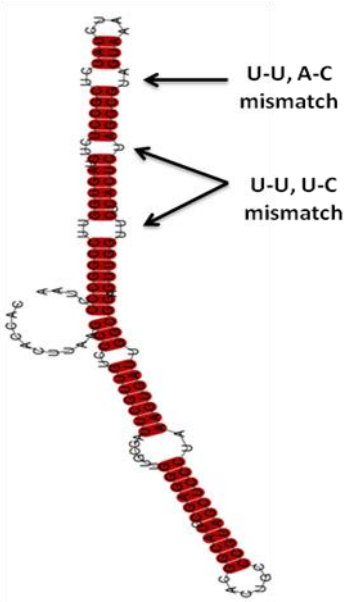

Fig 5.25: The predicted minimum free energy (MFE) secondary structures of ITS2 region of *M. darjeelingensis*

5.10.5 Phylogenetic tree reconstruction

The Profile Neighbor Joining (PNJ) tree based on the combined sequence-structure dataset of 19 different type species and strains of *Muscodor* genus resolved the *M. fengyangenesis* species as distinct monophyletic group (Group III). Twelve strains of *M. albus* did not clubbed into a single group (Group I). However, *Muscodor sp.* with accession number KF229762 clustered in group II along with *M. vitigenus*, *M. equiseti* and *M. yucatanensis* when using combined sequence and structure information for phylogenetic study.

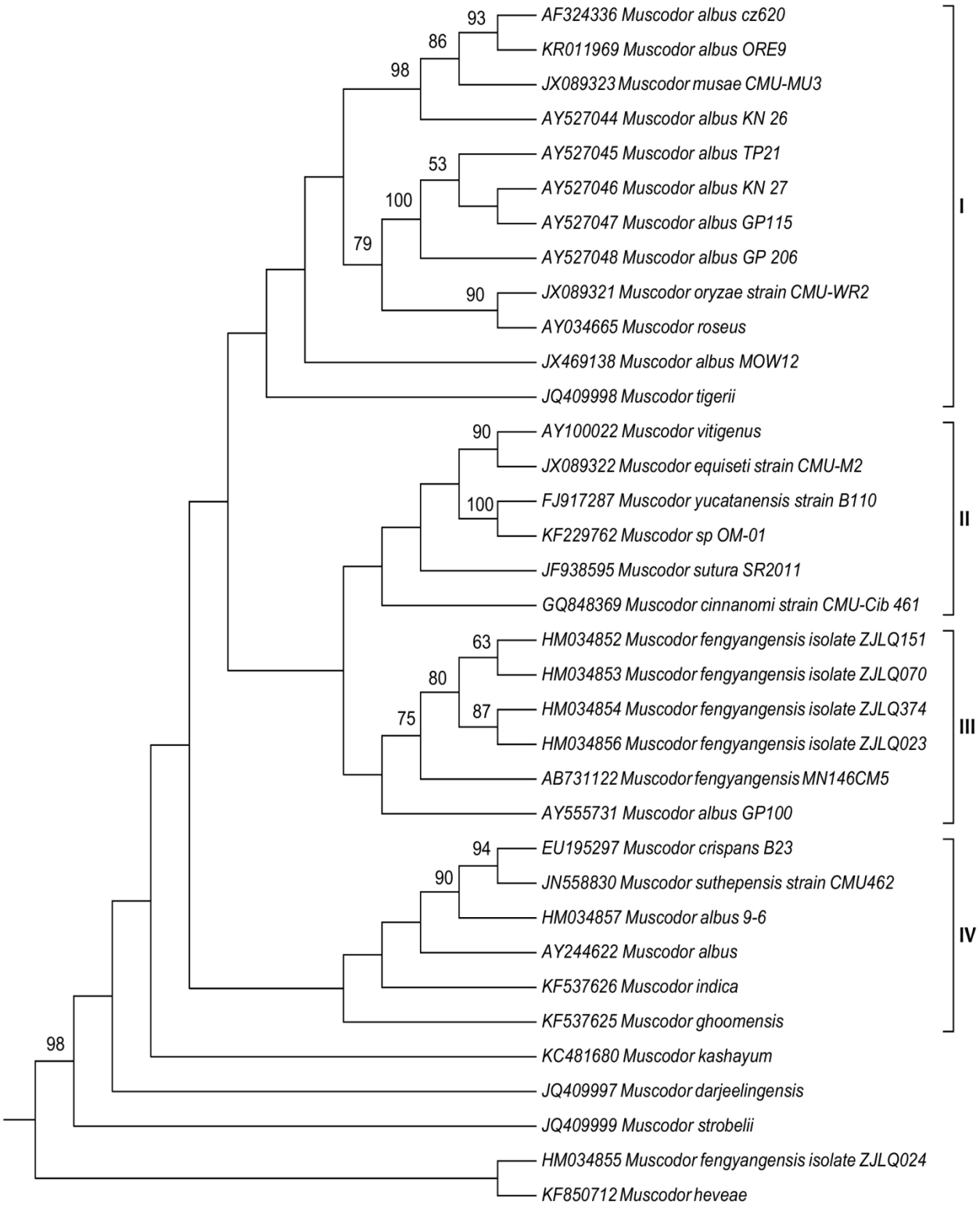

Fig 5.26: Profile Neighbor Joining (PNJ) tree of *Muscodor* species based on ITS sequence and structure information. The tree was generated by using General Time reversible model of evolution with 1000 bootstrap replicates.

Further, AY555731, AY244642 and HM034857, formally belonging to *M. albus,* emerged as a sister clade from group III and group IV respectively. Only *M. crispans* and *M. suthepensis* were

clustered significantly with high bootstrap support value in group IV while all other species viz. *M. ghoomensis*, *M. indica*, *M. kashayum*, *M. darjeelingensis*, *M. strobelii* and *M. heveae* were emerging out as sister clade (Fig 5.26). This also proved that *M. darjeelingensis* is a novel species isolated from *Cinnamomum camphora* in Darjeeling (Assam).

Hence, the use of an integrated sequence-structure based alignment along with phylogenetic tree formation appeared to be useful for accurate speciation thereby, improving the precision of phylogenetic analysis for identification of novel member species of *Muscodor* genus**.**

5.11 Optimization of culture conditions for optimal *in vitro* XO inhibitory activity

5.11.1 SSF in vitro XO inhibition

Out of the four agro-industrial residues evaluated for solid state production of XO inhibitor by #1 CCSTITD, none of the residue was found to be active against xanthine oxidase.

5.11.2 Selection of suitable medium for production of XO inhibitor

As evident from Fig 5.27, *in vitro* XO inhibitory activity of crude chloroform residue of #1 CCSTITD growing over different growth media were found to be significantly different by one way ANOVA ($F(6,14)=132.4$, $p=<0.0001$). According to Tukey's post-hoc analysis, mean XO inhibitory activity of crude chloroform residue obtained from PDB was highest and was exhibiting insignificant difference with allopurinol. Further, a significant difference in the XO inhibitory activity was observed between the chloroform residue obtained from PDB and MEB followed by CDB. No XO inhibitory activity was recorded by the crude chloroform residue obtained from RB, YEPDB and TSB. Hence, PDB was selected as a medium of choice for the production of xanthine oxidase inhibitor by #1 CCSTITD.

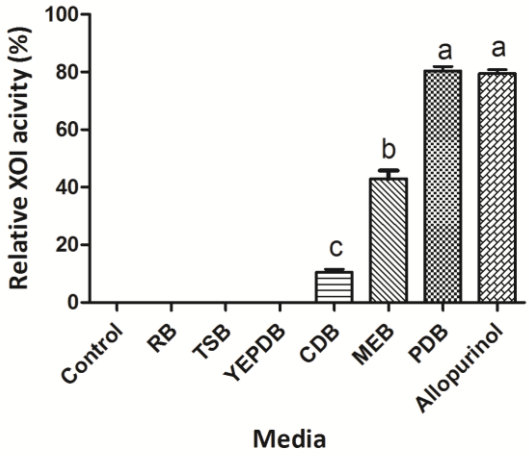

Fig 5.27: *in vitro* XO inhibitory activity of crude chloroform residue extracted from different media viz. PDB, MEB, CDB, RB, TSB and YEPDB. Data represented are mean ± SD values. Means with different letters are significantly different by Tukey's post-hoc test at $p<0.05$

5.11.3 Correlation between XO inhibitory activity and fungal biomass

As evident from Fig 5.28, XO inhibitory activity of #1 CCSTITD was growth associated till 7th day of incubation after further incubation the decline in XO inhibitory was observed with increasing biomass concentration.

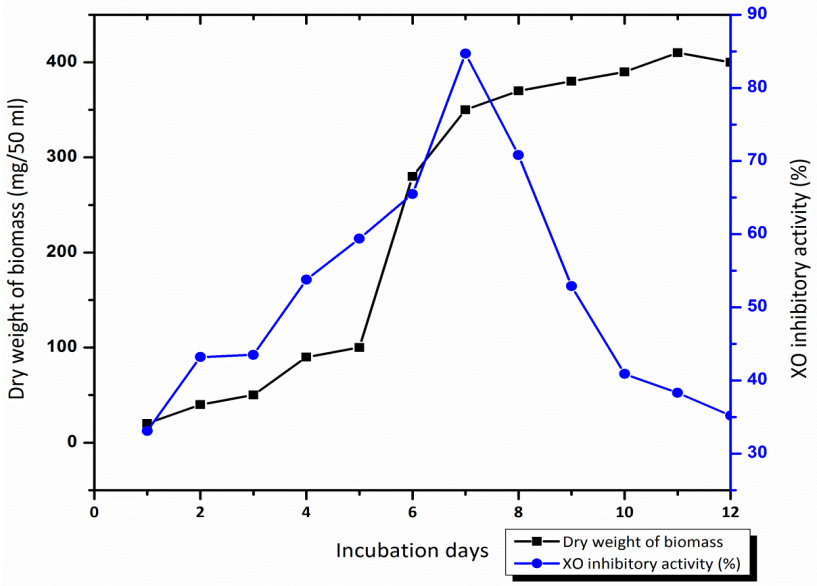

Fig 5.28: Correlation between biomass production and percentage XO inhibitory activity of #1 CCSTITD

5.12 Phytochemical testing of bioactive residue

The phytochemical testing of crude residue revealed the presence of alkaloids, carbohydrates, Flavanoids, glycosides and terpenoids (Table 5.12). The crude residue indicated the presence of alkaloids by forming a red precipitate while blue coloration/precipitate indicated the presence of amino acids/glycosides. A pinkish brown ring in the reaction mixture indicated the presence of terpenoids (Fig 5.29).

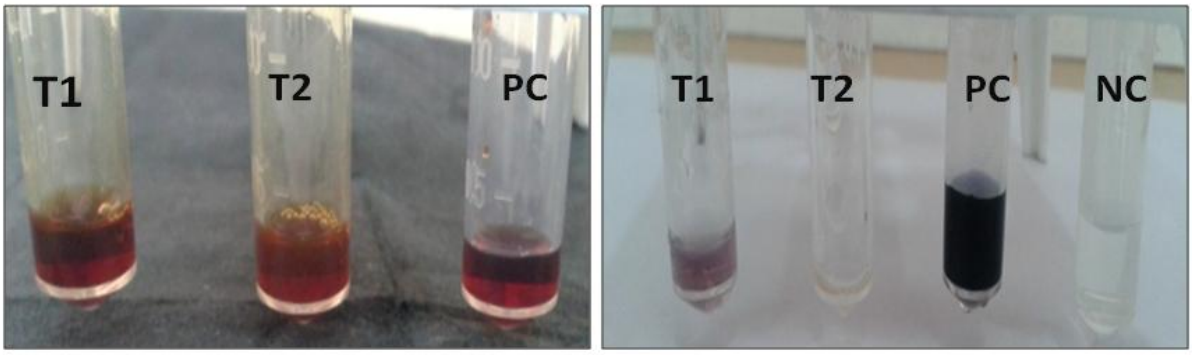

Fig 5.29: Phytochemical testing of crude chloroform residue of #1CCSTITD. a) Alkaloids test b) Ninhydrin test. T1 stands for crude chloroform residue of #1 CCSTITD, T2: crude residue of #1048 AMSTITYEL, PC: positive control, NC: Negative control

Table 5.12: Phytochemical nature of crude residue

Phytochemical test	Crude bioactive residue
Alkaloid	++
Amino acid	+
Anthraquinone	-
Carbohydrate	+++
Fats	-
Flavanoid	+
Glycoside	+
Resin	-
Saponin	-
Steroid	-
Tannin	-
Terpenoid	+

5.13 Purification and characterization of bioactive residue

5.13.1 TLC fractionation of bioactive residue

The crude chloroform residue of #1 CCSTITD (dark green in color) was subjected to TLC using different combinations of mobile phases (Table 5.13). Dichloromethane: Methanol in the ratio of 9.8:0.2 resolved the crude chloroform residue of #1 CCSTITD into 11 bands with R_f values 0.92, 0.88, 0.83, 0.81, 0.58, 0.52, 0.49, 0.37, 0.33, 0.26, 0.20 visualized under UV light (254 nm/ 365 nm) and iodine chamber over silica gel plates (Fig 5.30).

Table 5.13: Different mobile phases used for separation of crude residue of #1 CCSTITD on TLC

Solvents used	Ratio (v/v)	No of bands
Hexane: Ethyl acetate	1: 1	4
Hexane: Ethyl acetate	1.5: 0.5	5
Chloroform: Methanol	9.5: 0.5	6
Chloroform: Methanol	9.7: 0.3	7
Chloroform: Methanol: Ethyl acetate	9.7: 0.3: 2 drops	8
Chloroform: Methanol: Ethyl acetate	9.7: 0.3: 5 drops	6
Petroleum ether: Ethyl acetate	1.5: 0.5	4
Dichloromethane: Methanol	9.6: 0.4	7
Dichloromethane: Methanol	9.8: 0.2	11
Dichloromethane: Acetonitrile	9.8: 0.2	8
Ethyl acetate: acetic acid	9: 1	3

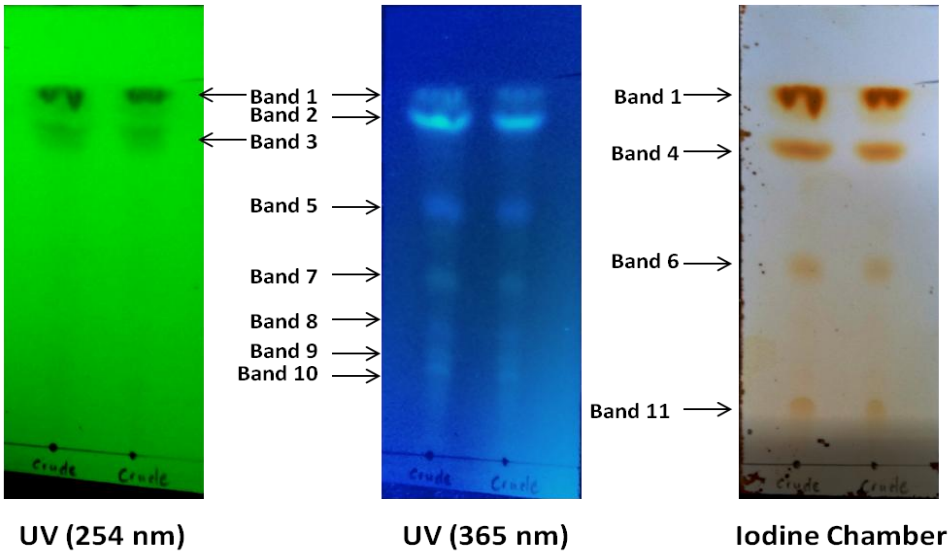

Fig 5.30: TLC profile of crude chloroform residue of #1 CCSTITD using dichloromethane: methanol (9.8:0.2) as mobile phase. The R_f values of Band 1- 11 was ranging between 0.92 to 0.20.

5.13.2 Purification by silica gel column chromatography

Based on the optimized mobile phase for fractionation of crude chloroform residue of #1 CCSTITD, the mobile phase for silica gel column chromatography was chosen. Different gradients (0.1 %) of dichloromethane: methanol starting from 100:0 to 0:100 were run and 500 column fractions (volume- 2 ml) were obtained which were further were clubbed into 18 fractions based on the TLC profile and were subjected to XO inhibitory assay (Fig 5.31). Of all the fractions, fraction 9 (7 mg) was found to exhibit potent XO inhibition using quantitative NBT assay as per One way-ANOVA ($F(19,18)= 37.28$, $p<0.0001$) and Tukey's post-hoc analysis (Table 5.14).

Table 5.14: Relative XO inhibition (%) of 18 column fractions using NBT microtiter plate assay

Fraction Number	XO inhibition (%)	Fraction Number	XO inhibition (%)
F-1	$34.22^{b} \pm 1.00$	F-10	$33.92^{b} \pm 0.71$
F-2	$29.98^{b} \pm 0.48$	F-11	$30.93^{b} \pm 3.16$
F-3	$23.58^{b} \pm 2.12$	F-12	$38.13^{b} \pm 5.32$
F-4	$34.76^{b} \pm 7.60$	F-13	$39.71^{b} \pm 1.18$
F-5	$32.79^{b} \pm 5.87$	F-14	$26.24^{b} \pm 2.79$
F-6	$33.83^{b} \pm 3.55$	F-15	$25.88^{b} \pm 2.22$
F-7	$41.08^{b} \pm 7.27$	F-16	$36.32^{b} \pm 2.55$
F-8	$34.44^{b} \pm 5.84$	F-17	$38.16^{b} \pm 2.22$
F-9	**$94.06^{a} \pm 1.10$**	F-18	$23.39^{b} \pm 1.24$

Data represented are mean ± SD of two replicates. Means with different superscript letters are different by Tukey's post-hoc analysis.

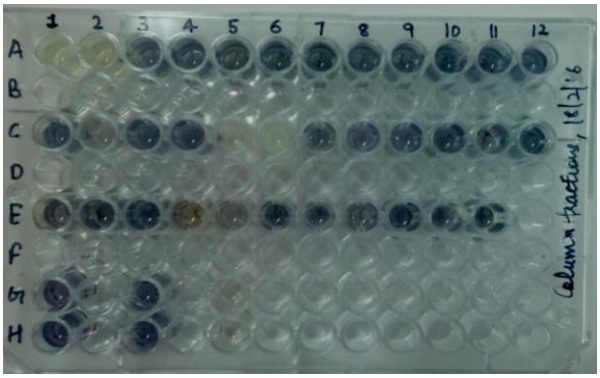

← Fig 5.31: *in vitro* NBT microtiter plate assay of 18 column fractions. Well A1-A2: Fraction 1; A3-A4: Fraction 2; A5-A6: Fraction 3; A7-A8: Fraction 4; A9-A10: Fraction 5; A11-A12: Fraction 6; C1-C2: Fraction 7; C3-C4: Fraction 8; C5-C6: Fraction 9; C7-C8: Fraction 10; C9-C10: Fraction 11; C11-C12: Fraction 12; E1-E2: Fraction 13; E3-E4: Fraction 14; E5-E6: Fraction 15; E7-E8: Fraction 16; E9-E10: Fraction 17; E11-E12: Fraction 18; G1,H1: Negative control (No inhibitor); G3,H3: Chloroform control; G5,H5: Positive Control (Allopurinol).

Further, fraction 9 exhibited highest XO inhibition of 89.85 % in Uric acid estimation assay as per One-way ANOVA ($F(16,32)= 16050$, $p<0.001$)). Bioactive fraction 9 (pale yellow color) was further analyzed on silica gel TLC plates using various combinations of solvent systems and showed single spot on TLC plate (Fig 5.32). The obtained R_f value in different mobile phases are listed in Table 5.15. The melting point was found to be > 250˚C.

Table 5.15: Different solvent system used for TLC analysis of fraction 9

Solvent system	**Ratio**	**R_f value**
Dichloromethane : Methanol	9.6:0.4	0.935
Hexane : Ethyl acetate	6:4	0.444
Dichloromethane : Acetonitrile	9.8:0.2	0.592
Chloroform : Methanol	9.8:0.2	0.6
Chloroform : Acetonitrile	9.8:0.2	0.307
Toluene : ethyl acetate	9.6:0.4	0.25
Ethyl acetate : acetic acid	9.2:0.8	0.903
Ethyl acetate : acetic acid	9.8:0.2	0.878

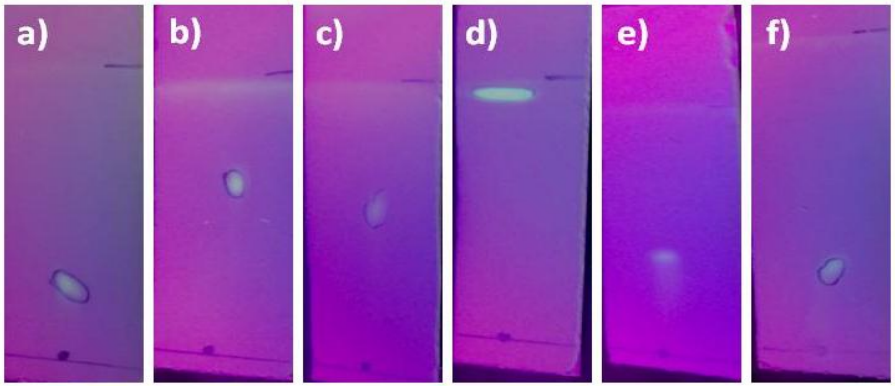

Fig 5.32: TLC analysis of bioactive fraction 9 on different solvent systems. a): Chloroform: Acetonitrile; b): Chloroform :Methanol; c): Dichloromethane:Acetonitrile; d) Dichloromethane:Methanol; e) Hexane: ethyl acetate; f): Toluene: Ethyl acetate.

5.14 Structure elucidation of bioactive fraction

The structure of bioactive fraction 9 was elucidated by LC/ESI-MS, NMR (H^1, C^{13}) and IR spectroscopic techniques. A single peak at 3.40 min was obtained in LC analysis (Fig 5.33). NMR (C^{13}) revealed the presence of carboxyl group due to resonance peak at 171.32 ppm (Fig 5.34). The low peak intensity at 171.32 ppm is attributed to the presence of quaternary carbon. In Proton-NMR (H^1- NMR), signal peak of the solvent (Chloroform-d) used for sample was observed at 7.24 ppm. Proton NMR spectra was found to be quite complex due to complex splitting pattern of large number of protons. A number of low intensity peaks were observed in the region of 5.8-7.0 ppm which represents olefenic protons [(C7,7'), C(8,8'), C(10,10'), C(11,11') C12,12'), C(14,14'), C(15,15')] associated with π-electron conjugated chain (Fig 5.35). The peaks ranging from 1.0 to 2.5 ppm were assigned to the protons of saturated methyl carbons [C(2,2'), C(16,16'), C(17,17'), C(18,18'), C(19,19'), C(20,20')]. The signals at 0.87, 1.27 and 2.20 ppm corresponds to the protons associated with methyl ($-CH_3$) groups at C17, C16 and C18 respectively. The resonance peak at 4.14 ppm was assigned to the axial proton at C(3,3') corresponding to presence of hydroxyl (–OH) group.

Further, the IR spectra of the bioactive fraction showed the presence of different functional groups viz. C-H stretch (2853.28 cm^{-1}, 2923.68 cm^{-1}), carboxyl group (1713.97 cm^{-1}) and CH_2 bending (1460.28 cm^{-1}) (Fig 5.36). From NMR and IR analysis, it was hypothesized that the structural characteristics of the bioactive fraction was found to be similar to that of Lutein. To further confirm the hypothesis, the mass spectrum of the bioactive fraction under study was compared to that of Lutein. The ESI-MS spectrum of the fraction was observed in the positive ion mode and the molecular mass of the bioactive fraction was found to be 569.35 (Fig 5.37) and this corresponds to the molecular weight of Lutein i.e. 569. The base ion peak, $[M+H-CH_3/H_2O]^+$, at *m/z* 553.35 with highest abundance (100 %) was observed corresponding to the loss of methyl group or hydroxyl group. A series of peaks viz. m/z: 313.17 (45 %), 531.6 (40 %), 288.4 (5 %) were also observed which either corresponds to cleavage within the conjugated double bond system or due to 3-hydroxy-ε-ring end-group formation. The observed mass spectrum was consistent with those reported for

Lutein. Based on NMR, IR and Mass spectrometry analysis, the structural features of the bioactive fraction 9 was identical to that of Lutein, a carotenoid pigment as per the available literature (Breemen et al., 1995; Boonnoun et al., 2012; LaFountain et al., 2013).

Hence, the chemical name of the fraction 9 was proposed to be **(1R,4R)-4-{(1E,3E,5E,7E,9E,11E,13E,15E,17E)-18-[(4R)-4-Hydroxy-2,6,6-trimethyl-1-cyclohexen-1-yl]-3,7,12,16-tetramethyl-1,3,5,7,9,11,13,15,17-octadecanonaen-1-yl}-3,5,5-trimethyl-2-cyclohexen-1-ol.** Hence, the proposed molecular mass calculated for $C_{40}H_{56}O_2$ $[M]^+$ is 569.3 (Fig 5.38). The Physical properties are listed in Table 5.16

Table 5.16: Physiochemical characteristics of bioactive fraction 9

Characteristics	**Observation**
Appearance	Pale yellow
Solubility	Soluble in Chloroform; Sparingly soluble in methanol
Nature	Slightly polar
Melting point	> 200°C
Sensitivity	Light sensitive

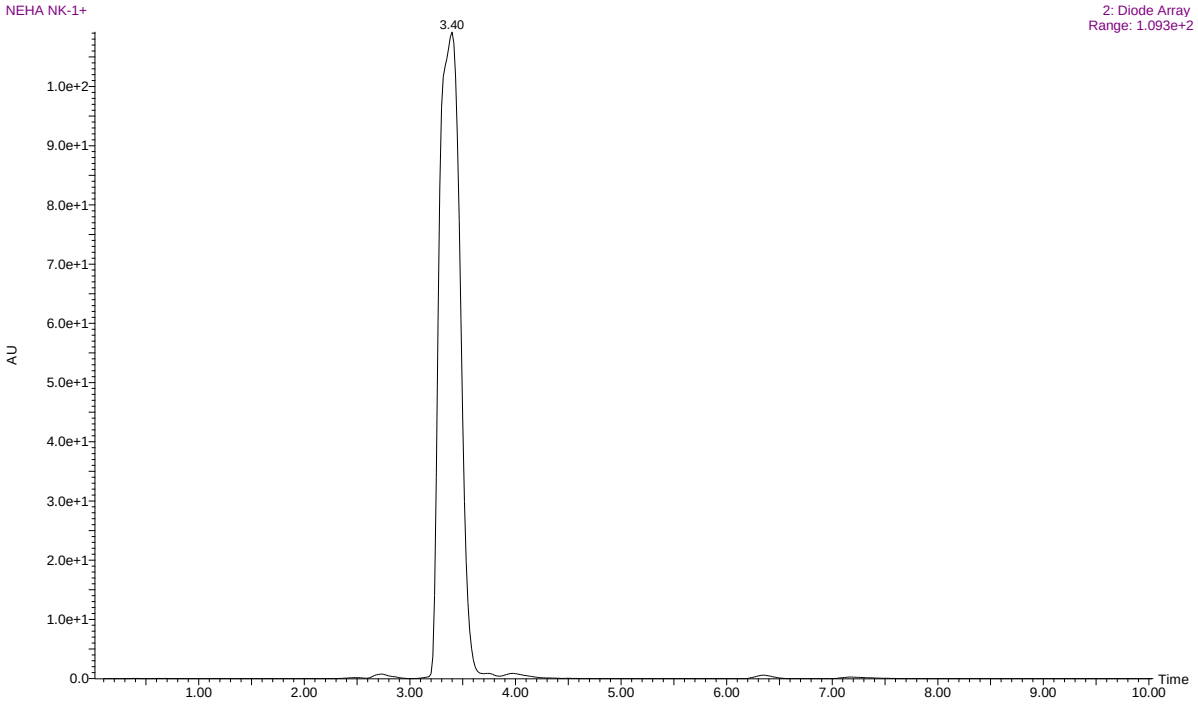

Figure 5.33: LC peak of bioactive fraction 9

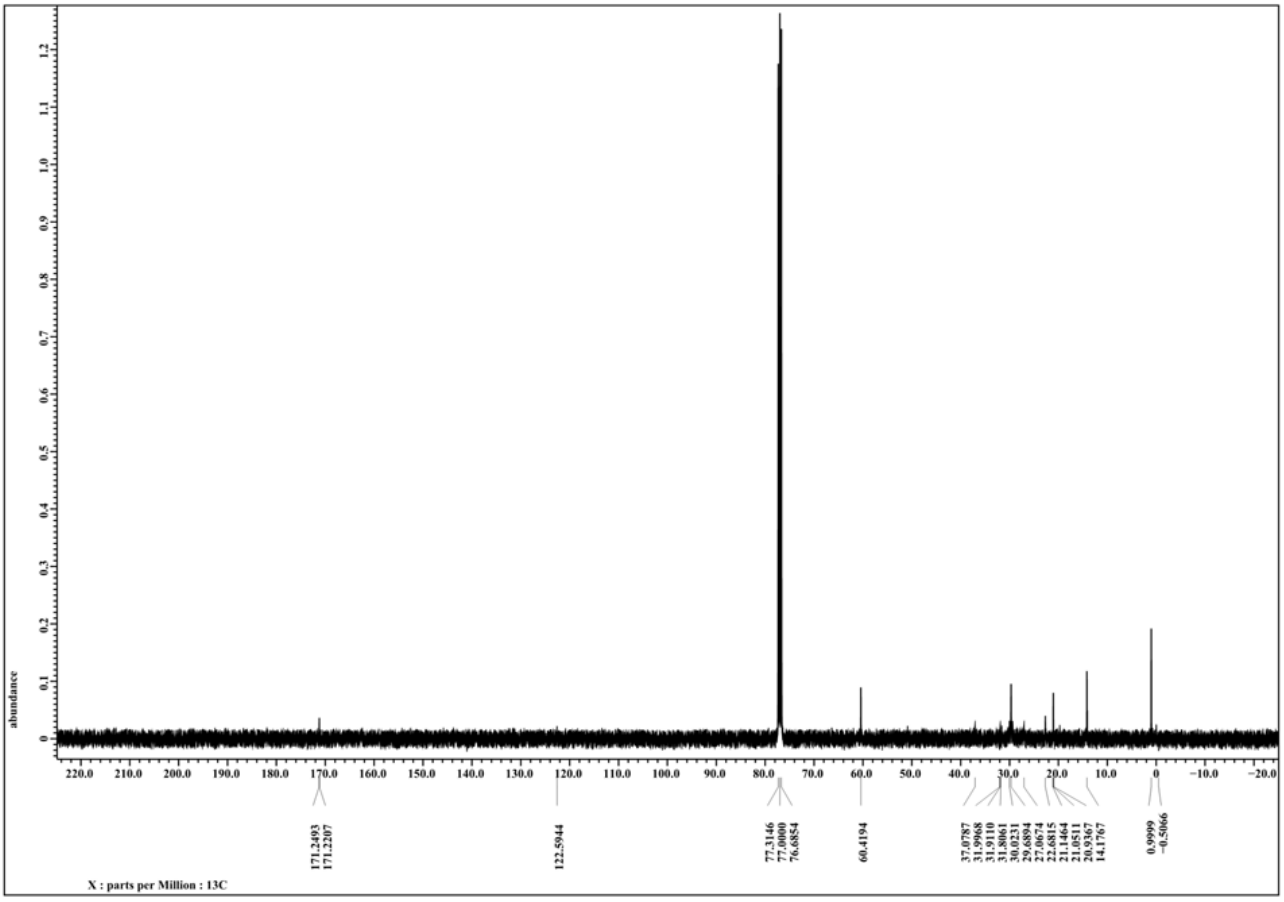

Fig 5.34: C^{13}-NMR of bioactive fraction 9

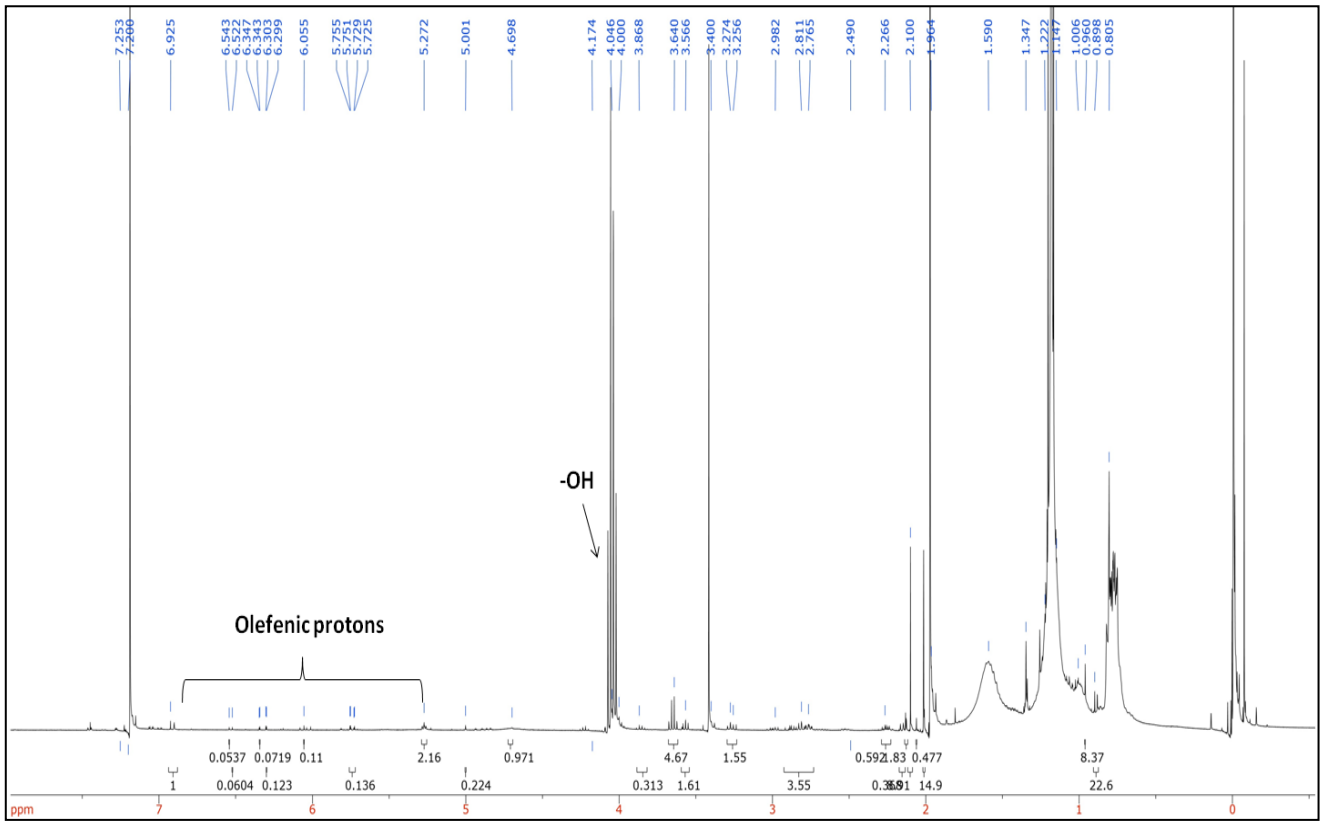

Fig 5.35: H^{1}-NMR of bioactive fraction 9

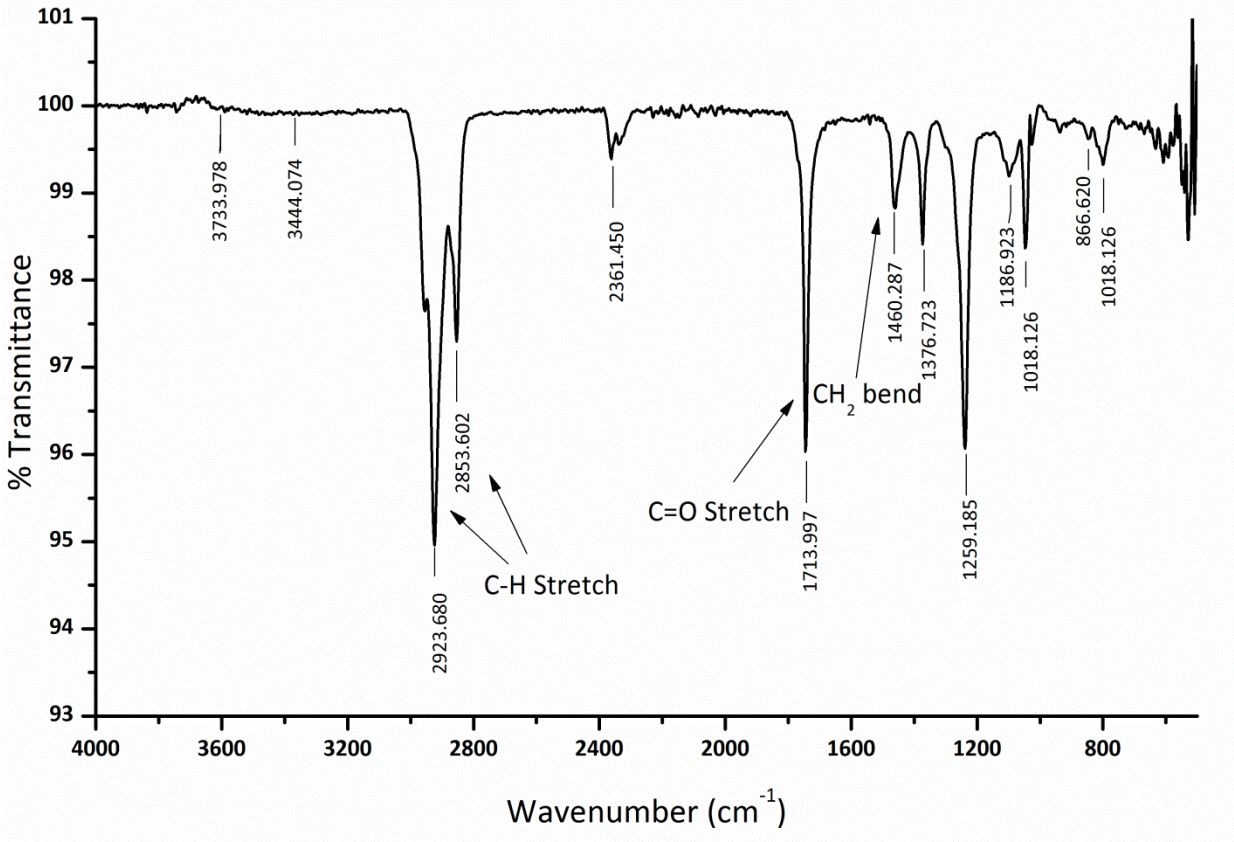

Fig 5.36: FTIR spectrum of bioactive fraction 9.

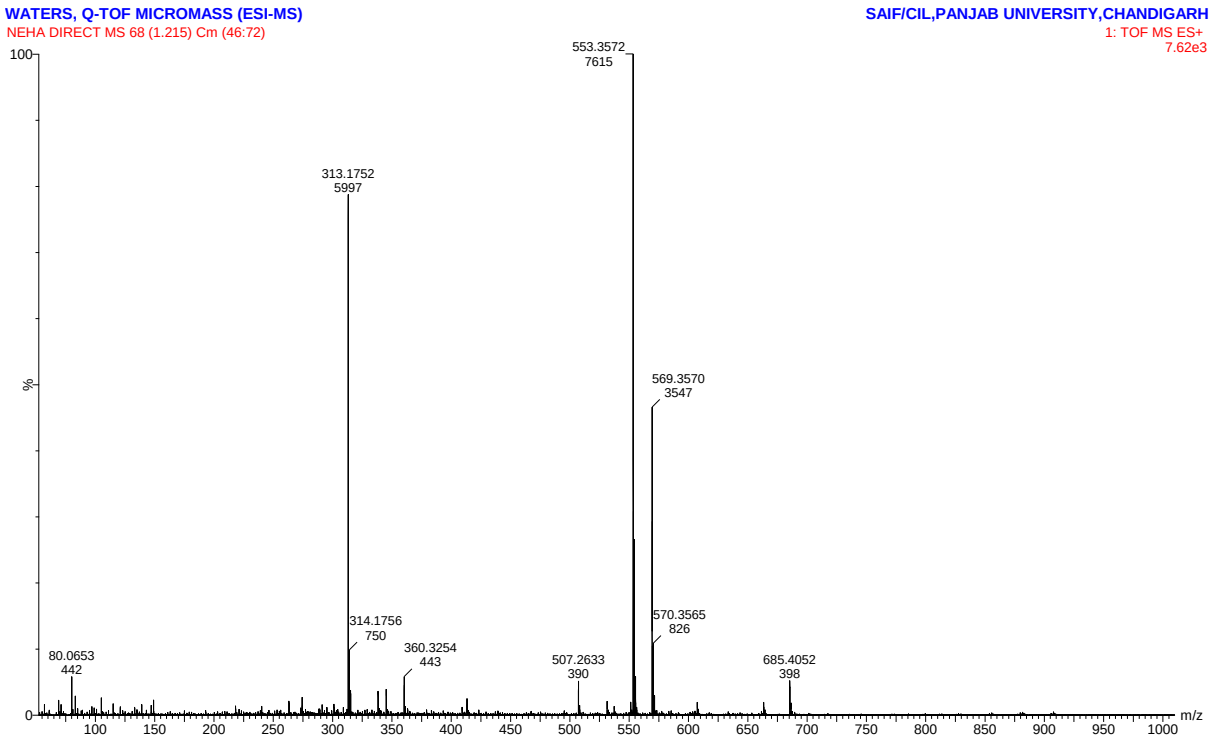

Fig 5.37: ESI-MS peaks of bioactive fraction 9

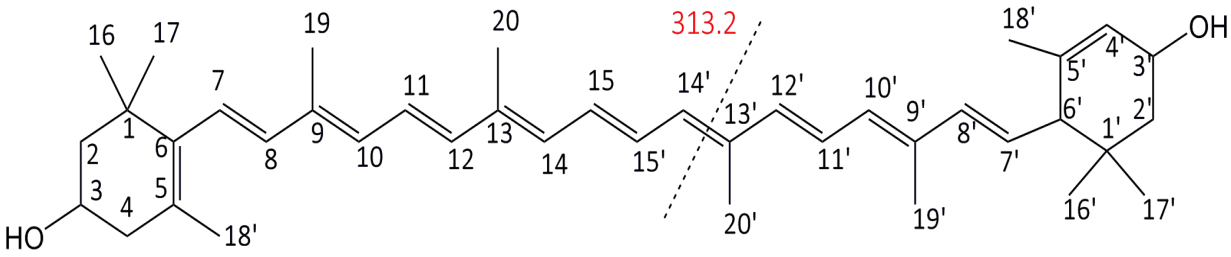

Fig 5.38: Proposed structure of bioactive fraction 9

5.15 Kinetic studies on the inhibition of xanthine oxidase by bioactive fraction

5.15.1 Lineweaver-Burk plot of bioactive fraction for xanthine oxidase inhibition

The mode of XO inhibition of bioactive fraction was deduced by plotting Lineweaver- Burk plot (Fig 5.39). With increasing concentration of inhibitor (Fraction 9), the K_m and V_{max} were found to decrease thereby indicating the mixed mode of inhibition. The K_i of the bioactive fraction was found to be 17.54 µM by using GraphPad Prism software V5.0.

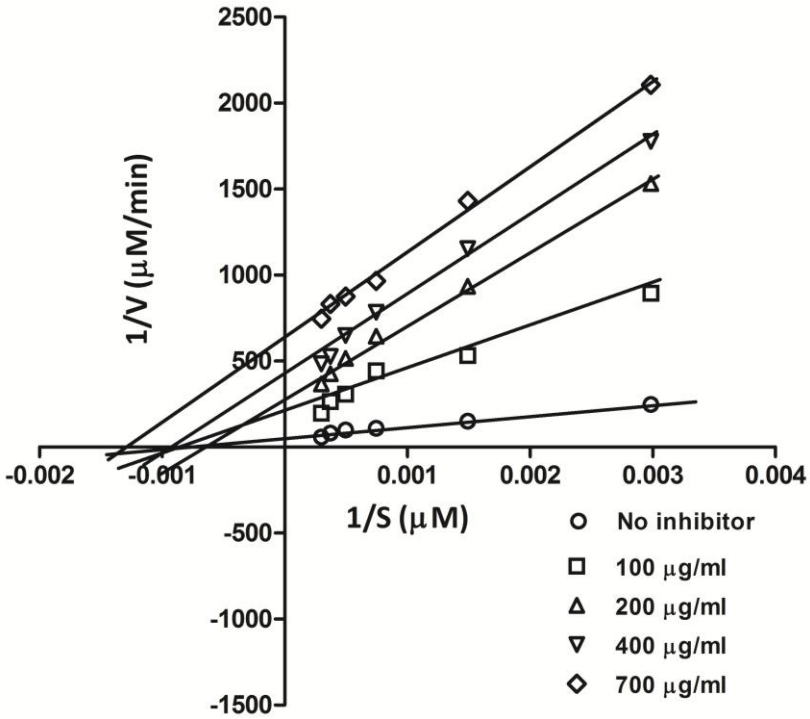

Fig 5.39: Lineweaver-Burk plot representing mixed type XO inhibition by bioactive fraction 9.

However, in case of allopurinol, increasing concentration of inhibitor resulted in a family of lines with a common intercept at 1/v resulting in increase in K_m but V_{max} being constant which indicates the competitive mode of inhibition with K_i value of 35.03 µM (Fig 5.40a). Further, Febuxostat exhibited mixed mode of XO inhibition with K_i of 14.5 µM (Fig 5.40b).

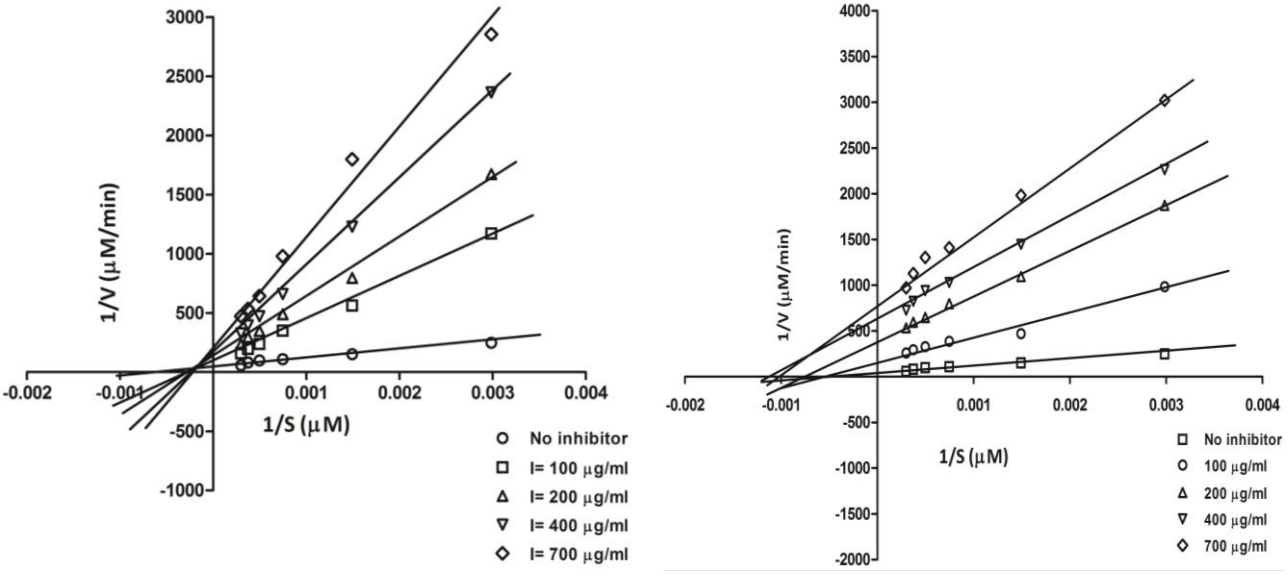

Fig 5.40: Lineweaver-Burk plot for XO inhibition a) Allopurinol; b) Febuxostat

Chapter 6

Discussion

Today, it is very well established that XO is a key enzyme which plays a important role in the progression of hyperuricemia and other oxidative stress related diseases such as hypertension, diabetes, obesity, chronic kidney disease (CKD), NAFLD, dyslipidemia and cardiovascular diseases (Gaffo et al., 2008; 2009; Han et al., 2014; Sah et al., 2015; Jalal et al., 2016; Mundhe and Mhasde, 2016). Being a hub of signaling in various biochemical and metabolic pathways, XO has been identified as a novel drug target, apart from its role in hyperuricemia and gout (Dawson and Walters, 2006; El-Bassossy and Watson, 2015; Gliozzi et al., 2016). The currently approved XO inhibitors which play a critical role in the urate lowering therapy are Allopurinol, a purine analogue while Febuxostat is a synthetic non-purine based selective inhibitor of XO (NP-SIXO). As genomics have provided insights on the correlation between presence of HLA-B*58:01 allele and occurrence of allopurinol hypersensitivity syndrome (AHS), HLA-B*58:01 may act as a biomarker for recommendation of allopurinol as a therapeutic molecule (Stamp et al., 2016). More emphasis is laid on NP-SIXO's to avoid expression of this gene. Hence, there is a demand for novel NP-SIXO's apart from Febuxostat which exhibit better efficacy and toxicological profile for oxidative stress management and anti-hyperuricemic therapy.

Plants, bacteria and fungi have been copious sources of novel chemical scaffolds which have been exploited for discovery and development of modern drugs. However, to prevent the rediscovery of already known bioactive compounds, pharmacologists and natural product chemists are more interested in exploring the biodiversity existing in undisturbed habitats and ecological niches (Katz and Baltz, 2016). Endophytic fungi inhabiting in distinct biotopes and ecological niches are the prime focus of research groups as these have already been proven to be metabolic factories of novel bioactive compounds with immense potential in pharmaceutical and agrochemical sectors (Strobel et al., 2004; Hardoim et al., 2015; Mercado-Blanco, 2015; Jia et al., 2016; Lugtenberg et al., 2016). Fungal endophytes produce a variety of compounds of different classes such as polyphenols, terpenes, peptides, alkaloids etc. exhibiting potent inhibitory action against various metabolic enzymes such as lipases, tyrosinase, HMG-CoA reductase and α-glucosidase (Gupta et al., 2014;

2015; Parthasarathy and Sathiyabama, 2015; Goutam et al., 2016). Exploration of XO inhibitors from endophytic fungi is a nascent approach with a very limited preliminary data (Shu et al., 2004; Song et al., 2004; Kapoor and Saxena, 2014; 2016). As we have propounded in the hypothesis that endophyte and the host plant exhibit a balanced antagonism which is mediated by a variety of signal molecules playing a critical role in the defense mechanism of the host as well as microbe. Oxidative stress is a common phenomenon encountered in this association wherein the fungi and the host strive to utilize the oxidative defense enzymes i.e. oxidases (oxidoreductases) to overcome the induced stress. This is accomplished by eliciting a battery of signaling molecules which inhibit the function of these oxidases thereby balancing the association (Hamilton et al., 2012).

Various endophytic fungi have been screened for exploration of antioxidant moieties however their role as inhibitors of these oxidative enzymes have largely been overlooked (Huang et al., 2007b; Phongpaichit et al., 2007; Srinivasan et al., 2010; Zeng et al., 2011; Yadav et al., 2014; Cui et al., 2015; Li et al., 2015a). Hence, in the present study, we have carried out a systematic screening of fungal endophytes inhabiting the medicinal plants in the biodiversity hotspots of India for production of XO inhibitors.

In the present study, *Fusarium sp*. exhibited highest colonization frequency followed by *Alternaria sp*. among the isolated endophytic fungal isolates. In other studies also, *Fusarium sp*, *Alternaria sp*, *Botryosphaeria sp.* have been found as predominant endophytes residing within the plants located in the tropical regions (Jena and Tayung, 2013; Nalini et al., 2014). The highest colonization frequency of endophytic fungal groups was exhibited by stem internal issue (vascular tissue) followed by leaf, stem and bark. Further, the fungal colonization was highest in *C. zeylanicum* followed by *C. malabaricum* and *A. marmelos*. In the present work, we have also encountered mycelia sterilia as an endophyte from different host plants. Quite frequently, sterile fungi have been specifically reported as endophyte from plants such as *Azadirachta indica, Jatropha curucs* and Mangroove trees existing in specific ecological niches (Arnold et al., 2000; Naik, 2009; Zakaria et al., 2016). Majority of the fungal endophytes isolated during the present work were belonging to

hyphomycetes. These findings were in accordance with the work of Naik et al., (2008) which also reported the highest occurrence of hyphomycetes.

The conventional method of screening XO inhibitory activity is by direct spectrophotometry wherein the formation of uric acid is estimated. However, while screening complex mixtures of natural products for the XO inhibitory activity by this approach may results in artifacts (Mashino et al., 2000). Many methods such as HPLC-UV, HPLC-MS, Flow injection analysis (FIA) system, fluorescence based microtiter plate assay, Immobilized metal affinity chromatography combined with ultrafiltration ultra-performance liquid chromatography mass spectrometry (UF-UPLC-MS), UF-LC-MS with high speed counter current chromatography (HSCCC), Centrifugal force LCMS (CF-LCMS) have been devised for screening of XO inhibitors more efficiently (Lam et al., 2006; Li et al., 2015b; Wang et al., 2016; Zhang et al., 2016; Liu et al., 2017). However, all these methods involve the utilization of high end equipments which are quite expensive, time consuming and laborious. Hence, in the present approach, we devised a superoxide anion radical scavenging based agar plate assay using xanthine as substrate and NBT as redox indicator for preliminary screening of culture filtrates of endophytic fungi. Our preliminary screening assay i.e. xanthine-NBT agar plate assay is a reliable, faster and cheaper method for large scale screening of XO inhibitors

In Xanthine-NBT agar plate XO inhibition assay, culture filtrates exhibiting more than 40 % inhibition of XO were further taken up for the quantitative estimation of XO inhibitory activity. In the pre-screen assay, three isolates viz. #1 CCSTITD, #1048 AMSTITYEL and #2 CCSTITD were found to exhibit XO inhibitory activity of more than 55 % which was similar to positive control Febuxostat as analyzed by One-way ANOVA and Post-hoc analysis (Kapoor and Saxena, 2014; 2016).

Two quantitative screening assays viz. NBT microtiter plate assay and uric acid estimation assay were further used for the identification of fungal endophytes possessing potent XO inhibitory potential. However, to optimally utilize the quantitative assays for XO inhibition, a pre-requisite is ascertaining the optimal conditions for the maximum XO activity. Hence, optimization of XO activity using microtiter plate based spectrophotometric assay was carried out which comprised of optimal

substrate concentration, enzyme concentration, pH and incubation time. Thus the assay conditions for optimal XO activity in a microtiter plate based spectrophotometric assay comprised of 2.5 mM xanthine, 15 mU/200 µl of xanthine oxidase, buffer of pH 7.8 and incubation time of 4 h. A substantial increase in the rate of enzymatic reaction was observed with increasing substrate concentration up to one point and thereafter it remained more or less constant over higher concentrations which were in accordance with the findings of Sharma et al., (2016). Furthermore, xanthine oxidase was found to be active in the pH range of 7.8-8.0 and displayed maximum activity in 4h. Numerous studies have also shown the pH range of 7.5-8.0 in Tris-HCl buffer for optimum XO activity (Egwim et al., 2005; Rashidi et al., 2009; Tao et al., 2014; Sharma et al., 2016). The K_m and V_{max} of the bovine milk XO was also determined to later on assess the effect of inhibitor on the K_m and V_{max} of the enzyme.

Based on the NBT microtiter plate assay, only those culture filtrates of endophytic fungi which inhibited XO by 70 % and above were taken into consideration for further studies. It was found that #1 CCSTITD clearly delineated from other 13 isolates exhibiting more than 70 % XO inhibitory activity as evident by One-way ANOVA and Tukey's post-hoc analysis. However, in the uric acid estimation assay only ten endophytic isolates exhibited significant 70 % reduction in uric acid production. However, in this assay also, we found that #1 CCSTITD clearly delineated from rest of the isolates in terms of XO inhibitory potential as compared to control. Febuxostat was found to be a strong inhibitor of XO in both quantitative assays. Further, Bland-Altman analysis indicated a bias which was having 95 % limits of agreement suggesting that #1 CCSTITD possess a potential to be taken up for further studies for the isolation of bioactive compound i.e. XO inhibitors. The analysis also showed #1048 AMSTITYEL to be the second potential isolate which could also be studied for the isolation of XO inhibitors. The Bland-Altman analysis also indicated NBT microtiter plate assay to be more sensitive assay as compared to the uric acid estimation assay.

At times, the activity of a bioactive molecule increases by removal of interfering substances from the culture broth. Hence, it was necessary to partially purify the culture broth of #1 CCSTITD

and #1048 AMSTITYEL using liquid-liquid extraction. The crude solvent residues of #1 CCSTITD and #1048 AMSTITYEL were re-analyzed by using quantitative NBT microtiter plate assay for XO inhibition. The chloroform solvent residues of both the isolates exhibited maximum XO inhibition amongst the different solvent residues obtained indicating it to be non-polar moiety. Similarly, chloroform extracts of wild growing mushrooms viz. *Suillus granulatus* (47.59 %) and *Hypholoma fasciculare* (77.67 %) exhibited moderate to good XO inhibition while *Tricholoma populinum* and *Suillus grevillei* exhibited remarkable XO inhibitory potential of 90. 96 % and 95.28 % respectively (Vanyolos et al., 2014). As NP-SIXO's is the current requirement in the pharmaceutical industry for urate lowering therapy (ULT). Hence, the purine detection test indicates that chloroform extracts of both isolates viz. #1 CCSTITD and #1048 AMSTITYEL were containing non-purine based compounds.

To statistically confirm the XO inhibitory potential of chloroform extracts of #1 CCSTITD and #1048 AMSTITYEL, we carried out the determination of IC_{50} using febuxostat and allopurinol as positive controls. IC_{50} is generally a maximal inhibition concentration of a substance wherein the biochemical function of the key enzymes is reduced to the half. This is a standard method used to compare the effectiveness of drugs. The crude chloroform residue of #1 CCSTITD exhibited a lower IC_{50} value as compared to #1048 AMSTITYEL but better than allopurinol. The crude chloroform extract of #1 CCSTITD exhibited lower IC_{50} value of 0.54 µg/ml as compared to Fusaruside and Phenolic compounds isolated from endophytic *Fusarium sp.* IFB-121 and *Chaetomium sp.* respectively (Shu et al., 2004; Huang et al., 2007a). Thus, based on the IC_{50} value of chloroform residue of #1 CCSTITD exhibited to be taken up for further purification of bioactive molecule.

No macroscopic and microscopic reproductive structures were seen in #1 CCSTITD when it was grown over different media and under different stress conditions which indicated #1 CCSTITD to be a sterile fungus. It emanated a strong fruity smell which was attributed to the complex mixture of volatile organic compounds (VOCs) and microscopically the hyphae was branched at 90˚ suggesting it to be possible member of *Muscodor* genus (Strobel et al., 2001; Zhang et al., 2010; Suwannarach et al., 2013; Meshram et al.,2013; Saxena et al., 2015). Morphologically, #1 CCSTITD differs from all

other *Muscodor* species by its fast colony growth rate, from *M. roseus, M. fengyangensis, M. musae, M. oryzae* and *M. suthepensis* by presence of cauliflower like structures and from *M. yucatanensis*, *M. equiseti, M. sutura* by the absence of swollen hyphae. It differs from *M. albus* and *M.vitigenus* by the presence of coiling structures.

The major constraint in identification and speciation of this fungus is its sterile nature and it cannot be solely identified on the basis of cultural characteristics and volatile organic compounds emitted by it. Hence, molecular phylogeny plays an integral role in identification of sterile fungi which predominantly exist as endophytes. The sequence analysis of ITS rRNA region has been the method of choice for phylogenetic and taxonomic placement studies of fungi (Rampersad, 2014). Therefore, molecular taxonomic tools were used in which we used *Muscodor* specific primers were used for amplification of ITS region (Ezra et al., 2010). Further, the ITS rDNA based phylogeny, DNA sequence polymorphism and pair wise distance analysis of nucleotide sites of ITS region indicated the emergence of novel species of the genus *Muscodor* named as *Muscodor darjeelingensis* (Saxena et al., 2014).

Multi-locus sequence based taxonomy is commonly adopted for precise speciation of various fungi (Donnell et al., 2012; Marques et al., 2013). However, the strategy is limited by the lack of sequence information from different nuclear regions of *Muscodor* species (Yuan et al., 2011). Thus, use of an integrated sequence-structure based alignment along with phylogenetic tree formation could be useful for accurate speciation and establishing the phylogenetic inter-relations between different species (Wolf et al., 2008). ITS1 and ITS2 conserved secondary structures have been deduced for a wide variety of eukaryotic groups including fungi (Barik et al., 2011), dinoflagellates (Thornhill and Lord, 2010) and nematodes (Ma et al., 2008) for gaining insights to illustrate phylogenetic relationships at different taxonomic levels (Schulz and Wolf, 2009). Thus, secondary structure prediction of ITS rDNA region appears to be a prominent method of delineating species identification and enhancing phylogenetic resolution.

From the present analysis it is clearly indicated that secondary structures of ITS1 of #1 CCSTITD (*M. darjeelingensis*), *M. kashayum*, and *M. tigerii* folded in X- shaped core structure but showed demarcation due to lack of sequence conservation in common core structure. On the other hand, ITS2 folding pattern of these three species shared similarities with minor differences in outer bulges of unpaired sequences. Further, *M. yucatanensis* and *M. satura* were identical but the two species exhibit marked differences based upon their ITS2 secondary structure folding pattern. Hence, the ITS1 region of *Muscodor* species was observed to be significantly variable as compared to ITS2 region at structural level. These findings are in accordance with Freire et al., (2012) in which the author explored the structural features of ITS1 and ITS2 marker of an obligate biotrophic fungus, *Phakopsora pachyrhizi*. The 5.8S region of #1 CCSTITD along with all *Muscodor* species was observed to be highly conserved and motif analysis confirmed the presence of conserved eukaryotic motifs (M1, M2 and M3) but with a single base substitution in Motif M1(C>U) and M3 (U>C). Similarly, single base substitution in motif M3 (U>C) was found in 5.8S region of *Colletotrichum gloeosporiodes* sensu lato species complex (Rampersad, 2014). However, *Phakopsora pachyrhizi* displayed three substitutions in motif M1 (C>U, A>G, U>C) and single substitution (U>C) in M3 (Freire et al., 2012). The PNJ tree resulted in the formation of monophyletic clades of individual *Muscodor* species. The proposed secondary structures provided supplementary information along with primary sequence information to generate reliable alignment and calculate robust as well as stable phylogenetic tree.

Endophytic *Muscodor* sp. have been reported to produce a mixture of VOCs primarily comprising of various alcohols, esters, acids, ketones, and lipophilic substances which are lethal to a wide variety of plant and human pathogenic fungi, bacteria as well as to nematodes and certain insects (Daisy et al., 2002; Strobel et al., 2001). The members of this genus are poorly explored for production of secondary metabolites (Boparai et al., 2015). More recently, VOCs and secondary metabolites production profile of epigenetic variants of *Muscodor yucatanensis* Ni30 were reported by cloning polyketide synthase (PKS) and non-ribosomal peptide synthetase (NRPS) genes. The epigenetic variant of *M. yucatanensis* differed considerably from the wild type morphologically as

well as in metabolites production profile. Each variant produced a different set of VOCs distinct from the wild type with several VOCs appearing only in the variant strains. The bioactive extrolite, Brefeldin A was isolated and characterized from the wild type. However, this metabolite was not detected the variant strain but instead, two other products were isolated and characterized as ergosterol and xylaguaianol C (Qadri et al., 2016).

Another pre-requisite for achieving maximum XO inhibitory activity is based upon optimizing the culture conditions. The bioactive fungus displayed maximum XO inhibitory activity over PDB in comparison to other fermentation medium such as CDB, RB, MEB, TSB and YEPDB which was analyzed statistically. Further, PDB has been used as a production medium of XO inhibitors in *Fusarium sp*. IFB-121, *Aspergillus terreus* and *Aspergillus niger* (Shu et al., 2004; Choudhary et al., 2004; Song et al., 2004).

The XO inhibitory activity was also found to exhibit positive correlation with increasing fungal biomass till 7th day of incubation. The fungal biomass increased slowly for the initial 48 h and then increased at an exponential rate till eight days. After which the growth became stationary. The reason of this may be attributed to the presence of abundant sugars in the production medium. The glucose concentration in the broth decreased rapidly in first four days, followed by a slow decrease. Further, the production of secondary metabolites starts on the second or third day and exhibit maximum yield during late logarithmic and initial stationary phase i.e. ninth or tenth day (Bundale et al., 2015). However, two phases are observed during the propagation of pharmaceutically metabolites producing micro-organisms. The first phase (trophophase) is characterized by rapid growth (biomass production) and the second phase (idiophase) is characterized by a slow growth and maximal productivity of metabolite. As the fungi grow it produces more and more metabolites thereby leading to increase in desired activity (Merlin et al., 2013). Various studies on optimization of incubation time period to achieve maximum secondary metabolite production have been carried out which also exhibit positive correlation between increasing fungal biomass and secondary

metabolite production till 8th day of incubation (Boonyapranai et al., 2008; Pradeep and Pradeep, 2013; Mathan et al., 2013).

Phytochemical testing of the crude extracts gives an indication of the nature of the compounds based upon which purification and visualization techniques are designed. Various polyphenolics, alkaloids, tannins, peptides, cerebrosides are reported to be potent XO inhibitors from plants and fungal extracts (Nagao et al., 1999; Van Hoorn et al., 2002; Lespade and Bercion, 2010). Phenolic compounds of Walnut leaf extract and ethyl acetate extracts of *Lycium arabicum* exhibited promising XO inhibitory activity (Wang et al., 2015; Trabsa et al., 2015). A novel cycloartane type triterpenoid, riparsaponin was isolated from the stem of *Homonoia riparia* and exhibited IC_{50} of 11.16 µM which was far better than the IC_{50} of #1 CCSTITD (Xu et al., 2014). Hydroxychavicol, a phenolic compound from *Piper* plant exhibited potent XO inhibitory potential (Murata et al., 2009). Further, hydroxychavicol derivatives named as nudibaccatumin A and B also exhibited XO inhibitory effect but with much less IC_{50} of 62.94 and 80.74 µM (Liu et al., 2015). A tripeptide with amino acid sequence of phenylalanine-cysteine-histidine, isolated from the aqueous extract of *Pleurotus ostreatus* exhibited remarkable XOI inhibitory potential with IC_{50} of 0.9 µM (Jang et al., 2014). Hespertin isolated from *Citrus auranticum* was found to posses strong XO inhibitory activity with IC_{50} of 16.48 µM (Liu et al., 2016).

The isolation of the bioactive compound from a solvent residue involves the employment of variety of analytical techniques to isolate the individual compounds and then subsequently identify the one possessing the desired bioactivity. Liquid - liquid fractionation is thus adopted to resolve the complex mixtures into smaller fractions. These fractions are further selected on the basis of bioactivity for further separation and isolation by TLC and column chromatography. Thus, bioassay guided fractionation is the most appropriate method to narrow down and isolate the bioactive molecules (Brady et al., 2000; Xin et al., 2009; Weller, 2012; Kumar et al., 2013; Guo et al., 2016; Lou et al., 2016). Various inhibitors have been identified from fungi/endophytic fungi using bioassay guided isolation methods (Kulanthaivel et al., 1993; Geng et al., 2013; Gupta et al., 2014). In the

present study, TLC fractionation of the crude chloroform extract was resolved into 11 bands of which bioactivity resided in fraction with R_f of 0.9. TLC chromatogram coupled with bio-autography assay has been used for identification of bioactive fraction from endophytic *Aspergillus terreus* MP15 which exhibited a promising anti-bacterial activity against gram positive bacteria (Yin et al., 2015). The silica gel column chromatography yielded 18 fractions of which significant XO inhibition was observed in fraction 9 as analyzed by one way ANOVA and Tukey's analysis. This fraction did not further split when re-chromatographed by TLC and HPLC suggesting it to be single entity. Fraction 9 is a yellow colored, unsaturated organic compound which is prone to oxidation in presence of light and temperature (Sowbhagya et al., 2004, Melendez-Martinez et al., 2007; Pratheesh et al., 2009)

Structural elucidation of this bioactive fraction was carried out by various spectral techniques including NMR (H^1 and C^{13}), ESI-MS and FTIR and was found to be a terpenoid. Thus, based on the NMR, FTIR and Mass spectra, the structure of the bioactive fraction was proposed to be β,ε-carotene-3,3'-diol commonly known as Lutein, a light sensitive carotenoid. ESI-MS, FTIR and NMR have been used for characterization of several enzyme inhibitors which have been isolated from fungal endophytes viz. *Xylaria feejeensis*, *Cladosporium* sp., *Colletotrichum* sp. TSC13, *Phomopsis vexans*, *Guignardia* sp. KcF8 (Artanti et al., 2012; Ai et al., 2014; Rivera-Chavez et al., 2015; Singh et al., 2015; Parthasarthy and Sathiyabama, 2015).

The proposed compound, Lutein exhibited a K_i of 17.54 µM which was quite close to Febuxostat. Even the mode of the inhibition was similar to Febuxostat i.e. mixed type. NMR (H^1), LC-MS, FTIR have been employed to deduce the structure of lutein (Aman et al., 2005; Boonnoun et al., 2012; Rodic et al., 2012; LaFountain et al., 2013). Lutein has been reported as a strong anti-oxidant (Sies et al., 1992; Sindhu et al., 2010; He et al., 2011), inflammatory modulator by reducing LPS and H_2O_2 induced phosphatidylinositol-3-kinase (PI3K) activity that inhibited NF-κB gene expression (Kim et al., 2008). Recently, Lutein has also been reported to induce α-1, 3-glucan accumulation on the cell wall surface of fungal plant pathogens (Otaka et al., 2016). Lutein has also been reported in reducing platelet derived growth factor (PDGF) including phosphorylation of PDGFR-β and its

downstream protein kinases/enzyme such as phospholipase C-ϒ, Akt and mitogen activated protein kinases (MAPKs) (Lo et al 2012). Being a plant carotenoid, lutein production has also been reported from microalga *Dunaliella salina* and it was observed that the under the influence of variable abiotic environmental stress conditions, the lutein production was increasing (Fu et al., 2014). Furthermore, Lutein has also been implicated in the scavenging of superoxide radicals thereby providing protecting effect against oxidative injury after ischemia reperfusion (Sato et al., 2011). Lutein has reported to act as potent enzyme inhibitor viz. human UDP glucuronosyl transferase (UGT) isoform (Zheng et al 2016), Cholinesterase (Ghanam et al., 2015) and porcine pancreatic lipase (Ong et al 2016). However, despite being a superoxide anion scavenger, lutein has not been evaluated or reported as a xanthine oxidase inhibitor so far. Till date, lutein has not been isolated from fungal endophytes. However, fungal endophytes are considered as important source of pharmaceuticals and are used in many industrial fermantative processes, such as the production of enzymes, vitamins, pigments, lipids, glycolipids, polysaccharides and polyhydric alcohols. The world of fungi offers an endless and rich source of biological diversity and exploitation.

Secondary metabolites production can serve multiple physiologic functions, many of which are common to both plants and microorganisms, and in a way it is intuitive that the same or similar compounds can be produced by ecologically associated entities. Thus, the continual efforts of researchers to exploit botanical diversity for the discovery of novel drugs has led to the finding of microbial strains able to synthesize bioactive compounds previously considered as typical plant products. In last two decades, it has become evident that all plants are inhabited by endophytic microorganisms, which are also capable of producing plant metabolites indicating that these compounds play a significant role in establishment and evolution of mutualistic inter-relations (Nicoletti and Fiorentino, 2015).

Further, this is the very first report highlighting the xanthine oxidase inhibitory activity of lutein isolated from novel endophytic *Muscodor* species. Thus, in the present study we have established that endophytic fungi could be a source of potential inhibitors of XO. Further, the

proposed fungal Lutein isolated from *M. darjeelingensis* could be further optimized using *in silico* methods like docking studies and quantitative structure activity relationship (QSAR) for achieving optimal activity and safe toxicological profile for further exploitation as therapeutic molecule for long term hyperuricemia management and oxidative stress related diseases.

Chapter 7

Conclusion

Conclusion

The present study establishes that endophytic fungi are novel source of non-purine selective inhibitors of xanthine oxidase (NP-SIXO) for the long term management of hyperuricemia and oxidative stress related disorders.

1. The present study is first systematic screening program exploiting endophytic fungi isolated from Indian medicinal plants as a source of novel xanthine oxidase inhibitors.
2. This is the first report of isolation of Lutein (Fraction 9), a dihydroxy-carotenoid from a novel endophytic fungus *Muscodor darjeelingensis* residing in stem internal tissue of *Cinnamomum camphora* in the Tiger Hills, Darjeeling.
3. In the present study, Lutein (Fraction 9) was found to exhibit potent xanthine oxidase inhibitory with K_i and mode of inhibition quite similar to that of Febuxostat which has not been reported so far.
4. Hence, we conclude that Lutein can serve as a novel scaffold for docking and QSAR studies in development of a novel XO inhibitor for long term management of Hyperuricemia as well as oxidative stress related diseases.

Being a nutraceutical, lutein holds an immense potential to be further developed as novel NPSIXO for urate lowering therapy among hyperuricemic patients with lesser or no adverse effects. Further, testing of lutein over hyperuricemic mice model and its effect on other enzymes of purine metabolic pathway is warranted.

Chapter 8

Bibliography

1. Agarwal A, Banerjee UC (2009): Screening of xanthine oxidase producing microorganisms using Nitroblue Tetrazolium based colorimetric assay method. Open Biotechnology Journal. 3: 46-49.
2. Agarwal A, Banerjee A, Banerjee UC (2011): Xanthine oxidoreductase: a journey from purine metabolism to cardiovascular excitation-contraction coupling. Critical Reviews in Biotechnology. 31(3): 264-80.
3. Aharwal RP, Kumar S, Sandhu SS (2016): Endophytic Mycoflora as a source of biotherapeutic compounds for disease treatment. Journal of Applied Pharmaceutical Science. 6 (10): 242-254.
4. Ahmad AR, Munim A, Elya B (2012): Study of antioxidant activity with reduction of DPPH radical and xanthine oxidase inhibitor of the extract of *Rueillia tuberosa* Linn Leaf. International Research Journal of Pharmacy. 3(11): 66-70.
5. Ai W, Wei X, Lin X, Sheng L, Wang Z, Tu Z, Yang X, Zhou X, Li J, Liu Y (2014): Guignardins AeF, spirodioxynaphthalenes from the endophytic fungus *Guignardia sp.* KcF8 as a new class of PTP1B and SIRT1 inhibitors. Tetrahedron. 70: 5806-5814.
6. Alam N, Yoon KN, Cha YJ, Kim JH, Lee RK, Lee TS (2011b): Appraisal of the antioxidant, phenolic compounds concentration, xanthine oxidase and tyrosinase inhibitory activities of *Pleurotus salmoneostramineus*. African Journal of Agricultural Research. 6(6): 1555-1563.
7. Alam N, Yoon KN, Lee KR, Kim HY, Shin PG, Cheong JC, Yoo YB, Shim MJ, Lee MW, Lee TS (2011a): Assessment of antioxidant and phenolic compound concentrations as well as xanthine oxidase and tyrosinase inhibitory properties of different extracts of *Pleurotus citrinopileatus* fruiting bodies. Mycobiology. 39 (1): 12-19.
8. Alam N, Yoon KN, Lee TS (2011d): Evaluation of the antioxidant and antityrosinase activities of three extracts from *Pleurotus nebrodensis* fruiting bodies. African Journal of Biotechnology. 10(11): 2978-2986.
9. Alam N, Yoon KN, Shin PG, Cheong JC, Yoo YB, Lee TS (2011c): Antioxidant, Phenolic compounds concentration, xanthine oxidase and tyrosinase inhibitory activities of *Pleurotus cornucopiae*. Australian Journal of Basic and Applied Science. 5 (3): 229-239.

10. Ali L, Khan AL, Hussain J, Al-Harrasi A, Waqas M, Kang SM, Al-Rawahi A, Lee IJ (2016): Sorokiniol: a new enzymes inhibitory metabolite from fungal endophyte *Bipolaris sorokiniana* LK12. BMC Microbiology. 16(103): 1-9.

11. Alvin A, Miller KI, Neilan BA (2014): Exploring the potential of endophytes from medicinal plants as sources of antimycobacterial compounds. Microbiological Research. 169: 483–495.

12. Aly A, Debbab A, Proksch P (2013): Fungal endophytes-secret producers of bioactive plant metabolites. Pharmazie. 68: 499-505.

13. Aly AH, Debbab A, Kjer J and Proksch P (2010): Fungal endophytes from higher plants: a prolific source of phytochemicals and other bioactive natural products. Fungal Diversity. 41: 1–16.

14. Aly AH, Debbab A, Proksch P (2011): Fungal endophytes: unique plant inhabitants with great promises. Applied Microbiology and Biotechnology. 90(6): 1829–1845.

15. Aman R, Biehl J, Carle R, Conrad J, Beifuss U, Schieber A (2005): Application of HPLC coupled with DAD, APcI-MS and NMR to the analysis of lutein and zeaxanthin stereoisomers in thermally processed vegetables. Food Chemistry. 92: 753-763.

16. Amirkia V, Heinrich M (2016): Natural products and drug discovery: a survey of stakeholders in industry and academia. Frontiers in Pharmacology. 6: 237.

17. Arnold AE (2005): Diversity and ecology of fungal endophytes in tropical forests. Biodiversity of fungi: their role in human life. In Current Trends in Mycological Research, D. Deshmukh, ed. (New Delhi, India: Oxford and IBH Publishing Co Pvt. Ltd.), pp. 49-68.

18. Arnold AE (2007): Understanding the diversity of foliar fungal endophytes: progress, challenges, and frontiers. Fungal Biology Reviews. 21: 51–66.

19. Arnold AE (2008): Endophytic fungi: hidden components of tropical community ecology. Tropical Forest Community Ecology. (S. Schnitzer and W. Carson, eds.) Blackwell Scientific, Inc. pp. 254-271.

20. Arnold AE, Lutzoni F (2007): Diversity and host range of foliar fungal endophytes: are tropical leaves biodiversity hotspots? Ecology. 88: 541–549.

21. Arnold AE, Maynard Z, Gilbert GS, Coley PD, Kursar TA (2000): Are tropical fungal endophytes hyperdiverse? Ecology Letters. 3: 267-274.

22. Artanti N, Tachibana S, Kardono LBS, Sukiman H (2012): Isolation of α-glucosidase inhibitors produced by an endophytic fungus *Colletotrichum sp.* TSC13 from *Taxus sumatrana.* Pakistan Journal of Biological sciences. 15(14): 673-679.

23. Aslan M, Ryan TM, Adler B, Townes TM, Parks DA, Thompson JA, Tousson A, Gladwin MT, Patel RP, Tarpey MM, Batinic-Haberle I (2001): Oxygen radical inhibition of nitric oxide-dependent vascular function in sickle cell disease. Proceedings of the National Academy of Sciences. 98: 15215–15220.

24. Aynehchi Y, Sormaghi MHS, Amin GH, Ghahreman A (1981): Survey of iranian plants for saponins, alkaloids, flavonoids and tannins. Pharmaceutical Biology. 19(2-3): 53-63.

25. Azmi SMN, Jamal P, Amid A (2012): Xanthine oxidase inhibitory activity from potential Malaysian medicinal plant as remedies for gout. International Food Research Journal. 19: 159-165.

26. Bacon CW, White JF (2000): Microbial endophytes. New York (NY): Marcel Dekker

27. Baker S, Satish S (2012): Endophytes: Natural warehouse of bioactive compounds. Drug Invention Today. 4(11): 548-553.

28. Bandoni AL, Mendiondo ME, Rondina RVD, Coussio JD (1976): Survey of Argentine medicinal plants, folklore and phytochemical screening. Economic Botany. 30(2): 161-185.

29. Baraf HSB, Becker M, Edwards NL, Gutierrez Urena SR, Sundy JS, Treadwell EL, Vazquez-Mellado J, Yood RA, Horowitz Z, Huang B, Maroli A, Waltrip R (2008a): Tophus response to pegloticase (PGL) therapy: pooled results from GOUT1 and GOUT2, PGL phase 3 randomized, double blind, placebo controlled trials. Arthritis and Rheumatology. 58: S176.

30. Baraf HSB, Matsumoto A, Maroli A, Waltrip R (2008b): Resolution of gouty tophi after twelve weeks of pegloticase treatment. Arthritis and Rheumatology. 58: 3632–3634.

31. Bardin T, Keenan RT, Khanna PP,Kopicko J, Fung M, Bhakta N, Adler S, Storgard C, Baumgartner S, So A (2016): Lesinurad in combination with allopurinol: a randomised, double-blind, placebo-controlled study in patients with gout with inadequate response to standard of care (the multinational CLEAR 2 study). Annals of the Rheumatic diseases. 0: 1-10.

32. Barik BP, Tayung K, Jagadev PN (2011): Molecular phylogeny and RNA secondary structure of *Fusarium* species with different lifestyles. Plant Pathology & Quarantine. 1(2): 205–219

33. Barnett HL, Hunter BB (1998): Illustrated genera of imperfect fungi. 4th edn. Macmillan, Publ Co, NewYork.

34. Becker MA, Kisicki J, Khosravan R, Wu J, Mulford D, Hunt B, MacDonald P, Joseph-Ridge N (2004): Febuxostat (TMX-67), a novel, non-purine, selective inhibitor of xanthine oxidase, is safe and decreases serum urate in healthy volunteers. Nucleosides, Nucleotides and Nucleic Acids. 23: 1111–1116.

35. Becker MA, Schumacher HR, Jr, Espinoza LR, Wells AF, MacDonald P, Lloyd E, Lademacher C (2010) The urate-lowering efficacy and safety of febuxostat in the treatment of hyperuricemia of gout: The CONFIRMS trial. Arthritis research & therapy. 12(2): R63.

36. Behera BC and Makhija U (2002): Inhibition of tyrosinase and xanthine oxidase by lichen species *Bulbothrix setschwanensis*. Current Science. 82: 61-66

37. Behera BC, Adawadkar B and Makhija U (2003): Inhibitory activity of xanthine oxidase and superoxide-scavenging activity in some taxa of the lichen family *Graphidaceae.* Phytomedicine. 10: 536–543.

38. Behera BC, Adawadkar B and Makhija U (2004): Capacity of some Graphidaceous lichens to scavenge superoxide and inhibition of tyrosinase and xanthine oxidase activities. Current Science. 87: 83-87.

39. Berdy J (2005): Bioactive microbial metabolites. The Journal of Antibiotics. 58(1): 455-463.

40. Berry CE, Hare JM (2004): Xanthine oxidoreductase and cardiovascular disease: molecular mechanisms and pathophysiological implications. Journal of Physiology (Lond). 555: 589–606.

41. Bhagat J, Kaur A, Kaur R, Yadav AK, Shrama V, Chadha BS (2016): Cholinesterase inhibitor (Altenuene) from an endophytic fungus *Alternaria alternata*: optimization, purification and characterization. Journal of Applied Microbiology. 121: 1015-1025.

42. Bharathi TR, Nadafi R, Prakash HS (2014): *in vitro* antioxidant and anti-inflammatory properties of different solvent extracts of *Memecylon talbotianum* Brandis. International Journal of Phytopharmacy. 4(6): 148-152

43. Billet L, Doaty S, Katz JD, Velasquez MT (2014): Review of Hyperuricemia as new marker for metabolic syndrome. ISRN Rheumatology. 2014: 852954, 7 pages.

44. Boonnoun P, Opaskonkun T, Prasitchoke P, Goto M, Shotipruk A (2012): Purification of free lutein from marigold flowers by Liquid Chromatography. Engineering Journal. 16(5): 145-155.

45. Boonyapranai K, Tungpradit R, Lhieochaiphant S, Phutrakul S (2008): Optimization of submerged culture for the production of Nnaphthoquinones pigment by *Fusarium verticillioide.* Chain Medical Journal of Science. 35(3) : 457-466.

46. Boparai J, Saxena S, Meshram V (2015): *In vitro* antimicrobial potential of Indian *Muscodor* species. Journal of Basic and Applied Mycology. 11: 22–25.

47. Borges F, Fernandes E, Roleira F (2002): Progress towards the discovery of xanthine oxidase inhibitors. Current Medicinal Chemistry. 9: 195–217.

48. Borowitzka M (2011): Pharmaceuticals from Algae. Biotechnology, vol. 7, Encyclopedia of Life Support System.

49. Boustie J, Grube M (2005): Lichens—a promising source of bioactive secondary metabolites. Plant Genetic Resources. 3(2): 273–287.

50. Brady SF, Wagenaar MM, Singh MP, Janso JE, Clardy J (2000): The Cytosporones, New Octaketide Antibiotics Isolated from an Endophytic Fungus. Organic Letters. 2(25): 4043-4046.

51. Breemen RBV, Schmitz HH, Schwartz SJ (1995): Fast Atom Bombardment Tandem Mass spectrometry of carotenoids. Journal of Agriculture and Food Chemistry. 43: 384-389.

52. Bruder G, Heid H, Jarasch ED, Keenan TW, Mather IH (1982): Characteristics of membrane-bound and soluble forms of xanthine oxidase from milk and endothelial cells of capillaries. Biochimica et Biophysica Acta. 4: 357–369.

53. Bundale S, Begde D, Nashikkar N, Kadam T, Upadhyay A (2015): Optimization of Culture Conditions for Production of Bioactive Metabolites by *Streptomyce*s spp. Isolated from Soil. Advances in Microbiology. 5:441-451.

54. Burns CM, Wortmann RL (2012): Latest evidence on gout management: what the clinician needs to know. Therapeutic Advances in Chronic Disease. 3(6): 271–286.

55. Cai H, Harrison DG (2000): Endothelial dysfunction in cardiovascular diseases: the role of oxidant stress. Circulation Research. 87(10): 840-4

56. Campion EW, Glynn RJ, Delabry LO (1987): Asymptomatic hyperuricemia. Risks and consequences in the normative aging study. The American Journal of Medicine. 82: 421-426.

57. Candan F (2003): Effect of *Rhus coriaria* L. (Anacardiaceae) on superoxide radical scavenging and xanthine oxidase activity. Journal of Enzyme Inhibition and Medicinal Chemistry. 18 (1): 59–62.

58. Cannon PJ, Stason WB, Demartini FE, Sommers SC, Laragh JH (1966): Hyperuricemia in primary and renal hypertension. The New England Journal of Medicine. 275(9): 457-64.

59. Card SD, Hume DE, Roodi D, McGill CR, Millner JP, Johnson RD (2015): Beneficial endophytic microorganisms of Brassica – A review. Biological Control. 90: 102-112.

60. Cengiz S, Cavas L, Yurdakoc K, Aksu S (2012): Inhibition of xanthine oxidase by Caulerpenyne from *Caulerpa prolifera.* Turkish Journal of Biochemistry. 37(4): 445–451.

61. Chaibriant H (2003): Stop marketing of proprietary medical product Desuric (benzbromarone) [press release]. URL: http://agmed.sante.gouv.fr.

62. Chandra Mouli K, Pragathi D, Naga Jyothi U, Shanmuga Kumar V, Himalaya Naik M, Balananda P, Suman B, Seshadri Reddy V, Vijaya T (2016): Leptin inhibitors from fungal endophytes (LIFEs):

Will be novel therapeutic drugs for obesity and its associated immune mediated diseases. Medical Hypotheses. 92: 48-53.

63. Chandra S (2012): Endophytic fungi: novel sources of anticancer lead molecules. Applied Microbiology and Biotechnology. 95(1): 47-59

64. Chandrappa CP, Anitha R, Jyothi P, Rajalakshmi K, Seema Mahammadi H, Govindappa M, Sharanappa P (2013): Phytochemical analysis and antibacterial activity of endophytes of *Embelia tsjeriam* cottamlinn. IJPBS. 3: 467- 473.

65. Chang WS, Lee YJ, Lu FJ, Chiang HC (1993): Inhibitory effects of flavonoids on xanthine oxidase. Anticancer Research. 13: 2165–2170.

66. Chen L, Zhang QY, Jia M, Ming QL, Yue W, Rahman K, Qin LP, Han T (2016): Endophytic fungi with antitumor activities: their occurrence and anticancer compounds. Critical Reviews in Microbiology. 42: 454–473.

67. Cheng SG, Koch U, Brunner JR (1988): Characteristics of purified cows' milk xanthine oxidase and its submolecular characteristics. Journal of Dairy Science. 71: 901–916.

68. Chien SC, Yang CW, Tseng YH, Tsay HS, Kuo YH, Wang SY (2009): *Lonicera hypoglauca* Inhibits Xanthine Oxidase and Reduces Serum Uric Acid in Mice. Planta Medicine. 75(4): 302-6.

69. Choi HK, Atkinson K, Karlson EW, Willett W, Curhan G (2004a): Purine-rich foods, dairy and protein intake, and the risk of gout in men. The New England Journal of Medicine. 350: 1093-1103.

70. Choi HK, Atkinson K, Karlson EW, Willett W, Curhan G (2004b): Alcohol intake and risk of incident gout in men: a prospective study. Lancet. 363(9417): 1277-81.

71. Chomcheon P, Wiyakrutta S, Sriubolmas N, Ngamrojanavanich N, Kengtong S, Mahidol C, Ruchirawat S, Kittakoop P (2009): Aromatase inhibitory, radical scavenging, and antioxidant activities of depsidones and diaryl ethers from the endophytic fungus *Corynespora cassiicola* L36. Phytochemistry. 70: 407-413.

72. Choudhary MI, Musharraf SG, Mukhmoor T, Shaheen F, Ali S, Rahman AU (2004): Isolation of bioactive compounds from *Aspergillus terreus.* Zeitschrift fur Naturforsch B. 59b: 324 – 328.

73. Cos P, Ying L, Calomme M, Hu JP, Cimanga K, Van Poel B, Pieters L, Vlietinck A, Vanden Berghe D (1998): Structure-activity relationship and classification of flavonoids as inhibitors of xanthine oxidase and superoxide scavengers. Journal of Natural Products. 61: 71-76.

74. Cota BB, Rosa LH, Caligiorne RB, Rabello ALT, Alves TMA, Rosa CA, Zani CL (2008): Altenusin, a biphenyl isolated from the endophytic fungus *Alternaria* sp., inhibits trypanothione reductase from Trypanosoma cruzi. FEMS Microbiology Letters. 285: 177–182.

75. Cragg GM, Newman DJ (2013): Natural products: A continuing source of novel drug leads. Biochimica et Biophysica Acta. 1830: 3670–3695.

76. Crittenden PD, Porter N (1991): Lichen forming fungi: Potential sources of novel metabolites. Trends in Biotechnology. 9: 409-414.

77. Cui H, Liu Y, Nie Y, Liu Z, Chen S, Zhang Z, Lu Y, He L, Huang X, She Z (2016): Polyketides from the Mangrove-Derived endophytic fungus *Nectria* sp. HN001 and their α-Glucosidase Inhibitory activity. Marine Drugs. 14(5) doi: 10.3390/md14050086.

78. Cui L, Guo TT, Ren ZX, Zhang NS, Wang ML (2015): Diversity and antioxidant activity of culturable endophytic fungi from alpine plants of *Rhodiola crenulata*, *R. angusta*, and *R. sachalinensis.* PLoS One. 10(3): e0118204.

79. Daisy BH, Strobel GA, Castillo U, Ezra D, Sears J, Weaver DK, Runyon JB (2002): Naphthalene, an insect repellent, is produced by *Muscodor vitigenus*, a novel endophytic fungus. Microbiology. 148: 3737–3741.

80. Dawson and Walters M (2006): Uric acid and Xanthine oxidase: Future therapeutic targets in the prevention of cardiovascular disease?. British Journal of pharmacology. 62(6): 633-644.

81. Demain AL (1999): Pharmaceutically active secondary metabolites of microorganisms. Applied Microbiology and Biotechnology. 52(4): 455-463.

82. Demain AL (2009): Antibiotics: Natural products essential to human health. Medicine Research reviews. 29 (6): 821-842.

83. Demain AL, Sanchez S (2009): Microbial drug discovery: 80 years of progress. The Journal of Antibiotics. 62: 5-16.

84. Desco MC, Asensi M, Marquez R, Martinez-Valls J, Vento M, Pallardo FV, Sastre J, Vina J (2002): Xanthine oxidase is involved in free radical production in type 1 diabetes: protection by allopurinol. Diabetes. 51: 1118–1124.

85. Deshmukh S, Verekar SA, Bhave SV (2015): Endophytic fungi: a reservoir of antibacterials. Frontiers in Microbiology. 5: 1-43.

86. Desire MH, Bernard F, Forsah MR, Assang CT, Denis ON (2012): Enzyme and Qualitative phytochemical screening of endophytic fungi isolated from *Lantana camara* linn Leaves. Journal of Applied Biology And Biotechnology. 2(06): 001-006.

87. Diaz-Torne C, Perez-Herrero N, Perez-Ruiz F (2015): New medications in development for the treatment of hyperuricemia of gout. Current Opinion in Rheumatology. 27: 164–169.

88. Donnell KO, Humber RA, Geiser DM, Kang S, Park B, Robert Varg, Crous PW, Johnston PR, Aoki T, Rooney AP, Rehner SA (2012): Phylogenetic diversity of insecticolous fusaria inferred from multilocus DNA sequence data and their molecular identification via FUSARIUM-ID and *Fusarium* MLST. Mycologia. 104: 427–445.

89. Egwim EC, Vunchi MA, Egwim PO (2005): Comparison of xanthine oxidase activities in cow and goat milks. Nigerian Society for Experimental Biology. 17(1): 1-6.

90. El-Bassossy HM, Watson ML (2015): Xanthine oxidase inhibition alleviates the cardiac complications of insulin resistance: effect on low grade inflammation and the angiotensin system. Journal of Translational medicine. 13(82).

91. Elion GB (1988): Nobel lecture. Burroughs Wellcome Co; Research Triangle Park, NC:. The purine path to chemotherapy.

92. Elion GB (1993): The quest for a cure. Annual Reviews in Pharmacology and Toxicology. 33: 1–23.

93. Elsebai MF, Tejesvi MV, Pirttila AM (2014): Endophytes as a novel source of bioactive new structures. Verma VC and Gange AC (eds.). Advances in Endophytic Research. 191–201.

94. Eyberger AL, Dondapati R, Porter JR (2006): Endophyte fungal isolates from *Podophyllum peltatum* produce podophyllotoxin. Journal of Natural Products. 69: 1121–1124.

95. Ezra D, Hess WM, Strobel GA (2004): New endophytic isolates of *Muscodor albus*, a volatile antibiotic-producing fungus. Microbiology. 150(12): 4023–4031.

96. Ezra D, Skovorodnikova J, Kroitor-Keren T, Denisov Y, Liarzi O (2010): Development of methods for detection and *Agrobacterium*-mediated transformation of the sterile, endophytic fungus *Muscodor albus*. Biocontrol Science and Technology. 20(1): 83-97.

97. Fang J, Alderman MH (2000): Serum uric acid and cardiovascular mortality the NHANES I epidemiologic follow-up study, 1971–1992. National Health and Nutrition Examination Survey. JAMA. 283: 2404–2410.

98. Faruque LI, Ehteshami-Afshar A, Wiebe N, Tjosvold L, Homik J, Tonelli M (2013): A systematic review and meta-analysis on the safety and efficacy of febuxostat versus allopurinol in chronic gout. InSeminars in arthritis and rheumatism. 43: 367–375.

99. Firakova S, Sturdikova M, Muckova M (2007): Bioactive secondary metabolites produced by microorganisms associated with plants. Biologia. 62: 251–257.

100. Fleischmann R, Kerr B, Yeh LT, Suster M, Shen Z, Polvent E, Hingorani V, Quart B, Manhard K, Miner JN, Baumgartner S (2014): Pharmacodynamic, pharmacokinetic and tolerability evaluation of concomitant administration of Lesinurad and febuxostat in gout patients with hyperuricaemia. Rheumatology. 53: 2167-2174.

101. Fox IH (1981): Metabolic basis for disorders of purine nucleotide degradation. Progress in endocrinology and metabolism. 30(6): 616-634.

102. Freeman BA, Crapo JD (1982): Biology of disease: free radicals and tissue injury. Lab Investigation. 47: 412–426.

103. Freire MCM, Roméria da Silva M, Zhang X, Almeida AMR, Stacey G, de Oliveira LO (2012): Nucleotide polymorphism in the 5.8S nrDNA gene and internal transcribed spacers in *Phakopsora pachyrhizi* viewed from structural models. Fungal Genetics and Biology. 49: 95–100.

104. Friedrich J, Dandekar T, Wolf M, Muller T (2005): ProfDist: a tool for the construction of large phylogenetic trees based on profile distances. Bioinformatics. 21: 2108–2109.

105. Friensen ML (2013): Microbially mediated plant functional traits. Molecular Microbial Ecology of the Rhizosphere, Volume 1, First Edition. Edited by Frans J. de Bruijn. Pp. 87-102.

106. Furukawa S, Fujita T, Shimabukuro M, Iwaki M, Yamada Y, Nakajima Y, Nakayama O, Makishima M, Matsuda M, Shimomura I (2004): Increased oxidative stress in obesity and its impact on metabolic syndrome. Journal of Clinical Investigation. 114(12): 1752-61.

107. Gaffo AL, Edwards NL, Saag KG (2009): Hyperuricemia and cardiovascular disease: how strong is the evidence for a causal link? Arthritis Research & Therapy. 11: 240.

108. Gaffo AL, Saag KG (2008): Management of Hyperuricemia and Gout in CKD. American Journal of kidney diseases. 52(5): 994–1009.

109. Garrod AB (1848): Observations on certain pathological conditions of the blood and urine in gout, rheumatism and Bright's disease. Trans M-Chir Soc Edinburgh. 31: 83-97.

110. Geng Y, Lu ZM, Huang W, Xu HY, Shi JS, Xu ZH (2013): Bioassay-Guided Isolation of DPP-4 Inhibitory fractions from extracts of submerged cultured of *Inonotus obliquus*. Molecules. 18: 1150-1161.

111. Ghanam K, Deshpande J, Juturu V (2015): Lutein and Zeaxanthin isomers inhibit cholinesterase and modulate the expression of inflammation-related genes: *In Vitro* models. International Journal of Ophthalmology and Clinical Research. 2:043.

112. Gilroy S, Białasek M, Suzuki N, Górecka M, Devireddy AR, Karpinski S, Mittler R (2016): ROS, calcium, and electric signals: key mediators of rapid systemic signaling in plants. Plant Physiol 171: 1606–1615.

113. Gliozzi M, Malara N, Muscoli S, Mollace V (2016): The treatment of hyperuricemia. International Journal of Cardiology. 213: 23-27.

114. GlobalData (2016): http://store.globaldata.com/market-reports/pharmaceuticals-andhealthcare/opportunityanalyzer-gout-opportunity-analysis-andforecast-to-2018#.Vso-VJflfQ.

115. Gojayev AS, Bankeu JK, Guliyev AA, Tsamo E, Choudhary MI (2011): Xanthine Oxidase inhibitory activity of natural compounds from *Ficus mucuso* WELW. (Moraceae). UOT. 581(577.16): 1.

116. Gonzalez DR, Treuer AV, Castellanos J, Dulce RA, Hare JM (2010): Impaired S-nitrosylation of the ryanodine receptor caused by xanthine oxidase activity contributes to calcium leak in heart failure. Journal of Biological Chemistry. 285(37): 28938-45.

117. Gouda S, Das G, Sen SK, Shin HS, Patra JK (2016) Endophytes: A Treasure House of Bioactive Compounds of Medicinal Importance. Frontiers in Microbiology. 7 (1538): 1-8.

118. Goutam J, Kharwar RN, Tiwari VK, Mishra A, Singh S (2016): Isolation and Identification of antibacterial compounds isolated from endophytic fungus *Emericella qaudrilineata* (RS-5). Natural Products Chemistry and Research. 4:2

119. Govindappa M, Channabasava R, Kumar KRS, Pushpalatha KC (2013): Antioxidant activity and phytochemical screening of crude endophytes extracts of *Tabebuia argentea* Bur. & K. Sch. American Journal of Plant Sciences. 4: 1641-1652.

120. Greenberg LE, Nguyen T, Miller SM (2001): Suspected Allopurinol induced aseptic meningitis. Pharmacotherapy. 21: 1007-1009.

121. Gu W (2009): Bioactive metabolites from *Alternaria brassicicola* ML-P08, an endophytic fungus residing in *Malus halliana*. World Journal of Microbiology Biotechnology. 25: 1677–1683.

122. Gunatilaka AA (2006): Natural products from plant-associated microorganisms: distribution, structural diversity, bioactivity, and implications of their occurrence. Journal of Natural Products. 69(3): 509-526.

123. Guo B, Wang Y, Sun X, Tang K (2008): Bioactive Natural Products from Endophytes: A Review. Applied Biochemistry and Microbiology. 44: 136-142.

124. Guo B, Dai JR, Ng S, Huang Y, Leong C, Ong W, Carte BK (2000) Cytonic acids A and B: novel tridepside inhibitors of hCMV protease from the endophytic fungus *Cytonaema* species. Journal of Natural Products. 63(5): 602-604.

125. Guo L, Wang C, Zhu WC, Xu FQ (2016): Bioassay-guided fractionation and identification of active substances from the fungus *Aspergillus tubingensis* against *Vibrio anguillarum.* Biotechnology & Biotechnological Equipment. 30(3): 602-606.

126. Guo LD, Hyde KD, Liew ECY (1998): A method to promote sporulation in palm endophytic fungi. Fungal Diversity. 1: 109–113

127. Gupta M, Saxena S, Goyal D (2014): Lipase inhibitory activity of endophytic fungal species of *Aegle marmelos*: a bioresource for potential pancreatic lipase inhibitors. Symbiosis. 64(3): 149-157.

128. Gupta M, Saxena S, Goyal D (2015): Potential pancreatic lipase inhibitory activity of an endophytic *Penicillium* species. Journal of Enzyme Inhibition and Medicinal Chemistry. 30(1): 15–21.

129. Gutman AB (1966): Uricosuric drugs, with special reference to probenecid and sulfinpyrazone. Advances in Pharmacology. 4: 91-142.

130. Gutman AB, Yu TF (1951): Benemid (pdi-n-propylsulfamyl-benzoic acid) as uricosuric agent in chronic gouty arthritis. Transactions of the Association of American Physicians. G4:279-288.

131. Guzik TJ, Sadowski J, Guzik B, Jopek A, Kapelak B, Przybylowski P, Wierzbicki K, Korbut R, Harrison DG, Channon KM (2006): Coronary artery superoxide production and nox isoform

expression in human coronary artery disease. Arteriosclerosis, thrombosis, and vascular biology. 26 (2): 333-339.

132. Halliwell B, Gutteridge MC (1982): Oxygen radicals and tissue damage. In: Caldarera CM, Harris P, eds. Advances in Studies on Heart Metabolism. Bologna: Cooperativa Libraria Universitaria Editrice Bologna. 403–411.

133. Hamburger S, Lipsky P, Simon L (2010): Safety and efficacy of long-term pegloticase (KRYSTEXXA™) treatment in adult patients with chronic gout refractory to conventional therapy. Arthritis and Rheumatology. 62(Suppl. 10): L12.

134. Hamilton CE, Gundel PE, Helander M, Saikkonen K (2012): Endophytic mediation of reactive oxygen species and antioxidant activity in plants: A review. Fungal Diversity. 54: 1–10

135. Han GM, Gonzalez S, DeVries D (2014): Combined effect of hyperuricemia and overweight/obesity on the prevalence of hypertension among US adults: result from the National Health and Nutrition Examination Survey. Journal of Human Hypertension. 28: 579–586.

136. Hanaee J, Rashidi MR, Delazar A, Piroozpanah S (2004): Onion, a potent Inhibitor of xanthine oxidase. Iranian Journal of Pharmaceutical Research. 4: 243-247.

137. Hande KR, Noone RM, Stone WJ (1984): Severe allopurinol toxicity: description and guidelines for prevention in patients with renal insufficiency. American Journal of Medicine. 76: 47–56.

138. Hardoim PR, van Overbeek LS, Berg G, Pirttila AM, Compant S, Campisano A, Doring M, Sessitsch A (2015): The hidden world within plants: ecological and evolutionary considerations for defining functioning of microbial endophytes. Microbiology and Molecular Biology Reviews. 79: 293–320.

139. Harvey AL, Edrada-Ebel R, Quinn RJ (2015): The re-emergence of natural products for drug discovery in the genomics era. Nature Reviews Drug Discovery. 14: 111–129.

140. Havlik J, Huebra RGDL, Hejtmankova K, Fernandez J, Simonova J, Melich M, Rada V (2010): Xanthine oxidase inhibitory properties of Czech medicinal plants. Journal of Ethnopharmacology. 132: 461–465.

141. He RR, Tsoi B, Lan F, Yao N, Yao XS, Kurihara H (2011): Antioxidant properties of lutein contribute to the protection against lipopolysaccharide-induced uveitis in mice. Chinese Medicine. 6:38

142. Heitzer T, Schlinzig T, Krohn K, Meinertz T, Munzel T (2001): Endothelial dysfunction, oxidative stress and risk of cardiovascular events in patients with coronary artery disease. Clinical Investigations and Reports. 104: 2673-2678.

143. Hendriani R, Sukandar EY, Anggadiredja K, Sukrasno (2016): *In vitro* Evaluation of xanthine oxidase inhibitory activity of selected medicinal plants. International Journal of Pharmaceutical and Clinical Research. 8(4): 235-238.

144. Higashi Y, Maruhashi T, Noma T, Kihara Y (2014): Oxidative stress and endothelial dysfunction: Clinical evidence and therapeutic implications. Trends in Cardiovascular Medicine. 2(4): 165-169.

145. Higashi Y, Noma K, Yoshizumi M, Kihara Y (2009): Endothelial function and oxidative stress in cardiovascular diseases. Circulation Journal. 73: 411–418.

146. Higgins P, Ferguson LD, Walters MR (2011): Xanthine oxidase inhibition for the treatment of stroke disease: a novel therapeutic approach. Expert Review of Cardiovascular Therapy. 9(4): 399-401.

147. Hofacker IL (2004): RNA secondary structure analysis using the Vienna RNA package. Current protocols in bioinformatics. Chapter 12: Unit 12.2. doi: 10.1002/0471250953.bi1202s04.

148. Hosoya T, Ohno I, Nomura S, Hisatome I, Uchida S, Fujimori S, Yamamoto T, Hara S (2014): Effects of topiroxostat on the serum urate levels and urinary albumin excretion in hyperuricemic stage 3 chronic kidney disease patients with or without gout. Clinical and Experimental Nephrology. 18: 876–884

149. Houston M, Estevez A, Chumley P, Aslan M, Marklund S, Parks DA, Freeman BA (1999): Binding of xanthine oxidase to vascular endothelium: kinetic characterization and oxidative impairment of nitric oxide-dependent signaling. Journal of Biological Chemistry. 274: 4985–4994.

150. Hoy SM (2016): Lesinurad: First Global Approval. Drugs. 76(4): 509-16

151. Huang WY, Cai YD, Hyde KD, Corke H, Sun M (2007a): Endophytic fungi from *Nerium oleander* L (Apocynaceae): main constituents and antioxidant activity. World Journal of Microbiology and Biotechnology. 23: 1253-1263.

152. Huang WY, Cai YZ, Xing J, Corke H, Sun M (2007b): A potential antioxidant resource: Endophytic fungi from medicinal plants. Economic Botany. 61(1): 14-30.

153. Hudaib MH, Tawaha KA, Mohammad MK, Assaf AM, Issa AY, Alali FQ, Aburjai TA, Bustanji YK (2011): Xanthine oxidase inhibitory activity of the methanolic extracts of selected Jordanian medicinal plants. Pharmacognosy Magazine. 7(28): 320–324.

154. Hyoung PS, Yoon SW, Park JM, Ohk SH, Yu JH, Bai DH (2000): Studies on xanthine oxidase inhibitor produced from *Aspergillus* sp. F184. Korean Journal of Applied microbiology and Biotechnology. 28(2): 92-96.

155. Iqbal J, Nelson JA, McCulley RL (2013): Fungal endophyte presence and genotype affect plant diversity and soil-to-atmosphere trace gas fluxes. Plant and Soil. 364: 15–27.

156. Irondi EA, Agboola SO, Oboh G, Boligon AA, Athayde ML, Shode FO (2016): Guava leaves polyphenolics-rich extract inhibits vital enzymes implicated in gout and hypertension *in vitro.* Journal of Intercultural Ethnopharmacology. 5(2): 122-130.

157. Izumida H, Adachi K, Mihara A, Yasuzawa T, Sano H (1997): Hydroxyakalone, a novel xanthine oxidase inhibitor produced by a marine bacterium, *Agrobacterium aurantiacum.* The Journal of Antibiotics. 50 (11): 916-918.

158. Izumida H, Adachi K, Nishijima M, Endo M, Miki W (1995): Akalone: A novel xanthine oxidase inhibitor produced by the marine bacterium, *Agrobacterium aurantiacum* sp. nov. Journal of Marine Biotechnology. 2: 115-118.

159. Jalal DI (2016): Hyperuricemia, the kidneys, and the spectrum of associated diseases: A Narrative Review. Current Medical Research and Opinion. DOI:10.1080/03007995.2016.1218840.

160. Jang IT, Hyun SH, Shin JW, Lee YH, Ji JH, Lee JS (2014): Characterization of an anti-gout xanthine oxidase inhibitor from *Pleurotus ostreatus.* Mycobiology. 42(3): 296-300.

161. Jayashankar CA, Andrews HP, Vijayasarathi, Pinnelli VB, Shashidharan B, Kumar HNN, Vemulapalli S (2016): Serum uric acid and low-density lipoprotein cholesterol levels are independent predictors of coronary artery disease in Asian Indian patients with type 2 diabetes mellitus. Journal of Natural Science, Biology and Medicine. 7(2): 161–165.

162. Jena SK, Tayung K (2013): Endophytic fungal communities associated with two ethno-medicinal plants of Similipal Biosphere Reserve, India and their antimicrobial prospective. Journal of Applied Pharmaceutical Science. 3:S7-S12.

163. Jia M, Chen L, Xin HL, Zheng CJ, Rahman K, Han T, Qin LP (2016): A Friendly Relationship between Endophytic Fungi and Medicinal Plants: A Systematic Review. Frontiers in Microbiology. 7: 906 doi: 10.3389/fmicb.2016.00906.

164. Jiao RH, Ge HM, Shi DH, Tan RX (2006): An apigenin-derived xanthine oxidase inhibitor from *Palhinhaea cernua*. Journal of Natural Products. 69: 1089–1091.

165. Jimenez MC, Curhan GC, Choi HK, Forman JP, Rexrode KM (2016): Plasma uric acid concentrations and risk of ischaemic stroke in women. European Journal of Neurology. 23(7): 1158-64.

166. Johnson LJ, de Bonth AC, Briggs LR, Caradus JR, Finch SC, Fleetwood DJ, Fletcher LR, Hume DE, Johnson RD, Popay AJ, Tapper BA, Simpson WR, Voisey CR, Card SD (2013a): The exploitation of epichloae endophytes for agricultural benefit. Fungal Diversity. 60: 171–188.

167. Johnson RJ, Nakagawa T, Sanchez-Lozada LG, Shafiu M, Sundaram S, Le M, Ishimoto T, Sautin YY, Lanaspa MA (2013b): Sugar, uric acid, and the etiology of diabetes and obesity. Diabetes. 62(10):3307-15.

168. Jothy SL, Zakaria Z, Sasidharan S (2011): Phytochemicals screening, DPPH free radical scavenging and xanthine oxidase inhibitory activities of *Cassia fistula* seeds extract. Journal of Medicinal Plants Research. 5(10): 1941-1947.

169. Kanbay M, Jensen T, Solak Y, Roncal-Jinenez C, Rivard C, Lanaspa MA, Nakagawa T, Johnson RJ (2016): Uric acid in metabolic syndrome: from an innocent bystander to a central player. European Journal of International Medicine. 29: 3-8.

170. Kantamreddi VSSN, Lakshmi YN, Kasapu VVVS (2010): Preliminary phytochemical analysis of some important indian plant species. International Journal of Pharmacy and Biological Science. 1(4): 351-357.

171. Kapoor N and Saxena S (2016): Xanthine oxidase inhibitory and antioxidant potential of Indian *Muscodor* species. 3Biotech. 6:248.

172. Kapoor N, Saxena S (2014): Potential xanthine oxidase inhibitory activity of endophytic *Lasiodiplodia pseudotheobromae*. Applied Biochemistry and Biotechnology. 173: 1360–1374.

173. Katz L, Baltz RH (2016): Natural product discovery: past, present, and future. Journal of Industrial Microbiology and Biotechnology. 43(2-3): 155-76.

174. Kaul S, Gupta S, Ahmed M, Dhar K (2012): Endophytic fungi from medicinal plants: a treasure hunt for bioactive metabolites. Phytochemistry Reviews. 11(4): 487-505.

175. Kennedy LD, Ajiboye VO (2010): Rasburicase for the prevention and treatment of hyperuricemia in tumor lysis syndrome. Journal of Oncology Pharmacy Practice. 16(3): 205–213.

176. Khan AL, Ali L, Hussain J, Rizvi TS, Al-Harrasi A, Lee IJ (2015): Enzyme Inhibitory Radicinol derivative from endophytic fungus *Bipolaris sorokiniana* LK12, associated with *Rhazya stricta.* Molecules. 20: 12198-12208.

177. Kim JH, Na HJ, Kim CK, Kim JY, Ha KS, Lee H, Chung HT, Kwon HJ, Kwon YG, Kim YM (2008): The non-provitamin A carotenoid, lutein, inhibits NF-κB-dependent gene expression through redox-based regulation of the phosphatidylinositol 3-kinase/PTEN/Akt and NF-κB-inducing kinase pathways: Role of H_2O_2 in NF-κB activation. Free Radical Biology and Medicine. 45: 885-896.

178. Kittleson MM, Hare JM (2005): Xanthine oxidase inhibitors: an emerging class of drugs for heart failure. European Heart Journal. 26: 1458-1460.

179. Komers R, Xu B, Schneider J, Oyama TT (2016): Effects of xanthine oxidase inhibition with febuxostat on the development of nephropathy in experimental type 2 diabetes. British Journal of Pharmacology. 173(17): 2573-88.

180. Kong LD, Cai Y, Huang WW, Cheng CHK, and Tan RX (2000a): Inhibition of xanthine oxidase by some chinese medicinal plants used to treat gout. Journal of Ethnopharmacology. 73: 199–207.

181. Kong LD, Zhang Y, Pan X, Tan RX, Cheng CHK (2000b): Inhibition of xanthine oxidase by Liquiritigenin and Isoliquiritigenin isolated from *Sinofranchetia chinensis.* Cellular and Molecular Life Sciences. 57(3): 500-505.

182. Kour A, Shawl A, Rehman S, Sultan P, Qazi P, Suden P, Khajuria RK, Verma V (2008): Isolation and identification of an endophytic strain of *Fusarium oxysporum* producing Podophyllotoxin from *Juniperus recurva*. World Journal of Microbiology and Biotechnology. 24: 1115–1121.

183. Krings M, Taylor TN, Hass H, Kerp H, Dotzler N, Hermsen EJ (2007): Fungal endophytes in a 400-million-yr-old land plant: infection pathways, spatial distribution, and host responses. New Phytologist. 174(3):648-57.

184. Kubo I, Masuoka N, Ha TJ, Tsujimoto K (2006): Antioxidant activity of anacardic acids. Food Chemistry. 99: 555-562.

185. Kudalkar P, Strobel G, Riyaz Ul Hasan S, Geary G, Sears J (2012): *Muscodor sutura,* A novel endophytic fungus with volatile antibiotic activities. Mycoscience. 53: 319–325.

186. Kulanthaivel P, Hallock YF, Boros C, Hamilton SM, Janzen WP, Ballas LM, Loomis CR, Jiang JB (1993): Balanol: A novel and potent inhibitor of protein kinase C from the fungus *Verticwum balanoides*. Journal of American chemical society. 115: 6452-6453.

187. Kumar S, Kaushik N, Proksch P (2013): Identification of antifungal principle in the solvent extract of an endophytic fungus *Chaetomium globosum* from *Withania somnifera.* Springerplus. 2:37.

188. Kumar US, Tiwari AK, Reddy SV, Aparna P, Rao RJ, Ali AZ, Rao JM (2005): Free-Radical-Scavenging and Xanthine Oxidase Inhibitory constituents from *Stereospermum personatum.* Journal of Natural Products. 68: 1615-1621.

189. Kuo CF, Grainge MJ, Zhang W, Doherty M (2015): Global epidemiology of gout: prevalence, incidence and risk factors. Rheumatology. 11(11): 649-62

190. Kusari S, Hertweck C, Spiteller M (2012): Chemical ecology of endophytic fungi: origins of secondary metabolites. Chemical Biology. 19(7): 792–798.

191. Kusari S, Lamshöft M, Spiteller M (2009a): *Aspergillus fumigatus* Fresenius, an endophytic fungus from *Juniperus communis* L. Horstmann as a novel source of the anticancer pro-drug deoxypodophyllotoxin. Journal of Applied Microbiology. 107: 1019–1030

192. Kusari S, Singh S, Jayabaskaran C (2014): Biotechnological potential of plant–associated endophytic fungi: hope versus hype. Trends in Biotechnology. 32(6): 297–303.

193. Kusari S, Zuhlke S, Spiteller M (2009b): An endophytic fungus from *Camptotheca acuminata* that produces camptothecin and analogues. Journal of Natural products. 72(1): 2–7

194. LaFountain AM, Pacheco C, Prum RO, Frank HA (2013): Nuclear magnetic resonance analysis of carotenoids from the burgundy plumage of the *Pompadour Cotinga* (Xipholena punicea). Archives of Biochemistry and Biophysics. 539: 133–141.

195. Lam LH, Sakaguchi K, Ukeda H, Sawamura M (2006): Flow injection determination of xanthine oxidase inhibitory activity and its application to food samples. Analytical Sciences. 22: 105-109.

196. Lanaspa MA, Cicerchi C, Garcia G, Li N, Roncal-Jimenez CA, Rivard CJ, Hunter B, Andres-Hernando A, Ishimoto T, Sanchez-Lozda L, Thomas J, Hodges RS, Mant CT, Johnson RJ (2012a) Counteracting Roles of AMP Deaminase and AMP Kinase in the Development of Fatty Liver. PLoS ONE. 7(11): e48801. doi:10.1371/journal.pone.0048801.

197. Lanaspa MA, Sanchez-Lozada LG, Choi YJ, Cicerchi C, Kanbay M, Roncal-Jimenez CA, Ishimoto T, Li N, Marek G, Duranay M, Schreiner G (2012b): Uric acid induces hepatic steatosis by generation

of mitochondrial oxidative stress: potential role in fructose-dependent and -independent fatty liver. Journal of Biological Chemistry. 287: 40732–40744.

198. Larkin MA, Blackshields G, Brown NP, Chenna R, McGettigan PA, Mcwilliam H, Valentin F, Wallace IM, Wilm A, Lopez R et al. (2007): Clustal W and Clustal X version 2.0. Bioinformatics 23: 2947–2948.

199. Lespade L, Bercion S (2010): Theoretical study of the mechanism of inhibition of xanthine oxidase by flavonoids and gallic acid derivatives. Journal of Physical Chemistry. 114: 921-928

200. Levita J, Sumiwi SA, Pratiwi TI, Ilham E, Sidiq SP, Moektiwardoyo M (2016): Pharmacological Activities of *Plectranthus scutellarioides* (L.) R.Br. leaves extract on cyclooxygenase and xanthine oxidase enzymes. Journal of Medicinal Plants research. 10(20): 261-269.

201. Li S, Tang Y, Liu C, Li J, Guo L, Zhang Y (2015b): Development of a method to screen and isolate potential xanthine oxidase inhibitors from *Panax japlcus* var via ultrafiltration liquid chromatography combined with counter-current chromatography. Talanta. 134: 665–673.

202. Li Y, Lai P, Chen J, Shen H, Tang B, Wu L, Weng M (2016): Extraction optimization of polyphenols, antioxidant and xanthine oxidase inhibitory activities from *Prunus salicina* Lindl. Food Science and Technology. 36(3): 520-5.

203. Li Y, Xu C, Yu C, Xu L, Miao M (2009): Association of serum uric acid level with non-alcoholic fatty liver disease: a cross-sectional study. Journal of Hepatology. 50(5): 1029–1034.

204. Li YL, Xin XM, Chang ZY, Shi RJ, Miao ZM, Ding J, Hao GP (2015a): The endophytic fungi of *Salvia miltiorrhiza* Bge.f. alba are a potential source of natural antioxidants. Botanical Studies An International Journal. 56:5.

205. Lin SY, Wang CC, Lu YL, Wu WC, Hou WC (2008): Antioxidant, anti-semicarbazide-sensitive amine oxidase, and anti-hypertensive activities of geraniin isolated from *Phyllanthus urinaria.* Food and Chemical Toxicology. 46: 2485–2492.

206. Lin WQ, Xie JX, Wu XM, Yang L, Wang HD (2014): Inhibition of xanthine oxidase activity by *Gnaphalium affine* Extract. Chinese Medical Sciences Journal. 29 (4): 225-230.

207. Liote F (2003): Hyperuricemia and Gout. Current Rheumatology Reports. 5: 227-234.

208. Liu HX, He MT, Tan H.B, Gu W, Yang SX, Wang YH, Li L, Long CL (2015): Xanthine oxidase inhibitors isolated from *Piper nudibaccatum*. Phytochemistry Letters. 12: 133–137.

209. Liu K, Wang W, Guo BH, Gao H, Liu Y, Liu XH, Yao HL, Cheng K (2016): Chemical evidence for potent xanthine oxidase inhibitory activity of ethyl acetate extract of *Citrus aurantium* L. dried immature fruits. Molecules. 21: 302; doi:10.3390/molecules21030302.

210. Liu L, Xiao A, Ma L, Li D (2017): Analysis of Xanthine Oxidase Inhibitors from *Puerariae flos* using centrifugal ultrafiltration coupled with HPLC-MS. Journal of Brazilian Chemical Society. 28(2): 360-366.

211. Liu X, Chen R, Shang Y, Jiao B, Huang C (2008): Lithospermic acid as a novel xanthine oxidase inhibitor has anti-inflammatory and hypouricemic effects in rats. Chemico-Biological Interactions. 176(2–3): 137-142.

212. Lo HM, Tsai YJ, Du WY, Tsou CJ, Wu WB (2012): A naturally occurring carotenoid, lutein, reduces PDGF and H_2O_2 signaling and compromises migration in cultured vascular smooth muscle cells. Journal of Biomedical Science. 19(18):1-9.

213. Lomax CA, Bagnara AS, Henderson JF (1975): Studies of the Regulation of Purine Nucleotide Catabolism. Canadian Journal of Biochemistry. 53: 231-241.

214. Lonardo A, Loria P, Leonardi F, Borsatti A, Neri P, Pulvirenti M, Verrone AM, Bagni A, Bertolotti M, Ganazzi D, Carulli N (2002): Fasting insulin and uric acid levels but not indices of iron metabolism are independent predictors of non-alcoholic fatty liver disease. A case–control study. Digestive and Liver Disease. 34(3): 204–211.

215. Lou J, Yu R, Wang X, Mao Z, Fu L, Liu Y, Zhou L (2016): Alternariol 9-methyl ether from the endophytic fungus *Alternaria* sp. Samif01 and its bioactivities. Brazilian journal of microbiology. 47: 96–101.

216. Lugtenberg BJJ, Caradus JR, Johnson LJ (2016): Fungal endophytes for sustainable crop production. FEMS Microbiology Ecology. 92:12.

217. Luk AJ, Simkin PA (2005): Epidemiology of hyperuricemia and gout. The American Journal of Managed Care. 11(15): S435-42.

218. Luo Y, Cobb RE, Zhao H (2014): Recent advances in natural product discovery. Current Opinion in Biotechnology. 30: 230–237.

219. Ma H, Overstreet RM, Subbotin SA (2008): ITS2 secondary structure and phylogeny of cyst-forming nematodes of the genus *Heterodera* (Tylenchida: Heteroderidae). Organisms, Diversity and Evolution, 8: 182–193.

220. Ma X, Wang WM, Bittner F, Schmidt N, Berkey R, Zhang L, King H, Zhang Y, Feng J, Wen Y, Tan L, Li Y, Zhang Q, Deng Z, Xiong X, Xiao S (2016): Dual and opposing roles of xanthine dehydrogenase in defense-associated reactive oxygen species metabolism in Arabidopsis. Plant Cell. 28: 1108–1126.

221. Maiuolo J, Oppedisano F, Gratteri S, Muscoli C, Mollace V (2016): Regulation of uric acid metabolism and excretion. International Journal of Cardiology. 213: 8–14.

222. Mallat SG, Kattar SA, Tanios BY, Jurjus A (2016): Hyperuricemia, Hypertension, and Chronic Kidney Disease: an emerging association. Current Hypertension Reports. 18:74

223. Mandala SM, Thornton RA, Rosenbach M, Milligan J, Garcia-Calvo M, Bull HG, Kurtz MB (1997): Khafrefungin, a novel inhibitor of sphingolipid synthesis. The Journal of Biological Chemistry. 272 (51): 32709-32714.

224. Marques MW, Lima NB, de Morais A, Jr M, Barbosa MAG, Souza BO, Michereff SJ, Phillips AJL, Câmara MPS (2013): Species of *Lasiodiplodia* associated with mango in Brazil. Fungal Diversity. 61(1): 181-193.

225. Mashino M, Takigawa Y, Saito N, Wong LQ, Mochizuki M (2001): Antioxidant activity and xanthine oxidase inhibition activity of reductic acid: Ascorbic acid analogue. Bioorganic & Medicinal Chemistry Letters. 10(24): 2783-5 ·

226. Mathan S, Subramanian V, Nagamony S (2013): Optimization and antimicrobial metabolite production from endophytic fungi *Aspergillus terreus* KC 582297. European Journal of Experimental Biology. 3(4):138-144.

227. Matsumoto K, Okamoto K, Ashizawa N, Nishino T (2011): FYX-051: a novel and potent hybrid-type inhibitor of xanthine oxidoreductase. Journal of Pharmacology and Experimental Therapeutics. 336: 95–103.

228. Meerson FZ, Kagon VE, Kozlov YP, Bellina LM, Arkkhipenko YV (1982): The role of lipid peroxidation in pathogenesis of ischemic damage and the antioxidant protection of the heart. Basic Research in Cardiology. 77: 465–485.

229. Meléndez-Martínez AJ, Vicario IM, Heredia FJ (2007): Review: Analysis of carotenoids in orange juice. Journal of Food Composition and Analysis. 20(7): 638–649.

230. Meng J, Li Y, Yuan X, lu Y (2016): Effects of febuxostat on insulin resistance and expression of high-sensitivity C-reactive protein in patients with primary gout. Rheumatology international. 23: 1-5.

231. Mercado-Blanco J (2015): Life of microbes inside the plant. In: Lugtenberg B (ed.). Principles of Plant-Microbe Interactions- Microbes for Sustainable Agriculture. Dordrecht, the Netherlands: Springer, 25–32.

232. Merlin JN, Christhudas IVSN, Kumar PP, Agastian A (2013): Optimization of growth and bioactive metabolite production: *Fusarium solani*. Asian Journal of pharmaceutical and clinical research. 6(3): 98-103.

233. Meshram V, Kapoor N, Saxena S (2013): *Muscodor kashayum* sp. nov. – a new volatile anti-microbial producing endophytic fungus. Mycology. 4(4): 196–204.

234. Michalak I, Chojnacka K (2015): Algae as production systems of bioactive compounds. Engineering in Life Sciences. 15: 160–176.

235. Mitchell A, Strobel G, Hess W, Vargas P, Ezra D (2008): *Muscodor crispans*, a novel endophyte from *Ananas ananassoides* in the Bolivian Amazon. Fungal Diversity. 31: 37–43.

236. Muller CA, Obermeier MM, Berg G (2016): Bio-prospecting plant-associated microbiomes. Journal of Biotechnology. 235: 171-80.

237. Mundhe SA, Mhasde DR (2016): The study of prevalence of hyperuricemia and metabolic syndrome in type 2 diabetes mellitus. International Journal of Advances in Medicine. 3(2): 241-249.

238. Murata K, Nakao K, Hirata N, Namba K, Nomi T, Kitamura Y, Moriyama K, Shintani T, Iinuma M, Matsuda H (2009): Hydroxychavicol: a potent xanthine oxidase inhibitor obtained from the leaves of betel, *Piper betle*. Journal of Natural Medicine. 63: 355–359.

239. Nagao A, Seki M, Kobayashi H (1999): inhibition of xanthine oxidase by Flavonoids. Bioscience, Biotechnology and Biochemistry. 63(10): 1787-1790.

240. Naik BS, Shashikala J, Krishnamurthy YL (2008): Diversity of fungal endophytes in shrubby medicinal plants of Malnad region, Western Ghats, Southern India. Fungal ecology. 1: 89–93.

241. Naik S (2009): Taxonomic placement for mycelia sterilia in endophytic fungal research: A molecular approach. Current science. 97(9):1276-1277 ·

242. Nalini MS, Sunayana N, Prakash HS (2014): Endophytic Fungal Diversity in Medicinal Plants of Western Ghats, India. International Journal of Biodiversity. 2014 (494213).

243. Narasimhan S (1982): Control of glycoprotein synthesis. UDP-GlcNAc: glycopeptide beta 4-N-acetylglucosaminyltransferase III, an enzyme in hen oviduct which adds GlcNAc in beta 1-4 linkage to the beta-linked mannose of the trimannosyl core of N-glycosyl oligosaccharides. Journal of Biological Chemistry. 257(17): 10235-42.

244. Newman DJ, Cragg GM (2012): Natural products as sources of new Drugs over the 30 years from 1981 to 2010. Journal of Natural Products. 75: 311-335.

245. Newman DJ, Cragg GM (2016): Natural Products as Sources of New Drugs from 1981 to 2014. Journal of Natural Products. 79: 629-661.

246. Newman DJ, Cragg GM (2015): Endophytic and epiphytic microbes as "sources" of bioactive agents. Frontiers in Chemistry. 3: 34.

247. Nguyen MT, Nguyen NT (2013): A new lupane triterpene from *Tetracera scandens* L., xanthine oxidase inhibitor. Natural products and Research. 27(1): 61-67.

248. Nguyen MTT, Awale S, Tezuka Y, Le Tran Q, Watanabe H, Kadota S (2004): Xanthine oxidase inhibitory activity of Vietnamese medicinal plants. Biological & Pharmaceutical Bulletin. 27: 1414–1421.

249. Nicoletti R and Fiorentino A (2015): Plant Bioactive Metabolites and Drugs Produced by Endophytic Fungi of Spermatophyta. Agriculture. 5: 918-970.

250. Nile SH and Khobragade CN (2011): Indian Phytochemical analysis, antioxidant and xanthine oxidase inhibitory activity of *Tephrosia purpurea* Linn. root extract. Journal of Natural Products and Resources. 2: 52-58.

251. Nile SH and Park SW (2014): HPTLC Analysis, antioxidant and antigout activity of Indian Plants. Iranian Journal of Pharmaceutical Research. 13 (2): 531-539.

252. Nisa H, Kamili AN, Nawchoo IA, Shafi S, Shameem N and Bandh SA (2015): Fungal endophytes as prolific source of phytochemicals and other bioactive natural products: A review. Microbial pathogenesis. 82: 50-59.

253. Nyhan WL (2005): Disorders of purine and pyrimidine metabolism. Molecular Genetics and Metabolism. 86(1-2): 25-33

254. Oloyed OI (2005): Chemical profile of unripe pulp of *Carica pagaya*. Pakistan Journal of Nutrition. 4: 379-381.

255. Ong SL, Mah SH, Lai HY (2016): Porcine Pancreatic Lipase Inhibitory agent isolated from medicinal herb and inhibition kinetics of extracts from *Eleusine indica* (L.) gaertner. Journal of Pharmaceutics. 2016:8764274.

256. Otaka J, Seo S, Nishimura M (2016): Lutein, a Natural Carotenoid, Induces α-1,3-Glucan accumulation on the cell wall surface of fungal plant pathogens. Molecules. 21:980.

257. Pacher P, Nivorozhkin A, Szabo C (2006): Therapeutic effects of xanthine oxidase inhibitors: renaissance half a century after the discovery of allopurinol. Pharmacology Reviews. 58: 87–114.

258. Palmieri VO, Grattagliano I, Portincasa P, Palasciano G (2006): Systemic oxidative alterations are associated with visceral adiposity and liver steatosis in patients with metabolic syndrome. The Journal of Nutrition. 136(12): 3022-6.

259. Pandey NR, Kaur G, Chandra M, Sanwal GG, Misra MK (2000): Enzymatic oxidant and antioxidants of human blood platelets in unstable angina and myocardial infarction. International Journal of Cardiology. 76(1): 33-38.

260. Papapostolou I, Georgiou CD (2010): Superoxide radical is involved in the sclerotial differentiation of filamentous phytopathogenic fungi: identification of a fungal xanthine oxidase. Fungal biology. 114: 387–395.

261. Parthasarathy R, Sathiyabama M (2015): Lovastatin-producing endophytic fungus isolated from a medicinal plant *Solanum xanthocarpum*. Natural Product Research. 29(24): 2282-2286.

262. Pedley AM, Benkovic SJ (2016): A new view into the regulation of purine metabolism-the purinosome. Trends in Biochemical Sciences. DOI: http://dx.doi.org/10.1016/j.tibs.2016.09.009.

263. Perez-Ruiz F, Calabozo C, Herrero-Beites A, Garcia-Erauskin G, Pijoan J (2000): Improvement in renal function in patients with chronic gout after proper control of hyperuricemia and gouty bouts. Nephron. 86: 287–291.

264. Phongpaichit S, Nikom J, Rungjindamai N, Sakayaroj J, Hutadilok-Towatana N, Rukachaisirikul V, Kirtikara K (2007): Biological activities of extracts from endophytic fungi isolated from *Garcinia* plants. FEMS Immunology and Medical Microbiology. 51: 517–525

265. Phuwapraisirisan P, Sowanthip P, Miles DH, Tip-pyang S (2006): Reactive radical scavenging and xanthine oxidase inhibition of Proanthocyanidins from *Carallia brachiata.* Phytotherapy research. 20: 458-461.

266. Pirttila AM, Frank C (2011): Endophytes of forest trees: biology and applications. Springer.

267. Porras-Alfaro A, Bayman P (2011): Hidden fungi, emergent properties: endophytes and microbiomes. Annual Reviews in Phytopathology. 49: 291-315

268. Pradeep FS, Pradeep BV (2013): Optimization of pigment and biomass production from *Fusarium moniliforme* under submerged fermentation conditions. International Journal of Pharmacy and Pharmaceutical Sciences. 5(3): 526-535.

269. Pratheesh VB, Benny N, Sujatha CH (2009): Isolation, stabilization and characterization of xanthophyll from Marigold Flower- *Tagetes Erecta*-L. Modern Applied Science. 3(2): 19-28.

270. Priti V, Ramesha BT, Singh S, Ravikanth G, Ganeshaiah KN, Suryanarayanan TS, Uma Shaanker R (2009): How promising are endophytic fungi as alternative sources of plant secondary metabolites? Current Science. 97(4): 477-478.

271. Priyanto LHA, Sukandar EY (2007): Xanthine oxidase inhibitor activity of terpenoid and pyrrole compounds from isolated from snake fruit (*Salacca edulis* Reinw) cv. Bongkok. Journal of Applied Sciences. 7(20): 3127-3130.

272. Puddu P, Puddu GM, Cravero E, Vizioli L, Muscari A (2012): Relationships among hyperuricemia, endothelial dysfunction and cardiovascular disease: molecular mechanisms and clinical implications. Journal of Cardiology. 59(3): 235-242.

273. Puri SC, Nazir A, Chawla R, Arora R, Riyaz-Ul-Hassan S, Amna T, Ahmad B, Verma V, Singh S, Sagar R, Sharma A, Kumar R, Sharma RK, Qazi GN (2006): The endophytic fungus *Trametes hirsuta* as a novel alternative source of podophyllotoxin and related aryl tetralin lignans. Journal of Biotechnology. 122: 494–510.

274. Puri SC, Verma V, Amna T, Qazi GN, Spiteller M (2005): An endophytic fungus from *Nothapodytes foetida* that produces camptothecin. Journal of Natural Products. 68(12): 1717–1719.

275. Qadri M, Nalli Y, Chaubey A, Ali A, Strobel GA, Vishwakarma RA, Hassan SRU (2016): An Insight into the secondary metabolism of *Muscodor yucatanensis*: small-molecule epigenetic modifiers induce expression of secondary metabolism-related genes and production of new etabolites in the endophyte. Microbial Ecology. DOI 10.1007/s00248-016-0901-y.

276. Raghuvanshi R, Kaul A, Bhakuni P, Mishra A, Misra MK (2007): Xanthine oxidase as a marker of myocardial infarction. Indian Journal of Clinical Biochemistry. 22(2): 90-92.

277. Rahman T, Hosen I, Islam MMT, Shekhar HU (2012): Oxidative stress and human health. Advances in Bioscience and Biotechnology. 3: 997-1019.

278. Rai and Agarkar (2014): Plant–fungal interactions: What triggers the fungi to switch among lifestyles? Critical reviews in Microbiology. 42(3): 428-438.

279. Raju R, Joseph SM, Pothen N, Abraham E, Scaria S, Mathews SM (2011): *in vitro* xanthine oxidase inhibitory activity of the fractions of *Tinospora cordifolia.* International Journal of Drug Formulation and Research. 2(5): 413-419.

280. Rambaut A (2007): FigTree, a graphical viewer of phylogenetic trees. Institute of evolutionary Biology University of Edinburgh.

281. Rampersad SN (2014): ITS1, 5.8S and ITS2 secondary structure modelling for intra-specific differentiation among species of the *Colletotrichum gloeosporioides* sensu lato species complex. SpringerPlus, 3: 684.

282. Rashidi MR, Soruaddin MH, Taherradeh F, Touyban A (2009): Catalytic activity and stability of xanthine oxidase in aqueous – organic mixtures. Biochemistry (Moscow). 74(1): 124-130.

283. Raviraja NS, Maria GL, Sridhar KR (2006): Antimicrobial evaluation of endophytic fungi inhabiting medicinal plants of the Western ghats of India. Life Science. 6: 515–520.

284. Ribeiro B, Valenta P, Baptista P, Seabra RM, Andrade PB (2007): Phenolic compounds, organic acids profiles and antioxidative properties of beefsteak fungus (*Fistulina hepatica*). Food and Chemical Toxicology. 45:1805–1813.

285. Richette P, Briere C, Honene-Claviert V, Loeuille D, Bardin T (2007): Rasburicase for tophaceous gout not treatable with allopurinol: An exploratory study. Journal of Rheumatology. 34: 1093–1098.

286. Rivera-Chávez J, Figueroa M, González MDL, Glenn AE, Mata R (2015): α-Glucosidase Inhibitors from a *Xylaria feejeensis* associated with *Hintonia latiflora.* Journal of Natural Products. 78 (4): 730–735

287. Rivera-Chávez J, González-Andrade M, González MDC, Glenn AE, Mata R (2013): Thielavins A, J and K: a-Glucosidase inhibitors from MEXU 27095, an endophytic fungus from *Hintonia latiflora.* Phytochemistry. 94: 198–205.

288. Rob D, Marek J, Dostálová G, Goláň L, Linhart A (2016): Correction: Uric Acid as a Marker of mortality and morbidity in Fabry Disease. PLOS ONE 11(11): e0166290.

289. Robles-Cervantes JA, Ramos-Zavala MG, Gonzalez-Ortiz M, Martinez-Abundis E, Valencia-Sandoval C, Torres-Chávez A, Espinel-Bermúdez C, Santiago-Hernández NJ, Hernández-González SO (2011): Relationship between serum concentration of uric acid and insulin secretion among adults with type 2 diabetes mellitus. International journal of endocrinology. 2011(107904): 1-4.

290. Rodic Z, Simonovska B, Albreht A, Vovk I (2012): Determination of lutein by high-performance thin-layer chromatography using densitometry and screening of major dietary carotenoids in food supplements. Journal of Chromatography A. 1231: 59- 65.

291. Rodriguez RJ, Henson J, Van Volkenburgh E, Hoy M, Wright L, Beckwith F, Kim YO, Redman RS (2008): Stress tolerance in plants via habitat-adapted symbiosis. ISME J. 2: 404–416.

292. Rodriguez RJ, White JF, Arnold AE, Redman RS (2009): Fungal endophytes: diversity and functional roles. New Phytologist. 182: 314-330.

293. Rosa LH, Vieira MLA, Cota BB, Johann S, Alves TMA, Zani CL, Rosa CA (2011): Endophytic Fungi of tropical forests: A promising source of bioactive prototype molecules for the treatment of neglected diseases, Drug Development - A Case Study Based Insight into Modern Strategies, Dr. Chris Rundfeldt (Ed.), ISBN: 978-953-307-257-9, InTech.

294. Ryu S, Chang Y, Kim SG, Cho J, Guallar E (2011): Serum uric acid levels predict incident nonalcoholic fatty liver disease in healthy Korean men. Metabolism. 60: 860–866.

295. Saag KG, Fitz-Patrick D, Kopicko J, Fung M, Bhakta N, Adler S, Storgard C, Baumgartner S, Becker MA (2016): Lesinurad Combined With Allopurinol: A Randomized, Double-Blind, Placebo-Controlled Study in Gout Patients With an Inadequate Response to Standard-of-Care Allopurinol (a US-Based Study). Arthritis and Rheumatology. 69(1): 203-212.

296. Sah OSP, Qing YX (2015): Associations between hyperuricemia and chronic kidney disease: a review. Nephro-urology Monthly. 7(3): 27233.

297. Sahgal G, Ramanathan S, Sasidharan S, Mordi MN, Ismail S, and Mansoor SM (2009): *In vitro* antioxidant and xanthine oxidase inhibitory activities of methanolic *Swietenia mahagoni* seed extracts. Molecules. 14: 4476-4485.

298. Saitou N, Nei M (1987): The Neighbour-Joining Method: A new method for reconstructing phylogenetic trees. Molecular Biology and Evolution. 4**:** 406-425.

299. Salkowski E (1897): Ueber die quantitative Bestimmung der Alloxurbasen im Harn mittelst des Silberverfahrens. Pflugers Archiv - European Journal of Physiology. 69: 268-306.

300. Sato Y, Kobayashi M, Itagaki S, Hirano T, Noda T, Sugawara M, Iseki K, Mizuno S (2011): Protective effect of lutein after ischemia-reperfusion in the small intestine. Food Chemistry. 127: 893–898.

301. Sawhney S, Mir M, Kumar S (2011): Phytochemical screening and antioxidant properties of *Bauhinia variegata* (bark). Journal of pharmaceutical science and technology. 3(8): 646-650.

302. Saxena S, Meshram V, Kapoor N (2014): *Muscodor darjeelingensis*, a new endophytic fungus of *Cinnamomum camphora* collected from north eastern Himalayas. Sydowia. 66(1): 2014–0055

303. Saxena S, Meshram V, Kapoor N (2015): *Muscodor tigerii* sp. nov.-Volatile antibiotic producing endophytic fungus from north eastern Himalayas. Annals of Microbiology. 65:47–57

304. Schultz J, Wolf M (2009): ITS2 sequence-structure analysis in phylogenetics: A how-to manual for molecular systematics. Molecular Phylogenetics and Evolution, 52: 520–523

305. Schulz B, Boyle C (2006): What are endophytes? In: Schulz BJE, Boyle CJC, Sieber TN, editors. Microbial Root Endophytes. Berlin, Germany: Springer-Verlag; 2006. pp. 1–13.

306. Schulz B, Boyle C, Draeger S, Roemmert AK, Krohn K (2002): Endophytic fungi: a source of novel biologically active secondary metabolites. Mycological Research. 106: 996–1004.

307. Schulz B, Wanke U, Drager S, Aust HJ (1993): Endophytes from herbaceous plants and shrubs: effectiveness of surface sterilization methods. Mycological Research. 97(12): 1447–1450

308. Schumacher HR, Becker MA, Lloyd E, MacDonald PA, Lademacher C (2009): Febuxostat in the treatment of gout: 5-yr findings of the FOCUS efficacy and safety study. Rheumatology (Oxford) 48: 188–19.

309. Scott F W, Trick KD, Stavric B, Braaten JT, Siddiqui Y (1981): Uric Acid-Induced decrease in rat insulin secretion. Proceedings of the Society for Experimental Biology and Medicine. 166: 123—128.

310. Seibel PN, Muller T, Dandekar T, Schultz J, Wolf M (2006): 4SALE a tool for synchronous RNA sequence and secondary structure alignment and editing. BMC Bioinformatics. 7: 498.

311. Senthilmurugan VG, Sekar R, Suresh K, Balamurugan S (2013): Phytochemical screening, enzyme and antibacterial activity analysis of endophytic fungi *Botrytis* sp isolated from *Ficus benghalensis*. International Journal of Pharmaceutical Research and Bioscience. 2(4): 264-273.

312. Sesh PSL, Venkatesan P, Jeyaraja K, Chandrasekar M, Pandiyan V (2015): Xanthine oxidase as a biochemical marker of dilated cardiomyopathy in dogs. Indian Journal of Animal Research. 49(2): 187-190.

313. Shah P, Bjornstad P, Johnson RJ (2016): Hyperuricemia as a potential risk factor for type 2 diabetes and diabetic nephropathy. Jornal Brasileiro de Nefrologia. 38(4): 386-387.

314. Sharma NK, Thakur S, Thakur N, Savitri, Bhalla TC (2016): Thermostable xanthine oxidase activity from *Bacillus pumilus* RL-2d isolated from manikaran thermal spring: production and characterization. Indian Journal of Microbiology. 56(1): 88–98.

315. Shen L, Shi DH, Song YC, Tan RX (2009): Chemical Constituents of liquid culture of endophyte IFB-E012 in *Artemisia annua.* Chinese Journal of Natural Products. 7(5): 354-356.

316. Shi Y, Evans JE, Rock KL (2003): Molecular identification of a danger signal that alerts the immune system to dying cells. Nature. 425: 516-521.

317. Shu RG, Wang FW, Yang YM, Liu YX, and Tan RX (2004): Antibacterial and xanthine oxidase inhibitory cerebrosides from *Fusarium sp.* IFB-121, an endophytic fungus in *Quercus variabilis*. Lipids. 39: 667-673.

318. Shweta S, Zuehlke S, Ramesha BT, Priti V, Mohana Kumar P, Ravikanth G, Spiteller M, Vasudeva R, Uma Shaanker R (2010): Endophytic fungal strains of *Fusarium solani*, from *Apodytes dimidiata* E. Mey. ex Arn (Icacinaceae) produce camptothecin, 10-hydroxycamptothecin and 9-methoxycamptothecin. Phytochemistry. 71(1): 117-22.

319. Sierla M, Waszczak C, Vahisalu T, Kangasjärvi J (2016): Reactive oxygen species in the regulation of stomatal movements. Plant Physiology. 171: 1569–1580.

320. Sies H, Stahl W, Sundquist AR (1992): Antioxidant functions of vitamins. Vitamins E and C, beta-carotene, and other carotenoids. Annals of the New York Academy of Sciences. 368: 7-19.

321. Sindhu ER, Preethi KC, Kuttan R (2010): Antioxidant activity of carotenoid lutein *in vitro* and *in vivo.* Indian Journal of Experimental Biology. 48(8): 843-8.

322. Singh B, Kaur T, Kaur S, Manhas RK, Kaur A (2015): An Alpha-Glucosidase Inhibitor from an endophytic *Cladosporium* sp. with potential as a biocontrol agent. Applied Biochemistry and Biotechnology. 175 (4): 2020–2034

323. Singh LP, Gill SS, Tuteja N (2011): Unraveling the role of fungal symbionts in plant abiotic stress tolerance. Plant Signaling and Behavior. 6: 75–191.

324. Singh V, Praveen V, tripathi D, Haque S, Somvanshi P, Katti SB, Tripathi CKM (2015): Isolation, characterization and antifungal docking studies of wortmannin isolated from *Penicillium radicum*. Scientific Reports. 5:11948.

325. Smith C, Heyne S, Richter AS, Will S, Backofen R (2010): Freiburg RNA Tools: a web server integrating IntaRNA, ExpaRNA and LocARNA. Nucleic Acids Research. 38: W373–W377

326. So A, Thorens B (2010): Uric acid transport and disease. Journal of Clinical Investigation. 120(6): 1791-9.

327. Song YC, Li H, Ye YH, Shan CY, Yang YM and Tan RX (2004): Endophytic naphthopyron metabolites are co-inhibitors of xanthine oxidase, SW1116 cell and some microbial growths. FEMS Microbiology Letters. 241: 67-72.

328. Song YS, Kim SH, Sa JH, Jin C, Lim CJ, Park EH (2003): Anti-angiogenic, antioxidant and xanthine oxidase inhibition activities of the mushroom *Phellinus linteus.* Journal of Ethnopharmacology. 88(1): 113-116.

329. Souza ADL, Rodrigues-Filho E, Souza AQL, Pereira JO, Calgarotto AK, Maso V, Marangoni S, Silva SLD (2008): Koninginins, phospholipase A inhibitors from endophytic fungus *Trichoderma koningii.* Toxicon. 51: 240–250.

330. Sowbhagya HB, Sampathu SR, Krishnamurthy (2004): Natural Colorant from Marigold-Chemistry and Technology. Food reviews International. 20(1): 33–50.

331. Sowndhararajan K, Joseph JM, Rajendrakumaran D (2012): *In vitro* xanthine oxidase inhibitory activity of methanol extracts of *Erythrina indica* Lam. leaves and stem bark. Asian Pacific Journal of Tropical Biomedicine. S1415-S1417.

332. Spiekermann S, Landmesser U, Dikalov S, Bredt M, Gamez G, Tatge H, Reepschläger N, Hornig B, Drexler H, Harrison DG (2003): Electron spin resonance characterization of vascular xanthine and NAD(P)H Oxidase activity in patients with coronary artery disease relation to Endothelium-Dependent Vasodilation. Circulation. 107: 1383-1389.

333. Sreejith M, Kannappan N, Santhiagu A, Marathakam A, Ajith PM, Jasemine S (2013): *In vitro* xanthine oxidase inhibitory and antioxidant activities of aerial parts of *Flacourtia sepiaria* Roxb. Oriental Pharmacy and Experimental Medicine. 13(2): 113–120.

334. Srinivasan K, Jagadish LK, Shenbhagaraman R, Muthumary J (2010): Antioxidant activity of Endophytic Fungus *Phyllosticta sp.* Isolated From *Guazuma Tomentosa.* Journal of Phytology. 2(6): 37–41.

335. Stamp LK, Day RO, Yun J (2016): Allopurinol hypersensitivity: investigating the cause and minimizing the risk. Naure Reviews Rheumatology. 12: 235–242.

336. Stierle A, Strobel G, Stierle D (1993) Taxol and taxane production by *Taxomyces andreanae*, an endophytic fungus of pacific yew. Science. 260: 214–216.

337. Stierle A, Strobel G, Stierle D, Grothaus P, Bignami G (1995): The search for a taxol-producing microorganism among the endophytic fungi of the Pacific yew, *Taxus brevifolia.* Journal of Natural Products. 58(9): 1315-24.

338. Stone JK, Polishook JD, White JRJ (2004): Endophytic fungi. In: Mueller G, Bills GF, Foster MS, editors. Biodiversity of fungi: Inventory and monitoring methods. Burlington: Elsevier. pp. 241–270.

339. Strobel G, Daisy B (2003): Bioprospecting for microbial endophytes and their natural products. Microbiology and Molecular Biology Reviews. 67(4): 491–502

340. Strobel G, Daisy B, Castillo U, Harper J (2004): Natural products from endophytic microorganisms. Journal of Natural Products. 67(2): 257-68.

341. Strobel GA (2015): Bioprospecting fuels from fungi. Biotechnology Letters. 37(5): 973-82.

342. Strobel GA, Dirske E, Sears J, Markworth C (2001): Volatile antimicrobials from *Muscodor albus*, a novel endophytic fungus. Microbiology. 147: 2943–295.

343. Sun DQ, Wu SJ, Liu WY, Lu QD, Zhu GQ, Shi KQ, Braddock M, Song D, Zheng MH (2016): Serum uric acid: a new therapeutic target for nonalcoholic fatty liver disease. Expert Opinion on Therapeutic Targets. 20(3): 1-13

344. Sun X, Guo LD (2012): Endophytic fungal diversity: review of traditional and molecular techniques. Mycology. 3:1: 65-76.

345. Sunahara N, Nogi K and Yokogawa K (1977): Production of xanthine Oxidase Inhibitor, 2, 8-Dihydroxyadenine, by *Alcaligenes aquamarines*. Agricultural and Biological Chemistry. 41(7): 1103-1109.

346. Sundy JS, Hershfield MS (2007): Uricase and other novel agents for the management of patients with treatment-failure gout. Current Rheumatology Reports. 9: 258–264.

347. Suresh E, Das P (2012): Recent advances in management of gout. QJM. 105: 407-417.

348. Suryanarayanan TS, Thirunavukkarasub N, Govindarajulub MB, Sassec F, Jansend R, Murali TS (2009): Fungal endophytes and bioprospecting. Fungal Biology Reviews. 23: 9-19.

349. Suwannarach N, Bussaban B, Hyde KD, Lumyong S (2010): *Muscodor cinnamomi,* a new endophytic species from *Cinnamomum bejolghota*. Mycotaxon. 114:15–23

350. Suwannarach N, Kumla J, Bussaban B, Hyde KD, Matsui K, Lumyong S (2013): Molecular and morphological evidence support four new species in the genus *Muscodor* from Northern Thailand. Annals of Microbiology. 63:1341-1351

351. Tamura K, Nei M (1993): Estimation of the number of nucleotide substitutions in the control region of mitochondrial DNA in humans and chimpanzees. Molecular Biology and Evolution. 10: 512-526.

352. Tamura K, Peterson D, Peterson N, Stecher G, Nei M, Kumar S (2011): MEGA5: Molecular Evolutionary Genetics Analysis Using Maximum Likelihood, Evolutionary Distance, and Maximum Parsimony Methods. Molecular Biology and Evolution. 28: 2731-2739.

353. Tan RX, Zou WX (2001): Endophytes: a rich source of functional metabolites. Natural Products Reports. 18: 448–459.

354. Tao H, Zhou J, Wu T, Cheng Z (2014): High-Throughput Superoxide anion radical scavenging capacity assay. Journal of Agricultural and Food Chemistry. 62: 9266−9272.

355. Tejesvi MV, Pirttila AM (2011): Potential of tree endophytes as sources for new drug compounds. In: Pirttila AM, Frank AC, editors. Endophytes of forest trees: Biology and applications. New York: Springer. pp. 295–311.

356. Thiombiano AME, Adama H, Jean BM, Bayala B, Nabèrè O, Roland MNT, Moussa C, Martin K, Jeanne MF, Samson G, Germaine NO (2014): *In vitro* Antioxidant, lipoxygenase and xanthine

oxidase inhibitory activity of fractions and macerate from *Pandiaka angustifolia* (vahl) Hepper. Journal of Applied Pharmaceutical Science. 4 (01): 009-013.

357. Thompson-Gorman SL, Zweier JL (1990): Evaluation of the role of xanthine oxidase in myocardial reperfusion injury. Journal of Biological Chemistry. 265(12): 6656-63.

358. Thornhill DJ, Lord JB (2010): Secondary Structure Models for the Internal Transcribed Spacer (ITS) Region 1 from Symbiotic Dinoflagellates. Protist. 161: 434-451.

359. Tiwari K (2015): The Future Products: Endophytic Fungal Metabolites. Journal of Biodiversity, Bioprospecting and Development. 2(1): 1-7.

360. Tousoulis D, Kampoli AM, Tentolouris C, Papageorgiou N, Stefanadis C (2012): The role of nitric oxide on endothelial function. Current Vascular Pharmacology. 10(1): 4-18.

361. Trabsa H, Baghiani A, Boussoualim N, Krache I, Khennouf S, Charef N, Arrar L (2015): Kinetics of Inhibition of Xanthine Oxidase by *Lycium arabicum* and its protective effect against oxonate-induced Hyperuricemia and renal dysfunction in Mice. Tropical Journal of Pharmaceutical Research. 14 (2): 249-256.

362. Tsai SF and Lee SS (2014): Neolignans as xanthine oxidase inhibitors from *Hyptis rhomboids.* Phytochemistry. 101: 121–127.

363. Tsuda H, Kawada N, Kaimori JY, Kitamura H, Moriyama T, Rakugi H, Takahara S, Isaka Y (2012): Febuxostat suppressed renal ischemiareperfusion injury via reduced oxidative stress Biochemical and Biophysical research communications. 427: 266–272.

364. Tung YT and Chang ST (2010): Inhibition of xanthine oxidase by *Acacia confusa* extracts and their phytochemicals. Journal of Agriculture and Food Chemistry. 58: 781–786.

365. Tuttle KR, Short RA, Johnson RJ (2001): Sex differences in uric acid and risk factors for coronary artery disease. American Journal of Cardiology. 87: 1411–4.

366. Umamaheswari M, Asokkumar K, Sivashanmugam AT, Remyaraju A, Subhadradevi V, Ravi TK (2009): *In vitro* xanthine oxidase inhibitory activity of the fractions of *Erythrina stricta* Roxb. Journal of Ethnopharmacology. 124: 646–648.

367. Umamaheswari M, AsokKumar K, Somasundaram A, Sivashanmugam T, Subhadradevi V, Ravi TK (2007): Xanthine oxidase inhibitory activity of some Indian medical plants. Journal of Ethnopharmacology. 109: 547–551.

368. Umamaheswari M, Chatterjee TK (2008): *In vitro* antioxidant activities of the fractions of *Coccinia Grandis* L. leaf extract. African Journal of Traditional Complementary and Alternative Medicine. 5(1): 61–73.

369. Umezawa H (1972): Enzyme Inhibitors of Microbial Origin. Univ. Tokyo Press p. 107.

370. Unno T, Sugimoto A, Kakuda T (2004): Xanthine oxidase inhibitors from the leaves of *Lagerstroemia speciosa* (L.) Pers. Journal of Ethnopharmacology. 93: 391-395.

371. Van den Berghe G, Vincent MF, Marie S (2006): Disorders of purine and pyrimidine metabolism. In: Fernandes J, Saudubray JM, van den Berghe G, Walter JH (eds) Inborn metabolic diseases: diagnosis and treatment. Springer, Heidelberg, pp 433–449.

372. Van Hoorn DEC, Nijveldt RJ, Leeuwen PAMV, Hofman Z, M'Rabet L, De Bont DBA , Norren KV (2002): Accurate prediction of xanthine oxidase inhibition based on the structure of flavonoids. European Journal of Pharmacology. 451: 111 – 118.

373. Vanyolos A, Orban-Gyapai O, Hohmann J (2014): Xanthine oxidase inhibitory activity of hungarian wild-growing mushrooms. Phytotherapy Research. 28: 1204–1210.

374. Venugopalan A, Srivastava S (2015): Endophytes as *in vitro* production platforms of high value plant secondary metabolites. Biotechnology Advances. 33: 873-87.

375. Verma VC, Gond SK, Mishra A, Kumar A, Kharwar RN, Gange AC (2009): Endophytic actinomycetes from *Azadirachta indica* A. Juss.: isolation, diversity and antimicrobial activity. Microbial Ecology. 57: 749–756

376. Wang GF, Shang YJ, Feng B, Jiao BH, Huang CG (2008a): Renierol from marine sponge *Haliclona sp*.: A natural inhibitor of xanthine oxidase with hypouricemic effects. Journal of enzyme inhibition and medicinal chemistry. 23(3): 406-10.

377. Wang SY, Yang CW, Liao JW, Zhen WW, Chu FH, Chang ST (2008b): Essential oil from leaves of *Cinnamomum osmophloeum* acts as a xanthine oxidase inhibitor and reduces the serum uric acid levels in oxonate-induced mice. Phytomedicine. 15: 940–945.

378. Wang X, Zhao M, Su G, Cai M, Zhou C, Huang J, Lin L (2015): The antioxidant activities and the xanthine oxidase inhibition effects of walnut (*Juglans regia* L.) fruit, stem and leaf. International Journal of Food Science and Technology. 50: 233–239.

379. Wang Y, Tang Y, Liu C, Shi C, Zhang Y (2016): Determination and isolation of potential a-glucosidase and xanthine oxidase inhibitors from *Trifolium pratense* L. by ultrafiltration liquid chromatography and high-speed countercurrent chromatography. Medicinal Chemistry Research. 25: 1020–1029.

380. Wani ZA, Ashraf N, Mohiuddin T, Riyaz-Ul-Hassan S (2015): Plant endophyte symbiosis, an ecological perspective. Applied Microbiology and Biotechnology 99: 2955-2965.

381. Ward HJ (1998): Uric acid as an independent risk factor in the treatment of hypertension. Lancet. 352: 670–671.

382. Weiqi Fu W, Paglia G, Magnúsdóttir M, Steinarsdóttir EA, Gudmundsson S, Palsson B, Andrésson OS, Brynjólfsson S (2014): Effects of abiotic stressors on lutein production in the green microalga *Dunaliella salina*. Microbial Cell Factories. 13(3):1-9

383. Weller MG (2012): A Unifying Review of Bioassay-Guided Fractionation, Effect-Directed Analysis and Related Techniques. Sensors. 12(7): 9181-9209.

384. Weng SC, Tarng DR, Chen YC, Wu MJ (2016): Febuxostat is superior to traditional urate-lowering agents in reducing the progression of kidney function in chronic kidney disease patients. Cogent Medicine. 3: 1213215.

385. Wheeler JG, Juzwishin KDM, Eiriksdottir G, Gudnason V, Danesh J (2005): Serum Uric Acid and Coronary Heart Disease in 9,458 Incident Cases and 155,084 Controls: Prospective Study and Meta-Analysis. PLOS Medicine. 2(3): 236-243.

386. White CR, Darley-Usmar V, Berrington WR, McAdams M, Gore JZ, Thompson JA, Parks DA, Tarpey MM, Freeman BA (1996): Circulating plasma xanthine oxidase contributes to vascular dysfunction in hypercholesterolemic rabbits. Proceedings of the National Academy of Sciences. 93: 8745–8749.

387. White JF, Bacon CW (2012): The secret world of endophytes in perspective. Fungal ecology. 5: 287-288.

388. White JF, Torres MS (2010): Is plant endophyte-mediated defensive mutualism the result of oxidative stress protection? Physiologia Plantarum. 138(4): 440-6.

389. Will S, Joshi T, Hofacker IL, Stadler PF, Backofen R (2012): LocARNA-P: Accurate boundary prediction and improved detection of structural RNAs. RNA. 18: 900–914.

390. Wolf M, Ruderisch B, Dandekar T, Schultz J, Muller T (2008): ProfDistS: (profile-) distance based phylogeny on sequence–structure alignments. Bioinformatics. 24: 2401–2402.

391. Wu X, Lee C, Muzny D, Caskey C (1989): Urate oxidase: primary structure and evolutionary implications. Proceedings of the National Academy of Sciences. 86: 9412–9416.

392. Xin ZH, Wang WL, Zhang YP, Xie H, Gu QQ, Zhu WM (2009): Pennicitrinone D, a new citrinin dimer from the halotolerant fungus *Penicillium notatum* B-52. The Journal of Antibiotics. 62:225-227.

393. Xu C, Wan X, Xu L, Weng H, Yan M, Miao M, Sun Y, Xu G, Dooley S, Li Y, Yu C (2015): Xanthine oxidase in non-alcoholic fatty liver disease and hyperuricemia: One stone hits two birds. Journal of hepatology. 62(6): 1412-9

394. Xu F, Zhao X, Yang L, Wang X, Zhao J (2014): A New Cycloartane-Type triterpenoid saponin xanthine oxidase inhibitor from *Homonoia riparia* Lour. Molecules. 19: 13422-13431.

395. Yadav M, Yadav A, Yadav JP (2014): *In vitro* antioxidant activity and total phenolic content of endophytic fungi isolated from *Eugenia jambolana* Lam. Asian Pacific Journal of Tropical Medicine. 7S1:S256-61.

396. Yaylaci S, Demir MV, Temiz T, Tamer A, Uslan MI (2012): Allopurinol-induced DRESS syndrome. Indian Journal of Pharmacology. 44(3): 412-414.

397. Ye YH, Zhu HL, Song YC, Liu JY, Tan RX (2005): Structural Revision of Aspernigrin A, reisolated from *Cladosporium herbarum* IFB-E002. Journal of Natural Products. 68: 1106-1108.

398. Yin OCJ, Ibrahim D, Lee CC (2015): Bioactive Compounds from *Aspergillus terreus* MP15, an endophytic Fungus Isolated from *Swietenia Macrophylla* Leaf. Malaysian Journal of Medical and Biological Research. 2(3): 262-272.

399. Yoon KN, Alam N, Lee JS, Lee KR, Lee TS (2011a): Detection of Phenolic compounds concentration and evaluation of antioxidant and anti-tyrosinase activities of various extracts from the fruiting bodies of *Lentinus edodes*. World Applied Science Journal. 12 (10): 1851-1859.

400. Yoon KN, Alam N, Lee KR, Shin PG, Cheong JC, Yoo YB, Lee TS (2011b): Antioxidant and antityrosinase activities of various extracts from the fruiting bodies of *Lentinus lepidus*. Molecules. 16: 2334–2347.

401. Yu MA, Sánchez-Lozada LG, Johnson RJ, Kang DH (2010): Oxidative stress with an activation of the renin-angiotensin system in human vascular endothelial cells as a novel mechanism of uric acid-induced endothelial dysfunction. Journal of Hypertension. 28: 1234–1242

402. Yuan ZL, Su ZZ, Mao LJ, Peng YQ, Yang GM, Lin FC, Zhang CL (2011): Distinctive endophytic fungal assemblage in stems of wild rice (*Oryza granulata*) in China with special reference to two species of *Muscodor* (Xylariaceae). Journal of Microbiology. 49(1): 15-23.

403. Zakaria L, Jamil MIM, Anuar ISM (2016): Molecular Characterisation of endophytic fungi from roots of Wild Banana (*Musa acuminata*). Tropical Life Science Research. 27(1): 153–162.

404. Zanabaatar B, Song JH, Seo GS, Noh HJ, Yoo YB and Lee JS (2010): Screening of Anti-gout Xanthine Oxidase Inhibitor from Mushrooms. Korean Journal of Mycology. 38(1): 85-87.

405. Zeng PY, Wu JG, Liao LM, Chen TQ, Wu JZ, Wong KH (2011): *In vitro* antioxidant activities of endophytic fungi isolated from the liverwort *Scapania verrucosa* Genetics and Molecular Research. 10 (4): 3169-3179.

406. Zerargui F, Boumerfeg S, Charef N, Baghiani A, Djarmouni M, Khennouf S, Arrar L, Zarga MHA, Mubarak MS (2015): Antioxidant Potentials and Xanthine Oxidase Inhibitory Effect of Two Furanocoumarins Isolated from *Tamus communis* L. Medicinal Chemistry. 11: 506-513.

407. Zhang C, Wang GP, Mao LJ, Komon-Zelazowska M, Yuan ZL, Lin FC, Druzhinina IS, Kubicek CP (2010): *Muscodor fengyangensis* sp. nov. from southeast china: morphology, physiology and production of volatile compounds. Fungal Biology. 114: 797–808.

408. Zhang HJ, Hu YJ, Xu P, Liang WQ, Zhou J, Liu PG, Cheng L, Pu JB (2016): Screening of Potential Xanthine Oxidase Inhibitors in *Gnaphalium hypoleucum* DC. By Immobilized Metal Affinity Chromatography and Ultrafiltration-Ultra Performance Liquid Chromatography-Mass Spectrometry. Molecules. 21: 1242.

409. Zhang J and Zhang Y (2016): Febuxostat (Uloric): A Xanthine oxidase inhibitor for the treatment of gout. In Innovative drug synthesis. First Edition. Edited by Jie Jack Li and Douglas S Johnson. John Wiley & Sons, Inc.

410. Zhang JY, Tao LY, Liang YJ, Chen LM, Mi YJ, Zheng LS (2010): Anthracenedione derivatives as anticancer agents isolated from secondary metabolites of the mangrove endophytic fungi. Marine Drugs. 8: 1469–1481.

411. Zheng YF, Min JS, Kim D, Park JB, Choi SW, Lee ES, Na K, Bae SK (2016): *In Vitro* Inhibition of Human UDP-Glucuronosyl-Transferase (UGT) Isoforms by Astaxanthin, β-Cryptoxanthin, Canthaxanthin, Lutein, and Zeaxanthin: Prediction of *in Vivo* Dietary Supplement-Drug Interactions. Molecules. 21(1052):1-11.

412. Zhu H, Chen Y, Huang C, Han Y, Zhang Y, Xie S, Chen X, Jin M (2015): Simultaneous determination of four Sudan dyes in rat blood by UFLC–MS/MS and its application to a pharmacokinetic study in rats. Journal of pharmaceutical analysis. 5(4): 239-248.

413. Zhu JX, Wang Y, Kong LD, Yang C, Zhang X (2004): Effects of *Biota orientalis* extract and its flavonoid constituents, quercetin and rutin on serum uric acid levels in oxonate-induced mice and

xanthine dehydrogenase and xanthine oxidase activities in mouse liver. Journal of Ethnopharmacology. 93(1): 133-40.

Chapter 9

Appendix

Appendix

Table 5.1: Endophytic fungi isolated from various tissues of medicinal plants collected from biodiversity hotspots of India

S.NO	Culture code	Plant name	Plant part	Sampling location	Tentative identification
1.	#4 AMSTYEL	*Aegle marmelos*	Stem	1	*Fusarium* sp.
2.	#7 AMSTYEL	*Aegle marmelos*	Stem	1	*Fusarium equiseti*
3.	#8 AMSTYEL	*Aegle marmelos*	Stem	1	Unidentified
4.	#9(b) AMSTYEL	*Aegle marmelos*	Stem	1	*Fusarium equiseti*
5.	#11 AMSTYEL	*Aegle marmelos*	Stem	1	*Neofusicoccum parvum*
6.	#18 AMSTYEL	*Aegle marmelos*	Stem	1	*Neofusicoccum* sp
7.	# 22 AMSTYEL	*Aegle marmelos*	Stem	1	*Fusarium* sp.
8.	# 23(b) AMSTYEL	*Aegle marmelos*	Stem	1	Unidentified
9.	# 32 AMSTYEL	*Aegle marmelos*	Stem	1	*Botryosphaeria* sp.
10.	#1003 AMSTITYEL	*Aegle marmelos*	Stem internal tissue	1	*Botryosphaeria* sp.
11.	#1010 AMSTITYEL	*Aegle marmelos*	Stem internal tissue	1	*Fusarium* sp.
12.	#1011 AMSTITYEL	*Aegle marmelos*	Stem internal tissue	1	*Fusarium* sp.
13.	#1013 AMSTITYEL	*Aegle marmelos*	Stem internal tissue	1	*Botryosphaeria* sp.
14.	#1022 AMSTITYEL	*Aegle marmelos*	Stem internal tissue	1	*Fusarium* sp.
15.	#1032 AMSTITYEL	*Aegle marmelos*	Stem internal tissue	1	*Botryosphaeria* sp.
16.	#1048 AMSTITYEL	*Aegle marmelos*	Stem internal tissue	1	*Lasiodiplodia psuedotheobromae*
17.	#1058 AMSTITYEL	*Aegle marmelos*	Stem internal tissue	1	*Fusarium* sp.
18.	#1069 AMSTITYEL	*Aegle marmelos*	Stem internal tissue	1	*Fusarium* sp.
19.	#1070 AMSTITYEL	*Aegle marmelos*	Stem internal tissue	1	*Fusarium* sp.
20.	#1088 AMSTITYEL	*Aegle marmelos*	Stem internal tissue	1	*Lasiodiplodia psuedotheobromae*
21.	#6 AMLWLS	*Aegle marmelos*	Leaf	2	*Fusarium incarnatum*
22.	#16 AMLWLS	*Aegle marmelos*	Leaf	2	*Muscodor kashayum* sp. *nov*
23.	#11 AMBAWLS	*Aegle marmelos*	Bark	2	Unidentified
24.	#20 AMSTWLS	*Aegle marmelos*	Stem	2	*Botryosphaeria* sp.

25.	#25 AMSTWLS	*Aegle marmelos*	Stem	2	Unidentified
26.	#33 AMSTWLS	*Aegle marmelos*	Stem	2	*Alternaria sp.*
27.	#37 AMSTWLS	*Aegle marmelos*	Stem	2	*Phaeoacremonium sp.*
28.	#47 AMSTWLS	*Aegle marmelos*	Stem	2	Unidentified
29.	#53 AMSTWLS	*Aegle marmelos*	Stem	2	Unidentified
30.	#59 AMSTWLS	*Aegle marmelos*	Stem	2	*Botryosphaeria stevensii*
31.	#1079 AMSTITWLS	*Aegle marmelos*	Stem internal tissue	2	*Lasiodiplodia theobromae*
32.	#1082 AMSTITWLS	*Aegle marmelos*	Stem internal tissue	2	*Lasiodiplodia pseudotheobromae*
33.	#1095 AMSTITWLS	*Aegle marmelos*	Stem internal tissue	2	Unidentified
34.	#1104 AMSTITWLS	*Aegle marmelos*	Stem internal tissue	2	*Barriopsis iraniana*
35.	#1111 AMSTITWLS	*Aegle marmelos*	Stem internal tissue	2	Unidentified
36.	#1118 AMSTITWLS	*Aegle marmelos*	Stem internal tissue	2	*Barriopsis iraniana*
37.	# 9 AMLBRT	*Aegle marmelos*	Leaf	3	*Fusarium* sp.
38.	#1005 AMLBRT	*Aegle marmelos*	Leaf	3	*Alternaria marmelos sp. nov*
39.	#1006 AMLBRT	*Aegle marmelos*	Leaf	3	*Fusarium* sp.
40.	#1007 AMLBRT	*Aegle marmelos*	Leaf	3	*Fusarium* sp.
41.	#1016 AMLBRT	*Aegle marmelos*	Leaf	3	*Fusarium* sp.
42.	#1 CCBD	*C. camphora*	Bark	4	*Fusarium* sp.
43.	# 2 CCBD	*C. camphora*	Bark	4	*Penicillium* sp.
44.	#1 CCSTITD	*C. camphora*	Stem internal tissue	4	*Muscodor darjeelingensis sp. nov*
45.	#2 CCSTITD	*C. camphora*	Stem internal tissue	4	*Muscodor tigerii sp.nov*
46.	#6 CCSTITD	*C. camphora*	Stem internal tissue	4	*Muscodor ghoomensis sp.nov.*
47.	#6(b) CCSTITD	*C. camphora*	Stem internal tissue	4	*Muscodor indica sp.nov.*
48.	#36 CCSTITD	*C. camphora*	Stem internal tissue	4	*Alternaria* sp.
49.	#1639 CCSTITD	*C. camphora*	Stem internal tissue	4	*Muscodor camphora sp. nov.*
50.	#4 CMBABRT	*C. malabaricum*	Bark	3	*Bionectria* sp.
51.	#12 CMBABRT	*C. malabaricum*	Bark	3	*Bionectria* sp.

52.	#18 CMBABRT	*C. malabaricum*	Bark	3	*Bionectria* sp.
53.	#49 CMBABRT	*C. malabaricum*	Bark	3	Unidentified
54.	#12 CMBANEY	*C. malabaricum*	Bark	5	*Alternaria* sp.
55.	#18 CMBANEY	*C. malabaricum*	Bark	5	*Alternaria* sp.
56.	#20 CMBANEY	*C. malabaricum*	Bark	5	*Lasiodiplodia* sp.
57.	#4 CMLBRT	*C. malabaricum*	Leaf	3	*Xylaria* sp.
58.	#26CMLBRT	*C. malabaricum*	Leaf	3	Unidentified
59.	#27 CMLBRT	*C. malabaricum*	Leaf	3	*Aspergillus* sp.
60.	#29 CMLBRT	*C. malabaricum*	Leaf	3	Unidentified
61.	#40 CMLBRT	*C. malabaricum*	Leaf	3	*Alternaria* sp.
62.	#1 CMLNEY	*C. malabaricum*	Leaf	5	*Aspergillus sp.*
63.	#2 CMLNEY	*C. malabaricum*	Leaf	5	*Nigrospora* sp.
64.	#17 CMLNEY	*C. malabaricum*	Leaf	5	Unidentified
65.	#18 CMLNEY	*C. malabaricum*	Leaf	5	*Fusarium* sp.
66.	#23 CMLNEY	*C. malabaricum*	Leaf	5	*Fusarium* sp.
67.	#29 CMLNEY	*C. malabaricum*	Leaf	5	Unidentified
68.	# 37 CMLNEY	*C. malabaricum*	Leaf	5	Unidentified
69.	#11 CMSTNEY	*C. malabaricum*	Stem	5	*Pestalotiopsis sp.*
70.	#13 CMSTNEY	*C. malabaricum*	Stem	5	*Pestalotiopsis sp.*
71.	#28 CMSTNEY	*C. malabaricum*	Stem	5	*Curvularia* sp.
72.	#36 CMSTNEY	*C. malabaricum*	Stem	5	Mycelia sterilia
73.	#43 CMSTNEY	*C. malabaricum*	Stem	5	*Acremonium* sp.
74.	# 54 CMSTNEY	*C. malabaricum*	Stem	5	*Pestalotiopsis* sp
75.	#55 CMSTNEY	*C. malabaricum*	Stem	5	Unidentified
76.	#64 CMSTNEY	*C. malabaricum*	Stem	5	*Phaeoacremonium* sp
77.	#68 CMSTNEY	*C. malabaricum*	Stem	5	Unidentified
78.	#79 CMSTNEY	*C. malabaricum*	Stem	5	Unidentified

79.	#92CMSTITNEY	*C. malabaricum*	Stem internal tissue	5	Unidentified
80.	#96 CMSTITNEY	*C. malabaricum*	Stem internal tissue	5	Unidentified
81.	#1622 CMSTITNEY	*C. malabaricum*	Stem internal tissue	5	Unidentified
82.	#1 CMSTITBRT	*C. malabaricum*	Stem internal tissue	3	*Pestalotiopsis* sp.
83.	#43 CMSTITBRT	*C. malabaricum*	Stem internal tissue	3	Unidentified
84.	#50 CMSTITBRT	*C. malabaricum*	Stem internal tissue	3	Unidentified
85.	#29 CZSTITBRT	*C. malabaricum*	Stem internal tissue	3	*Pestalotiopsis* sp.
86.	#33 CZSTITBRT	*C. malabaricum*	Stem internal tissue	3	*Fusarium sp.*
87.	#41 CZSTITBRT	*C. malabaricum*	Stem internal tissue	3	*Alternaria sp.*
88.	#47 CZSTITBRT	*C. malabaricum*	Stem internal tissue	3	*Fusarium sp*
89.	#5 CZBAWLS	*C. zeylanicum*	Bark	2	*Fusarium oxysporum*
90.	#20 CZBAWLS	*C. zeylanicum*	Bark	2	Unidentified
91.	#28 CZBAWLS	*C. zeylanicum*	Bark	2	*Glomerella sp*
92.	#30 CZBAWLS	*C. zeylanicum*	Bark	2	*Glomerella sp*
93.	#1CZBAPLM	*C. zeylanicum*	Bark	6	*Lasiodiplodia sp.*
94.	#3CZBAPLM	*C. zeylanicum*	Bark	6	*Pestalotiopsis* sp.
95.	#7CZBAPLM	*C. zeylanicum*	Bark	6	*Pestalotiopsis sp.*
96.	#14CZBAPLM	*C. zeylanicum*	Bark	6	*Fusarium sp.*
97.	#16CZBAPLM	*C. zeylanicum*	Bark	6	*Fusarium sp.*
98.	#18CZBAPLM	*C. zeylanicum*	Bark	6	*Alternaria sp.*
99.	#27CZBAPLM	*C. zeylanicum*	Bark	6	Unidentified
100.	#29CZBAPLM	*C. zeylanicum*	Bark	6	*Colletotrichum sp.*
101.	#36CZBAPLM	*C. zeylanicum*	Bark	6	*Alternaria sp.*
102.	#42CZBAPLM	*C. zeylanicum*	Bark	6	*Nigrospora* sp.
103.	#44CZBAPLM	*C. zeylanicum*	Bark	6	*Aspergillus sp.*
104.	#48CZBAPLM	*C. zeylanicum*	Bark	6	*Fusarium oxysporum*
105.	#50CZBAPLM	*C. zeylanicum*	Bark	6	*Colletotrichum sp*

106.	#52CZBAPLM	*C. zeylanicum*	Bark	6	*Penicillium* sp.
107.	#56CZBAPLM	*C. zeylanicum*	Bark	6	*Fusarium sp.*
108.	#1CZLPLM	*C. zeylanicum*	Leaf	6	*Alternaria sp.*
109.	#3CZLPLM	*C. zeylanicum*	Leaf	6	*Xylaria sp.*
110.	#7CZLPLM	*C. zeylanicum*	Leaf	6	Unidentified
111.	#11CZLPLM	*C. zeylanicum*	Leaf	6	Mycelia sterilia
112.	#16CZLPLM	*C. zeylanicum*	Leaf	6	*Phomopsis* sp.
113.	#22CZLPLM	*C. zeylanicum*	Leaf	6	*Alternaria sp.*
114.	#23 (a) CZLPLM	*C. zeylanicum*	Leaf	6	*Fusarium sp.*
115.	#23(b) CZLPLM	*C. zeylanicum*	Leaf	6	*Fusarium sp.*
116.	#24CZLPLM	*C. zeylanicum*	Leaf	6	*Lasiodiplodia sp.*
117.	#25CZLPLM	*C. zeylanicum*	Leaf	6	*Lasiodiplodia sp.*
118.	#26CZLPLM	*C. zeylanicum*	Leaf	6	*Cladosporium sp.*
119.	#30CZLPLM	*C. zeylanicum*	Leaf	6	*Hypoxylon sp.*
120.	#31CZLPLM	*C. zeylanicum*	Leaf	6	*Botryosphaeria sp.*
121.	#32CZLPLM	*C. zeylanicum*	Leaf	6	*Botryosphaeria sp.*
122.	#33CZLPLM	*C. zeylanicum*	Leaf	6	*Botryosphaeria sp.*
123.	#35CZLPLM	*C. zeylanicum*	Leaf	6	*Fusarium sp.*
124.	#38CZLPLM	*C. zeylanicum*	Leaf	6	Unidentified
125.	#42(a)CZLPLM	*C. zeylanicum*	Leaf	6	*Alternaria sp.*
126.	#43CZLPLM	*C. zeylanicum*	Leaf	6	*Fusarium sp.*
127.	#44CZLPLM	*C. zeylanicum*	Leaf	6	*Xylaria sp.*
128.	#56CZLPLM	*C. zeylanicum*	Leaf	6	*Fusarium sp.*
129.	#58CZLPLM	*C. zeylanicum*	Leaf	6	*Chaetomium* sp.
130.	#64CZLPLM	*C. zeylanicum*	Leaf	6	Unidentified
131.	#65CZLPLM	*C. zeylanicum*	Leaf	6	*Arthriniumsp.*
132.	#63CZSTITPLM	*C. zeylanicum*	Stem internal tissue	6	*Xylaria sp.*

133.	#6610 CZSTITBRT	*C. zeylanicum*	Stem internal tissue	3	*Muscodor strobelii* sp.*nov*
134.	#23CZSTITG	*C. zeylanicum*	stem	7	*Fusarium sp.*
135.	#2 CRSTBRT	*Cathranthus roseus*	Stem internal tissue	3	*Pestalotiopsis* sp.
136.	#5 CRSTBRT	*Cathranthus roseus*	Stem internal tissue	3	Unidentified
137.	#6 CRSTBRT	*Cathranthus roseus*	Stem internal tissue	3	*Hypoxylon* sp.
138.	#17 CRSTBRT	*Cathranthus roseus*	Stem internal tissue	3	*Fusarium oxysporum*
139.	#22 CRSTBRT	*Cathranthus roseus*	Stem internal tissue	3	Unidentified
140.	#26 CRSTBRT	*Cathranthus roseus*	Stem internal tissue	3	*Pestalotiopsis* sp.
141.	#29 CRSTBRT	*Cathranthus roseus*	Stem internal tissue	3	*Cladosporium* sp.
142.	#42 CRSTBRT	*Cathranthus roseus*	Stem internal tissue	3	*Fusarium* sp.
143.	#43 CRSTBRT	*Cathranthus roseus*	Stem internal tissue	3	*Alternaria* sp.
144.	#16 CRLBRT	*Cathranthus roseus*	Stem internal tissue	3	*Fusarium sp.*
145.	1CSSTOT	*Camellia sinensis*	Stem	8	*Schizophyllum sp.*
146.	2CSSTOT	*Camellia sinensis*	Stem	8	*Schizophyllum sp.*
147.	4CSSTOT	*Camellia sinensis*	Stem	8	*Schizophyllum sp.*
148.	7CSSTOT	*Camellia sinensis*	Stem	8	*Neofusicoccum sp.*
149.	8CSSTOT	*Camellia sinensis*	Stem	8	Unidentified
150.	14NOBASVNP	*Nerium oleander*	Bark	9	Unidentified
151.	19NOBASVNP	*Nerium oleander*	Bark	9	*Gibberella sp.*
152.	1PNLNEY	*Piper nigrum*	Leaf	5	*Alternaria sp.*
153.	2PNLNEY	*Piper nigrum*	Leaf	5	*Alternaria sp.*
154.	5PNLNEY	*Piper nigrum*	Leaf	5	*Alternaria sp.*
155.	#4 RSLBRT	*Rauwolfia serpentina*	Leaf	3	*Fusarium solani*
156.	#16 RSLBRT	*Rauwolfia serpentina*	Leaf	3	*Gibberella sp.*
157.	#16 RSBANEY	*Rauwolfia serpentina*	Bark	5	*Fusarium sp.*
158.	#23(a) RSSTNEY	*Rauwolfia serpentina*	Stem	5	*Fusarium sp.*
159.	1TCSTITPLM	*T. cordifolia*	Stem internal tissue	6	*Colletotrichum sp.*

160.	4TCSTITPLM	*T. cordifolia*	Stem internal tissue	6	Unidentified
161.	11TCSTITPLM	*T. cordifolia*	Stem internal tissue	6	*Alternaria sp.*
162.	16TCSTITPLM	*T. cordifolia*	Stem internal tissue	6	*Hypoxylon sp.*
163.	21TCSTITPLM	*T. cordifolia*	Stem internal tissue	6	Unidentified
164.	33TCSTITPLM	*T. cordifolia*	Stem internal tissue	6	*Fusarium sp.*
165.	41TCSTITPLM	*T. cordifolia*	Stem internal tissue	6	Unidentified
166.	42TCSTITPLM	*T. cordifolia*	Stem internal tissue	6	*Alternaria sp.*
167.	46TCSTITPLM	*T. cordifolia*	Stem internal tissue	6	*Hypoxylon sp.*
168.	45TCSTITPLM	*T. cordifolia*	Stem internal tissue	6	Unidentified
169.	51TCSTITPLM	*T. cordifolia*	Stem internal tissue	6	*Curvularia sp.*
170.	53TCSTITPLM	*T. cordifolia*	Stem internal tissue	6	*Fusarium sp.*
171.	59TCSTITPLM	*T. cordifolia*	Stem internal tissue	6	*Fusarium sp*
172.	61TCSTITPLM	*T. cordifolia*	Stem internal tissue	6	Unidentified
173.	76TCSTITPLM	*T. cordifolia*	Stem internal tissue	6	*Fusarium equiseti*
174.	83TCSTITPLM	*T. cordifolia*	Stem internal tissue	6	*Fusarium sp.*
175.	88TCSTITPLM	*T. cordifolia*	Stem internal tissue	6	*Fusarium sp.*
176.	105TCSTITPLM	*T. cordifolia*	Stem internal tissue	6	*Fusarium sp.*
177.	107TCSTITPLM	*T. cordifolia*	Stem internal tissue	6	*Fusarium sp.*
178.	#2(a) TMDSTYEL	*T. divaricata*	stem	1	*Fusarium oxysporum*
179.	#2(b) TMDSTYEL	*T. divaricata*	stem	1	*Fusarium oxysporum*
180.	#3 TMDSTYEL	*T. divaricata*	stem	1	Unidentified
181.	#4 TMDSTYEL	*T. divaricata*	stem	1	*Fusarium solani*

1: Yelandur, Karnataka; 2: Wayanad, Kerala; 3: Biligirirangana Temple (BRT) wildlife sanctuary; 4: Darjeeling, West Bengal; 5: Neyyar, Kerala; 6: Palampur, Himachal Pradesh; 7: Guwahati; 8: Ooty; 9: Silent Valley National Park, Kerala.

S.No	Species Name	Minimum Free Energy (kcal/mol)	
		ITS1	ITS2
1	*M. albus*	-64.74	-53.49
2	*M. roseus*	-74.60	-51.20
3	*M. crispans*	-74.60	-51.70
4	*M. yucatanensis*	-63.40	-45.70
5	*M. vitigenus*	-69.90	-59.20
6	*M. satura*	-57.00	-54.30
7	*M. cinnanomi*	-98.60	-60.10
8	*M. equiseti*	-75.40	-54.80
9	*M. musae*	-81.10	-67.10
10	*M. suthepensis*	-73.10	-52.80
11	*M. fengyangenesis*	-91.55	-45.96
12	*M. kashayum*	-59.70	-46.40
13	*M. darjeelingensis*	-60.20	-46.40
14	*M. tigerii*	-59.90	-46.40
15	*M. strobelii*	-48.70	-38.50
16	*M. ghoomensis*	-54.00	-44.40
17	*M. indica*	-44.80	-42.60
18	*M. heveae*	-82.80	-50.10
19	*M. oryzae*	-101.20	-59.30

Table 5.11: Delta G required for the formation of secondary structure of ITS1 and ITS2 marker region of different *Muscodor* species

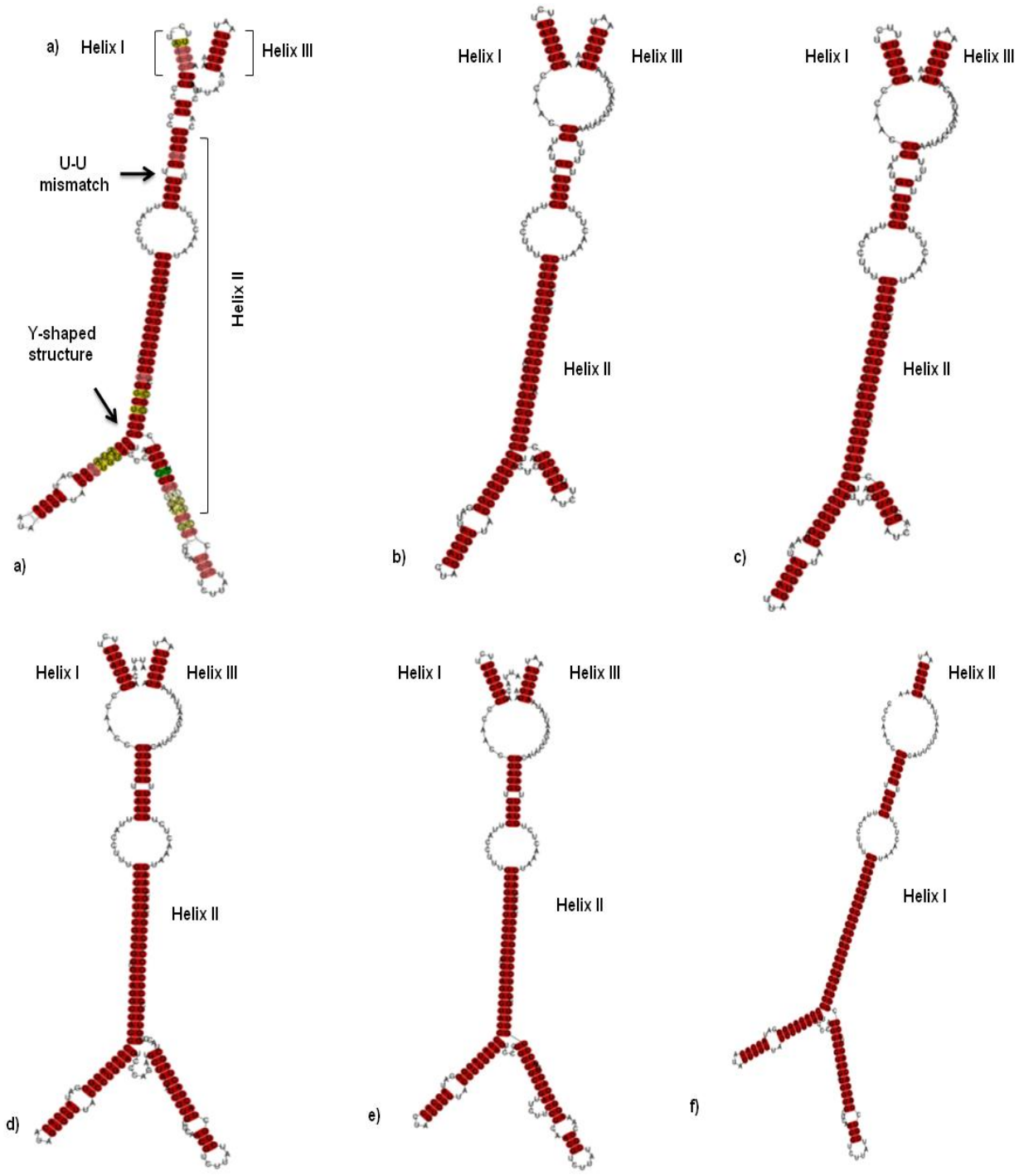

Fig 5.18: The predicted minimum free energy (MFE) secondary structures of ITS1 region from six different *Muscodor* species (a) *Muscodor albus* (Consensus structure) (b) *M. yucatanensis* (c) *M. satura* (d) *M. roseus* (e) *M. suthepensis* (f) *M. crispans.* All the species formed common three helix configuration core structure except *M. crispans* which was folded in two helix arrangement.

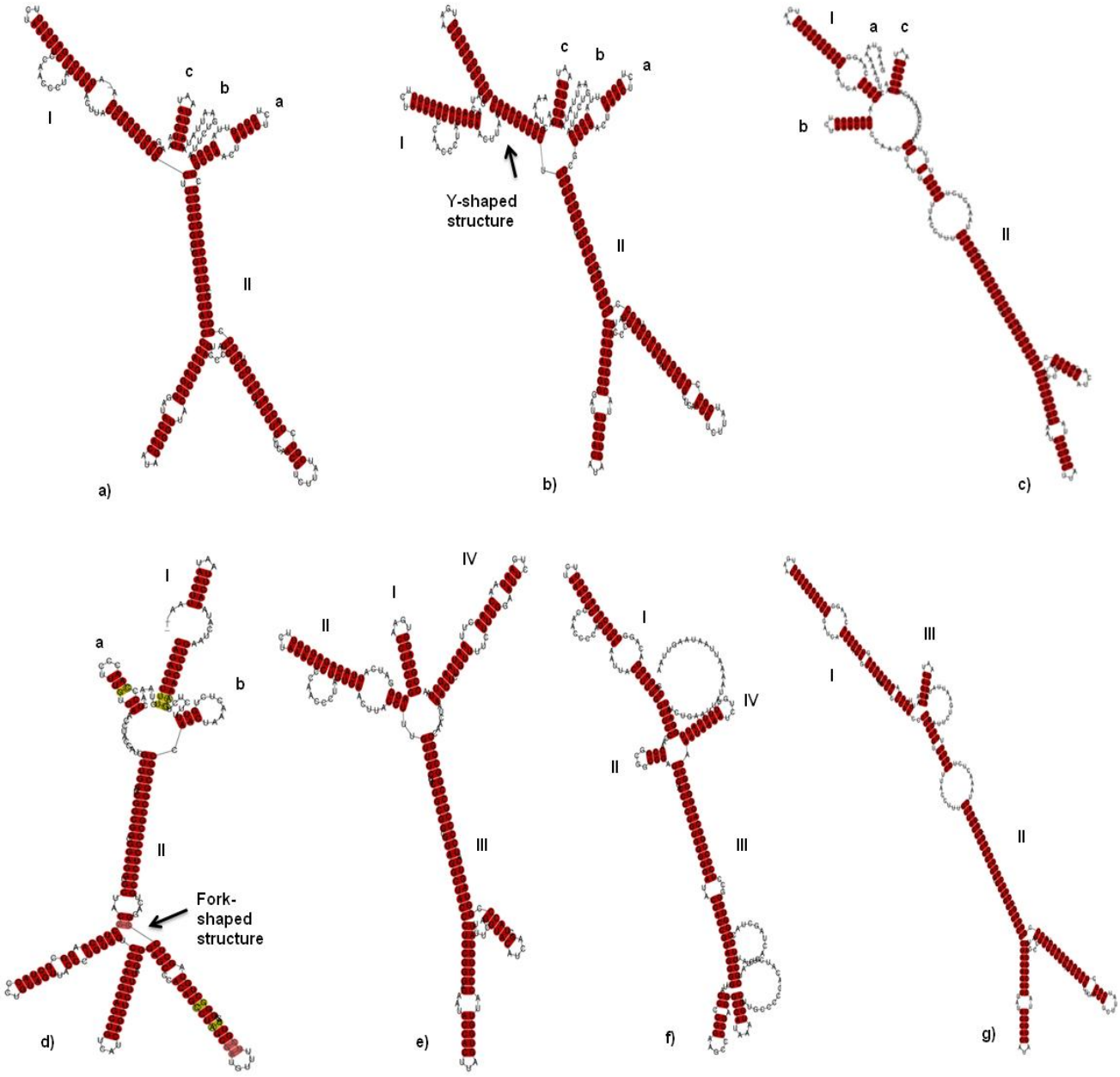

Fig 5.19: The predicted minimum free energy (MFE) secondary structures of ITS1 region from seven different *Muscodor* species (a) *Muscodor musae* (b) *M. cinnanomi* (c) *M. equiseti* (d) *M. fengyangenesis* (e) *M. vitigenus* (f) *M. heveae* (g) *M. oryzae.*

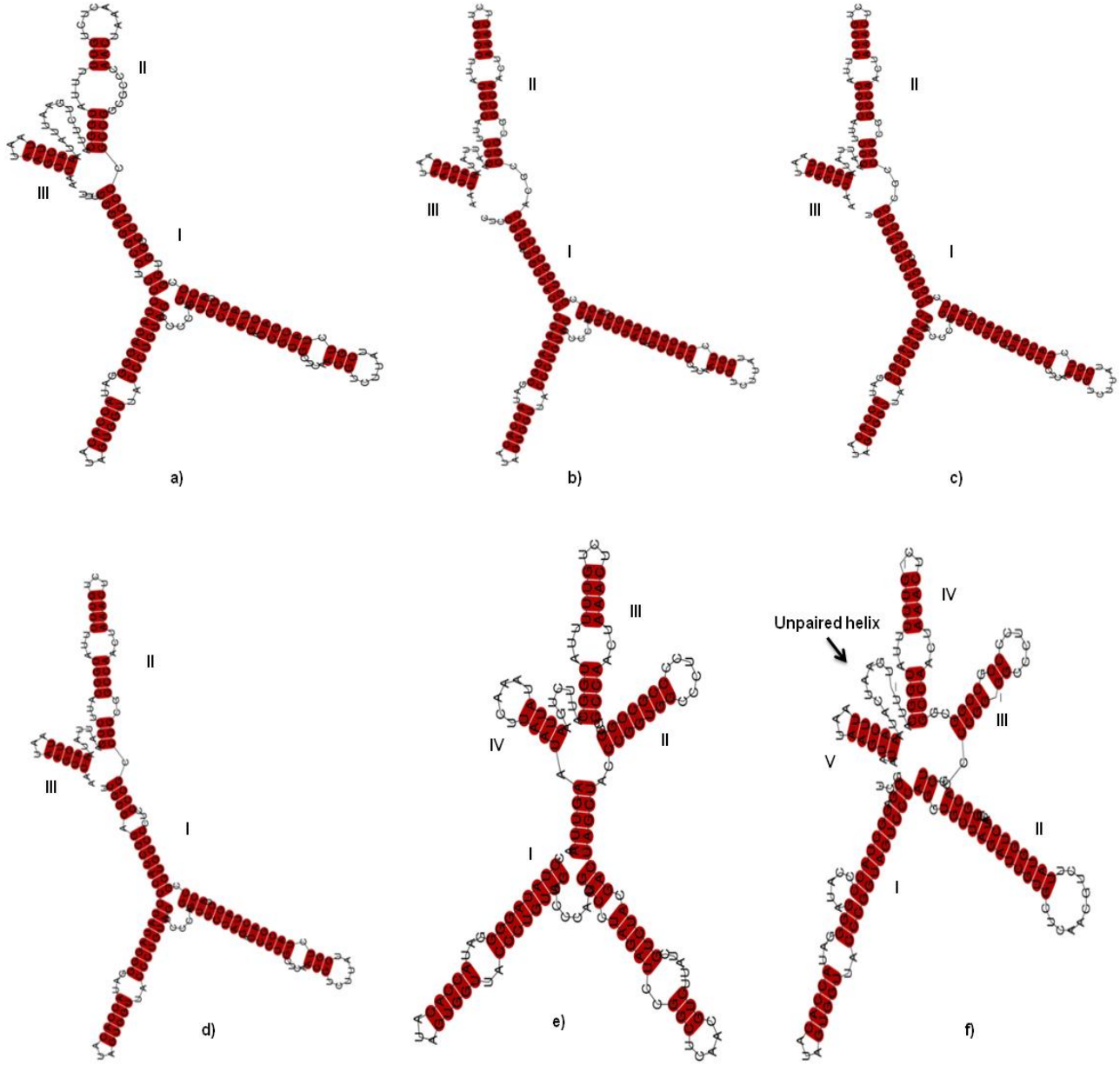

Fig 5.20: The predicted minimum free energy (MFE) secondary structures of ITS1 region from six different *Muscodor* species (a) *Muscodor ghoomensis* (b) *M. kashayum* (c) *M. tigerii* (d) *M. darjeelingensis* (e) *M. indica* (f) *M. strobelii.* All the six species folded in common X-shaped, three-helix configured core structure.

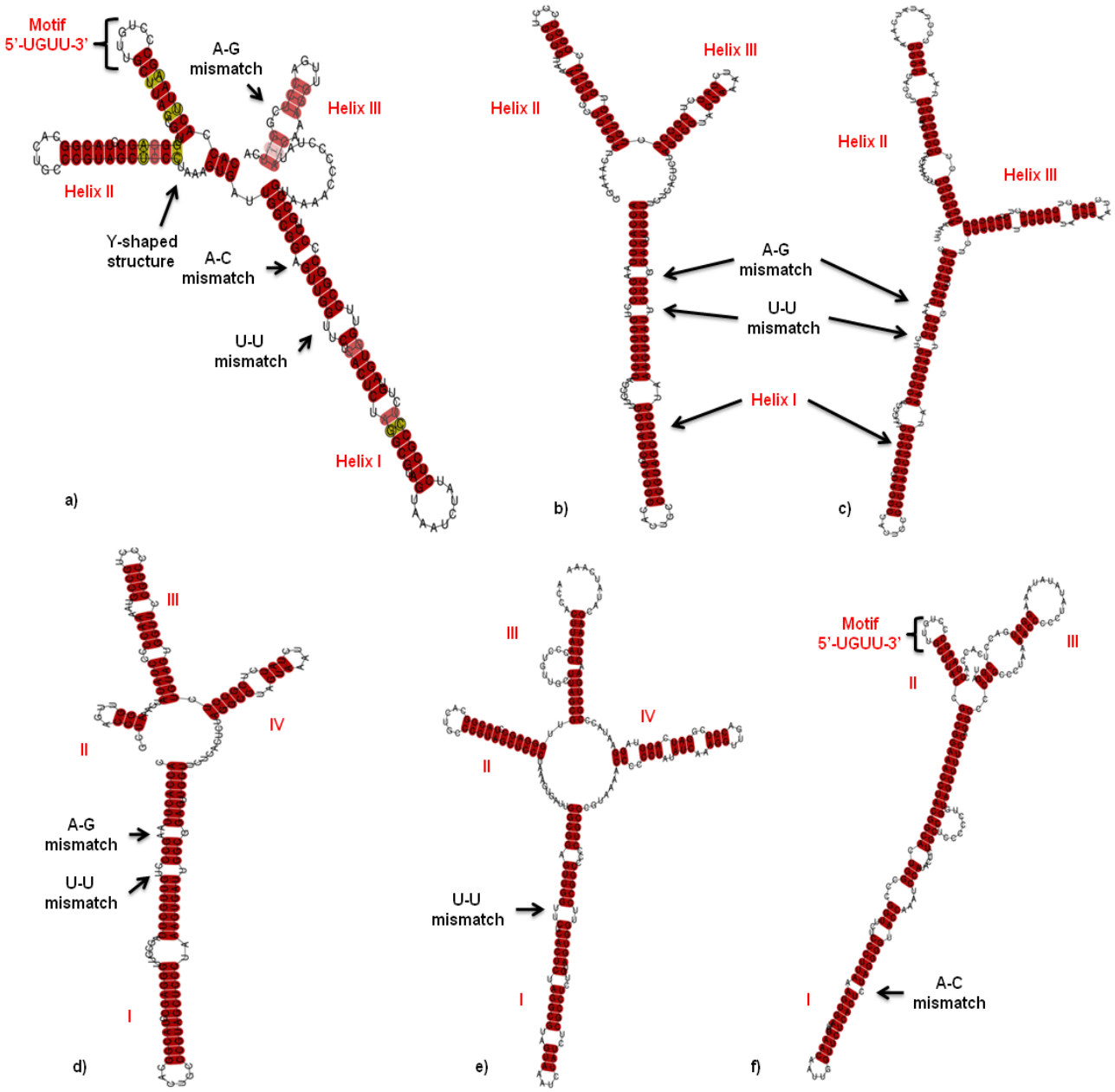

Fig 5.22: The predicted minimum free energy (MFE) secondary structures of ITS2 region from six different *Muscodor* species (a) *Muscodor albus* (Consensus structure) (b) *M. roseus* (c) *M. oryzae* (d) *M. suthepensis* (e) *M. cinnanomi* (f) *M. heveae.* Conserved motif 5'-UGGU-3' and U-U mismatch was detected.

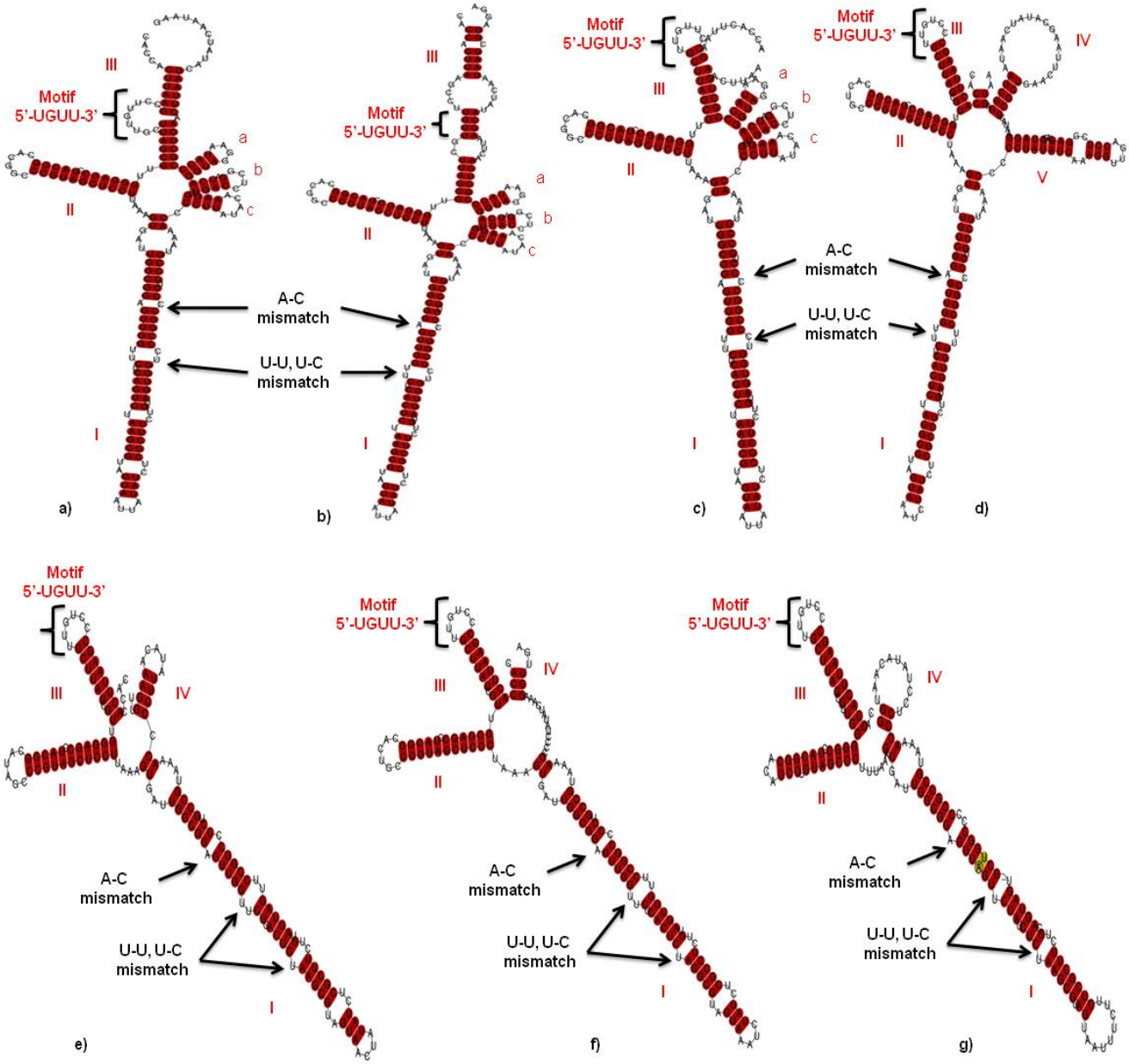

Fig 5.23: The predicted minimum free energy (MFE) secondary structures of ITS2 region from seven different *Muscodor* species (a) *Muscodor equiseti* (b) *M. vitigenus* (c) *M. satura* (d) *M. musae* (e) *M. yucatanensis* (f) *M. crispans* (g) *M. fengyangenesis* (consensus structure).

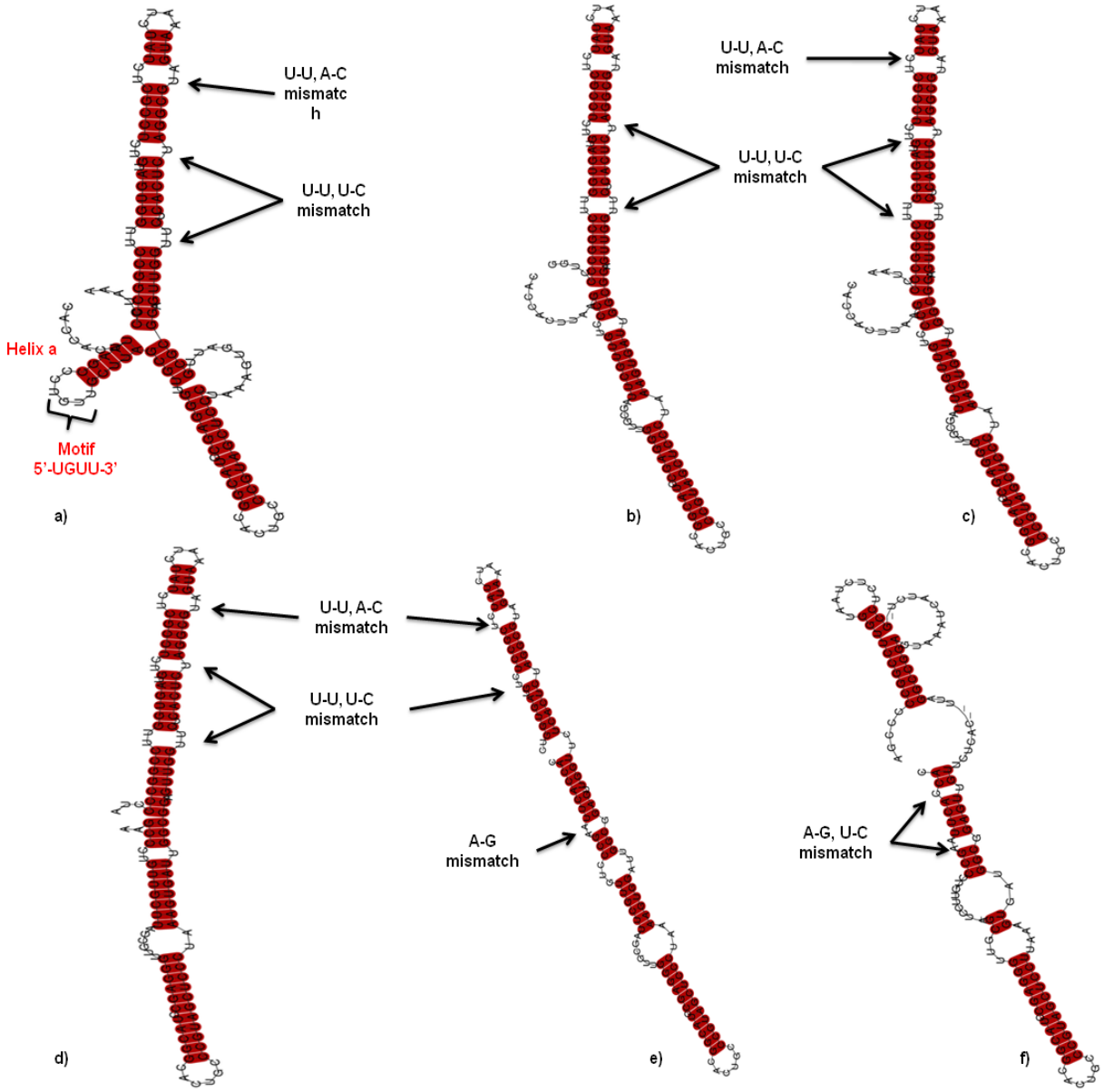

Fig 5.24: The predicted minimum free energy (MFE) secondary structures of ITS2 region from six different *Muscodor* species (a) *Muscodor ghoomensis* (b) *M. kashayum* (c) *M. darjeelingensis* d) *M. tigerii* (e) *M. indica* (f) *M. strobelii*

3 Biotech (2016)6:248
DOI 10.1007/s13205-016-0569-5

ORIGINAL ARTICLE

Xanthine oxidase inhibitory and antioxidant potential of Indian *Muscodor* species

Neha Kapoor[1] · **Sanjai Saxena**[1]

Received: 27 September 2016 / Accepted: 11 November 2016

Abstract Xanthine oxidase is a key enzyme responsible for hyperuricemia, a pre-disposing factor for Gout and oxidative stress-related diseases. Only two clinically approved xanthine oxidase inhibitors Allopurinol and Febuxostat are currently used for treatment of hyperuricemia. However, owing to their side effects there is a need for new non-purine-based selective inhibitors of xanthine oxidase. In the process of exploring novel xanthine oxidase inhibitors and anti-oxidants, we screened the culture filtrate of 07 novel species of *Muscodor*, a sterile endophytic fungi isolated from *Cinnamomum* and *Aegle marmelos*. Chloroform extract of *M. darjeelingensis* exhibited the maximum xanthine oxidase inhibition in the qualitative and quantitative assays. The IC_{50} of chloroform extract of *M. darjeelingensis* was 0.54 µg/ml which was much lower to Allopurinol but higher when compared to Febuxostat. 88% reduction in uric acid production was recorded *by M. darjeelingensis* chloroform extract which was similar to allopurinol. The maximum anti-oxidant activity was exhibited by *M. indica* against the gallic acid standard in the DPPH-free radical assay. Anti-oxidant activity index of *M. indica* was 7.7, which was followed by *M. kashayum* with 5.4. *M. darjeelingensis* exhibited a moderate anti-oxidant activity with anti-oxidant activity index of 1.63 in the DPPH assay. The present study is the very first report of *Muscodor* species exhibiting xanthine oxidase inhibitory and anti-oxidant activity together. Chloroform extract of *M. darjeelingensis* and *M. indica* stand out as potential candidates for isolation and characterization of the xanthine oxidase inhibitor and anti-oxidant compound, respectively.

Keywords Endophytic fungi · DPPH assay · Enzyme inhibitor · Muscodor · Hyperuricemia

Introduction

Hyperuricemia is a pre-disposing factor of gout which has been recognized as a lifestyle disease affecting adult population in the developed as well as developing countries (Kuo et al. 2015). Hyperuricemia results due to high serum urate levels which is attributed to it's over production or under-excretion. The therapeutic strategies of treatment of hyperuricemia are by excretion of excessive uric acid or blocking the uric acid production. The later strategy appears to be safer since it involves the inhibition of Xanthine oxidase (XO), the key enzyme responsible for the production of uric acid. Till date, only Allopurinol and Febuxostat have been clinically approved as XO inhibitors for the treatment of hyperuricemia and gout. However, there is a demand for new non-purine-based selective inhibitors of Xanthine oxidase (NP-SIXO's) owing to the side effects of currently used drugs.

Over last two decades, endophytic fungi have been well recognized as fountainheads of novel bioactive compounds possessing anti-cancer, anti-microbial, and anti-oxidant properties as well as putative sources of phytochemicals. However, exploration of these microorganisms for NP-SIXO's is very limited as evident from the literature (Kapoor and Saxena 2014).

The genus *Muscodor* emerged with the discovery of sterile endophytic fungus *Muscodor albus* from the branch of cinnamon plant in Honduras (Worapong et al. 2001).

✉ Sanjai Saxena
sanjaibiotech@yahoo.com; ssaxena@thapar.edu

[1] Department of Biotechnology, Thapar University, Patiala, Punjab 147004, India

Published online: 17 November 2016

Since then over 19 species have been added to the genus *Muscodor* on the basis of morphological, volatile gas composition, phenetic, and genetic makeup from Central/South America, Northern Territory of Australia, Thailand, China, and India (Meshram et al. 2014; Saxena et al. 2014a).

Till date, only volatile organic compounds (VOCs) produced by *Muscodor* have been explored and exploited for their antimicrobial, anti-insecticidal, and anti-fungal properties (Newman and Cragg 2015; Saxena et al. 2014b). Secondary metabolites of *Muscodor* species have not been explored extensively; there is only a single report on antimicrobial activity (Boparai et al. 2015). Hence, *Muscodor* species can be a novel source of new and diverse bioactive moieties which could be exploited by the pharmaceutical and the agrochemical industry.

Thus, in the present investigation, we have evaluated the in vitro xanthine oxidase inhibitory and antioxidant potential of non-volatile secondary metabolites of Indian *Muscodor* species.

Materials and methods

Production of secondary metabolites

Indian *Muscodor* species viz. *Muscodor strobelii*, *M. darjeelingensis*, *M. tigerii*, *M. kashayum*, *M. ghoomensis*, *M. indica,* and *M. camphora* were inoculated in potato dextrose broth for secondary metabolite production. Briefly, 5 mm mycelial plug of 3–4 day-old culture was inoculated into 100 ml pre-sterilized Potato Dextrose Broth (pH 5.1) followed by incubation at 26 ± 2 °C, 120 rpm for 7 days. Subsequently, the fungal mass was separated by filtration through Whatman filter paper No. 4 followed by centrifugation at 10,000 rpm for 10 min. The supernatant so obtained was subjected to qualitative XOI assay.

Qualitative screening of XO inhibition

Qualitative screening of XO inhibition was carried out as per the procedure of Kapoor and Saxena (2014). The method comprised of preparation of Xanthine–Nitroblue tetrazolium (NBT) plates using 0.8% agar, 1.5 mg/ml Xanthine, and 0.11 mg/ml NBT. 5 mm wells were prepared aseptically with a sterile cork borer. Subsequently, 40 µl of reaction mixture containing 30 µl of each culture filtrate, 0.04 U of xanthine oxidase (source: bovine milk), and 10 mmol/L of Tris–HCl buffer was dispensed into each well followed by overnight incubation at 37 °C. The control well consisted of 30 µl of un-inoculated broth and 0.04 U of XO. Allopurinol and Febuxostat (1 mM) were used as positive controls. Appearance of a blue-colored halo indicated the XO activity in control well while reduction in diameter of blue-colored halo in comparison to control-indicated XO inhibition. All the tests were carried out in triplicates. The halo diameter was recorded and data were represented as mean ± SD values.

Metabolite extraction from the culture filtrates

The cell-free supernatant of each culture was extracted thrice with chloroform in the ratio of 1:2. The organic layers were pooled followed by dehydration with anhydrous sodium sulphate. The solvent was evaporated till dryness at room temperature so as to get chloroform fraction residue. The fraction so obtained was weighed and reconstituted in methanol.

Quantitative estimation of xanthine oxidase inhibition

NBT assay

The crude chloroform fractions of cultures were subjected for determination of XOI as described by Aggarwal and Banerjee (2009) with slight modifications. The crude fractions were pre-incubated with bovine milk xanthine oxidase at 37 °C for 1 h prior to assay. The reaction was initiated by addition of 130 µL of xanthine (10 mM) followed by 30 µl of NBT. After the incubation, the amount of formazan formed was estimated by measuring the absorbance at 575 nm using a microplate reader (Biotek Powerwave 340, USA). Allopurinol and Febuxostat were used as positive control. Control reaction mixture consisted of substrate, enzyme, and NBT without any inhibitor. All the reactions were performed in triplicates.

Uric acid estimation assay

This assay was carried out as per the method of Chang et al. (1993), wherein the reaction mixture comprised of 10 µl of crude chloroform extract and 990 µl of xanthine buffer solution (200 µM). The reaction was initiated by addition of 5 µl of XO solution. Subsequently, the reaction mixture was mixed properly followed by incubation at 25 °C for 15 min. The reaction was terminated by adding 1 N HCl solution. Subsequently, the reaction was aborted by adding 1 N HCl solution. The concentration of uric acid was measured by taking absorbance value at 290 nm. Allopurinol and Febuxostat were used as positive controls. The percentage inhibition of xanthine oxidase was calculated by following formula:

$$\%\,\text{Inhibition} = [(A-B)-(C-D)]/(A-B) \times 100\%,$$

where *A* is the OD at 290 nm with enzyme but without sample, *B* is the OD at 290 nm without sample and enzyme, *C* is the OD at 290 nm with sample and enzyme, and *D* is the OD at 290 nm with sample but without enzyme.

Free radical scavenging activity by DPPH assay

Antioxidant potential of the chloroform extracts of cultures were determined by the procedure of Ho et al. (2012) with minor modifications. Briefly, the reaction mixture comprised of 100 µl of sample extract (1 mg/ml) mixed with 100 µL DPPH solution (1, 1-diphenyl-2-picrylhydrazyl, Sigma, Final concentration = 4 µg/ml). Allopurinol and Febuxostat were also evaluated for their antioxidant potential. The control comprised of 100 µl of methanol and 100 µl of DPPH solution. The titer plate was then incubated at 25 °C for 30 min in dark. The sudden decrease in absorbance was measured at 517 nm and the DPPH scavenging activity was calculated using the following formula:

$$\text{DPPH scavenging activity } (\%) = [\text{Acontrol} - \text{ATest}]/\text{Acontrol} \times 100.$$

The test was performed in triplicates and data were represented as mean ± SD. The antioxidant capacity was expressed as the antioxidant activity index (AAI) determined by following formula

AAI = final concentration of DPPH (µg/ml)/IC_{50} of sample (µg/ml).

An AAI of 0.5 and below indicated a poor anti-oxidant, when AAI was between 0.5 and 1.0 it is moderate anti-oxidant,and when the AAI is in the range of 1.0 and 2.0 it is considered as a strong anti-oxidant, while above 2 AAI indicated a very strong anti-oxidant (Scherer and Godoy 2009).

Test for purine

The chloroform fraction of *Muscodor* species exhibiting the best XO inhibition was test for the presence of purine moieties using a silver precipitation test (Kapoor and Saxena 2014). Briefly the assay involved 0.5 ml of test sample (Stock-1 mg/ml) in test tube and excess of ammonium hydroxide was added to it followed by addition of 0.5 ml of 0.1 M silver nitrate solution. Appearance of white precipitate, which is Purine-Ag+ complex, indicates the presence of purine. Allopurinol (purine analogue) was used as positive control, and Febuxostat, being non-purine in nature, served as negative control.

Table 1 Xanthine oxidase inhibition of Indian *Muscodor* species by qualitative and quantitative assay

Treatment	% XO inhibition		% Reduction in uric acid production
	Xanthine plate assay	NBT assay	
Control (no inhibitor)	0^{e}	0^{g}	0^{g}
Febuxostat*	59.4 ± 1.0^{a}	99.2 ± 0.0^{a}	99.5 ± 0.0^{a}
M. darjeelingensis	59.4 ± 1.0^{a}	91.4 ± 0.8^{b}	88.1 ± 0.0^{b}
Allopurinol*	58.6 ± 1.0^{a}	88.0 ± 0.5^{b}	86.7 ± 0.0^{b}
M. tigerii	56.7 ± 0.9^{a}	77.0 ± 0.5^{c}	74.0 ± 0.0^{c}
M. kashayum	54.9 ± 1.0^{a}	76.0 ± 1.0^{c}	70.3 ± 0.0^{c}
M. strobelii	48.6 ± 3.1^{b}	40.2 ± 1.9^{e}	40.2 ± 2.6^{d}
M. camphora	46.7 ± 1.8^{b}	46.7 ± 1.8^{d}	39.7 ± 0.0^{d}
M. ghoomensis	31.6 ± 3.8^{c}	37.6 ± 2.7^{e}	24.2 ± 0.0^{e}
M. indica	18.2 ± 1.9^{d}	28.6 ± 4.5^{f}	18.7 ± 1.6^{f}

* Represent commercial inhibitors of Xanthine Oxidase (XO). All values presented are Mean ± SD of triplicate readings

Mean values represented by same alphabets are not significantly different by Tukey's post hoc analysis at $p \leq 0.05$

Results

Qualitative XO inhibition assay

Muscodor darjeelingensis chloroform extract (CE) exhibited the highest inhibition of XO (59.4%) all the *Muscodor* species tested. This was similar to the clinically approved first NP-SIXO, Febuxostat used as a standard. It was closely followed by *M. tigerii* with 56.7% inhibition which was marginally lower to allopurinol exhibiting 58.6% XO inhibition in the assay. In the qualitative assay, *M. indica* CE exhibited the least XO inhibition. Febuxostat, Allopurinol, *M. darjeelingensis* CE, *M. tigerii* CE, and *M. kashayum* CE exhibited a similar XO inhibition profile in the plate assay based on Tukey's post hoc analysis (Table 1; Fig. 1).

Quantitative XO inhibition

In the quantitative NBT-based XO inhibition assay, Febuxostat exhibits 99.2% inhibition of the XO activity which was closely followed by *M. darjeelingensis* with 91.4% inhibition. Allopurinol tested as a purine-based XO inhibitor exhibited only 88% reduction in the XO activity during the in vitro assay. *M. tigerii* and *M. kashayum* CE extracts exhibited a moderate inhibition of 77% and 76%, respectively. Tukey's post hoc analysis suggested that *M. darjeelingensis* CE and Allopurinol possessed similar potency for XO inhibition. These findings corroborated

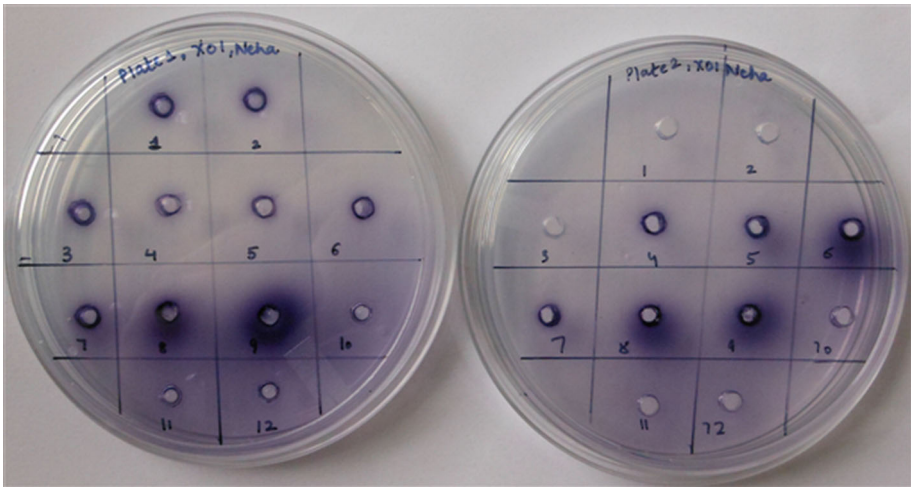

Fig. 1 Qualitative NBT plate assay of chloroform residues of *Muscodor* species

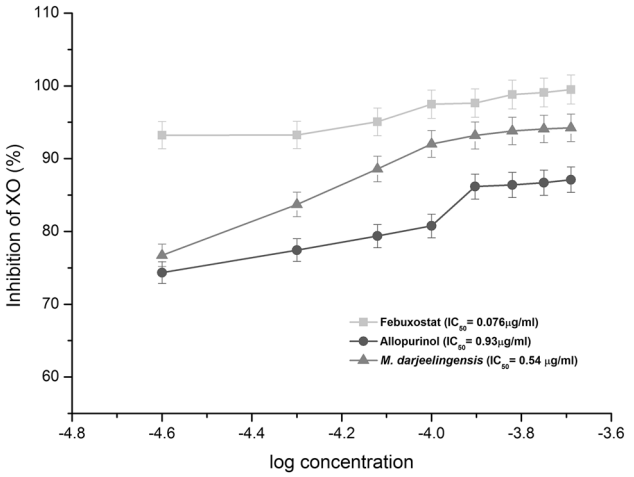

Fig. 2 Dose-response curve of chloroform residue of *M. darjeelingensis* for inhibition of xanthine oxidase. Allopurinol and Febuxostat was used as the positive control

with the reduction in uric acid production, with maximum reduction in Febuxostat, followed by *M. darjeelingensis*, Allopurinol, and *M. tigerii* (Table 1). Further, *M. darjeelingensis* CE exhibited an IC_{50} value of 0.54 µg/ml for XO in the in vitro assay (Fig. 2).

Free radical scavenging assay

Muscodor indica CE exhibited the highest free radical scavenging activity among the isolates tested and was quite similar to the Gallic acid, the standard anti-oxidant used in the DPPH assay. The IC_{50} value was 0.5 µg/ml for *M. indica* CE as compared to 7 µg/ml of Gallic acid. It also exhibited the highest AAI of 7.7 as compared to Gallic acid (Table 2; Fig. 3). *M. ghoomensis* CE exhibited the least antioxidant activity as well as AAI.

Purine detection test

Muscodor darjeelingensis CE did not exhibit presence of any purine moiety in the purine detection test. Febuxostat also gave a negative purine test indicating that it is a NP-SIXO while Allopurinol was found to be positive for purine.

Discussion and conclusion

Hyperuricemia is a biochemical abnormality which results in gout apart from oxidative stress-related diseases. Hence, the lowering plasma uric acid levels within normal range is extremely important and can be achieved by blocking the uric acid production. Till date, only Allopurinol and Febuxostat have been clinically used for the treatment of hyperuricemia and gout; however, they have severe side effects which demand exploration of new XO inhibitors which are non- purine in nature and have lesser side effects as compared to synthetic chemicals. Endophytic fungi are relatively under tapped resources of XO inhibitors which could enter the drug discovery pipeline as anti-hyperuricemic agents. In the present study, CE of *M. darjeelingensis* was found to have a significantly lower IC_{50} value as compared to Fusaruside and Phenolic compounds isolated from endophytic *Fusarium* sp. IFB-121 and *Chaetomium* sp., respectively (Shu et al. 2004; Huang et al. 2007). Further phytochemicals like Isoliquiritigenin, Liquiritigenin, and Cinnamaldehyde exhibited an IC_{50} of 12.6, 14.29 and 8.4 µg/ml, respectively, which was much higher than 0.54 µg/ml of CE of *Muscodor darjeelingensis* (Wang et al. 2008). Earlier, we have reported that CE of another endophytic fungus *Lasiodiploda pseudotheobromae* exhibited a potent XO inhibition with an IC_{50} of

Table 2 Free radical scavenging activity by DPPH Assay

Species	Scavenging activity (%)	IC_{50} (μg/ml)	Antioxidant activity index (AAI)
Gallic acid (standard)*	73.9 ± 1.3^{a}	7.00	0.6
M. indica	71.6 ± 0.9^{ab}	0.52	7.7
M. strobelii	69.8 ± 2.6^{abc}	1.47	2.7
M. darjeelingensis	68.0 ± 3.8^{bc}	2.45	1.6
M. kashayum	65.4 ± 3.8^{c}	0.74	5.4
M. camphora	48.5 ± 3.2^{d}	5.64	0.7
M. tigerii	46.5 ± 1.7^{d}	47.32	0.08
M. ghoomensis	46.4 ± 4.9^{d}	133.30	0.03

* Represent commercial inhibitors of Xanthine Oxidase (XO). All values presented are Mean ± SD of triplicate readings

Mean values represented by same alphabets are not significantly different by Tukey's post hoc analysis at $p \leq 0.05$

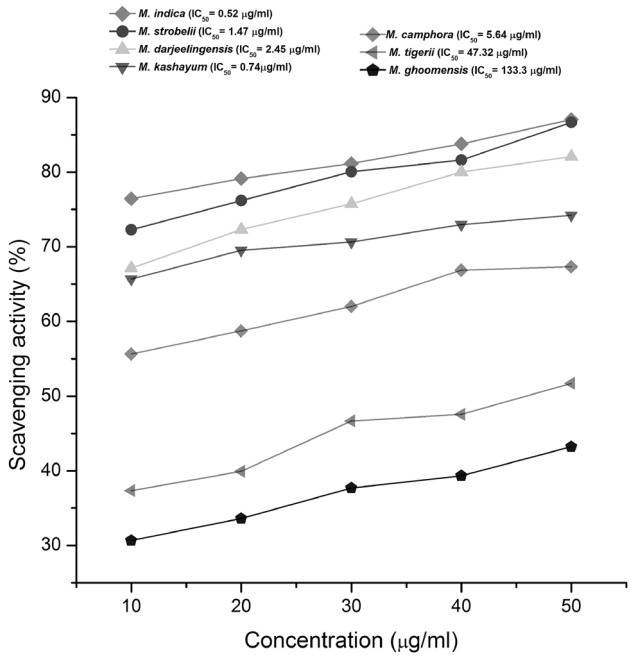

Fig. 3 Dose-response curve of chloroform residue of Indian *Muscodor* species for antioxidant activity by DPPH assay

0.61 μg/ml (Kapoor and Saxena 2014); however, the CE of *M. darjeelingensis* exhibits a still lower IC_{50} for XO inhibition warranting potential for isolation and characterization of the bioactive moiety.

The XO inhibitory activity by endophytic fungi probably is attributed to their survival strategy to overcome the metabolically aggressive environment inside the plant. Further, they may also exhibit anti-oxidant potential to overcome the oxidative stress based defense mechanism of plants. Hence, we found that *M. indica* expressed highest anti-oxidant activity index when compared to the standard anti-oxidant Gallic acid. *Muscodor tigerii* and *M. ghoomensis* exhibited the least anti-oxidant activity index when compared to gallic acid. The IC_{50} of DPPH scavenging activity of *M. indica* was significantly low when compared to endophytic fungus *Cladosporium velox* TN-9S isolated from *T. cordifolia* (Singh et al. 2016). Endophytic fungi are increasingly being explored for their anti-oxidant activity; however, they are seldom being reported for both anti-oxidant and Xanthine oxidase inhibitory activity which are interconnected. Hence, in the present investigation, we have tried to establish both XO inhibitory as well as anti-oxidant activity of *Muscodor* species isolated from India primarily from *Cinnamomum* sp. and *Aegle marmelos*. Both *Cinnamomum* and *Aegle marmelos* are medicinal plants which have been previously reported to possess anti-oxidant potential (Upadhya et al. 2004; Mathew and Abraham 2006; Jayaprakasha et al. 2006; Prasad et al. 2009; Reddy and Urooj 2013). Further, it can be hypothesized that endophytes generally mimic the medicinal properties of their host.

Thus, it can be concluded from the present study that *M. darjeelingensis* possesses a potent XOI activity while *M. indica* possesses potent anti-oxidant activity which warrants further investigation for further isolation and characterization of bioactive compounds.

Acknowledgements The Authors thank the Department of Biotechnology (National Biodiversity Development Board) for financial assistance through project no. BT/PR/10083/NDB/52/95/2007 under which this repository was created.

Compliance with ethical standards

Conflict of interest There is no conflict of interest.

References

Aggarwal A, Banerjee UC (2009) Screening of xanthine oxidase producing microorganisms using nitroblue tetrazolium based colorimetric assay method. Open Biotechnol J 3:46–49

Boparai JK, Saxena S, Meshram V (2015) *In vitro* antimicrobial potential of Indian *Muscodor* species. J Basic Appl Mycol 11:22–25

Chang WS, Lee YJ, Lu FJ, Chiang HC (1993) Inhibitory effects of flavonoids on xanthine oxidase. Anticancer Res 13:2165–2170

Ho R, Violette A, Cressend D, Raharivelomanana P, Carrupt PA, Hostettmann K (2012) Antioxidant potential and radical-scavenging effects of flavonoids from the leaves of *Psidium cattleianum* grown in French Polynesia. Nat Prod Res 26:274–277

Huang WY, Cai YZ, Hyde KD, Corke H, Sun M (2007) Endophytic fungi from *Nerium oleander* L (Apocynaceae): main constituents and antioxidant activity. World J Microbiol Biotechnol 23:1253–1263

Jayaprakasha GK, Ohnishi-Kameyama M, Ono H, Yoshida M, Jaganmohan Rao L (2006) Phenolic constituents in the fruits of *Cinnamomum zeylanicum* and their antioxidant activity. J Agric Food Chem 54:1672–1679

Kapoor N, Saxena S (2014) Potential xanthine oxidase inhibitory activity of endophytic *Lasiodiplodia pseudotheobromae*. Appl Biochem Biotechnol 173:1360–1374

Kuo CF, Grainge MJ, Zhang W, Doherty M (2015) Global epidemiology of gout: prevalence, incidence and risk factors. Rheumatology 11:649–662

Mathew S, Abraham TE (2006) *In vitro* antioxidant activity and scavenging effects of *Cinnamomum verum* leaf extract assayed by different methodologies. Food Chem Toxicol 44:198–206

Meshram V, Kapoor N, Saxena S (2014) *Muscodor strobelii*, a new endophytic species from South India. Mycotaxon 128:93–104

Newman DJ, Cragg GM (2015) Endophytic and epiphytic microbes as "sources" of bioactive agents. Front Chem 3:34. doi:10.3389/fchem.2015.00034

Prasad KN, Yang B, Dong X, Jiang G, Zhang H, Xie H, Jiang Y (2009) Flavonoid contents and antioxidant activities from *Cinnamomum* species. Innov Food Sci Emerg Technol 10:627–632

Reddy VP, Urooj A (2013) Antioxidant properties and stability of *Aegle marmelos* leaves extracts. J Food Sci Technol 50:135–140

Saxena S, Meshram V, Kapoor N (2014a) *Muscodor tigerii* sp. nov.-Volatile antibiotic producing endophytic fungus from the Northeastern Himalayas. Ann Microbiol 65:47–57

Saxena S, Meshram V, Kapoor N (2014b) *Muscodor darjeelingensis*, a new endophytic fungus of *Cinnamomum camphora* collected from northeastern Himalayas. Sydowia 66:55–67

Scherer R, Godoy HT (2009) Antioxidant activity index (AAI) by the 2, 2-diphenyl-1-picrylhydrazyl method. Food Chem 112:654–658

Shu RG, Wang FW, Yang YM, Liu YX, Tan RX (2004) Antibacterial and xanthine oxidase inhibitory cerebrosides from Fusarium sp. IFB-121, and endophytic fungus in *Quercus variabilis*. Lipids 39:667–673

Singh B, Sharma P, Kumar A, Chadha P, Kaur R, Kaur A (2016) Anti-oxidant and in vivo genoprotective effects of phenolic compounds identified from an endophytic *Cladosporium velox* and their relationship with host plant *Tinospora cordifolia*. J Ethnopharmacol. doi:10.1016/j.jep.2016.10.018

Upadhya S, Shanbhag KK, Suneetha G, Balachandra Naidu M, Upadhya S (2004) A study of hypoglycemic and antioxidant activity of *Aegle marmelos* in alloxan induced diabetic rats. Indian J Physiol Pharmacol 48:476–480

Wang SY, Yang CW, Liao JW, Zhen WW, Chu FH, Chang ST (2008) Essential oil from leaves of *Cinnamomum osmophloeum* acts as a xanthine oxidase inhibitor and reduces the serum uric acid levels in oxonate-induced mice. Phytomedicine 15:940–945

Worapong J, Strobel GA, Daisy BH, Castillo U, Baird G, Hess WM (2001) *Muscodor albus* anam. gen. et sp. nov., an endophyte from *Cinnamomum zeylanicum*. Mycotaxon 79:67–79

Appl Biochem Biotechnol (2014) 173:1360–1374
DOI 10.1007/s12010-014-0927-x

Potential Xanthine Oxidase Inhibitory Activity of Endophytic *Lasiodiplodia pseudotheobromae*

Neha Kapoor · Sanjai Saxena

Received: 7 February 2014 / Accepted: 17 April 2014 /
Published online: 7 May 2014

Abstract Xanthine oxidase is considered as a potential target for treatment of hyperuricemia. Hyperuricemia is predisposing factor for gout, chronic heart failure, atherosclerosis, tissue injury, and ischemia. To date, only two inhibitors of xanthine oxidase viz. allopurinol and febuxostat have been clinically approved for used as drugs. In the process of searching for new xanthine oxidase inhibitors, we screened culture filtrates of 42 endophytic fungi using in vitro qualitative and quantitative XO inhibitory assays. The qualitative assay exhibited potential XO inhibition by culture filtrates of four isolates viz. #1048 AMSTITYEL, #2CCSTITD, #6AMLWLS, and #96 CMSTITNEY. The XO inhibitory activity was present only in the chloroform extract of the culture filtrates. Chloroform extract of culture filtrate #1048 AMSTITYEL exhibited the highest inhibition of XO with an IC_{50} value of 0.61 μg ml^{-1} which was better than allopurinol exhibiting an IC_{50} of 0.937 μg ml^{-1} while febuxostat exhibited a much lower IC_{50} of 0.076 μg ml^{-1}. Further, molecular phylogenetic tools and morphological studies were used to identify #1048 AMSTITYEL as *Lasiodiplodia pseudotheobromae*. This is the first report of an endophytic *Lasiodiplodia pseudotheobromae* from *Aegle marmelos* exhibiting potential XO Inhibitory activity.

Keywords Xanthine oxidase · Endophytic fungi · Allopurinol · *Aegle Marmelos* · *Lasiodiplodia*

Introduction

Hyperuricemia is a biochemical abnormality which is clinically marked by overproduction or under excretion of uric acid leading to enhanced serum urate level beyond 6–7 mg dl^{-1} [1]. Gout is a debilitating metabolic disease which is increasingly getting prevalent predominantly due to changes in lifestyle and aging populations suffering with chronic hyperuricemia. Approximately 4.64 million adults globally are suffering from hyperuricemia and gout [2]. It is well established that xanthine oxidase (XO) is responsible for uric acid production by converting hypoxanthine into xanthine, and xanthine in turn into uric acid [3, 4]. Apart from gout, XO is also implicated in chronic heart failure [5, 6], atherosclerosis, tissue injury, and ischaemia [7, 8].

N. Kapoor · S. Saxena (✉)
Department of Biotechnology, Thapar University, Patiala, Punjab 147004, India
e-mail: sanjaibiotech@yahoo.com

Sanjai Saxena
e-mail: ssaxena@thapar.edu

Cornerstone of prevention and treatment of gout is anti-hyperuricemia therapy either by uricosuric drugs or XO inhibitors. Uricosuric drugs enhance the urinary excretion of uric acid while XO inhibitors (XOI) block the terminal step of uric acid biosynthesis thereby decreasing the plasma uric acid concentration. XOI are preferred over uricosuric and anti-inflammatory drugs because of lesser side effects [9]. Allopurinol, an analogue of hypoxanthine, has been the basis of hyperuricemic therapy; however, owing to its side effects and interference in other reactions of purine metabolism [10], non-purine inhibitors are being explored which could selectively inhibit the conversion of hypoxanthine and xanthine to uric acid. Febuxostat was the first synthetic non-purine based XOI approved by USFDA in 2009 for people suffering from allopurinol hypersensitivity syndrome. Thus, allopurinol and febuxostat are the only two molecules which have been used as oral XOI's in the last four decades.

Hence, there is a growing demand of new chemical templates which possess better in vitro inhibition of XO, have favorable toxicological profile and longer anti-hyperuricemic effect as compared to allopurinol and febuxostat. Endophytic fungi colonize the plants internally without apparent symptoms of their ubiquitous existence and are increasingly being prospected as underexplored resource of novel chemical entities exhibiting medicinal properties for their use as antimicrobials, anti-oxidants, cytotoxic, neuroprotective, and insulin mimetic activities in the last decade [11].

Bio-prospecting endophytic fungi for XO inhibition is a nascent area with very scanty preliminary data [12]. We carried out an in vitro screening program of xanthine oxidase inhibition by cell free culture filtrate of 42 endophytic fungi of plants inhabiting in the Western Ghats and north-east regions of India.

Here, we report the potential of a lead extract from the culture filtrate of endophytic fungal isolate # 1048 AMSTITYEL which induced higher inhibition of xanthine oxidase as compared to the positive control, allopurinol. The fungus was identified using molecular and morphological approaches for its exploitation in the isolation of the XOI and its evaluation as a pharmacophore for treatment of hyperuricemia.

Materials and Methods

Isolation of Endophytic Fungi

The plant material was collected from conserved forest area of Western Ghats and North eastern Himalayas. Each collected sample was properly labelled and placed in a sterile bag and stored at 4 °C until further use. Healthy stems and leaves of collected samples were surface sterilized by dipping in 1 %*w*/*v* sodium hypochlorite solution for 2–3 min, followed by washing with 70 % ethanol for 1 min, and then final washing by 30 % ethanol for 30–45 s [13]. The surface-sterilized samples were then cross-sectioned into 1–3 mm pieces with a sterile blade which were aseptically inoculated onto pre-sterilized potato dextrose agar (PDA) plates. The plates were incubated at 26±2 °C for 8–10 days with 12 h light/dark cycles. Hyphal tips of fungi emerging out of the inoculated plant tissues were picked up with sterile inoculation needle and sub-cultured on PDA plates. The active cultures were preserved as pure cultures over PDA slants containing 10 % glycerol.

Production of Culture Filtrates and Isolation of Bioactive Fraction

Liquid cultures of endophytic fungi were prepared by the procedure of Rodriguez et al., 2000 [14]. Concisely, the method comprised of inoculation of 100 ml pre-sterilized potato dextrose

broth (pH 5.1) aseptically with 5 mm mycelial disc of 7-day-old culture of endophytic fungus followed by incubation at 26±2 °C, 120 rpm for 15 days. After the culmination of incubation period, the mycelial mass was separated using Whatman filter paper no.4 followed by centrifugation at 10,000 rpm for 10 min at room temperature. The supernatant was then passed through 0.22 μm nitrocellulose membrane making it cell free. The cell free broths were stored at −20 °C until subjected to qualitative screening for XO inhibition.

Liquid–liquid extraction of the broth was adopted for isolation of the bioactive fraction [15]. Briefly, ethyl acetate was used to extract the cell free filtrate in ratio of 2:1. This process was repeated thrice, and the organic layers so obtained were pooled and subsequently dehydrated using anhydrous sodium sulphate. The remaining aqueous layer was extracted with chloroform following same procedure. The fractions so obtained were weighed, reconstituted in methanol and stored at −20°C until further use.

Qualitative Screening for Inhibitors of Xanthine Oxidase

Xanthine–nitroblue tetrazolium (NBT) agar plate method was used as preliminary screening assay for xanthine oxidase inhibitors. The method is based upon reduction in the diameter of blue halo formed by formazan due to reactive oxygen species produced by xanthine oxidase during conversion of xanthine into uric acid.

The assay was carried out by preparing plates containing 0.8 % agar, 1.5 mg ml^{-1}xanthine, and 0.11 mg ml^{-1} NBT. After solidification, 5-mm wells were prepared with sterile cork borer. In each test well, 30 μl of culture filtrate, 0.04 U of xanthine oxidase (source: bovine milk, Sigma-Aldrich), 10 mmol l^{-1} of tris-HCl buffer were dispensed while the control well was dispensed with 30 μl of un-inoculated broth. Allopurinol and febuxostat (50 mmol l^{-1}) were used as the positive control in place of culture filtrate. Febuxostat was gifted by Ranbaxy Research Laboratories, Gurgaon, India. All the treatments were incubated at 37 °C for 24 h. After the incubation is over, the plates were observed for reduction or absence of blue colored halo formation confirming the presence of xanthine oxidase inhibiting moiety. The halo diameter was recorded and data was represented as mean ± SD values.

Quantitative Analysis of XOI

The endophytic fungi showing maximum XO inhibitory activity on xanthine-NBT agar plate assay were further screened for their inhibitory potential quantitatively by using two spectrophotometric assays viz. NBT assay and the uric acid estimation assay.

(a) Nitroblue tetrazolium assay: the selected bioactive residue was screened for XO inhibition using microtitre plate-based nitroblue tetrazolium assay as described by Agarwal et al., 2009 [16] with slight modifications. The assay was based upon the formation of blue colored product formazan due to interaction of NBT with superoxide radicals generated during the oxidation of xanthine to uric acid with XO. The reduction in the intensity of blue colored product indicated xanthine oxidase inhibition.

Briefly, 0.125 mmol l^{-1} bioactive residue was incubated with 0.04 U of xanthine oxidase for 1 h at 37 °C, and the reaction was initiated by adding 6.7 mmol l^{-1} xanthine (substrate) followed by addition of 0.25 mmol l^{-1} NBT. After 30 min incubation at 37 °C, the amount of formazan formed in the reaction was estimated by measuring absorbance at 575 nm Biotek throughput reader, Powerwave 340. The control comprised of 6.7 mmol l^{-1} xanthine, 0.04 U of xanthine oxidase, 0.25 mmol l^{-1} NBT, and 6.58 mmol l^{-1} tris-HCl buffer. Positive control was same as that of control except that

it contains 6.25 mmol l^{-1} allopurinol/febuxostat and 0.325 mm ol l^{-1} of tris-HCl buffer. All the test and control experiments were performed in triplicates.

(b) Uric acid estimation assay: the assay was carried out as per the method of Chang et al., 1993 [17] to establish the production of uric acid from xanthine which is dependent on the XO activity. Briefly, 200 μM xanthine buffer solution was prepared by dissolving xanthine (3.0 mg) in the 100 ml of 0.1 M phosphate buffer (pH 7.8) solution by gentle heating. The sample extract (ethyl acetate/chloroform) was diluted with methanol and dissolved in the phosphate buffer solution to obtain a concentration of 1 mg/ml. The assay mixture was prepared by adding 10 μl of sample solution to 990 μl of xanthine buffer solution. The reaction was initiated by adding 5 μl of xanthine oxidase enzyme solution. The mixture was vortexed and incubated at 25ºC for 15 min, and further reaction was stopped by adding 1 N HCl solution. The concentration of uric acid was measured by taking absorbance value at 290 nm. Allopurinol and febuxostat served as positive controls. The inhibitory percentage of xanthine oxidase was calculated by:

$$\%\text{Inhibition} = [(\text{A}-\text{B})-(\text{C}-\text{D})]/(\text{A}-\text{B}) \times 100\%$$

Where *A* is the OD at 290 nm with enzyme but without sample, *B* is the OD at 290 nm without sample and enzyme, *C* is the OD at 290 nm with sample and enzyme, and *D* is the OD at 290 nm with sample but without enzyme.

Test for Purine

The fraction of interest was subjected to purine detection test based on precipitation of Ag^{+} ions with purine [18]. Briefly, to the 1 ml of sample (stock 1 mg/ml), ammonium hydroxide was added in excess followed by a few drops of 0.1 M silver nitrate solution. Formation of white precipitate, which is a purine complex with Ag^{+} ions, confirms the presence of purine. Allopurinol (purine analogue) and xanthine were used as positive control, and febuxostat, being non-purine in nature, was used as negative control.

Identification of Potential Endophytic Fungi

Microscopic Identification of Endophytic Fungi

Morphotaxonomic studies of the endophytic fungal isolate (#1048AMSTITYEL) were done by mounting the culture in lactophenol cotton blue and then observing under Nikon Stereozoom microscope (Nikon SMZ 745 T) coupled with NIS element D 3.2 software and Nikon Eclipse Compound microscope (E100). For tentative identification, the culture was grown over pine leaf agar (PLA) for 4–6 weeks at 26 °C with 12 h light period (near UV to cool white light) to support sporulation. Micrometry was carried out using Image J software with at least 30 observations per structure. Colony appearance, color, colony growth rate along with its microscopic structures like hyphal characteristics, conidia, and other cellular bodies were critically observed and recorded.

Molecular Phylogenetic Identification of Endophytic Fungi

The fungal mycelium was freeze-dried, and the genomic DNA isolation was carried out using the Wizard® Genomic DNA purification kit (Promega, USA). Briefly describing, 0.5 g of

fresh fungal mycelia were crushed to very fine powder in mortar and pestle using liquid nitrogen. The powdered mycelia were then transferred to microcentrifuge tube and further processed as per the manufacturer's instructions for the isolation of genomic DNA.

Phylogenetic relationship was accomplished by carrying out partial 5.8S and flanking ITS rDNA gene sequencing. The ITS rDNA amplification was performed in My Cycler™ Thermal cycler, Bio-Rad, USA using universal primer pair ITS1 (5′ CTTGGTCATTTAGAGGAAGT AA 3′) and ITS4 (5′ TCCTCCGCTTATTGATATG 3′) as designed by White et al., 1990 [19]. Amplification reaction was carried out in 25 μl reaction mixture volume comprising of 20 ng of extracted genomic DNA, 0.8 μM of each primer (ITS1 and ITS4), 2.5 mM of dNTP, 1.5 mM $MgCl_2$, 1.5 U of Taq DNA polymerase in 10× Taq buffer with following thermal cycling parameters—an initial denaturation at 96ºC for 5 min followed by 39 cycles of 95ºC for 45 s, 60ºC for 45 s, 72ºC for 45 s, followed by final extension at 72ºC for 5 min. PCR amplicon was purified using mini-columns (Wizard® SV Gel and PCR clean up system kit, Promega, USA) according to the manufacturer's protocol. Purified PCR product was sent for direct sequencing to Chromus Biotech Pvt. Ltd, Bangalore. The obtained chromatograms were manually edited and checked using Sequencher ver. 5 (www.genecodes.com) and submitted in the GenBank under the accession number KF540145.

The final consensus sequence was subjected to BLAST searches to ascertain the putative positional homology with closely related organisms based on sequence similarity results and phylogenetic inference. The obtained sequence along with selected reference taxa were aligned using ClustalW in MEGA 5.2 [20]. The alignment was inspected and adjusted manually wherever necessary. Alignment gaps were treated as missing characters. Evolutionary history was inferred by neighbor-joining method [21] using the maximum composite likelihood (MCL) model [22] to calculate the evolutionary distances. Bootstrap analysis (1000 bootstrap) was conducted to infer the consensus tree for the representation of phylogenetic diversity and evolutionary relationship.

Results

A total of 42 endophytic fungal isolates from different parts of medicinal parts were investigated for the xanthine oxidase inhibition activity (Table 1). Among these, 33 % cultures were isolated from *Aegle marmelos* while remaining 67 % of cultures were isolated *Cinnamomum camphora*, *Cinnamomum malabaricum*, *Cinnamomum zeylanicium*, *Tinospora cordifolia*, *Rauvolfia serpentina*, wild ginger, *Tabernaemontana divaricata*, *Camellia sinensis*, *Jatropha*, and *Nerium oleander*. The prevalent species among isolated mycoflora comprised of *Lasiodiplodia*, *Fusarium* and *Muscodor* (Table 1).

In the preliminary screening i.e., xanthine-NBT plate assay, the allopurinol and febuxostat exhibited reduction in halo size by 44.2 and 55.8 %, respectively, indicating the XO inhibition. The cell-free filtrates which exhibited the same or higher level of reduction in the halo size as induced by allopurinol were considered to be the producers of potential XO inhibitors. It was observed that culture filtrates of four isolates viz. #1048 AMSTITYEL, #2CCSTITD, #6AMLWLS, and #96 CMSTITNEY exhibited a potential in vitro xanthine oxidase inhibition with reduction in halo size by 54.8, 46, 44.2, and 42.4 %, respectively (Table 2).

The ethyl acetate fractions and chloroform fractions of the culture filtrates were isolated and were tested for XO inhibition. The ethyl acetate fraction did not exhibit any inhibitory action on xanthine oxidase while the chloroform fraction exhibited XO

Table 1 Endophytic fungi isolated from different medicinal plants and screened for xanthine oxidase inhibition

	Culture code	Identification	Host plant	Sampling location	XO inhibition
1.	#6AMLWLS	*Fusarium sp.*	*Aegle marmelos*	Wayanad wildlife sanctuary, Karnataka	++
2.	#16AMLWLS	*Muscodor sp.*	*Aegle marmelos*	Wayanad wildlife sanctuary, Karnataka	+
3.	#1006AMLBRT	*Fusarium sp.*	*Aegle marmelos*	BRT wildlife sanctuary, Karnataka	+
4.	#1007AMLBRT	Unidentified	*Aegle marmelos*	BRT wildlife sanctuary, Karnataka	−
5.	#1016AMLBRT	*Fusarium sp.*	*Aegle marmelos*	BRT wildlife sanctuary, Karnataka	+
6.	#7AMSTYEL	*Fusarium sp.*	*Aegle marmelos*	Yelandur, Karnataka	−
7.	#9(b)AMSTYEL	*Fusarium sp.*	*Aegle marmelos*	Yelandur, Karnataka	−
8.	#23(b)AMSTYEL	*Lasiodiplodia sp.*	*Aegle marmelos*	Yelandur, Karnataka	−
9.	#1022AMSTYEL	Unidentified	*Aegle marmelos*	Yelandur, Karnataka	+
10.	#1048AMSTITYEL	*Lasiodiplodia sp.*	*Aegle marmelos*	Yelandur, Karnataka	+++
11.	#1013AMSTITYEL	*Lasiodiplodia sp.*	*Aegle marmelos*	Yelandur, Karnataka	−
12.	#1069AMSTITYEL	*Fusarium sp.*	*Aegle marmelos*	Yelandur, Karnataka	−
13.	#1070AMSTITYEL	*Fusarium sp.*	*Aegle marmelos*	Yelandur, Karnataka	−
14.	##11AMSTITYEL	*Fusarium sp.*	*Aegle marmelos*	Yelandur, Karnataka	++
15.	#1CCBD	Unidentified	*Cinnamomum camphora*	Tiger hills, Darjeeling,WB	−
16.	#2CCBD	Unidentified	*Cinnamomum camphora*	Tiger hills, Darjeeling, WB	−
17.	#2CCSTITD	*Muscodor sp.*	*Cinnamomum camphora*	Tiger hills, Darjeeling, WB	++
18.	#1639CCSTITD	*Muscodor sp.*	*Cinnamomum camphora*	Tiger hills, Darjeeling, WB	+
19.	#2CMLNEY	Unidentified	*Cinnamomum malabaricum*	Neyyar, Kerala	−
20.	#40CMLBRT	*Botryosphaeria sp.*	*Cinnamomum malabaricum*	BRT wildlife sanctuary, Karnataka	−
21.	#21CMSTITNEY	Unidentified	*Cinnamomum malabaricum*	Neyyar, Kerala	+
22.	#52CMSTITNEY	Unidentified	*Cinnamomum malabaricum*	Neyyar, Kerala	−
23.	#54(b)CMSTITNEY	Unidentified	*Cinnamomum malabaricum*	Neyyar, Kerala	−

Table 1 (continued)

	Culture code	Identification	Host plant	Sampling location	XO inhibition
24.	#96CMSTITNEY	Unidentified	*Cinnamomum malabaricum*	Neyyar, Kerala	++
25.	#6610CMSTITBRT	*Muscodor sp.*	*Cinnamomum malabaricum*	BRT wildlife sanctuary, Karnataka	+
26.	#5CZBAWLS	*Fusarium solani*	*Cinnamomum zeylanicium*	Wayanad wildlife sanctuary, Karnataka	−
27.	#52CZSTITBRT	*Heliotales sp.*	*Cinnamomum zeylanicium*	BRT wildlife sanctuary	−
28.	#2162CZSTITG	Unidentified	*Cinnamomum zeylanicium*	Guwahati, Assam	−
29.	#2CSSTOT	*Schizophyllum* sp.	*Camellia sinensis*	Ooty	−
30.	#23JTLSVNP	Unidentified	*Jatropha*	Silent Valley, Kerala	−
31.	#19NOBASVNP	Gibberella sp.	*Nerium oleander*	Silent Valley, Kerala	−
32.	#16RSBANEY	Fusarium sp.	*Rauvolfia serpentina*	Neyyar, Kerala	+
33.	#16RSLBRT	Fusarium sp.	*Rauvolfia serpentina*	BRT wildlife sanctuary, Karnataka	+
34.	#2(a)TMDSTYEL	Fusarium sp.	*Tabernaemontana divaricata*	Yelandur, Kerala	−
35.	#2(b)TMDSTYEL	Fusarium sp.	*Tabernaemontana divaricata*	Yelandur, Kerala	−
36.	#4TICSTITPLM	Unidentified	*Tinospora cordifolia*	Palampur	−
37.	#11TICSTITPLM	Unidentified	*Tinospora cordifolia*	Palampur	−
38.	#46TICSTTPLM	Unidentified	*Tinospora cordifolia*	Palampur	−
39.	#51TICSTITPLM	Unidentified	*Tinospora cordifolia*	Palampur	−
40.	#13(a)WGSTNEY	Unidentified	*Wild ginger*	Neyyar, Kerala	+
41.	#15WGSTNEY	Unidentified	*Wild ginger*	Neyyar, Kerala	−
42.	#15(a)WGSTNEY	Unidentified	*Wild ginger*	Neyyar, Kerala	−

Table 2 In vitro xanthine oxidase inhibitory activity of culture filtrates by xanthine-NBT agar plate assay

Culture code	Enzyme activity* as halo formed (diameter mm)	Inhibition (%age)
Control	11.33±0.58	0
Allopurinol	6.33±0.58	44.2±3.9
Febuxostat	5.00±0.00	55.8±0.0
#1048AMSTITYEL	5.17±0.29	54.8±1.3
#2CCSTITD	6.17±0.29	46.0±0.5
#6AMLWLS	6.33±0.58	44.2±4.7
#96CMSTITNEY	6.50±0.50	42.4±3.8
##11AMSTITYEL	6.83±0.29	39.8±0.0
#16AMLWLS	7.17±0.29	37.1±6.1
1639CCSTITD	7.33±0.58	35.3±3.2
1006AMLBRT	7.50±0.50	33.6±2.9
16RSLBRT	7.50±0.50	33.6±2.9
22AMSTYEL	7.67±0.29	31.8±0.8
1016AMLBRT	7.83±0.29	30.9±0.8
#21CMSTITNEY	8.00±0.00	29.2±6.3
6610CMSTITBRT	8.00±0.00	29.2±6.3
16RSBANEY	8.17±0.29	28.3±1.1
52CMSTITNEY	8.50±0.50	24.7±2.2
1069 AMSTITYEL	8.83±0.76	22.1±5.6
15(a) WGSTNEY	8.83±0.29	22.1±1.6
1007AMLBRT	9.00±0.00	20.3±7.1
54(B)CMSTITNEY	9.00±0.00	20.3±7.1
46TICSTITPLM	9.00±0.00	20.3±7.1
5CZBAWLS	9.00±0.00	20.3±7.1
7AMSTYEL	9.17±0.29	19.4±1.8
1CCBD	9.17±0.29	19.4±1.8
19NOBASVNP	9.17±0.29	19.4±1.8
2(A)TMDSTYEL	9.17±0.29	19.4±1.8
11TICSTITPLM	9.17±0.29	19.4±1.8
15WGSTNEY	9.17±0.29	19.4±1.8
1022AMSTITYEL	9.33±0.58	17.6±1.6

inhibition in the xanthine-NBT assay. Further, the inhibitory potential of the chloroform fraction was established using spectrophotometric quantitative assays viz. NBT assay and the uric acid estimation assay.

NBT Assay

As evident from the qualitative NBT assay, #1048 AMSTITYEL exhibited 82.2 % inhibition in enzyme activity during the enzyme assay and was similar to the positive control allopurinol exhibiting 82.6 % inhibition; however, febuxostat exhibited 99.2 % inhibition (Fig. 1) while #6AMLWLS, #2 CCSTITD, and #96 CMSTITNEY exhibited 65.9, 59.9, and 54.2 % inhibition of enzyme activity. Further confirmation of enzyme inhibition was assessed though uric acid estimation assay.

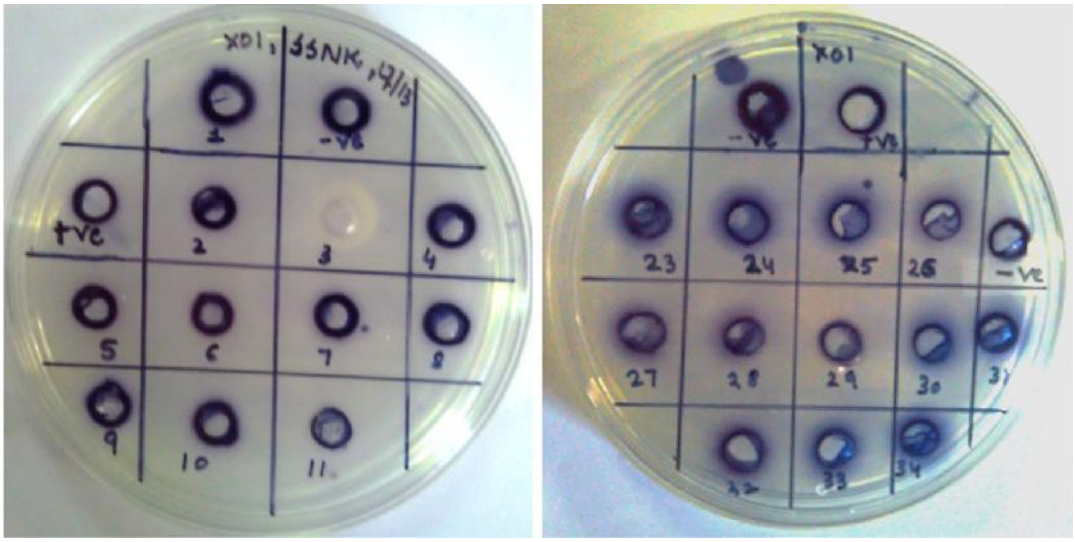

Fig. 1 NBT assay of allopurinol and the chloroform extracts of culture filtrates of selected fungi exhibiting potential XO inhibition

Uric Acid Estimation Assay

In the uric acid estimation assay, it became clearly evident that out of the four selected isolates, maximal inhibition of uric acid inhibition was caused by chloroform fraction of #1048 AMSTITYEL i.e., by 84.1 %, followed by #2CCSTITD and #6 AMLWLS. #96 CMSTITNEY did not exhibit any activity in the uric acid estimation assay. Allopurinol and febuxostat exhibited a 53.9 and 100 % reduction in uric acid formation during the assay, respectively. Thus, based on NBT as well as uric acid estimation assay, it was inferred that #1048 AMSTITYEL, #2CCSTITD, and #6AMLWLS were true producers of xanthine oxidase inhibitors with maximum inhibition by #1048 AMSTITYEL (Fig. 2a, b). Further IC_{50} value of # 1048 AMSTITYEL was 0.61 μg ml^{-1} as compared to allopurinol and febuxostat which exhibited an IC_{50} value of 0.93 μg ml^{-1} and 0.076 μg ml^{-1}, respectively (Fig. 3) indicating the presence of bioactive entity in the chloroform fraction residue of #1048 AMSTITYEL which has as potential XO inhibitory activity.

The purine detection test was positive for allopurinol and xanthine; however, it was negative for febuxostat and chloroform extract of #1048AMSTITYEL suggesting non-purine nature of the inhibitor (Fig. 4).

Morphotaxonomic Description

Over PDA, the colony was fast growing covering the 90 mm plate in 7 days; floccose, initially white later turning to grey colored, with formation of aerial hyphae (Fig. 5a). Over PLA, the colony was slow to moderately growing (76.02±1.89 mm in 14 days), downy, green to brown colored with rough margins (Fig. 5b). Hypha (2.66−) 3.83±0.79 (−4.97) μm thick, highly branched, brown colored, septate, broad, thick walled. Conidia (19.95−) 25.9±3.16 (−31.5)×(11.84−) 13.55±1.4 (−15.88) μm single celled, oval shaped, double walled, multi-nucleate (Fig. 6). Conidiogenous cells were simple, cylindrical to subobpyriform, holoblastic, paraphyses when present are cylindrical and sometimes septate (Fig. 7). Hence, on the basis of morphological and microscopic analysis, the culture was tentatively identified as *Lasiodiplodia* species [23, 24].

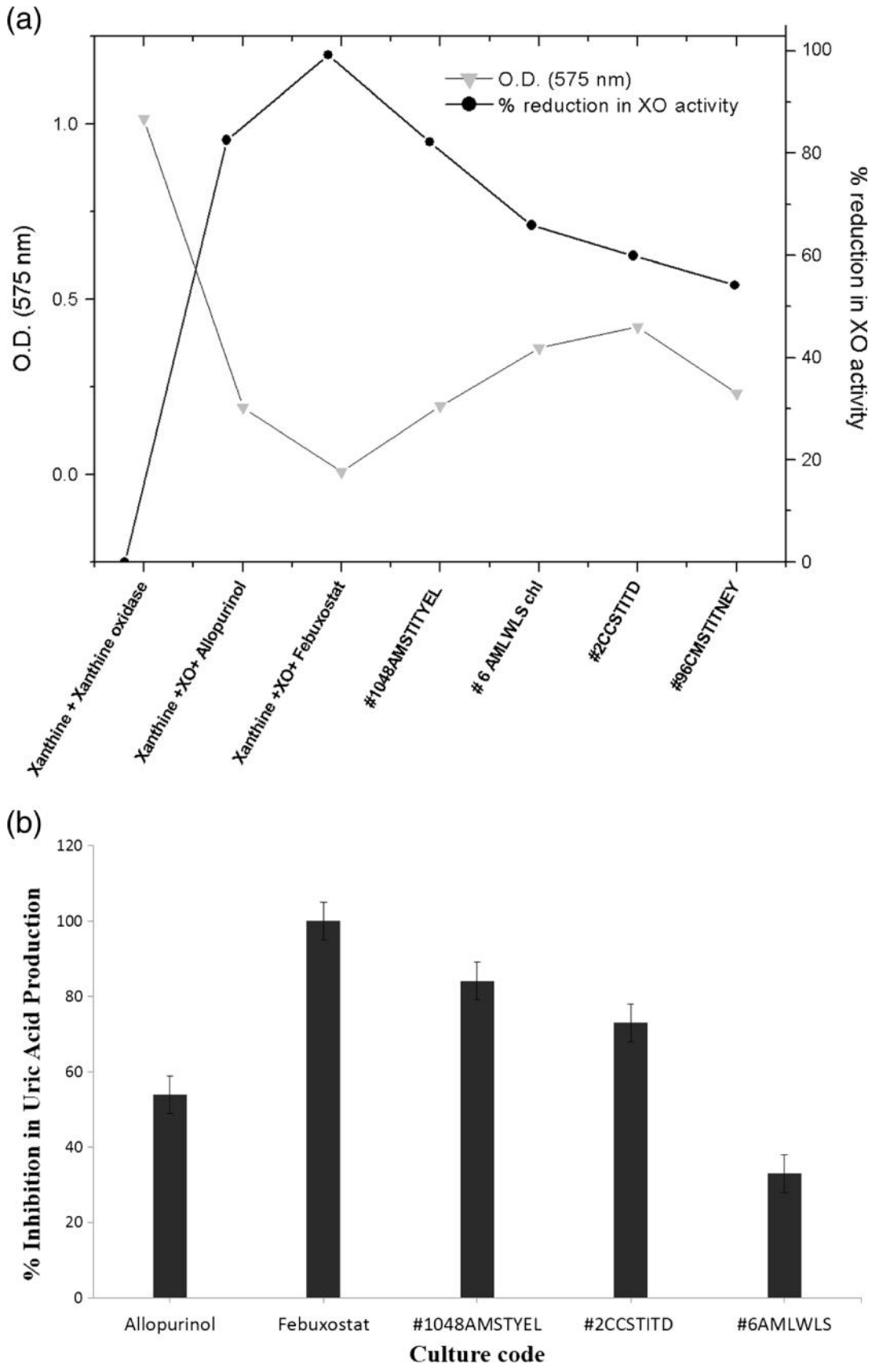

Fig. 2 Inhibition of xanthine oxidase by chloroform extracts of culture filtrate of selected fungi and allopurinol by **a** NBT reduction assay and **b** uric acid estimation assay to confirm the inhibition of XO

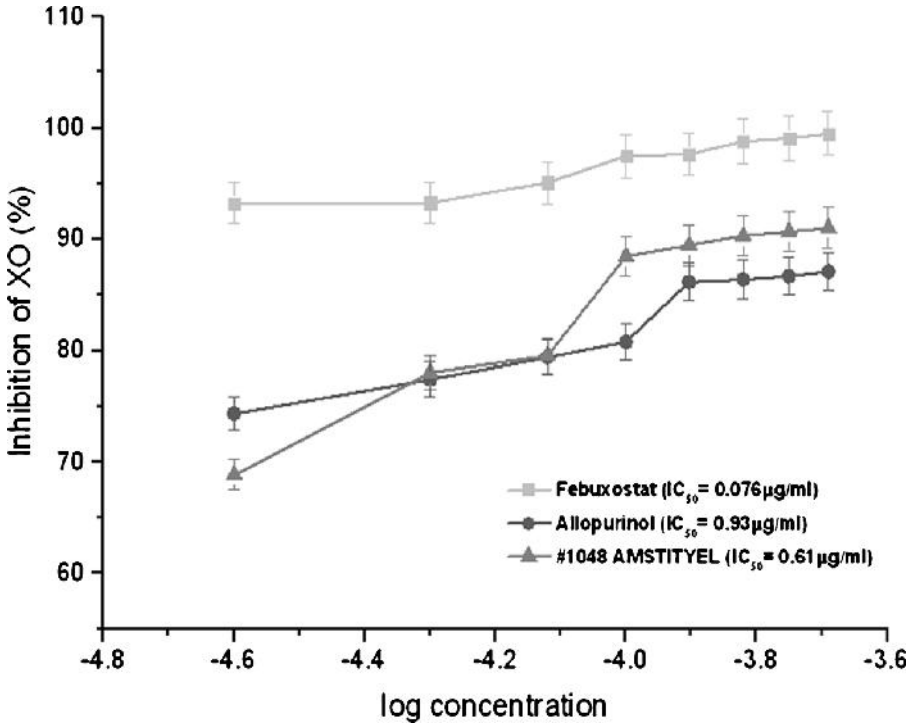

Fig. 3 Dose–response curves for inhibition of Xanthine oxidase chloroform extract of culture filtrate of #1048 AMSTITYEL. Allopurinol and febuxostat was used as the positive control

Molecular Phylogenetic Identification

Evolutionary relationship of the putative taxon, #1048AMSTITYEL, was established by subjecting the ITS region-based sequence to BLAST similarity search. The result showed 99 % sequence identity with *Lasiodiplodia pseudotheobromae* followed by 98 % identity with *L. theobromae* and *L. iranensis* confirming that it belongs to *Lasiodiplodia* lineage. It also exhibited 97 % sequence identity with *L. viticola*, *L. crassispora*, *L. rubropurpurea* and *L. parva*. The phylogenetic map was divided into two clades (Fig. 8). In clade I,

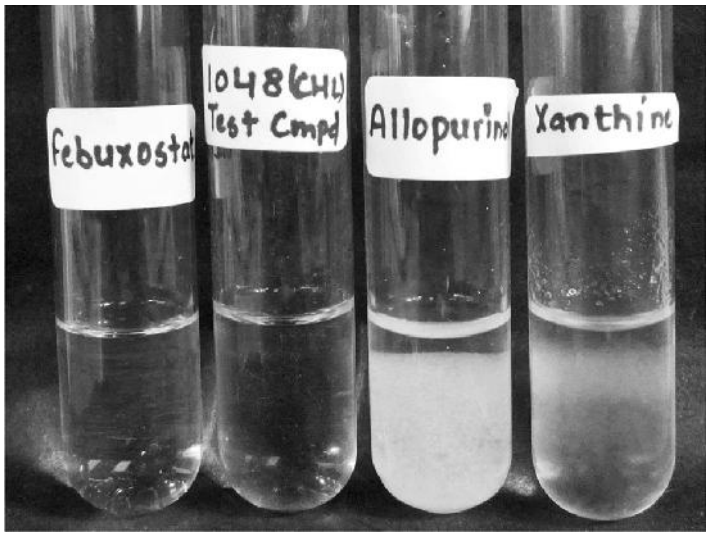

Fig. 4 Test for the presence of purine in chloroform extract of 1048AMSTITYEL. Allopurinol and Xanthine was used as positive control. Febuxostat (non-purine) was chosen as negative control

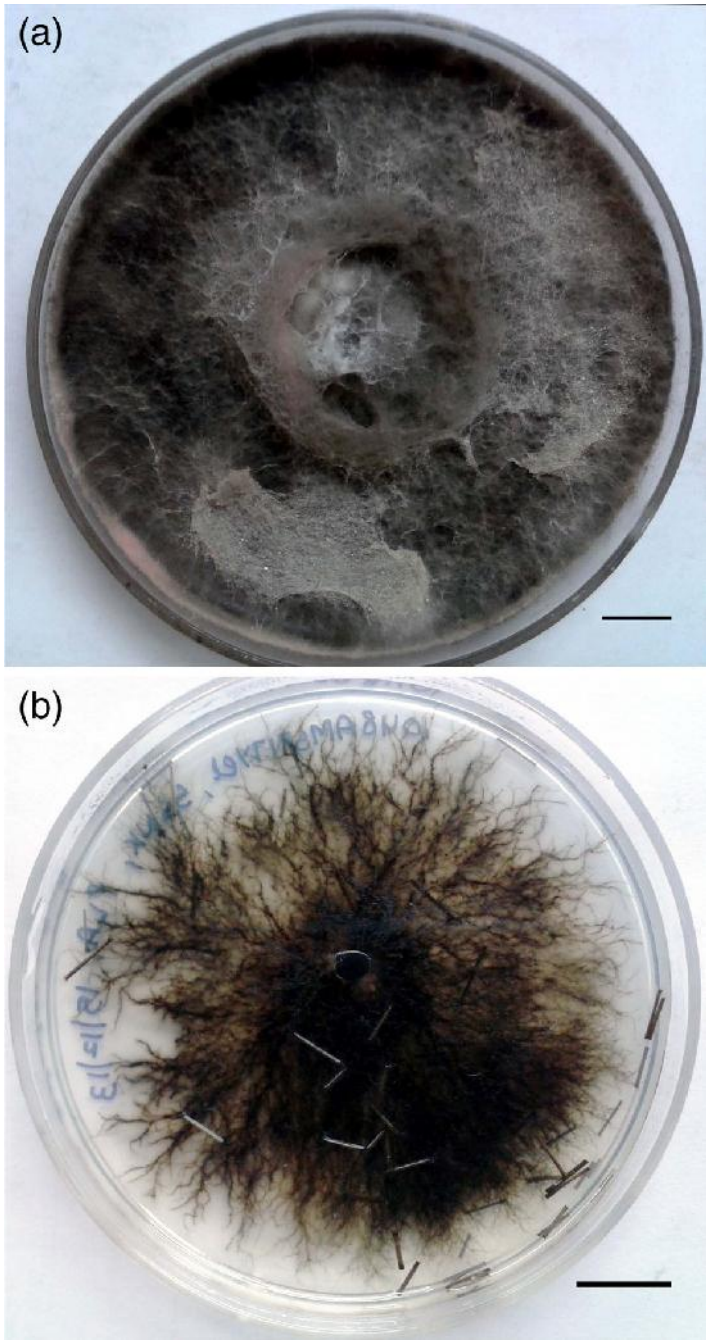

Fig. 5 Morphological features of #1048 AMSTITYEL. **a** On PDA. **b** On PLA (pine leaf agar)

#1048AMSTITYEL was clustered with three strains of *L. psuedotheobromae* and two strains of *L. theobromae*. It was very evident that 1048AMSTITYEL belongs to *L. pseudotheobromae*. Clade II grouped *L. parva*, two strains of *L. crassispora*, and *L. viticola*. *Aspergillus niger* was used as out group to root the tree.

Discussion and Conclusion

Hyperuricemia is recognized as a metabolic disorder which plays an important role in development of gout and related oxidative stress related diseases like cancer and

Fig. 6 Microscopic features of spores of # 1048 AMSTITYEL

cardiovascular disease. Until date, only febuxostat and allopurinol have been clinically used to lower plasma uric acid concentration by blocking the biosynthesis of uric acid. However, due to several severe side effects of these drugs on prolonged usage, safer alternatives are being explored from natural resources.

Fig. 7 Conidial arrangement of #1048 AMSTITYEL as seen under the microscope

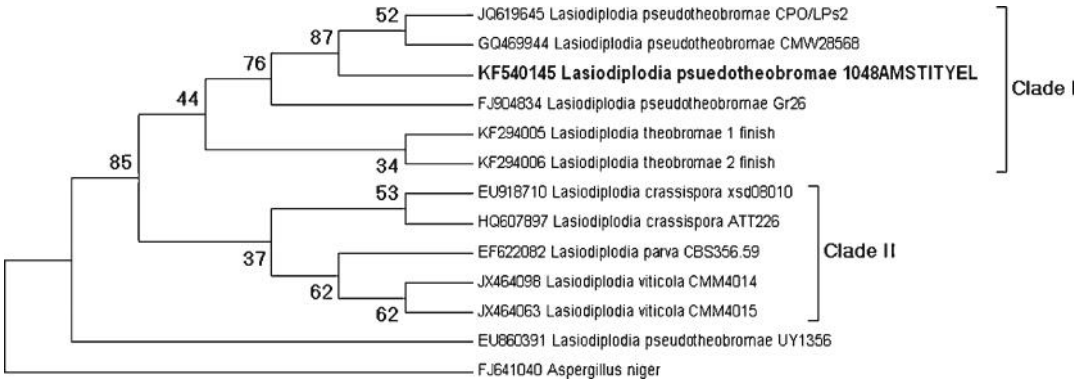

Fig. 8 Phylogenetic tree showing ITS-based molecular taxonomy and phylogenetic analysis of #1048 AMSTITYEL

Several plant extracts and phytochemicals have been found to possess XOI activities. Seed extracts of *Cassia fistula* [25], *Swietenia mahagoni* [26], and root extract of *Tephrosia purpurea* [27] exhibited promising xanthine oxidase inhibition. Liquiritigenin and isoliquiritigenin exhibited an IC_{50} of 12.6 μg ml^{-1} and 14.29 μg ml^{-1}, respectively for xanthine oxidase inhibition. Similarly, cinnamaldehyde isolated from the essential oil of *Cinnamomum osmophloeum* exhibited an IC_{50} of 8.4 μg ml^{-1} [28].

Apart from medicinal plants/phytochemicals, endophytic fungi offer themselves as a relatively untapped source of natural products which could inhibit XO and probably enter the drug discovery pipeline as an anti-hyperuricemic drug. There exist limited studies on the use of endophytic fungi as sources of xanthine oxidase inhibitory compounds. Fusaruside is a XOI which has been isolated from endophytic *Fusarium* sp. IFB–121 with an IC_{50} of 32.9 μg ml^{-1} [29]. Phenolic compounds isolated from endophytic *Chaetomium* sp. residing in *Nerium oleander* L. (Apocyanaceae) exhibited an IC_{50} of 109.8 μg ml^{-1} for xanthine oxidase inhibition [30].

The production of XO inhibitory compounds by endophytic fungi might be required for their survival and reproduction inside the host plant or would be a result of their modified metabolism for their survival. The present study is the first report of XOI producing endophytic fungus from *Aegle marmelos*. The chloroform fraction of isolate #1048AMSTITYEL identified as *L. pseudotheobromae*, exhibited prominent xanthine oxidase inhibition potential with IC_{50} better than allopurinol but higher as compared to febuxostat. It is expected that further purification of the chloroform extract would improve the inhibition kinetics of xanthine oxidase which would be helpful in arriving to the exact IC_{50} of the pure compound. Further purification and characterization of this compound are underway for possible development into a drug for hyperuricemia management and gout treatment.

Acknowledgment The authors are thankful to the Head of the Department of Biotechnology, Thapar University, Patiala, Punjab for providing the necessary infrastructure to carry out the research work. The authors would like to acknowledge Shri Vinod Arora, Vice-President (Pharma Research) and Ms. Jyoti Srivastava, Ranbaxy Research laboratories, Gurgaon, India for providing febuxostat as a gift sample. This research received no specific grant from any funding agency in the public, commercial, or not-for-profit sectors.

References

1. Neogi, T. (2011). *New England Journal of Medicine, 364*, 443–452.
2. Zhu, Y., Pandya, B. J., & Choi, H. K. (2011). *Arthritis and Rheumatism, 63*, 3136–3141.
3. Fukunari, A., Okamoto, K., Nishino, T., Eger, B. T., Pai, E. F., Kamezawa, M., et al. (2004). *Journal of Pharmacology and Experimental Therapeutics, 311*, 519–528.

4. Glantzounis, G. K., Tsimoyiannis, E. C., Kappas, A. M., & Galaris, D. A. (2005). *Current Pharmaceutical Design, 11*, 4145–4151.
5. Farquharson, C. A. J., Butler, R., Hill, A., Belch, J. J. F., & Struthers, A. D. (2002). *Circulation, 106*, 221–226.
6. Berry, C. E., & Hare, J. M. (2004). *Journal of Physiology, 555*, 589–606.
7. Chambers, D. E., Parks, D. A., Patterson, G., Roy, R., McCord, J. M., Yoshida, S., et al. (1985). *Journal of Molecular and Cellular Cardiology, 17*, 145–152.
8. Boueiz, A., Damarla, M., & Hassoun, P. M. (2008). *American Journal of Physiology - Lung Cellular and Molecular Physiology, 294*, 830–840.
9. Liebman, S. E., Taylor, J. G., & Bushinsky, D. A. (2007). *Current Rheumatology Reports, 9*, 251–257.
10. Arellano, F., & Sacristan, J. A. (1993). *Annals of Pharmacotherapy, 27*, 337–343.
11. Zhang, H. W., Song, Y. C., & Tan, R. X. (2006). *Natural Product Reports, 23*, 753–771.
12. Song, Y. C., Li, H., Ye, Y. H., Shan, C. Y., Yang, Y. M., & Tan, R. X. (2004). *FEMS Microbiology Letters, 241*, 67–72.
13. Pterini, O. (1986). In Fokkema & J. Van Den Heuvel (Eds.), *Microbiology of phylosphere. Taxonomy of endophytic fungi of aerial plant tissues* (pp. 175–187). Cambridge: Cambridge University press.
14. Rodrigues, K. F., Manfred, H., & Christa, W. (2000). *Journal of Basic Microbiology, 40*(4), 261–267.
15. Choudhary, M. I., Musharraf, S. G., Mukhmoor, T., Shaheen, F., Ali, S., & Rehman, A. U. (2004). *Journal of Biosciences, 59*, 324–327.
16. Agarwal, A., & Banerjee, U. C. (2009). *The Open Biotechnology Journal, 3*, 46–49.
17. Chang, W., Lee, Y., Lu, F., & Chiang, H. (1993). *Anticancer Research, 13*, 2165–2170.
18. Salkowski, E. (1898). *Pflugers Archiv - European Journal of Physiology, 69*, 268-306.
19. White, T. J., Bruns, T. D., Lee, S., & Taylor, J. W. (1990). Amplification and direct sequencing of fungal ribosomal RNA genes for phylogenies. In M. A. Innis, D. H. Gelfand, J. J. Sninsky, & T. White (Eds.), *PCR protocols: A guide to methods and applications* (pp. 135–322). San Diego: Academic.
20. Tamura, K., Peterson, D., Peterson, N., Stecher, G., Nei, M., & Kumar, S. (2011). *Molecular Biology and Evolution, 28*, 2731–2739.
21. Saitou, N., & Nei, M. (1987). *Molecular Biology and Evolution, 4*, 406–425.
22. Tamura, K., Nei, M., & Kumar, S. (2004). *Proceedings of the National Academy of Sciences (USA), 101*, 11030–11035.
23. Abdollahzadeh, J., Javadi, A., Goltapeh, E., Mohammadi, Zare, R., & Phillips, A. J. L. (2010). *Persoonia, 25*, 1–10.
24. Damn, U., Pedro, W. C., & Fourei, H. P. (2007). *Mycologia, 5*(99), 664–680.
25. Jothy, S. L., Zakaria, Z., & Sasidharan, S. (2011). *Journal of Medicinal Plants Research, 5*(10), 1941–1947.
26. Sahgal, G., Ramanathan, S., Sasidharan, S., Mordi, M. N., Ismail, S., & Mansoor, S. M. (2009). *Molecules, 14*, 4476–4485.
27. Nile, S. H., & Khobragade, C. N. (2011). *Journal of Natural Products and Resources, 2*, 52–58.
28. Wang, S. Y., Yang, C. W., Liao, J. W., Zhen, W. W., Chu, F. H., & Chang, S. T. (2008). *Phytomedicine, 15*, 940–945.
29. Shu, R. G., Wang, F. W., Yang, Y. M., Liu, Y. X., & Tan, R. X. (2004). *Lipids, 39*, 667–673.
30. Huang, W. Y., Cai, Y. Z., Kevin, D., Corke, H. H., & Sun, M. (2007). *World Journal of Microbiology and Biotechnology, 23*, 1253–1263.

DOI 10.12905/0380.sydowia66(1)2014-0055

Muscodor darjeelingensis, a new endophytic fungus of *Cinnamomum camphora* collected from northeastern Himalayas

Sanjai Saxena*, Vineet Meshram & Neha Kapoor

Department of Biotechnology, Thapar University, Patiala, Punjab, 147004, India

Saxena S., Meshram V. & Kapoor N. (2014) *Muscodor darjeelingensis*, a new endophytic fungus of *Cinnamomum camphora* collected from northeastern Himalayas. – Sydowia 66 (1): 55–67.

Muscodor species are sterile, volatile producing endophytic fungi with antimicrobial properties. The current study reports the new species *Muscodor darjeelingensis* from internal stem tissue of *Cinnamomum camphora*. The fungus produces white colonies over potato dextrose agar (PDA) medium with sterile ropy mycelial filaments. Scanning electron microscopy photographs showed formation of thick sterile mycelium with cauliflower-like structures. The phylogenetic analysis based on ITS1-5.8S-ITS2 confirms its identity as a new species in the genus *Muscodor*. The fungus also produces a unique mixture of 27 volatile organic compounds (VOCs) predominantly 2, 6-Bis (1, 1-dimethylethyl)-4-(1-oxopropyl) phenol, 1, 6-Dioxacyclododecane-7, 12-dione and 4-octadecylmorpholine. A consortium of these volatiles exhibited inhibitory effect over a tested battery of pathogenic microorganisms. Out of 25 tested pathogenic microorganisms, the VOCs inhibit the growth of five fungal pathogens by 50–70 %, while considerable inhibition was observed against *Candida* species and *Pseudomonas aeruginosa*.

Keywords: Darjeeling, anamorphic fungi, ITS rDNA, volatile antimicrobials, sp. nov.

Over the last five decades there has been continuous search for isolating and exploring fungi that produce volatile organic compounds (VOCs) and have antimicrobial activity but none of them was found to be as magnificent as the endophytic *Muscodor* species. *Muscodor* species produce a multitude of antimicrobial volatile carbon compounds. Studies of *Muscodor* species in different geographical regions and exploring its volatile organic spectrum could possibly provide insights into the ecological role in nature (Strobel 2012). To date 12 *Muscodor* species have been reported from different parts of the world with potential antimicrobial and insecticidal efficacy (Suwannarach *et al.* 2013). Several *Muscodor* species and strains *viz. M. albus* Worapong, Strobel & W. M. Hess strains *MFC2,* 1-4 1.3s, *MOW12, M. equiseti* Suwannarach & Lumyong, *M. fengyangensis* C. L. Zhang, *M. musae* Suwannarach & Lumyong, *M. suthepensis* Suwannarach & Lumyong (Sopalun *et*

* e-mail: sanjaibiotech@yahoo.com

al. 2003, Atmosukarto *et al.* 2005, Zhang *et al.* 2010, Banerjee *et al.* 2013, Suwannarach *et al.* 2010, 2013) have been isolated from the biodiversity hotspot areas of South east Asia.

The current study reports the existence of a novel *Muscodor* species in the internal stem tissue of *Cinnamomum camphora* growing in Tiger Hill area of Darjeeling, West Bengal, India. The fungus possesses antifungal activity against both the filamentous and non filamentous fungi. Morphological, molecular and chemical characteristics distinguish it from the earlier reported *Muscodor* species. Thus, based on its unique features, the isolate #1 CCSTITD represents a new species, for which the name *Muscodor darjeelingensis* is proposed.

Materials and methods

Plant sample collection, endophytic fungal isolation and preservation

Healthy twigs of *Cinnamomum camphora* were collected from the peak of Tiger Hills in Darjeeling, West Bengal, during the forest forays in March 2011. Plant samples were kept in sterile packets and stored at 4 °C until further use. Isolation of endophytic fungi was done in presence of *Muscodor albus* cz620 which allows the growth of *Muscodor* or related species by the virtue of volatiles produced by it. In one quadrant of the commercially available partitioned Petri plate pre-sterilised potato dextrose agar (PDA) was poured whereas in the three other quadrants water agar (WA) was dispensed and allowed to solidify. Actively growing *M. albus* cz620 was inoculated over the PDA quadrant and incubated at 24 ± 1 °C for the next four days for the production of VOCs. The plant material (5 × 5 mm) was surface sterilised using 2 % sodium hypochlorite for 2–3 min followed by 70 % ethanol for 1 min and 30 % ethanol for 30 s. These were then finally rinsed with sterile distilled water and allowed to air dry under aseptic condition. The plant material was sliced into fine sections of 1–2 mm. These were placed over the remaining column of the plate. The plates were sealed and incubated at 26 ± 2 °C for 14 days with alternating cycles of light and dark for 12 hours. The fungi sprouting from the host tissues were further subcultured onto fresh PDA plates and then subsequently transferred to PDA slants supplemented with 10 % glycerol (Ezra *et al.* 2004, Strobel *et al.* 2007, Mitchell *et al.* 2008). The holotype was submitted in living form to the National Fungal Culture Collection of India, Agharkar research Institute, Pune (NFCCI 3095).

Morphology

The fungus was identified on the basis of morphological characters. It was grown on six different media comprising PDA, malt extract agar (MEA), corn meal agar (CMA), Czapek Dox agar (CDA), synthetischer nährstoffarmer agar (SNA) and water agar (WA). The mycelial mass of the seven days old fungus was teased into fine filaments and then mounted with lactophenol

cotton blue. The microscopic characters were observed using a Nikon stereozoom microscope (Nikon SMZ 745T) coupled with NIS element D 3.2 software and a Nikon eclipse compound microscope (E100). Microscopic measurements were done using Image J software with at least 30 observations per structure. Colony texture, colour, growth rate, pigment and VOC production along with microscopic structures like hyphal characteristics and other cellular bodies were critically observed and recorded according to Guo *et al.* (1998) and Mitchell *et al.* (2008).

DNA extraction, sequence assembly and phylogenetic analysis

Genomic DNA extraction of the isolate was carried out by scrapping off the cultured mycelia from a 3–4 days old culture with pre-sterilized inoculation loop and grounded to very fine powder with liquid nitrogen in pestle and mortar. Further DNA extraction was performed by Wizard® genomic DNA purification kit (Promega, USA) following manufacturer instructions.

The conserved internal transcribed spacer region (ITS1-5.8S-ITS2) was amplified using the *M. albus* specific primer pair as described by Ezra *et al.* (2009). The reaction mixture for the amplification of ITS region contained 1µl of extracted genomic DNA, 25mM $MgCl_2$, 2.5mM dNTP, 10 pmol/µl of each primer, 1.5U of Taq DNA polymerase (Bangalore Genei) in 10X Taq buffer making the reaction volume to 25µl. Thermal cycling parameters used were previously described by Ezra *et al.* (2009). The PCR product of approximately 400–500 bp was purified by Wizard® SV gel and PCR clean up system kit (Promega, USA). The purified amplicon was sequenced using BDTV 3.1 cycle sequencing kit on ABI 3730 XI genetic analyzer by Xcleris Genomics, Xcleris labs, Gujarat.

The obtained sequence #1CCSTITD was aligned in Sequencher, Version 5 (Gene Codes, Ann, Arbor, MI) and deposited in the GenBank JQ409997. The sequence was subjected to similarity search using BLAST against the database maintained by NCBI. Sequences of already reported *Muscodor* species were retrieved from GenBank and aligned with the sequence of #1CCSTITD using Clustal W in MEGA 5 (Tamura *et al.* 2011). Distance-based analysis of the ITS region alignment was done by Neighbor-joining method (Saitou & Nei 1987) using the Tamura-Nei model (Tamura & Nei 1993) and the rate variation among sites was modelled with a gamma distribution (shape parameter = 5). Gaps were coded as missing characters. Clade stability was assessed by 1000 bootstrap replicates.

Computation of genetic distances

The genetic relatedness of *Muscodor darjeelingensis* with already reported species of *Muscodor* was deduced by determination of pair wise distances implemented in MEGA 5.2. This distance is the proportion (p) of nucleotide sites at which two sequences being compared are different. It is obtained by dividing the number of nucleotide differences by the total number

of nucleotides compared. Gaps were coded as missing characters, and Maximum Composite Likelihood was chosen as a model for the analysis.

The levels of DNA polymorphism such as number of variable sites (η), haplotypes, haplotype diversity, nucleotide diversity (π), evolutionary models were deduced with DNASp5 (Librado & Rozas 2009).

Scanning electron microscopy

Scanning electron microscopy of *M. darjeelingensis* was done by the procedure described by Ezra *et al.* (2004). Briefly, agar blocks of seven days old fungus were placed in 2.5 % glutaraldehyde in 0.1 M phosphate buffer (pH 7.2) overnight at 4 °C. Next day they were washed twice with the same buffer for 10 min each. The fungal material was slowly dehydrated using different gradients of acetone (30–100%), critical-point dried and coated with gold palladium using putter coater. The images were then recorded in high vacuum mode using a Zeiss Evo40 scanning electron microscope between 307 X – 2.02 KX magnification at 15 kV EHT (Ezra *et al.* 2004, Kudalkar *et al.* 2012).

Volatile analysis of *M. darjeelingensis*

Volatiles produced by seven days old *M. darjeelingensis* were evaluated using solid phase microextraction (SPME) syringe having a stable flex fibre made up of 50/30 divinylbenzene/carboxen on polydimethylsiloxane (Supelco, Sigma Aldrich). The baked SPME fiber was placed inside the Petri plate through a small hole bored inside the plate. The fibre was exposed to the vapour phase for 45 min. The SPME syringe was then injected for 30 s in the Shimadzu QP 2010 plus gas chromatograph with thermal desorption system TD 20. A RTX column (diphenyl 95 %, dimethyl polysiloxane 5 %) with 30 m × 0.25 mm ID and 0.25 mm DF was used for separating of the fungal volatiles. The column was programmed at 100 °C for 2 min and the temperature was then raised to 250 °C for 2 min and then finally to 300 °C for 13 min. The carrier gas was helium and the initial column head pressure was 94.4 KPa. Data acquisition and processing was done on GCMS solution software. The compounds obtained after GC/MS analysis were then subtracted from the control plate containing only PDA medium. The compounds obtained were tentatively identified based on their high quality matching (above 70 %) with database of National institute of Standard and Technology (NIST) compounds (NIST05) and compared with all reported species of *Muscodor* to date (Ezra *et al.* 2004, Kudalkar *et al.* 2012).

Bioassay of VOCs produced by *M. darjeelingensis*

Antimicrobial activity of the volatiles produced by *M. darjeelingensis* was evaluated using a simplified bioassay as described by Strobel *et al.* (2001). Two mm agar strip was removed from the centre in order to check the

movement of any diffusible inhibitory compound from the *Muscodor* sp. to the test microorganism(s). One half of the Petri plate was inoculated with a mycelial plug of an actively growing culture of *M. darjeelingensis*, The plates were sealed and incubated at 24 ± 2 °C for five days for production of the VOCs. The test bacteria or yeast were subsequently streaked in the other two quadrants whereas for testing filamentous fungi, three mm mycelial plugs were inoculated over the remaining PDA quadrants. The control plates were devoid of *M. darjeelingensis* thus allowing the test bacteria or the fungi to grow normally. Antimicrobial action of VOCs was determined by monitoring the difference in growth of microbes in test and control plates. (Mitchell *et al.* 2010). Each test was performed in triplicates and their mean and SD was calculated.

Results and discussion

Taxonomy

Muscodor darjeelingensis S. Saxena, Meshram & N. Kapoor, **sp. nov.** – Figs. 1–5. MycoBank no.: MB 804025, GenBank no.: JQ409997

D i a g n o s i s . – Differs from all other *Muscodor* species by its fast colony growth rate; from *M. roseus, M. fengyangensis, M. musae, M. oryzae* and *M. suthepensis* by presence of cauliflower like structures and from *M. yucatanensis*, *M. equiseti, M. sutura* by the absence of swollen hyphae. It differs from *M. albus* and *M. vitigenus* by the presence of coiling structures.

E t y m o l o g y . – '*darjeelingensis*' refers to the collection site Darjeeling.

H o l o t y p e . – INDIA, West Bengal, Darjeeling, Tiger Hills, 27° 13'–26° 27'N 88° 53'–87°59'E, endophytic fungus from internal stem tissue of *Cinnamomum camphora*, 23 March 2011, *leg*. Sanjai Saxena (Holotype: CCSTITD #1 in metabolic inactive state; ex type culture: National Fungal Culture Collection of India, NFCCI-3095). rDNA sequence ex-holotype: JQ409997

T e l e o m o r p h . – Not observed.

D e s c r i p t i o n . – Contrasting to the other slow growing *Muscodor* species, this endophytic fungal isolate grows rapidly over PDA and MEA and covers 90 mm Petri plate within five days when incubated at 24±2 °C with 12 h photoperiods (Fig. 1). The fungal colony is floccose and white turning to brown after ten days. It generates septate and branched hyphae which are (3.9)6.3±1.7(9) µm wide grown on CDA (Fig. 2). The mycelium branches at a certain angle and terminates into coils which are 37.30 × 36.54 µm wide. On MEA the isolate produces a thick and broad mycelium that forms fishing-net like structures with (4.4)7.4±1.7(10.7) µm wide hyphae. The hyphae branch at right angles and terminally form gigantic coiling structures which are up to 134 µm wide. The fungus produces fruity smell but does not produce any pigment or conidial structure *in vitro*.

Variation in growth rate and morphology was observed when grown on different media. Over CDA and SNA, the isolate was floccose, moderately growing with a mean colony size of 46.6 mm and 67 mm. When grown over CMA and WA hyaline colonies are formed which were growing slowly with a

mean colony diameter of 32 mm and 23 mm, respectively after seven days incubation. The culture produces VOCs with a strong fruity smell exclusively on PDA, MEA, and CDA. Volatile production was comparably higher on PDA than on MEA and CDA. The hyphae are septate, branched at right angle forming coiling structures either centrally or terminally. The average width of the hyphae on CMA, CDA, SNA and WA medium was 3.5±1.2µm, 6.5±0.9 µm, 6.6±1.4 µm and 6.2±1.3 µm, respectively, whereas the mean diameter of the coils were 71.3 µm, 149.6 µm, 93.8 µm, respectively (Fig. 3).

Scanning electron microscopy

The scanning electron micrographs of *M. darjeelingensis* exhibited the characteristic features of *Muscodor* species i.e. long, sterile and right-angled ropy hyphae that terminate into coils. The hyphae further fuse to form a ropy mycelium. The isolate also produces cauliflower-like structure but did not produce any sporulating structures (Figs. 4–5).

Muscodor darjeelingensis differs in morphology from the other type strains of *Muscodor*. *Muscodor crispans* A. M. Mitch., Strobel, W. M. Hess, Pérez-Vargas & Ezra and *M. sutura* Kudalkar, Strobel & Riyaz-Ul-Hassan form a similar cauliflower-like structure but they differ in mycelial arrangement with *M. crispans* forming a wavy hyphal mass and *M. sutura* showing a 'knitting pattern' mycelium. *Muscodor roseus* Worapong, Strobel & W. M. Hess, *M. cinnamomi* Suwannarach, Bussaban, K. D. Hyde & Lumyong, *M. musae, M. oryzae* Suwannarach & Lumyong and *M. suthepensis* have ropy mycelia with coils but lack cauliflower-like structures. *Muscodor yucatanensis* and *M. equiseti* have ropy mycelia with swollen hyphae. *Muscodor albus* and *M. vitigenus* have straight hyphae without any coils or cauliflower-like structures.

Internal transcribed spacer (ITS)-based phylogenetic analysis of *M. darjeelingensis*

The phylogenetic diversity of *M. darjeelingensis* was inferred on the basis of ITS region sequence analysis. BLAST similarity search showed 97 % sequence similarity with *M. cinnamomi*, *M. crispans*, *M. albus* cz620. It also showed 92 % sequence similarity with *M. sutura*, *M. vitigenus* and 86 % sequence similarity with *M. yucatanensis*. The Neighbor-joining tree revealed two separate clades of *Muscodor* species: Clade I with *M. albus, M. cinnamomi*, *M. crispans*, *M. musae, M. oryzae, M. roseus* and *M. darjeelingensis* and *M. suthepensis* appearing as a basal sister to the rest of clade I with 99 % bootstrap support. *Muscodor equiseti, M. fengyangensis, M. sutura, M. vitigenus* and *M. yucatanensis* grouped in Clade II. *Xylaria arbuscula* and *Peziza badia* were taken as outgroup (Fig. 6).

DNA sequence polymorphism analysis can provide insights into the significant evolutionary factors acting on the population and species and can be employed to compare alternative evolutionary scenarios. The number of pol-

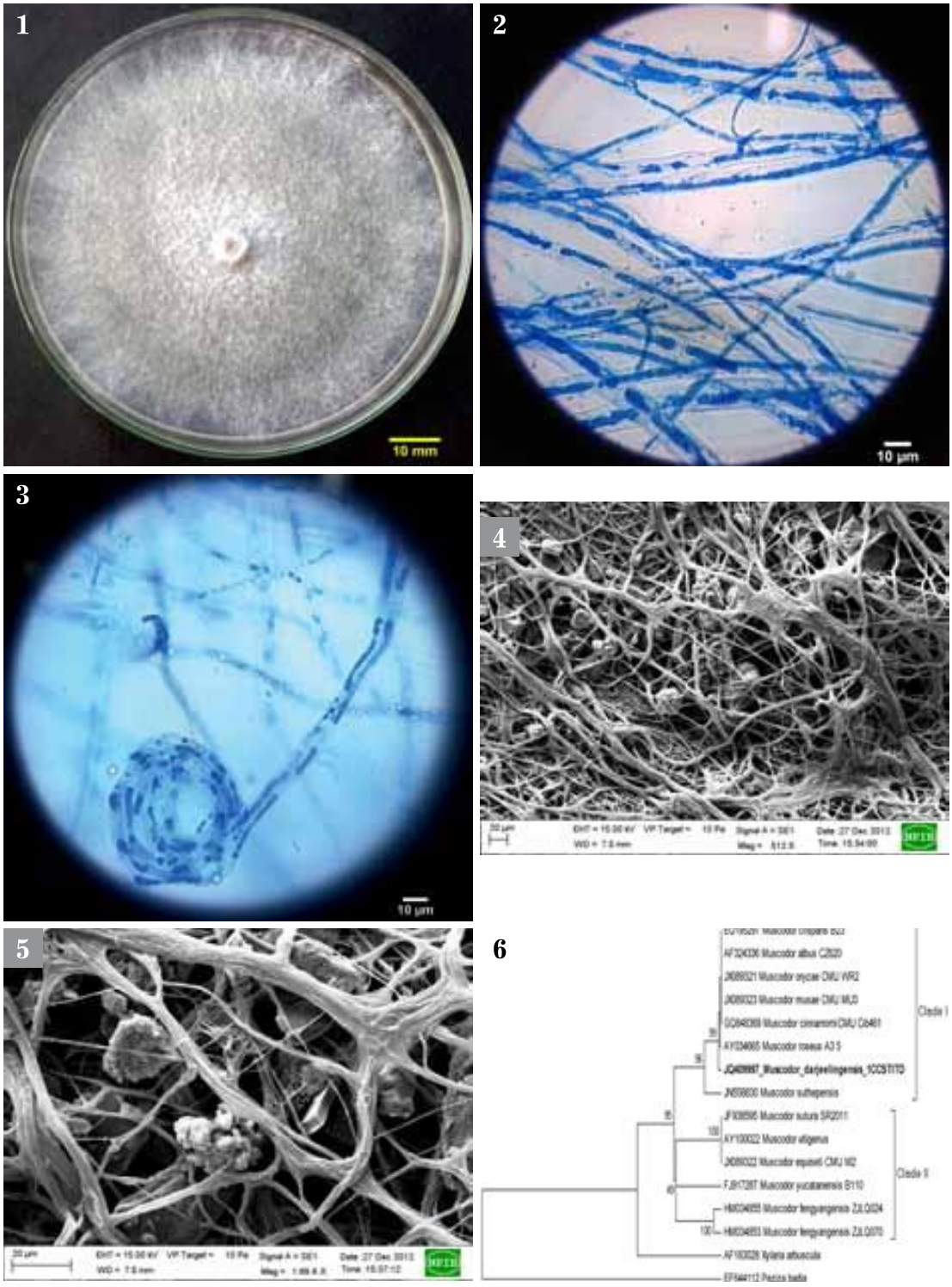

Figs. 1–5. Morphological features of *Muscodor darjeelingensis*. Strain #1 CCSTITD after seven days of growth. **1.** Culture characteristics on PDA. **2.** Hyphae stained with lactophenol cotton blue on CDA. **3.** Hyphae forming coils on SNA. **4–5.** SEM of the mycelial arrangement and of cauliflower-like structures.

Fig. 6. Neighbour-joining tree based on ITS1-5.8S-ITS2 region; optimal tree with sum of branch length = 0.685; bootstrap support values (1000 replicates) given at the nodes.

ymorphic or segregating sites (η), nucleotide diversity (π) and number of haplotypes of ITS region are shown in Tab. 1. Fu & Li's (1993) D* and F* statistics, and Tajimas test (Tajima 1989) revealed that the ITS region locus evolved neutral and was thus suitable for the phylogenetic analysis. Besides grouping all the *Muscodor* species into eight haplotypes, this locus showed 28 % of nucleotide variation which was quite higher than 2.7 % as observed in five strains of *Muscodor fengyangensis* (Zhang *et al.* 2010) and was also above the range (>3 %) for intra-specific variation (Nilsson *et al.* 2008).

Pair-wise distance proportion of nucleotide sites of the ITS region sequence comparisons between all the known species of *Muscodor* and *Muscodor darjeelingensis* (Tab. 2) exhibited concordance to the phylogenetic as well as DNA polymorphism data thereby indicating the novelty of *M. darjeelingensis*.

Tab. 1. Nucleotide properties of the ITS region of the *Muscodor darjeelingensis*

Locus	ITS1-5.8S-ITS2	
No. of sites	534	
No. of variable or polymorphic sites (η)	150	
No. of haplotypes	8	
Haplotype	Hap_1: 5	[JX089323 (*M. musae*), JX089321 (*M. oryzae*), GQ848369 (*M. cinnamomi*), EU195297 (*M. crispans*), AF324336 (*M. albus* cz620)]
	Hap_2: 3	[JX089322 (*M. equiseti*), JF938595 (*M. sutura*), AY100022 (*M. vitigenus)*]
	Hap_3: 1	[JN558830 (*M. suthepensis*)]
	Hap_4: 1	[HM034855 (*M. fengyangensis* ZJLQ024)]
	Hap_5: 1	[HM034853 (*M. fengyangensis* ZJLQ070)]
	Hap_6: 1	[FJ917287 (*M. yucatanensis*)]
	Hap_7: 1	[AY034665 (*M. roseus*)]
	Hap_8: 1	[JQ409997 (*M. darjeelingensis*)]
Haplotype diversity	0.892±0.063	
Nucleotide diversity (π)	0.08254	
Tejima's D	Not significant	
Fu & Li's D*	Not significant	
Fu & Li's F*	Not significant	

Volatile analysis of *Muscodor darjeelingensis*

Muscodor darjeelingensis produced a blend of 27 volatile compounds which were tentatively identified by comparing the GC/MS spectra with the NIST database (Tab. 3). The most abundant volatile was 2,6-bis(1,1-dimethylethyl)-4-(1-oxopropyl) phenol. Other important volatiles produced were 1,6-dioxacyclododecane-7,12-dione, 3,7-octadien-2-ol, 2,6-dimethyl. It also produces some unknown volatile compounds which could not be identified with the NIST data. *Muscodor darjeelingensis* has a unique gas chemistry completely different from the other *Muscodor* species which predominantly produce propanoic acid, methyl esters, azuelene, naphthalene deriva-

Tab. 2. *p*-Distance of nucleotide sites among the ITS sequences compared between *Muscodor darjeelingensis* and 12 species of *Muscodor*

	1	2	3	4	5	6	7	8	9	10	11	12	13	14	15
JQ409997(1)															
JX089323 (2)	0.004														
JX089322 (3)	0.071	0.062													
JX089321 (4)	0.004	0.000	0.062												
JN558830 (5)	0.038	0.031	0.067	0.031											
JF938595 (6)	0.071	0.062	0.000	0.062	0.067										
HM034855 (7)	0.173	0.161	0.125	0.161	0.169	0.125									
HM034853 (8)	0.164	0.152	0.110	0.152	0.160	0.110	0.014								
GQ848369 (9)	0.004	0.000	0.062	0.000	0.031	0.062	0.161	0.152							
FJ917287 (10)	0.071	0.062	0.036	0.062	0.059	0.036	0.107	0.093	0.062						
EU195297 (11)	0.004	0.000	0.062	0.000	0.031	0.062	0.161	0.152	0.000	0.062					
AY100022 (12)	0.071	0.062	0.000	0.062	0.067	0.000	0.125	0.110	0.062	0.036	0.062				
AY034665 (13)	0.007	0.002	0.065	0.002	0.039	0.065	0.164	0.156	0.002	0.065	0.002	0.065			
AF324336(14)	0.004	0.000	0.062	0.000	0.031	0.062	0.161	0.152	0.000	0.062	0.000	0.062	0.002		
EF644112 (15)	0.597	0.602	0.603	0.602	0.585	0.603	0.697	0.682	0.602	0.575	0.062	0.603	0.598	0.602	
AF163028 (16)	0.155	0.169	0.198	0.169	0.161	0.198	0.212	0.201	0.168	0.189	0.169	0.198	0.173	0.169	0.562

Tab. 3. Composition of the volatiles produced by *Muscodor darjeelingensis* after seven days of incubation at 24±2 °C on potato dextrose agar (PDA) entrapped using a solid-phase micro-extraction (SPME) fibre and GC/MS analysis

Retention time	Name of compound	Quality	% Area of peak	Molecular formula	Mass (Da)
2.034	1H-Benzimidazol-5-amine, 2-methyl	71	1.51	$C_8H_9N_3$	147
2.649	3,7-Octadien-2-ol, 2,6-dimethyl	81	5.23	$C_{10}H_{18}O$	154
2.817	Unknown	61	0.29		
3.185	2-furanmethanol,5-ethenyltetrahydro-.alpha.,.alpha.,5-trimethyl-, trans	86	0.11	$C_{10}H_{18}O_2$	170
3.528	2,3,5,8-tetramethyldecane	86	0.32	$C_{14}H_{30}$	198
3.996	2-Cyclohexen-1-one,3,5.5-methyl-; Seudenone	87	1.21	$C_7H_{10}O$	110
4.266	Acetic acid, 2-ethylhexyl ester	90	0.26	$C_{10}H_{20}O_2$	172
5.868	Unknown				
5.967	2-Acetoxytridecane	85	0.83	$C_{15}H_{30}O_2$	242
11.317	2,5-cyclohexadiene-1,4-dione,2,6-bis(1,1-dimethylethyl)-	88	0.90	$C_{14}H_{20}O_2$	220
11.455	Beta.-aminoaethyl-morpholin	92	2.35	$C_6H_{14}N_{2O}$	130
12.217	Bis(2-ethylhexyl) ether	80	0.11	$C_{16}H_{34}O$	242
12.352	Acorenone	73	0.18	$C_{15}H_{24}O$	220
14.219	Pentanoic acid, 2,2,4-trimethyl-3-carboxyisopropyl, isobutyl ester	79	0.09	$C_{16}H_{30}O_4$	286
14.292	Phenol, 2,4,6-tris(1,1-dimethylethyl)	72	0.20	$C_{18}H_{30}O$	262
15.044	2,6-Bis(1,1-dimethylethyl)-4-(1-oxopropyl)phenol	91	6.11	$C_{17}H_{26}O_2$	262
15.293	1,6-Dioxacyclododecane-7,12-dione	78	5.90	$C_{10}H_{16}O_4$	200
16.129	Unknown	67	0.06	$C_{15}H_{24}O_2$	236
16.286	Unknown	64	4.33	$C_{14}H_{22}O_2$	222
18.275	Phosphorin, 2,4,6-tris(1,1-dimethylethyl)	69	2.31	$C_{17}H_{29}P$	264
18.571	Benzene, Hexaethyl	72	1.91	$C_{18}H_{30}$	246
19.156	Phenol, 2,4,6-tris(1,1-dimethylethyl)-	74	0.41	$C_{18}H_{30}O$	262
20.659	4-octadecylmorpholine	94	6.29	$C_{22}H_{45}NO$	339
24.942	Unknown	45	0.07		
28.435	6-Undecylamine	88	0.22	$C_{11}H_{25}N$	171
40.600	Unknown	62	0.41		
42.529	Oleic Acid, Propyl Ester	74	0.93	$C_{21}H_{40}O_2$	324

tives and thujopsene. *Muscodor darjeelingensis* produces both aliphatic and aromatic heterocyclic compounds which predominantly belong to alcohols, acids, esters, ketones and amines. It also produces phosphorine which is known for its antimicrobial potential.

Bioassay of VOCs produced by *Muscodor darjeelingensis*

The VOCs produced by *M. darjeelingensis* do not show a killing effect but an inhibitory effect on the tested spectrum of bacteria, yeast and fungi. Only 56 % of the test panel microbes exhibited a retarded growth pattern when exposed to the VOC's. After 72 hours of exposure of the five days old culture, VOCs inhibited the growth of *Lasiodiplodia theobromae, Alternaria alternata, Rhizoctonia solani, Cercospora beticola* and *Penicillium chrysogenum* by 50–70 % while 30–40 % reduction was observed in *Arthrinium phaeospermum, Talaromyces marneffei, Colletotrichum gloeosporioides* and *Botrytis cinerea*. *Muscodor albus* was resistant to the VOCs produced by *M. darjeelingensis*. The pathogenic yeasts *Candida glabrata*, *C. vishvanathi*, *C. albicans* and a bacterial isolate (*Pseudomonas aeruginosa* MTCC 3541) were significantly inhibited when exposed to VOCs. *Staphylococcus epidermidis* exhibited partial and *Escherichia coli* (MTCC 1032) complete resistance against the VOCs (Tab. 4).

Tab. 4. Antimicrobial activity of volatile organic compounds produced by *M. darjeelingensis* after 72 h of exposure

Species name	Growth inhibition (%)
Fungi	
Alternaria alternata	61.36
Arthrinium phaeospermum	31.70
Aspergillus flavus	26.56
Aspergillus niger	24.69
Bionectria ochroleuca	11
Botrytis cinerea MTCC 359	30.49
Cercospora beticola	57.57
Colletotrichum gloeosporioides MTCC 9623	40.9
Fusarium solani	41.11
Fusarium oxysporum	17.3
Lasiodiplodia theobromae	70.83
Muscodor albus cz620	0
Penicillium chrysogenum	48.89
Phomopsis theiocola MTCC 373	19.23
Rhizoctonia solani MTCC 4634	32.22
Talaromyces marneffei	42.5
Candida glabrata MTCC 3019	++
Candida albicans MTCC 183	++
Candida albicans MTCC 854	++
Candida viswanathii MTCC 1629	++
Bacteria	
Escherichia coli MTCC 1302	-
Pseudomonas aeruginosa MTCC 3541	+++
Pseudomonas aeruginosa MTCC 647	+
Staphylococcus epidermidis MTCC 2639	+

+ Sign indicates the severity of inhibition

Acknowledgements

We thank the Department of Biotechnology (National Biodiversity Development Board) for sponsoring the project no. BT/PR/10083/NDB/52/95/2007. We acknowledge Dr. Gary Strobel, MSU-Bozeman, USA, for providing *M. albus* cz620 type strain, plant pathogenic fungi, and for constructive discussions. We also gratefully acknowledge the help of Dr. Naresh M. Meshram and Ms. Salam Rita Devi, Division of Entomology, IARI, PUSA, New Delhi for SEM analysis and Shri Ajay Kumar from ARIF, JNU, New Delhi, for GC/MS analysis.

References

Atmosukarto I., Castillo U., Hess W. M., Sears J., Strobel G. (2005) Isolation and characterization of *Muscodor albus* I-41.3s, a volatile antibiotic producing fungus. *Plant Science* **169**: 854–861.

Banerjee D., Pandey A., Jana M., Strobel, G. (2013) *Muscodor albus* MOW 12 an endophyte of *Piper nigrum* L. (Piperaceae) collected from North East India produces volatile antimicrobials. *Indian Journal of Microbiology* DOI 10.1007/s12088-013-0400-5.

Ezra D., Hess W. M., Strobel G. A. (2004) New endophytic isolates of *Muscodor albus*, a volatile antibiotic-producing fungus. *Microbiology* **12**: 4023–4031.

Ezra D., Skovorodnikova J., Kroitor-Keren T., Denisov Y., Liarzi O. (2009) Development of methods for detection and *Agrobacterium*-mediated transformation of the sterile, endophytic fungus *Muscodor albus*. *Biocontrol Science and Technology* **20**: 83–97.

Fu Y. X., Li W. H. (1993) Statistical tests of neutrality of mutations. *Genetics* **133**: 693–709.

Guo L. D., Hyde K. D., Liew E. C. Y. (1998) A method to promote sporulation in palm endophytic fungi. *Fungal Diversity* **1**: 109–113.

Kudalkar P., Strobel G., Riyaz-Ul-Hasan S., Geary G., Sears J. (2012) *Muscodor sutura*, a novel endophytic fungus with volatile antibiotic activities. *Mycoscience* **53**: 319–325.

Librado P., Rozas J. (2009) DnaSP v5: a software for comprehensive analysis of DNA polymorphism data. *Bioinformatics* **25**: 1451–1452.

Mitchell A., Strobel G., Hess W., Vargas P., Ezra D. (2008) *Muscodor crispans*, a novel endophyte from *Ananas ananassoides* in the Bolivian Amazon. *Fungal Diversity* **31**: 37–43.

Mitchell A. M., Strobel G. A., Moore E., Robinson R., Sears J. (2010) Volatile antimicrobials from *Muscodor crispans*, a novel endophytic fungus. *Microbiology* **156**: 270–277.

Nilsson R. H., Kristiansson E., Ryberg M., Hallenberg N., Larsson K. H. (2008) Intraspecific ITS variability in the kingdom fungi as expressed in the international sequence databases and its implications for molecular species identification. *Evolutionary Bioinformatics* **4**: 193–201.

Saitou N., Nei M. (1987) The neighbor-joining method: A new method for reconstructing phylogenetic trees. *Molecular Biology Evolution* **4**: 406–425.

Sopalun K., Strobel G. A., Hess W. M., Worapong J. (2003) A record of *Muscodor albus*, an endophyte from *Myristica fragrans*, in Thailand. *Mycotaxon* **88**: 239–247.

Strobel G. A., Dirske E., Sears J., Markworth C. (2001) Volatile antimicrobials from *Muscodor albus*, a novel endophytic fungus. *Microbiology* **147**: 2943–295.

Strobel G. (2012) *Muscodor albus* – the anatomy of an important biological discovery. *Microbiology today* May 108–111.

Strobel G. A., Katreena K., Hess W. M., Sears J., Ezra D., Vargas P. N. (2007) *Muscodor albus* E-6, an endophyte of *Guazuma ulmifolia* making volatile antibiotics: isolation, characterization and experimental establishment in host plant. *Microbiology* **153**: 2613–2620.

Suwannarach N., Bussaban B., Hyde K. D., Lumyong S. (2010) *Muscodor cinnamomi*, a new endophytic species from *Cinnamomum bejolghota*. *Mycotaxon* **114**: 15–23.

Suwannarach N., Kumla J., Bussaban B., Hyde K. D., Matsui K., Lumyong S. (2013) Molecular and morphological evidence support four new species in the genus *Muscodor* from northern Thailand. *Annuals of Microbiology*. DOI 10.1007/s13213-012-0593-6.

Tajima F. (1989) Statistical method for testing the neutral mutation hypothesis by DNA polymorphism. *Genetics* **123**: 585–595.

Tamura K., Nei M. (1993) Estimation of the number of nucleotide substitutions in the control region of mitochondrial DNA in humans and chimpanzees. *Molecular Biology and Evolution* **10**: 512–526.

Tamura K., Peterson D., Peterson N., Stecher G., Nei M., Kumar S. (2011) MEGA5: molecular evolutionary genetics analysis using Maximum Likelihood, Evolutionary Distance, and Maximum Parsimony methods. *Molecular Biology and Evolution* **28**(10): 2731–2739.

Zhang H. W., Song Y. C., Tan R. X. (2006) Biology and chemistry of endophytes. *Natural Product Reports* **23**: 753–771.

Zhang C. L., Wang G. P., Mao L. J., Komon-Zelazowska M., Yuan Z. L., Lin F. C., Druzhinina I. S., Kubicek C. P (2010) , *Muscodor fengyangensis* sp. nov. from South East China: morphology, physiology and production of volatile compounds. *Fungal Biology* **114**(10): 797–808.

(Manuscript accepted 14 October 2013; Corresponding Editor: I. Krisai-Greilhuber)

Ann Microbiol
DOI 10.1007/s13213-014-0834-y

ORIGINAL ARTICLE

Muscodor tigerii sp. nov.-Volatile antibiotic producing endophytic fungus from the Northeastern Himalayas

Sanjai Saxena · Vineet Meshram · Neha Kapoor

Received: 22 August 2013 / Accepted: 3 February 2014

Abstract Genus *Muscodor* came into existence with the discovery of *Muscodor albus*, a sterile endophytic fungus that produces a medley of volatile organic moieties possessing strong antimicrobial activity. The current paper reports *Muscodor tigerii* as a novel endophytic fungus from the stem internal tissue of *Cinnamomum camphora* growing in the Tiger Hill area of Darjeeling, West Bengal, India. *M. tigerii* exhibited distinct morphological, molecular and physiological features than previously reported *Muscodor* species. The fungus possesses all the morphological features described till date in genus *Muscodor* making it remarkably unique. The strong fruity smell of the fungus is attributed to 22 volatile organic compounds (VOCs), predominantly 4-Octadecylmorpholine, 1-Tetradecanamine,N,N-dimethyl and 1,2-Benzenedicarboxylic acid, mono(2-ethylhexyl) ester. The in vitro VOC stress assay completely suppressed the growth of *Alternaria alternata* and *Cercospora beticola* while growth of other fungal species was inhibited in a range of 10 %-70 %. The growth of *Candida albicans* in the presence of VOC was reduced by 50 %-65 % while in bacteria 50 %-80 % reduction in growth was observed. Thus, *M. tigerii* stands as a potential candidate to be further developed into a biocontrol agent.

Keywords Anamorphic fungus · Tiger hills · *Cinnamomum camphora* · ITS-rDNA

S. Saxena (✉) · V. Meshram · N. Kapoor
Department of Biotechnology, Thapar University, Patiala, Punjab, India 147001
e-mail: sanjaibiotech@yahoo.com

S. Saxena
e-mail: ssaxena@thapar.edu

Published online: 02 March 2014

Introduction

Endophytes comprise of an extremely diverse group of microorganisms that are ubiquitous in plants and maintain a symptomless and unobtrusive union with their hosts for at least a period of their life cycle (Stone et al. 2000; Kusari et al. 2012). Endophytes play an important role in plant symbiosis, rescuing their host from microbial infiltration and stressful conditions (Shipunov et al. 2008). The genetic recombination of the endophytes with the host plant enables them to mimic the biological properties of their host and produce analogous bioactive metabolites (Zhao et al. 2011; Kusari et al. 2012). Thus, endophytic microorganisms are considered as a lucrative source of bioactive metabolites with promising applications in the agrochemical and pharmaceutical industries (Strobel and Daisy 2003; Kudalkar et al. 2012).

Muscodor is a genus of sterile endophytic fungi that has been isolated from tropical rainforest areas of Australia, Central and South America and South-east Asia (Zhang et al. 2010; Suwannarach et al. 2013). To date, twelve species have been described in this genus based on ITS sequencing and volatile gas composition analysis and hyphal structures using a scanning electron microscope (SEM) (Suwannarach et al. 2013). The fungus has a remarkable ability to produce volatile antibiotics that are lethal against plant and human pathogens, nematodes and insects (Strobel 2006). Hence, *Muscodor* spp. stands out as a potential candidate as a biocontrol agent in post harvest technology with possible replacement of hazardous chemical fumigants like methyl bromide and; therefore, it is considered to be a promising source of eco-friendly antimicrobial compounds thus exhibiting mycofumigation potential (Strobel et al. 2001; Mercier et al. 2007).

The Northeastern Himalayas are located at the junction of Indo-Burma biodiversity hotspots. The hotspots cover the Indian states of Arunachal Pradesh, Sikkim and the Darjeeling district of West Bengal (Mcneely et al. 1990). The

Northeastern Himalayas harbour a rich diversity of over 7,500 plant species out of which 1,500 are endemic (Chatterjee et al. 2006). *Cinnamomum camphora* is an evergreen plant native to India, China, Taiwan and Japan. The medicinial properties of the camphor plant have been explored since antiquity as a panacea for diarrhoea, muscular spasm, bronchitis, rheumatism, etc. Camphor oil is used as an antiseptic, anti-inflammatory, diuretic, rubefacient, odontalgic, laxative and as well as an insecticide (Chelliah 2008). It also inhibits the production of aflatoxin B1 produced by *Aspergillus flavus* (Singh et al. 2008). Microbial symbionts of *Cinnamomum camphora* have been poorly studied. The plant harbours *Aspergillus fumigatus, Alternaria cineraria, Curvularia lunata, Nigrospora oryzae, Periconia* sp. *Pestalotiopsis* sp. *Phomopsis* sp. and several sterile fungi as endophytes (Kharwar et al. 2012). Another astonishing feature of the camphor plant is the use of its endophytic fungal wealth like *Colletotrichum, Fusarium* and *Aspergillus clavatus* for synthesis of gold and silver nanoparticles (Verma et al. 2010). However, the current study reports *Muscodor* species #2 CCSTITD from the stem internal tissue of the camphor plant growing in the Tiger Hill area of Darjeeling, West Bengal, India. The endophytic fungus produces a unique set of volatile compounds, which possess antimicrobial activity and could be further used to identify the particular *Muscodor* species. Morphological, molecular and chemical characteristics of #2 CCSTITD distinguishes it from earlier reported *Muscodor* species. Based on its distinctive features, #2 CCSTITD is introduced as a new species of *Muscodor* genus for which the name *Muscodor tigerii* is proposed.

Materials and methods

Fungal isolation and preservation

Healthy and mature plant parts (leaf and stems) of *Cinnamomum camphora* were collected from the Tiger hill area, Darjeeling, West Bengal during March 2011. Plant samples were kept in sterile packets and stored at 4 °C till further use. The fungal isolation was done using *Muscodor albus* CZ620 as a screening tool as reported by Ezra et al. (2004). Briefly, Potato Dextrose Agar (PDA) was poured into one quadrant of the four sectioned commercially available Petri plates. An actively growing agar plug of *M. albus* CZ 620 was placed over the PDA medium while other quadrants of the Petriplates contained water agar (WA). The plates were then incubated at 24 °C for four days for Volatile Organic Compounds (VOCs) production by *M. albus*. The plant samples were washed under running tap water; air dried and cut into small segments of 5 mm, then the plant segments were surface sterilized with 75 % ethanol for 30 s, 2 % sodium hypochlorite for 3 min and 95 % ethanol under a laminar flow hood. The sterile plant segments were placed in the other quadrants containing WA thereby exposing the plant segments to VOC's of *M. albus* arising in the plates. The fungi emerging out of the host tissue was aseptically subcultured onto a fresh PDA plate so as to obtain pure isolates which were further preserved on PDA slants supplemented with 10 % glycerol (Ezra et al 2004; Strobel et al. 2007; Mitchell et al. 2008).

Morphotaxonomy

Morphological and microscopic characters of *M. tigerii* were studied by growing the fungus on four different media comprising of PDA, CDA (Czapek Dox Agar), WA and SNA (Synthetischer Nahrstoffarmer agar). Morphotaxonomic studies of the endophytic fungal isolate was done by mounting the culture in lactophenol cotton blue and then observing under a Nikon Stereozoom microscope (Nikon SMZ 745 T) coupled with NIS element D 3.2 software and a Nikon Eclipse Compound microscope (E100). Micrometry was done using ocular

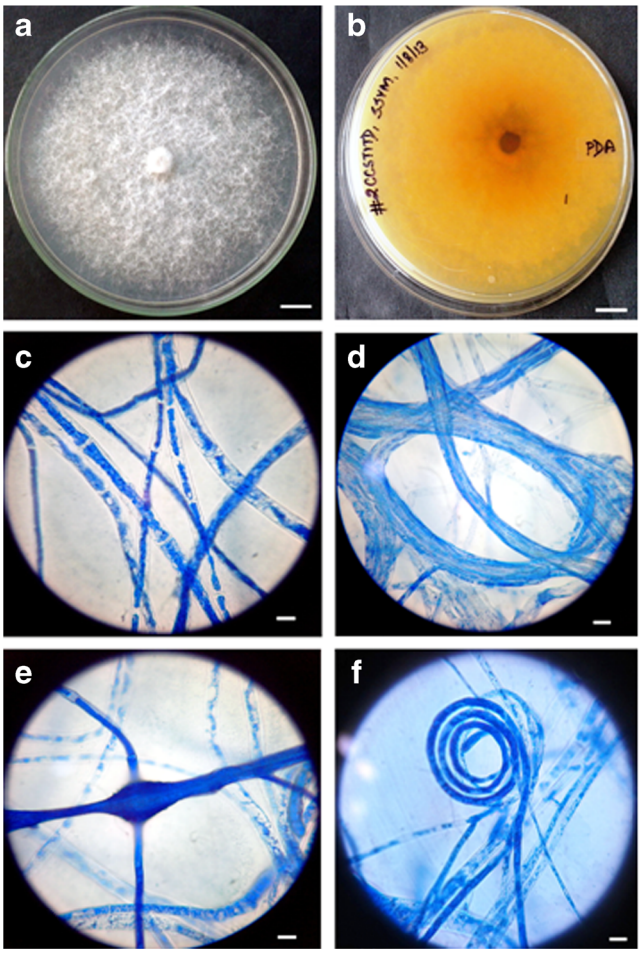

Plate 1 Morphological traits of *Muscodor tigerii* (#2 CCSTITD) over PDA. (**a**) Morphological features, front view (**b**) Brown colored pigment production, reverse view. (**c**) Sterile hyphae (**d**) Ropy mycelium. (**e**) Swollen hyphae (**f**) Coil formation of fungal hyphae. Bar 1(**a**) and 1(**b**) = 10mm, 1(**c**)-1(**f**) = 10μm

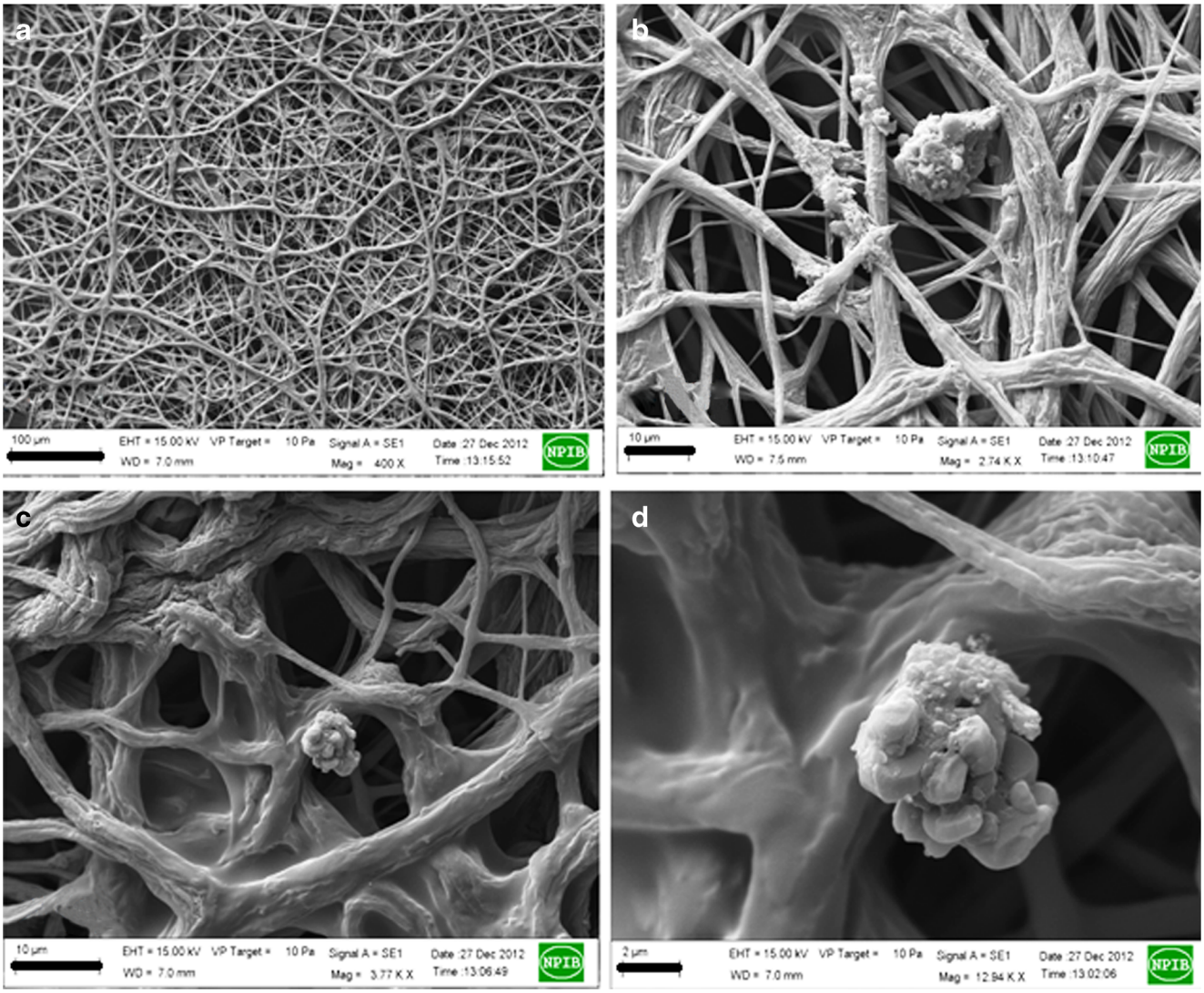

Plate 2 Scanning electron micrograph of 10-day old *Muscodor tigerii* (#2 CCSTITD) including (**a**) Sterile mycelial web, bar- 100 µm (**b**) right angle branching, bar 10 µm (**c**) ropy mycelium with nondescript hyphal projection, Bar=10 µm (**d**) Close view of nondescript hyphal projections. Bar=2µm

and stage scale and further confirmed by Image J software with at least 30 observations per structure. The colony appearance, color, colony growth rate, pigment and VOCs production along with its microscopic structures like hyphal characteristics and other cellular bodies were minutely observed and recorded (Guo et al. 1998; Mitchell et al. 2008).

DNA Extraction, Sequence Assembly and Phylogenetic Analysis

Total fungal genomic DNA isolation was carried out with the Wizard® Genomic DNA purification kit (Promega, USA) as per instructions of the manufacturer. The ITS1-5.8S-ITS2 region was amplified using the *M. albus* specific primer pair as described by Ezra et al. (2010). The reaction mixture composition for the amplification of the ITS region comprised of 1 µl of extracted genomic DNA, 25 mM $MgCl_2$, 2.5 mM dNTP, 10 pmol/µl of each primer, 1.5 U of Taq DNA polymerase (Bangalore Genei) in 10X Taq buffer of the 25 µl reaction volume. Thermal cycling conditions used were previously described by Ezra et al. (2010). The PCR product of approximately 400-500 bp was purified by the Wizard® SV Gel and PCR clean up system kit (Promega, USA). The purified amplicon was sequenced by Xcleris Genomics, Xcleris labs, Gujarat.

The chromatograms of the isolate *M. tigerii* was edited and aligned in Sequencher, Version 5 (Gene Codes, Ann, Arbor, MI). The homology of the *M. tigerii* was ascertained by subjecting the final sequence of the isolate to a sequence similarity search using BLAST against the database maintained by NCBI. Sequences showing the highest sequence similarity with the sequence of *M. tigerii* were aligned using MUSCLE in MEGA5.2 (Tamura et al. 2011). Distance based analysis of the ITS region alignment was done

Table 1 Synopsis of the advanced BLAST search homology analysis of ITS-5.8S ribosomal gene sequence of *Muscodor tigerii*

Species	GenBank Acc. No.	Query Coveage	Sequence similarity
Muscodor cinnamomi CMU Cib-461	GQ848369	99 %	98 %
Muscodor crispans B23	EU195297	99 %	98 %
Muscodor albus CZ620	AF324336	99 %	98 %
Muscodor roseus A3-5	AY034665	99 %	98 %
Muscodor sp. AB2011	JN426991	99 %	98 %
Muscodor sp. VC01	KF229754	99 %	98 %
Xylariaceae sp. M26	JX298899	99 %	98 %
Sordariomycetes sp. FL0969	JQ760598	99 %	98 %
Sordariomycetes sp. FL0502	JQ760221	99 %	98 %
Muscodor suthepensis	JN558830	99 %	90 %
Muscodor oryzae	JX089321	99 %	98 %
Muscodor musae	JX089323	99 %	98 %
Muscodor equiseti	JX089322	91 %	93 %
Muscodor sutura	JF938595	91 %	93 %
Muscodor vitigenus	AY100022	91 %	93 %
Muscodor yucatanensis	FJ917287	90 %	86 %
Muscodor fengyangensis ZJLQ024	HM034855	81 %	90 %

by the Neighbor-joining method (Saitou and Nei 1987) using the p-distance method (Nei and Kumar 2000) of nucleotide substitution, and the rate variation among sites was modeled with a gamma distribution (shape parameter= 5). Gaps were considered as missing data. One thousand bootstrap replicates were taken into account to infer the consensus tree for the representation of evolutionary relationship. The DNA sequence obtained in the present study has been deposited in the GenBank under accession number JQ409998.

Computation of genetic distances

The genetic relatedness of *Muscodor tigerii* with already reported species of *Muscodor* was established by determination of pair wise distances implemented in MEGA5.2. Genetic distance is the proportion (p) of nucleotide sites at which two sequences being compared are different from each other. It is obtained by dividing the number of nucleotide differences by the total number of nucleotides compared. Gaps were coded as missing characters, and Maximum Composite Likelihood was chosen as a model for the analysis.

The levels of DNA polymorphism such as number of variable sites (η), haplotypes, haplotype diversity, nucleotide diversity (π), evolutionary models were deduced with DNASp5 (Librado and Rozas 2009).

Scanning electron microscopy

Agar plugs of 10 day old fungal samples were placed in 2.5 % glutaraldehyde in 0.1 M phosphate buffer (pH 7.2) overnight at 4 °C. The next day they were washed twice with 0.1 M phosphate buffer for 10 min each. Subsequently, the samples were slowly dehydrated using acetone graded series (10 min.

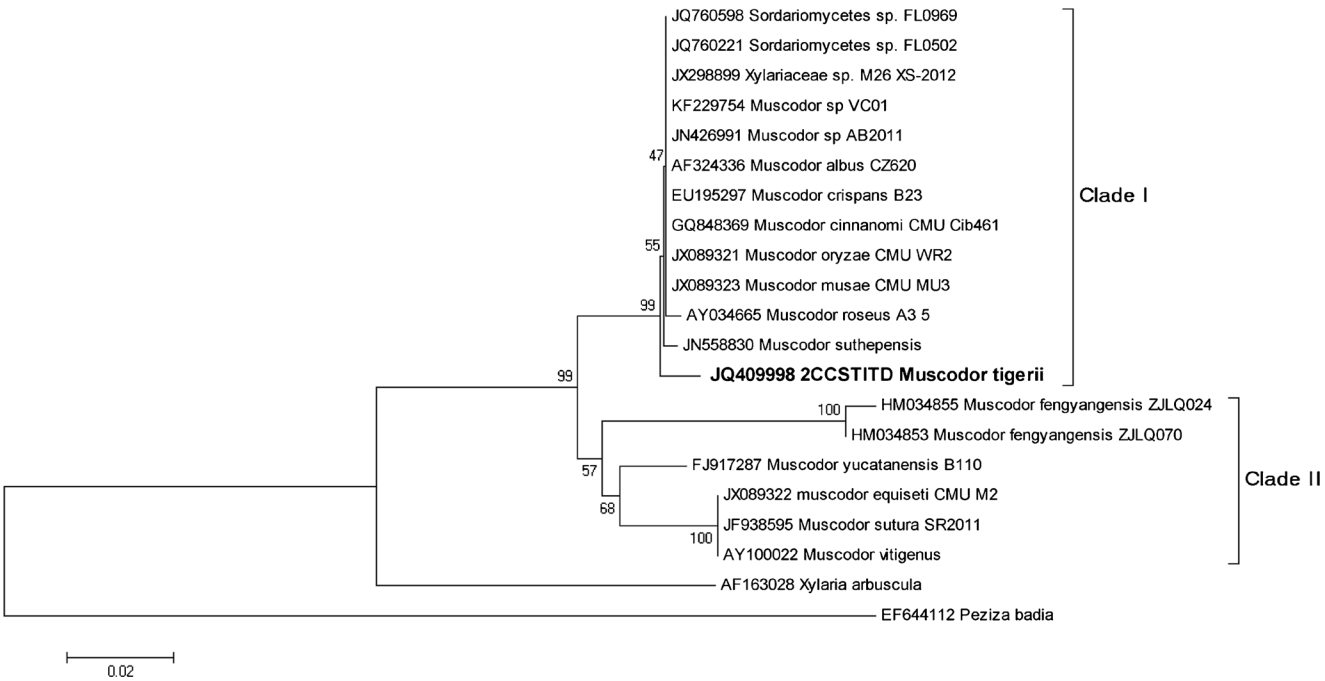

Fig. 1 The Neighbor-joining tree based on the ITS1-5.8S-ITS2 region. The optimal tree with the sum of branch length=0. 452 is shown. The percentage of replicate trees in which the associated taxa clustered together in the bootstrap test (1,000 replicates)

Table 2 Nucleotide properties of the ITS region of the *Muscodor tigerii*

Locus	ITS1-5.8S-ITS2
No. of sites	704
No. of variable or polymorphic sites (η)	139
No. of haplotypes	08
Haplotype	Hap_1:10 [JX089323 (*M. musae*), JX089321 (*M. oryzae*), GQ848369 (*M. cinnamomi*), EU195297 (*M. crispans*), AF324336 (*M. albus* CZ620), JN426991 (*Muscodor* sp. AB2011), KF229754 (*Muscodor* sp. VC-01), JX298899 (*Xylariaceae* sp. M26) JQ760598 (*Sordariomycetes* sp.), JQ760221 (*Sordariomycetes* sp. Isolate FL0502)]
	Hap_2:3 [JX089322 (*M. equiseti*), JF938595 (*M. sutura*), AY100022 (*M. vitigenus*)]
	Hap_3:1 [JN558830 (*M. suthepensis*)]
	Hap_4:1 [HM034855 (*M. fengyangenensis* ZJLQ024)]
	Hap_5:1 [HM034853 (*M. fengyangenensis* ZJLQ070)]
	Hap_6:1 [FJ917287 (M. *yucatanensis*)]
	Hap_7:1 [AY034665 (*M. roseus*)]
	Hap_8:1 [JQ409998 (*M. tigerii*)]
Haplotype diversity	0.771±0.092
Nucleotide diversity (π)	0.06222
Tejima's D	Not significant
Fu and Li's D*	Not significant
Fu and Li's F*	Not significant

each at 30, 40, 50, 60, 70, 80, 95 and 100 %). The samples were then brought to critical point drying and coated with Gold palladium using sputter coater. The images were then recorded in high vacuum mode using a Zeiss Evo40 scanning electron microscope between 400 X – 12.94 KX magnification at 15 kV EHT (Ezra et al. 2004; Kudalkar et al. 2012)

Volatile analysis of *Muscodor tigerii*

A solid phase microextraction (SPME) syringe having a stable flex fiber made up of 50/30 divinylbenzene/carboxen on polydimethylsiloxane (Supelco, Sigma Aldrich) was used to trap the VOCs produced by a 10 day old culture of *M. tigerii* following the method of Ezra et al. (2004). The fiber was exposed for 45 min by placing the SPME syringe through a small bore made using a sterile needle over the headspace of culture in the Petri dish. Subsequently the fiber was injected for 30 s in the Shimadzu QP 2010 plus gas chromatograph with thermal desorption system TD 20. An RTX column (diphenyl 95 %, dimethyl polysiloxane 5 %) with 30 m x 0.25 mm ID and 0.25 mm DF was used for separating of the fungal volatiles. The column was programmed at 100 °C for 2 min and the temperature was then raised to 250 °C for 2 min and then finally to 300 °C for 13 min. The carrier gas was helium and the initial column head pressure was 94.4 KPa. Data acquisition and processing was done on GCMS solution software. The compounds obtained after GC/MS analysis were then subtracted from the control plate consisting only PDA medium. The obtained compounds were then tentatively identified based on their high quality matching (above 70 % similarity) with the database of the National institute of Standard and Technology compounds (NIST05) and compared with all reported species of *Muscodor* to date (Ezra et al. 2004; Kudalkar et al. 2012)

Bioassay of VOC's produced by *M. tigerii*

Antimicrobial activity of the volatiles produced by *M. tigerii* were tested using dual culture volatile bioassay technique against a spectrum of pathogenic fungi, yeasts and bacteria. One half of the 90 mm plate was comprised of PDA whereas the remaining part consisted of PDA, Mueller Hinton Agar (MHA) and Yeast Extract Peptone Dextrose agar (YEPDA) for growing pathogenic fungi, bacteria and yeast cultures, respectively. Agar strips were removed to create compartments in the plate and thereby prohibiting the movement of any diffusible inhibitory compound from the *Muscodor* sp. to the test microorganism(s). One compartment of the plate was inoculated with an agar plug of actively growing *M. tigerii*. The plates were sealed and incubated at 24±2 °C for five days for VOC production. An array of twenty pathogenic microorganisms comprising of 13 fungi, four *Candida* and two bacterial strains

Table 3 p-Distance of nucleotide sites among the ITS sequences compared between *Muscodor tigerii*, *Sordariomycetes, Xylaria* and *Muscodor* spp

	1	2	3	4	5	6	7	8	9	10	11	12	13	14	15	16	17	18	19	20
JQ409998 (1)																				
AF324336 (2)	0.009																			
GQ848369 (3)	0.009	0.000																		
EU195297 (4)	0.009	0.000	0.000																	
JX089323 (5)	0.009	0.000	0.000	0.000																
JX089321 (6)	0.009	0.000	0.000	0.000	0.000															
JN426991 (7)	0.009	0.000	0.000	0.000	0.000	0.000														
KF229754 (8)	0.009	0.000	0.000	0.000	0.000	0.000	0.000													
JX298899 (9)	0.009	0.000	0.000	0.000	0.000	0.000	0.000	0.000												
JQ760598 (10)	0.009	0.000	0.000	0.000	0.000	0.000	0.000	0.000	0.000											
JQ760221 (11)	0.009	0.000	0.000	0.000	0.000	0.000	0.000	0.000	0.000	0.000										
AY034665 (12)	0.011	0.003	0.003	0.003	0.003	0.003	0.003	0.003	0.003	0.003	0.003									
JN558830 (13)	0.011	0.003	0.003	0.003	0.003	0.003	0.003	0.003	0.003	0.003	0.003	0.006								
FJ917287 (14)	0.048	0.038	0.038	0.038	0.038	0.038	0.038	0.038	0.038	0.038	0.038	0.041	0.041							
JF938595 (15)	0.055	0.045	0.045	0.045	0.045	0.045	0.045	0.045	0.045	0.045	0.045	0.048	0.048	0.032						
JX089322(16)	0.055	0.045	0.045	0.045	0.045	0.045	0.045	0.045	0.045	0.045	0.045	0.048	0.048	0.032	0.000					
AY100022 (17)	0.055	0.045	0.045	0.045	0.045	0.045	0.045	0.045	0.045	0.045	0.045	0.048	0.048	0.032	0.000	0.000				
HM034853 (18)	0.086	0.075	0.075	0.075	0.075	0.075	0.075	0.075	0.075	0.075	0.075	0.079	0.079	0.065	0.079	0.079	0.079			
HM034855 (19)	0.093	0.082	0.082	0.082	0.082	0.082	0.082	0.082	0.082	0.082	0.082	0.086	0.086	0.072	0.086	0.086	0.086	0.006		
AF163028 (20)	0.160	0.150	0.150	0.150	0.150	0.150	0.150	0.150	0.150	0.150	0.150	0.154	0.146	0.175	0.180	0.180	0.180	0.204	0.214	
EF644112 (21)	0.584	0.576	0.576	0.576	0.576	0.576	0.576	0.576	0.576	0.576	0.576	0.584	0.584	0.628	0.656	0.656	0.656	0.698	0.720	0.642

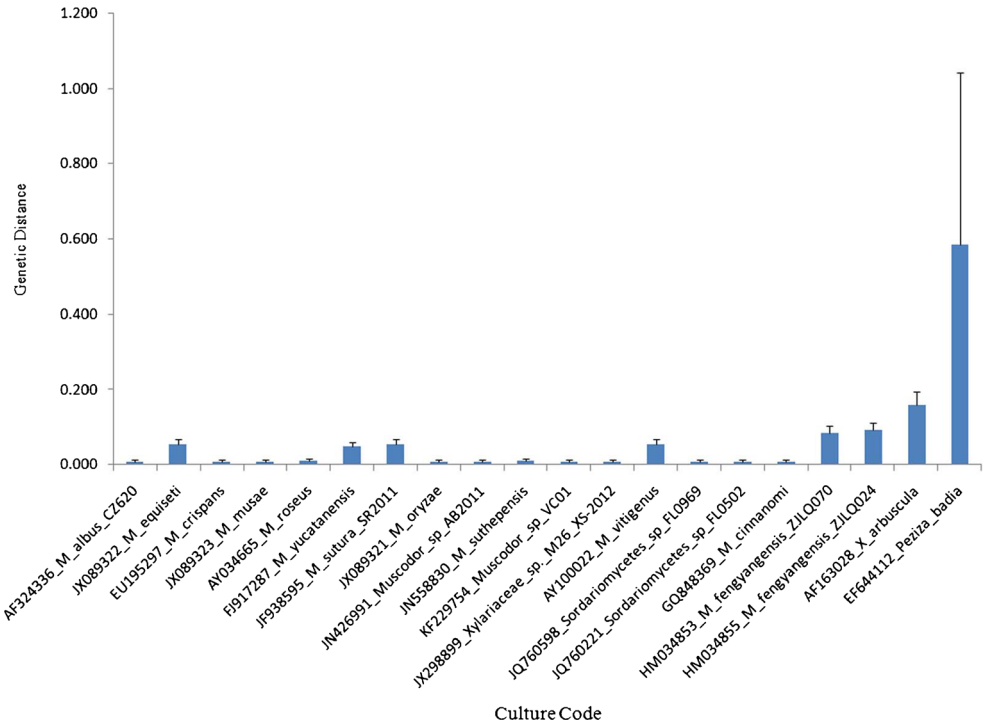

Fig. 2 Phylogenetic distance of *Muscodor tigerii* to congeneric species. Shown are p-distance values calculated by MEGA5.0

were tested in the study. *Muscodor albus* CZ 620 was used as a positive control. Individual test fungi were inoculated by placing a 3 mm plug of seven days old culture on the remaining compartments whereas bacteria and yeasts were tested by individual inoculation in other quadrants. Correspondingly, the control plates were comprised of only inoculated test bacteria or fungi and were devoid of isolated *M. tigerii* allowing it to grow normally. Antimicrobial action of VOCs was determined by monitoring the difference in growth of microorganisms in test and control plates (Mitchell et al. 2010; Suwannarach et al. 2013). All the tests were performed in triplicates and values calculated as mean±SD.

Results and Discussion

Taxonomy

Muscodor tigerii S. Saxena, Meshram & N. Kapoor, sp. nov. Plate 1 and 2

MycoBank no.:805271; GenBank no.: JQ 409998

Diagnosis: Differs from all other *Muscodor* species by its fast colony growth rate. Distinct from *M. fengyangensis*, *M. equiseti, M. musae, M. oryzae,* and *M. suthepensis* by presence of nondescript extracellular bodies. Varies from *M. cinnamomi*, *M. sutura*, *M. crispans*, *M. albus* and *M. vitigenus* by presence of swollen hyphae and coiling structures, respectively. It differs from *M. roseus* and *M. yucantanensis* by brown colored colonies.

Etymology: '*tigerii*' refers to the collection site Tiger hills, Darjeeling.

Holotype: India, West Bengal, Darjeeling, Tiger Hills, 27°13'-26°27'N 88°53'- 87°59' E, endophytic fungi from stem internal tissue of *Cinnamomum camphora*, 23 March 2011, leg. Sanjai Saxena (Holotype: CCSTITD #2; ex type culture: National Fungal Culture Collection of India, NFCCI- 3172)

Teleomorph: not observed

rDNA sequence ex-holotype: JQ409998

Latin description: Opponens ad tardus *Muscodor* crescentis species, hoc endophytic fungal dissociari crescit celeriter platam infra 7 dies Petri 90 mm super PDA et tenet medium in incubatis cum 24±2 ° C, 12 h photoperiod (Plate 1a,1b). Ad fungal coloniam floccosus, candidus coloris fusci quod vertitur post 15 diebus. Hyphis ramosis, septatis, qui generat, et (4.58)-7.8±1.9-(11.76) μm latae (Plate 1c). Hyphis [(9.8)-21.37±5.58-(26.54) μm] fuse densam ropy mycelium (Plate 1d). Quaedam sunt, quae etiam in crassis supra auctus (14.74)-36.84±10.86-(54.22) X (9.07)-25.32±11.28-(47.26) μm (Plate 1e). Et terminatur in quodam angulo orbis ramos ex hyphis quae (37.24)-43.85±9.4-(62.35) μm latae (Plate 1f). Fungus producit fruity odore, sed non parit aliquam fructificatio corpora probavimus in vitro sub conditionibus.

Description: Contrasting to the slow growing *Muscodor* species, this endophytic fungal isolate rapidly grows over PDA medium and covers 90 mm Petri plate within seven days when incubated at 24±2 °C with 12 h of photoperiod (Plate 1a,1b). The fungal colony was floccose, white colored which turns to brown after 15 days. It generates septate and branched hyphae which are (4.58)-7.8±1.9-(11.76) μm

Table 4 Composition of the volatiles produced by *Muscodor darjeelingensis* after seven days incubation at 24±2 °C on potato dextrose agar (PDA) entrapped using a solid-phase micro-extraction (SPME) fibre and GC/MS analysis

Retention time	Possible name	Relative %	Molecular Formula	Mass (Da)	SI
8.841	Morpholine, 3-methyl-2-phenyl	0.30	$C_{11}H_{15}NO$	177	81
12.323	Lilial	0.51	$C_{14}H_{20}O$	204	79
14.495	Unknown	0.16			64
14.750	Phenol,2,6-bis(1,1-dimethylethyl) -4-(1-methyl propyl)-	0.18	$C_{17}H_{26}O_2$	262	80
14.816	Unknown	3.11			62
15.543	4-Octadecylmorpholine	10.64	$C_{22}H_{45}NO$	339	86
15.812	Asarone	2.66	$C_{12}H_{16}O_3$	208	92
17.251	Unknown	0.19			62
17.822	Carotol	0.68	$C_{15}H_{26}O$	222	74
19.00	Phytol	1.74	$C_{20}H_{40}O$	296	84
19.658	1,2-Benzenedicarboxylic acid, bis(2-methylpropyl) ester	0.65	$C_{16}H_{22}O_4$	278	90
20.298	1-Tetradecanamine,N,N-dimethyl	8.32	$C_{16}H_{35}N$	241	97
20.583	Unknown	0.58			65
31.468	1,2-Benzenedicarboxylic acid, mono(2-ethylhexyl) ester	6.55	$C_{16}H_{22}O_4$	278	96
35.721	Squalene	2.24	$C_{30}H_{50}$	410	78
36.400	Geranyl linalool	2.17	$C_{20}H_{34}O$	290	77
36.648	Bisacodyl	1.64	$C_{22}H_{19}NO_4$	361	86
36.787	Unknown	0.44			44
38.140	Unknown	1.49		416	68
38.368	Cholest-5-en-3-ol (3.beta.)-	1.26	$C_{27}H_{46}O$	386	80
39.378	Campesterol	0.80	$C_{28}H_{48}O$	400	82
39.703	Stigmasterol	1.67	$C_{29}H_{48}O$	412	78

wide (Plate 1c). Hyphae [(9.8)-21.37±5.58 (26.54) μm] fuse to thick ropy mycelium (Plate 1d). Swollen hyphae are also present at some places which measures (14.74)-36.84± 10.86-(54.22) x (9.07)-25.32±11.28-(47.26) μm (Plate 1e). The hyphae branches at a certain angle and terminates into coils which are (37.24)-43.85±9.4-(62.35) μm wide (Plate 1f). The fungus produces a fruity smell but does not produce any fruiting bodies under tested in vitro conditions.

Growth rate and morphological characters varies when grown over different media. Over CDA and SNA, the isolate was floccose, moderately growing with mean colony size of 59 mm and 45 mm. The fungus produces brown color soluble pigment over CDA medium after 15 days of incubation. When grown over WA, the fungus forms hyaline colonies, which were slow growing with the mean colony diameter of 27 mm after seven days incubation. The fungal culture produces VOCs with a strong fruity smell only on PDA and CDA. Volatile production was comparably higher in PDA than from CDA. Microscopic studies reveal that hyphal fabrication is septate, branched at a right angle forming coiling structures either centrally or terminally. The average width of the hyphae on CDA, SNA and WA medium was (3.09)-5.02±1.17-(6.51) μm, (2.41)-3.73±0.92-(6.41) μm, and (2.18)-3.42± 1.01-(5.99) respectively, whereas the average diameter of the coils are 47.66±9.05 μm, 47.50±7.38 μm and 40.20± 11.61 μm, respectively.

Scanning electron microscopy

The scanning electron micrographs of *M. tigerii* exhibited the true features of *Muscodor* species forming long, sterile ropy mycelium that terminates into coils. The hyphae further fuse to form ropy mycelium. The isolate also produces nondescript extracellular bodies but did not produce any sporulating bodies (Plate 2).

Muscodor tigerii exhibited variation in morphology from the other type strains of *Muscodor. M. crispans* and *M. sutura* forms similar kind of structures but they are different in their mycelial arrangement whereas *M. crispans* forms a wavy hyphal mass and *M. sutura* displays a knitting pattern of mycelia. *M. roseus, M. cinnamomi, M. musae, M. oryzae* and *M. suthepensis* possess ropy mycelia with coils but lack cauliflower like structural bodies thereby differentiating it from *M. tigerii. M. yucatanensis* and *M. equiseti* shows ropy mycelia with swollen hyphae making it remarkably different from *M. tigerii. M. albus* and *M. vitigenus* exhibited straight hyphae without any coils or cauliflower bodies, thus, differentiating it from the *M. tigerii*.

Internal transcribed spacer (ITS)-based phylogenetic analysis of *M. tigerii*

The evolutionary relationship of the *M. tigerii* was established on the basis of ITS region sequence analysis. The sequence on subjecting to a BLAST similarity search showed 98 % sequence similarity with *M. cinnamomi* CMU Cib461 (Suwannarach et al. 2010), *M. crispans* B23 (Mitchell et al. 2008), and *M. albus* CZ620 (Strobel et al. 2001) suggesting that the isolate belongs to *Muscodor* lineage (Table 1). In addition to this, it also showed 93 % sequence similarity with *M. sutura* SR-2011, *M. vitigenus* and 86 % sequence identity with *M. yucatanensis* (Daisy et al. 2002).

The Neighbor-joining phylogram of ITS region depicted divergence of *Muscodor* sp. into two separate clades viz: Clade I and Clade II. Clade I clustered *M. cinnamomi*, 2 *Sordariomycetes* species, *Xylariaceae* sp. M26, *Muscodor* sp. AB-2011, *Muscodor* sp. VC-01, *M. albus* CZ620, *M. crispans* B23, *M. roseus, M. oryze, M. musae, M. suthepensis* and *M. tigerii* (#2CCSTITD) emerged as a basal sister to the rest of the members of clade I with a significant bootstrap support value. *M. yucatnensis, M. sutura, M. equiseti, M. vitigenus* and *M. fengyangensis* were grouped in Clade II with adequate branch support value. *Xylaria arbuscula* and *Peziza badia* was taken as an outgroup (Fig. 1).

DNA sequence polymorphism analysis can provide insights into the various significant evolutionary factors acting on the population and species and can be employed to compare alternative evolutionary relationships. The number of polymorphic or segregating sites (η), nucleotide diversity (π) and number of haplotypes of ITS region are shown in Table 2. Fu and Li's (1993) D* and F* statistics, and Tajimas test (Tajima 1989) revealed that ITS region locus evolved neutral and was, thus, suitable for the phylogenetic analysis.

Based on the genetic distance analysis of ITS region, it was evident that *M. tigerii* is different from already reported species of *Muscodor*. Concordant results of the phylogenetic and DNA polymorphism analysis confirmed *M.tigerii* to be a new species (Table 3, Fig. 2).

Volatile analysis of *M. tigerii*

Muscodor tigerii produced a mixture of 22 volatile compounds which were tentatively identified by comparing the GC/MS spectra in the NIST Database (Table 4). Of all the compounds produced, 4-Octadecylmorpholine was the most abundant covering 10.64 % of all the compounds present in the air space of the plate. Other important volatiles produced were 1-Tetradecanamine,N,N-dimethyl, 1,2-Benzenedicarboxylic acid, mono(2-ethylhexyl) ester, squalene and phytol. It also produces some unknown volatile moieties which could not be identified using the NIST database. The VOCs produced by the fungus were broadly categorized into three categories, steroids, terpenoids and aliphatic & aromatic compounds. The first category comprised of campesterol and stigmasterol which are steroidal in nature and are used in anticancer therapeutics (Ghosh et al. 2010; Choi et al. 2010). The second category includes caratol, phytol and squalene which are terpenoids having isoprene units in them and are known antibacterial compounds (Togashi et al. 2010). The third category includes aliphatic and aromatic compounds having polar groups in them like phenol, ether, amine and acid derivatives e.g., 4-Octadecylmorpholine and 1,2-Benzenedicarboxylic acid, mono(2-ethylhexyl) ester. These compounds have been previously reported to possess antibacterial and antifungal potential. The VOC profile of *M. tigerii* is different from the previously reported *Muscodor* species, which dominantly produces esters of propanoic acid, azuelene, naphthalene derivatives and thujopsene. The volatiles produced by *M. tigerii* are unique and have not been reported by any other *Muscodor* species so far.

Table 5 Growth inhibition of the test organisms by the volatile organic compounds (VOC's) produced by *M. tigerii* after 72 h of exposure

Test species	Mean diameter in (mm)		Growth inhibition (%)
	Test	Control	
FUNGI			
Alternaria alternata	0	11±1.41	100
Aspergillus flavus	9.5 ±2.08	16±0.00	40.62
Artheminium phaeospermum	16.75±2.63	24±1.41	30.2
Bionectria ochroleuca	12.25±1.50	16±1.41	23.43
Botrytis cinerea	18.75±1.50	20.5±0.71	8.53
Cercospora beticola	0	16.5±2.12	100
Colletotrichum gloeosporioides	16.5±1.73	16.5±0.71	0
Fusarium oxysporum	15.75±0.50	25.5±0.71	38.23
Fusarium solani	19.75±0.50	22.5±2.12	12.22
Lasiodiplodia theobromae	32.75±2.50	36±0.00	9.02
Muscodor albus	8.75±0.96	9.5±0.71	7.8
Penicillium marneffei	6±1.41	21±1.41	71.42
Phomopsis theiocola	10.5±1.29	16.5±0.71	36.36
Rhizoctonia solani	12.75±0.50	45±0.00	71.67
YEASTS			
Candida albicans	6.25±0.5	18.5±3.54	62.21
Candida albicans	8.5±1.73	18.5±0.71	54.04
Candida albicans	8.5±1.91	20.5±3.54	58.53
Candida vishwanathi	7.5±1.91	20.5±0.71	63.41
BACTERIA			
Staphylococcus aureus	6.57±1.37	32.86±0.18	80.01
Pseudomonas aeruginosa	7.52±1.13	15.88±2.63	51.1

Bioassay of VOC's produced by *Muscodor tigerii*

The VOC produced by *M. tigerii* exhibits antifungal and antibacterial activity against the tested spectrum of bacteria, yeast and fungi. An array of 20 microorganisms were tested, out of which the growth of two fungal pathogens *Alternaria alternata* and *Cercospora beticola* were completely suppressed by the VOC whereas fungal pathogens like *Rhizoctonia solani*, *Penicillium marneffei*, *Aspergillus flavus* showed sensitivity toward volatiles. Their growth was inhibited by 72 %,42 % and 40.2% while *M.albus* cz 620 remains unaffected to VOCs. The growth of candidal isolates was also retarded by 54-63 % while *Staphylococcus aureus* and *Pseudomonas aeruginosa* exhibited 81 % and 51 % inhibition, respectively (Table 5).

Discussion

Emergence of resistance in microbes against the current armenterium of drugs and hazardous effect of methyl bromide and sulphur dioxide over the ozone layer is a burgeoning problem. Many efforts have been made over last two decades to rectify this, but it still remains an unsolved issue. The inherent property of the microorganism can be harnessed to produce bioactive secondary metabolites which will help in solving the current scenario. Plants harbour countless number of microorganisms which either exist as a pathogen or a symbiont inside the host tissue or are referred as endophytes. The predominant class of microorganisms, which resides as endophytes, belong to the fungal kingdom. Endophytes have been isolated from various habitats of the world, but their maximum diversity lies in the tropical rainforest. Endophytes are synthetic chemists par excellence, which reside within the plants, thereby offering themselves for future exploitation in medicinal and agrochemical industries. *Muscodor* is a genus of sterile endophytic fungi that produces volatile antimicrobial compounds. Over the past two decades, there has been a continual search for isolating the newer biotypes of this organism. The current study introduces *M. tigerii* from the internal tissue of the medicinal plant *Cinnamomum camphora* as a new species in genus *Muscodor*. Morphological, genetic and chemical profile demarcates it from the earlier reported species. *M. tigerii* bears all the morphological features described to date in the genus *Muscodor*, and, thus, it can be concluded as the most evolved one. The VOCs produced by *M. tigerii* induces inhibitory or lethal effect over the spectrum of plant and human pathogens tested in in vitro antimicrobial studies. Further studies are warranted to determine their efficacy in food preservation in post harvest technology. Apart from this, studies on plant-microbe interaction will facilitate our present knowledge on the beneficial effects of microorganisms associated with plants. The life cycle of Muscodor needs to be unveiled.

Acknowledgments The authors thank Department of Biotechnology (National Biodiversity Development Board) for financial assistance through project no. BT/PR/10083/NDB/52/95/2007. We also acknowledge Dr. Gary Strobel, MSU-Bozeman, USA for providing *M. albus* CZ620 type strain and constructive discussions. We extend our gratitude to Dr. AvneetPal Singh, Assistant Professor, Punjab University, Patiala, Punjab for his advice in taxonomic identification. We also gratefully acknowledge the help of Dr. Naresh M. Meshram and Ms. Salam Rita Devi, Division of Entomology, IARI, PUSA, New Delhi for SEM analysis and Shri Ajay Kumar from ARIF, JNU, New Delhi for GC/MS analysis.

References

Chatterjee S, Saikia A, Dutta P, Ghosh D, Pangging G, Goswami AK (2006) Biodiversity Significance Of North East India.wwf-India 172 B Lodi Estate New Delhi 110003

Chelliah DA (2008) Biological Activity Prediction Of An Ethno Medicinal Plant *Cinnamomum Camphora* Through Bio-Informatics. Ethnobotanical Leafl 12:181–190

Choi JM, Lee EO, Lee HJ, Kim KH, Ahn KS, Shim BS, N-Ii K, Song MC, Baek NM, Kim SH (2010) Identification Of Campesterol From *Chrysanthemum coronarium* L. And Its Antiangiogenic Activities. Phytother Res 21(10):954–959

Daisy BH, Strobel GA, Castillo U, Ezra D, Sears J, Weaver DK, Runyon JB (2002) Naphthalene, an insect repellent, is produced by *Muscodor vitigenus*, a novel endophytic fungus. Microbiology 148:3737–3741

Ezra D, Hess WM, Strobel GA (2004) New Endophytic Isolates Of *Muscodor albus*, A Volatile Antibiotic-Producing Fungus. Microbiology 12:4023–4031

Ezra D, Skovorodnikova J, Kroitor-Keren T, Denisov Y, Liarzi O (2010) Development Of Methods For Detection And *Agrobacterium*-Mediated Transformation Of The Sterile, Endophytic Fungus *Muscodor albus*. Biocontrol Sci Tech 20(1):83–97

Fu YX, Li WH (1993) Statistical tests of neutrality of mutations. Genetics 133:693–709

Ghosh T, Maity TP, Singh J (2010) Evaluation Of Antitumor Activity Of Stigmasterol, A Constituent Isolated from *Bacopa monnieri* Linn Aerial Parts Against Ehrlich Ascites Carcinoma In Mice. Orient Pharm Exp Med 11:41–49

Guo LD, Hyde KD, Liew ECY (1998) A Method To Promote Sporulation In Palm Endophytic Fungi. Fungal Divers 1:109–113

Kharwar RN, Maurya AL, Verma VC, Kumar A, Gond SK, Mishra A (2012) Diversity And Antimicrobial Activity Of Endophytic Fungal Community Isolated From Medicinal Plant *Cinnamomum camphora*. Natl Acad Sci India Sect B Biol Sci 82(4):557–565

Kudalkar P, Strobel G, Riyaz Ul Hasan S, Geary G, Sears J (2012) *Muscodor sutura*, A Novel Endophytic Fungus With Volatile Antibiotic Activities. Mycoscience 53:319–325

Kusari S, Hertweck C, Spiteller M (2012) Chemical Ecology of Endophytic Fungi: Origins Of Secondary Metabolites. Chem Biol 19:792–798

Librado P, Rozas J (2009) Dnasp V5: A Software For Comprehensive Analysis Of Dna Polymorphism Data. Bioinformatics 25:1451–1452

Mcneely JA, Miller KR, Reid W, Mittermeier R, Werner T (1990) Conserving The World's Biological Diversity. Iucn, Wri, World Bank, Wwf Us, Ci, Usa

Mercier J, Santamaria JIJ, Guerra PT (2007) Development Of The Volatile Producing Fungus *Muscodor albus* Worapong, Strobel,

And Hess As A Novel Antimicrobial Bio-Fumigant. Rev Fitopatol 25(2):173–179

Mitchell A, Strobel G, Hess W, Vargas P, Ezra D (2008) *Muscodor Crispans*, A Novel Endophyte From *Ananas ananassoides* In The Bolivian Amazon. Fungal Divers 31:37–43

Mitchell AM, Strobel GA, Moore E, Robinson R, Sears J (2010) Volatile Antimicrobials From *Muscodor crispans*, A Novel Endophytic Fungus. Microbiology 156:270–277

Nei N, Kumar S (2000) Molecular Evolution And Phylogenetics. Oxford University Press, New York

Saitou N, Nei M (1987) The Neighbor-Joining Method: A New Method For Reconstructing Phylogenetic Trees. Mol Biol Evol 4:406–425

Shipunov A, Newcombe G, Raghavendra AKH, Anderson CL (2008) Hidden Diversity Of Endophytic Fungi In An Invasive Plant. Am J Bot 95(9):1096–1108

Singh P, Shrivastava B, Kumar A, Dubey NK (2008) Fungal Contamination Of Raw Materials Of Some Herbal Drugs And Recommendation Of *Cinnamomum camphora* Oil As Herbal Fungitoxicant. Microb Ecol 56:555–560

Stone JK, Bacon CW, White JF (2000) An Overview Of Endophytic Microbes: Endophytism Defined. In: Bacon C, White J (eds) Microbial Endophytes. Dekker, New York, pp 3–30

Strobel G (2006) *Muscodor albus* And Its Biological Promise. J Ind Microbiol Biotechnol 33:514–522

Strobel G, Daisy B (2003) Bioprospecting For Microbial Endophytes And Their Natural Products. Microbiol Mol Biol R 4:491–502

Strobel GA, Dirske E, Sears J, Markworth C (2001) Volatile Antimicrobials From *Muscodor albus*, A Novel Endophytic Fungus. Microbiology 147:2943–295

Strobel GA, Katreena K, Hess WM, Sears J, Ezra D, Vargas PN (2007) *Muscodor albus* E-6, An Endophyte Of *Guazuma ulmifolia* Making Volatile Antibiotics: Isolation, Characterization And Experimental Establishment In Host Plant. Microbiology 153: 2613–2620

Suwannarach N, Bussaban B, Hyde KD, Saisamorn L (2010) *Muscodor cinnamomi,* a new endophytic species from *Cinnamomum bejolghota*. Mycotaxon 114:15–23

Suwannarach N, Kumla J, Bussaban B, Hyde KD, Matsui K, Lumyong S (2013) Molecular And Morphological Evidence Support Four New Species In The Genus *Muscodor* From Northern Thailand. Ann Microbiol. doi:10.1007/S13213-012-0593-6

Tajima F (1989) Statistical Method For Testing The Neutral Mutation Hypothesis By Dna Polymorphism. Genetics 123:585–59

Tamura K, Peterson D, Peterson N, Stecher G, Nei M, Kumar S (2011) Mega5: Molecular Evolutionary Genetics Analysis Using Maximum Likelihood, Evolutionary Distance, And Maximum Parsimony Methods. Mol Biol Evol 28(10):2731–2739

Togashi N, Hamashima H, Shiraishi A, Inoue Y, Takano A (2010) Antibacterial Activities Against *Staphylococcus aureus* of Terpene Alcohols With Aliphatic Carbon Chains. J Essent Oil Res 22:263–269

Verma VC, Kharwar RN, Gange AC (2010) Biosynthesis Antimicrobial Silver Nanoparticles By The Endophytic Fungus *Aspergillus clavatus*. Nanomedicine 5:33–40

Zhang C, Wang G, Mao LJ, Komon-Zelazowska M, Yuan ZL, Lin FC, Druzhinina IS, Kubicek CP (2010) *Muscodor fengyangensis* sp. Nov. From Southeast China: Morphology, Physiology and Production Of Volatile Compounds. Fungal Biol 114:797–808

Zhao J, Shan T, Mou T, Zhou L (2011) Plant-Derived Bioactive Compounds Produced By Endophytic Fungi. Mini Rev Med Chem 11(2):159–168

4th BIENNIAL
INTERNATIONAL CONFERENCE ON
NEW DEVELOPMENTS IN DRUG DISCOVERY FROM NATURAL PRODUCTS AND TRADITIONAL MEDICINES

DDNP TM
NIPER-2014

Local Organizing Committee is pleased to award the Best Poster Prize to Mr./Ms./Dr. Neha Kapoor for poster presentation during the conference held from 20-22 November, 2014 organized by the Department of Natural Products, National Institute of Pharmaceutical Education and Research (NIPER), Sector - 67, S.A.S. Nagar, Punjab, INDIA.

Prof. I.P. Singh
Joint Organizing Secretary

Prof. Sanjay Jachak
Joint Organizing Secretary

Prof. K.K. Bhutani
Organizing Secretary-cum-Convenor

Thesis

ORIGINALITY REPORT

%2	%	%2	%0
SIMILARITY INDEX	INTERNET SOURCES	PUBLICATIONS	STUDENT PAPERS

PRIMARY SOURCES

1	Advances in Endophytic Research, 2014. Publication	%2

EXCLUDE QUOTES	ON	EXCLUDE MATCHES	< 1%
EXCLUDE BIBLIOGRAPHY	ON		